UNIVERSITY OF LIVERPOOL

**The University of Liverpool**

# Proteins, which are upregulated at early time points following *Apc* deletion, are involved in intestinal tumourigenesis and represent potential colorectal cancer biomarkers

**Thesis submitted in accordance with the requirements of the University of Liverpool for the degree of Doctor in Philosophy by**

**Dr Shahram Ali Ibrahim**

**November 2014**

# ACKNOWLEDGEMNTS

First and foremost I offer my sincerest gratitude to my first supervisor, Dr John Jenkins, who has supported me throughout my thesis with his patience and knowledge whilst allowing me the room to work in my own way. I attribute the level of my PhD degree to his encouragement and effort and without him this thesis, too, would not have been completed or written. One simply could not wish for a better or friendlier supervisor.

I would also like to show my deepest gratefulness to my second supervisor, Professor Mark Pritchard, for helping me to focus and for keeping me on track throughout the study. His support, guidance and advice throughout the research project, as well as his pain-staking effort in proof reading the drafts, are greatly appreciated. Indeed, without his guidance, it would have taken me much more time to put the topic together. Also, if I would remember someone as a role model, it would be Mark.

Thanks to Dr Karen Reed from the University of Cardiff for providing me with the animal samples and thanks to Dr Paul Sutton for providing me with the clinical samples. These samples were the corner stone for this project. I am also thankful to Professor Barry Campbell who accepted to be my mentor and advisor. I benefited from his sincere advice and constructive criticism. I highly acknowledge the help that Dave Berry, Dr Abdalla Hanedi, Dr Carrie Duckworth, Sue Courtney and other staff and colleagues gave me during the course of my work in the Department of Gastroenterology. Without them things could have been much more difficult.

I would also like to thank my government, our Prime Minister Mr Nicheervan Barzani and Mr Bariz Barzani for funding my studies and for supporting me and all other Kurdish students all over the world.

A special thanks to my family. Words cannot express how grateful I am to my mother and my brother and sisters for all of the sacrifices that they have made on my behalf. At the end I would like to express appreciation to my beloved wife who was always my support in the moments when there was no one to answer my queries.

## Table of contents

## List of abbreviations

**A**

| | |
|---|---|
| ACF | aberrant crypt foci |
| AFAP | attenuated familial adenomatous polyposis |
| AJCC | American Joint Committee on Cancer |
| AML | acute myeloid leukaemia |
| ANOVA | analysis of variance |
| AOM | azoxymethane |
| APC | adenomatous polyposis coli |
| APES | 3-aminopropyltriethoxysilane |
| AS | alternative splicing |

**B**

| | |
|---|---|
| Bcl2 | B cell lymphoma 2 |
| BNF | beta naphthoflavone |
| BrdU | 5-bromo-2-deoxyuridine |

**C**

| | |
|---|---|
| CA | carbohydrate antigen |
| CBC | crypt base columnar |
| CDC5L | Cell division cycle 5-like |
| CEA | carcinoembryonic antigen |
| CHRPE | congenital hypertrophy of the retinal pigment epithelium |
| CID | beta catenin inhibitory domain |
| CIMP | CpG island methylator phenotype |
| CIN | chromosomal instability |
| CK1γ | casein kinase 1 gamma |
| COX | cyclooxygenase |
| CpG | cytosin-phosphate-guanin |
| CRC | colorectal cancer |
| CtBP | C terminal binding protein |
| CTC | Computed tomographic colonography |
| cyp1A1 | cytochrome P450 subfamily1 A1 |

**D**

| | |
|---|---|
| DAB | diaminobenzidine |
| DCC | deleted in colorectal cancer |
| DDX5 | DEAD box protein 5 |
| dip | diploid |
| DMEM | Dulbecco's Modified Eagle Medium |
| Dsh | dishevelled |
| DSS | dextran sodium sulphate |

**E**

| | |
|---|---|
| ELISA | enzyme linked immunosorbent assay |

**F**

| | |
|---|---|
| FABP6 | Fatty acid binding protein 6 |
| FACS | fluorescence activated cell sorting |
| FAP | familial adenomatous polyposis |
| FCS | foetal calf serum |
| FIT | faecal immunochemical testing |
| FOBT | faecal occult blood test |
| FS | flexibile sigmoidoscopy |
| Fz | frizzled |

**G**

| | |
|---|---|
| gFOBT | guaiac faecal occult blood test |
| GIT | gastrointestinal tract |
| GSKβ | glycogene synthase kinase beta |
| GTP | Guanosine-5-phosphate |

**H**

| | |
|---|---|
| H and E | haematoxylin and eosin |
| HIV | human immunodeficiency virus |
| HMGB1 | High-mobility group protein B1 |

**I**

| | |
|---|---|
| IBD | inflammatory bowel disease |
| ICC | Immunocytochemistry |
| iFOBT | immunochemical faecal occult blood test |
| IHC | immunohistochemistry |
| IPA | Ingenuity pathway analysis |
| iTRAQ | isobaric tag for relative and absolute quantification |

**L**

| | |
|---|---|
| LEF | lymphoid enhancing factor |
| LGr5 | leucine rich repeat containing G protein coupled receptor 5 |
| LOH | loss of heterozygosity |

**M**

| | |
|---|---|
| MAM | methylazoxy methanol |
| MAP | MUTYH associated polyposis |
| MAPK | mitogen-activated protein kinase |
| MCR | mutation cluster region |
| MIC1 | macrophage inhibitory cytokine 1 |
| Min | multiple intestinal neoplasia |
| MMP | matrix metalloproteinases |
| MMR | mismatch repair |

| | |
|---|---|
| mRNA | messenger RNA |
| MS | Mass spectrometry |
| MSI | microsatellite instability |
| MUTYH | MutY homolog |

**N**

| | |
|---|---|
| NAP1L1 | Nucleosome assembly protein 1-like 1 |
| NCL | Nucleolin |
| NHPCC | hereditary non polyposis colorectal cancer |
| NPM | Nucleophosmin |

**P**

| | |
|---|---|
| PBS | phophate buffered saline |
| PHB | Prohibitin |
| pre-mRNA | precursor mRNA |
| PTEN | Phosphatase and tensin homolog |

**Q**

| | |
|---|---|
| qRT-PCR | quantitative reverse transcription polymerase chain reaction |

**R**

| | |
|---|---|
| RAGE | receptor for advanced glycation end products |
| RIPA | radioimmunoprecipitation assay |
| RNAi | RNA interference |
| RP | Ribosomal protein |
| RPL6 | Ribosomal protein L6 |

**S**

| | |
|---|---|
| SD | standard deviation |
| SDS | sodium dodecyl sulphate |
| SFRS2 | Splicing factor, arginine/serine-rich 2 |
| siRNA | small interfering RNA |
| SR | serine rich |
| STK11 | serine/threonine kinase11 |

**T**

| | |
|---|---|
| TBS | tris buffered saline |
| TCF | T cell factor |
| Tcf4 | Transcriptional factor 4 |
| TEMED | tetramethylethylenediamine |
| *Tgfbr2* | transforming growth factor beta receptor 2 |
| TGFβ | transforming growth factor beta |
| TIMP | Tissue inhibitor of metalloproteinase type |
| TNM | tumour node metastasis |

**U**

| | |
|---|---|
| UICC | International Union against Cancer |

**W**

| | |
|---|---|
| WB | western blot |
| WHO | world health organisation |
| Wnt | wingless/Int1 |

**Proteins, which are upregulated at early time points following *Apc* deletion, are involved in intestinal tumourigenesis and represent potential colorectal cancer biomarkers**


## Abstract

Colorectal cancer is a potentially curable disease if diagnosed at its earliest stages. However, as the current tools for early diagnosis of colorectal cancer are suboptimal, this condition is still a major health issue in the UK and the whole world. Each year nearly 40,000 new cases are diagnosed in the UK. Approximately half of these patients have advanced disease at the time of diagnosis and this is associated with a less favourable prognosis. Therefore, there is still an urgent need for better colorectal cancer screening tools. Moreover, it has long been suggested that *APC* deletion is an early and major event in the initiation of more than 80% of all colorectal cancers. However, the molecular events that occur following *APC* deletion are yet to be fully understood. Working on an acute *Apc* deletion animal model, our group has identified several candidate biomarker proteins. It is postulated that studying these proteins will reveal new aspects about early colorectal tumourigenesis. We hypothesised that these proteins are upregulated very early following *Apc* deletion and are involved in various aspects of colorectal cancer development, therefore they are potential biomarkers and/or therapeutic targets for this disease.

Most of the project's aims were addressed using immunohistochemical assessment of the expression of several candidate biomarkers in a novel *in vivo* model of acute *Apc* deletion ($AhCre^{+}Apc^{fl/fl}$ mouse), a model of established early intestinal neoplasia ($Apc^{Min/+}$ mouse) and a model of invasive disease ($AhCreER^{T+}Apc^{fl/+}Pten^{fl/fl}$ mouse) as well as clinical samples from patients with early and advanced colorectal cancer. Mechanistic studies were carried out using the human colonic adenocarcinoma cell lines, HCT116 and HT29.

In the animal models, deletion of *Apc* resulted in an early activation of the Wnt signalling pathway as indicated by nuclear localisation of Beta catenin. Six (NAP1L1, RPL6, SFRS2, PHB, FABP6 and NCL) out of the nine candidate biomarker proteins tested and two proposed partner molecules (Cyclin E and CDC5L), demonstrated obvious differential patterns of expression in areas where Apc loss had induced Wnt pathway activation. Specific knockdown studies of

selected members of this protein list in human colon adenocarcinoma cell lines using siRNA identified important effects of these proteins on critical cellular functions such as proliferation and apoptosis. NAP1L1 and RPL6 knockdown had an inhibitory effect on cell proliferation and survival and caused a simultaneous increase in apoptosis. SFRS2 knockdown caused increased abundance of nuclear CDC5L and vice versa. SFRS2 down regulation had marginal effects on cell proliferation and cell survival and resulted in a small reduction in the amount of apoptosis. In contrast, CDC5L knockdown caused a dramatic inhibition of cellular proliferation, loss of the G2 cell cycle peak and a significant increase in the amount of apoptosis and caspase 8 activity. HCT116 cells with a *p53* deletion were more sensitive to toxicity of experimental (transfection) reagents and SFRS2 knockdown in these cells caused obvious inhibition of cell proliferation with increased apoptosis.

Immunohistochemical staining of the candidate biomarker proteins in human samples of colorectal cancer generally supported the results shown in animal studies for early stages of the disease. Moreover, it demonstrated reduced nuclear expression of Beta catenin, nuclear relocalisation of CDC5L and cytoplasmic displacement of SFRS2 in the more advanced stages of colorectal cancer. PHB showed increased cytoplasmic staining in Dukes' stage A and B cancers. These results were backed up by appropriate scoring systems.

Our results concerning these proteins in colorectal cancer are novel and agree with several studies by other research groups describing their roles in other cancers or cancer models. Due to the relatively late detection of lesions in humans, the early changes which were observed in animals might have been missed in humans. NAP1L1, RPL6, SFRS2 and NCL showed early overexpression during colorectal tumourigenesis. These proteins therefore have the potential as screening biomarkers. Due to their role in regulating cellular proliferation, NAP1L1, RPL6 and CDC5L are potential therapeutic targets for colorectal cancer. PHB is also a potential marker for Dukes' stage A and B cancers. Mechanistically, the interplay between SFRS2 and CDC5L during colorectal tumourigenesis is a promising case to follow.

Based on this study and other studies conducted in our group, the above proteins are promising screening, predictive or prognostic markers as well as potential therapeutic targets for colorectal cancer.

# Chapter one

# Introduction

# 1. Introduction

## 1.1 Epidemiology of colorectal cancer

### 1.1.1 Worldwide incidence and mortality

Colorectal cancer (CRC) is the third most common cancer and second leading cause of cancer-related death in Europe and according to the World Health Organisation (WHO) it meets the criteria for mass screening [1]. It is considered the fourth most common cancer and second most common cause of cancer related death in the UK [2]. Approximately 40,700 cases were diagnosed in 2010 in the UK and 15,700 people died in the same year [2]. Moreover, research suggests that more than 90% of bowel cancer patients will survive for more than five years if diagnosed at the earliest stages. However, currently less than half of the cases are localised to the colon at time of diagnosis [3].

### 1.1.2 Types of colorectal cancer

Ninety five percent of CRCs are adenocarcinomas. This means that they arise from the glandular element of the bowel lining. The glands produce mucus, a substance that acts as a lubricant in the bowel. Two of the rare morphological types of bowel adenocarcinoma are mucinous (cells lie in pools of mucus) and signet ring (mucus fills the individual cell, pushing the nucleus to one side giving it this particular shape) tumours [2]. Other less common tumours of the bowel include squamous cell carcinoma, neuroendocrine tumours, sarcomas (mostly leimyosarcoma, of smooth muscle origin) and lymphomas (1%) [2].

### 1.1.3 Distribution of colorectal cancer

More cases of CRC are diagnosed in the left than right side of the large bowel as shown in figure 1.1 below.

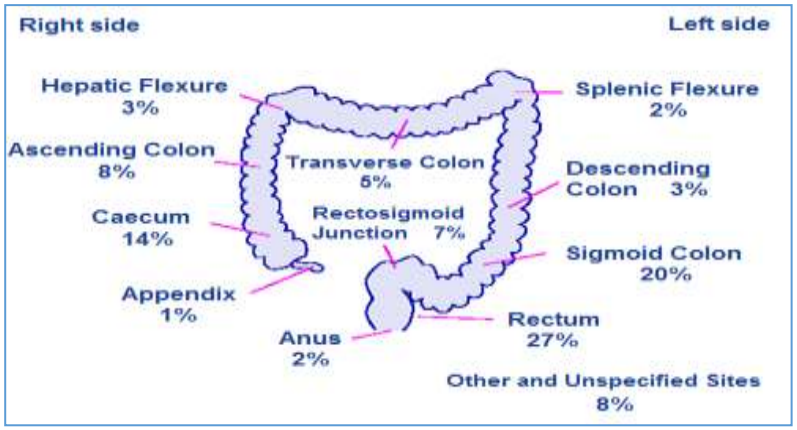


**Figure 1.1 UK percentage distribution of cases within the large intestine, 2007-2009 [2]. Cancer Research UK. http://www.cancerresearchuk.org/cancer-info/cancerstats/types/bowel/incidence/19Nov2013.**

### 1.1.4 Staging of colorectal cancer

Treatment strategies and prognosis vary according to the stage of CRC. Accurate prognostic prediction of patients is important for improving treatment selection [4]. Moreover, due to the critical role of lymph node involvement in determining the outcome of CRC [4], the International Union against Cancer (UICC) and the American Joint Committee on Cancer (AJCC) recommend the Tumour, Node, Metastasis (TNM) system for staging CRC [5]. However, the modified Dukes' staging [6, 7] is still also being used [5].

The table below (1.1) shows the two commonly used staging systems for CRC. The table is produced from data on the Cancer research UK website [2].

| *TNM* | | *Modified Dukes'* |
|---|---|---|
| Stage 0 | Carcinoma *in situ* | |
| Stage I | Tumour invades submucosa (T1)<br>Tumour invades musularis propria (T2)<br>No nodal involvement nor distant metastasis (N0, M0) | A |
| Stage II, a<br>b | Tumour invades serosa (T3)<br>Tumour invades beyond serosa (locally) (T4)<br>No nodal involvement nor distant metastasis (a & b) | B |
| Stage III, a<br>b<br>c | 1-3 regional lymph nodes involved (N1), (T1, T2)<br>1-3 regional lymph nodes involved (N1), (T3, T4)<br>4 or more regional lymph nodes involved (N2) , any T, not distant metastasis | C |
| Stage IV | Any T and N with distant metastasis (M1) | D |

**Table 1.1 Staging systems commonly used in CRC**

Nowadays there is a concept that molecular diagnostics are equally important, if not more so, to anatomical factors in the staging of many solid tumours and that in future, classic morphology might give way to these molecular markers [5].

### 1.1.5 Grading of colorectal cancer

Grading CRCs also has important therapeutic and prognostic implications. Grading of CRC is based on the morphology of cells and their degree of differentiation. As normal cells grow and mature they become more specialised for their role and position in the body (differentiation). Pathologists grade CRCs as:

- Grade 1 (Low), very similar to normal cells
- Grade 2 (Moderate), moderately abnormal

- Grade 3 (High), highly abnormal

Low grade tumours unlike high grade ones tend to grow more slowly and are less likely to metastasise [2].

### 1.1.6 Risk factors

The average lifetime risk for the development of sporadic CRC is about 5% [8]. High consumption of red meat and low intake of dietary fibre increase the chance of developing bowel cancer [2]. Being overweight has also been shown to be a risk factor since at least 10% of all cases of colorectal cancer diagnosed in the UK are related to this problem [9]. Among other risk factors are inactivity and drinking more than 30 grams (4 units) of alcohol per day [10]. Chronic diseases such as diabetes mellitus and inflammatory bowel disease also increase the risk of developing bowel cancer [2].

#### Genetics

Evidence suggests that a person's genetic makeup accounts for 35% of the risk of developing colorectal cancer [11]. A first degree relative with colorectal cancer doubles the chance of a person developing the disease compared to an average risk individual [10]. Interestingly however, the majority of cases of colorectal cancer occur in individuals without a family history of such disease (sporadic CRC, 70-80% of cases) [10]. Moreover, around 20% of those who develop colorectal cancer have one or more family members with this condition (familial CRC) [9]. Known predisposing inherited conditions represent 5-10% of all cases of colorectal cancer (hereditary CRC) [9]. Most common of these conditions are hereditary non polyposis colorectal cancer (NHPCC) and familial adenomatous polyposis (FAP) [12].

#### Hereditary disorders predisposing to colorectal cancer

A good classification of hereditary disorders predisposing to CRC was made in 1998 by Lynch and Lynch [13]. This classification included pattern of inheritance, associated germinal mutations, polyp information, other associated malignancies, non-cancerous features, population screening, surgical and/or prophylactic strategies and DNA testing in asymptomatic individuals as well as genetic counselling [14]. These hereditary disorders include

- Familial adenomatous polyposis (FAP)
- Attenuated familial adenomatous polyposis (AFAP)

- I1307K mutation in Ashkenazi Jews
- Juvenile polyposis coli
- Peutz-Jeghers syndrome
- Slight adenomatous polyposis of the colon and Burt's colorectal cancer
- Hereditary non-polyposis colorectal cancer (HNPCC)
- Familial colorectal cancer
- Familial ulcerative colitis and Crohn's disease

All but the last two are inherited in an autosomal dominant pattern [14].

FAP is an autosomal dominant disorder characterised by extensive polyposis of the colon (hundreds to thousands of polyps) that leads to cancer at an early age (typically less than 40 years). It affects people inheriting a germ line mutation in the *APC* gene, which is localised on chromosome 5q21 and is found in 60-80% of families with FAP [14, 15]. Polyps may also appear in the upper gastrointestinal tract (GIT) and tumours may affect other organs such as the brain and thyroid gland. Moreover, FAP patients may have other clinical problems such as congenital hypertrophy of the retinal pigment epithelium (CHRPE), jaw cysts, sebaceous cysts, and osteomas [14]. Gardner's syndrome is a phenotypic variant of FAP that also shows epidermoid cysts, jaw osteomas, CHRPE, fibromas, and desmoid tumours [16]. Moreover, FAP patients may develop extra colonic malignancies such as stomach, small intestine and periampullary cancers in addition to sarcomas [16]. The average age of cancer development in FAP is 39 years but it is not uncommon in teens and early adulthood [13].

AFAP presents with fewer polyps (average 5-10 and often less than 100) with predilection for the proximal colon. It may also be associated with gastric fundic cystic gland polyps and duodenal adenomas. Cancers tend to develop at later ages [13]. Importantly, 16%–40% of patients with less than 100 polyps carry the bi-allelic inactivation of the MutY homolog (MUTYH) based-excision repair gene, a condition called MUTYH-associated polyposis (MAP). AFAP and MAP have very similar phenotypes [17].

Turcot's syndrome is characterised by 50 to 100 adenomas in the colon and cancers of the central nervous system. Medulloblastomas occur when APC is defective while

multiform glioblastomas develop when *hMLH1* and *hPMS2* genes are mutated [13]. Juvenile polyposis patients show 10 or more juvenile hamartomatous polyps in the colon but also in the stomach and small intestine. It is defined by mutations in the tyrosine-phosphate *(PTEN)* gene [18]. Peutz-Jegher's syndrome in addition to hamartomatous polyps in the gastrointestinal tract (GIT) is also characterised by mucocutaneous melanin pigmentation, usually of the perioral area. The defective gene encodes for the serine-therionine kinase 11 (STK11) [18].

HNPCC patients only occasionally develop polyps, but never abundantly. Its diagnosis needs the exclusion of FAP. However, adenomas are bigger and more villous. HNPCC patients are prone to other malignancies such as endometrial, ovarian, small intestinal, gastric, ureteric, and renal pelvis cancers [13]. CRC in HNPCC develops at an early age and predominantly in the right colon [19]. Moreover, the average age for cancer development is 44 years with a rapid adenoma to carcinoma progression [13]. HNPCC develops due to defects in the DNA mismatch repair system (MMR) genes, mainly *hMLH1* and *hMSH2* and therefore tumours show microsatellite instability (MSI) [19].

**Age**

There is a progressive increase in the chance of developing colorectal cancer after the age of 40 with a sharp rise in incidence after 50 (figure 1.2) [9, 12].

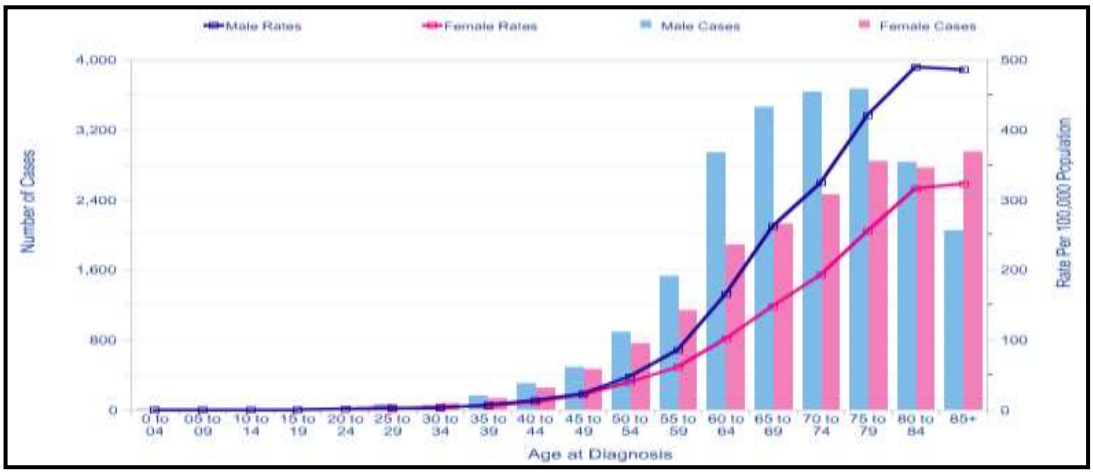


**Figure 1.2 Number of New Cases and Age-Specific Incidence Rates, UK, 2008 [2]. Cancer Research UK. http://www.cancerresearchuk.org/cancer-info/cancerstats/types/bowel/incidence/19Nov2013.**

**Adenomatous polyps**

Incidence of colorectal adenomas is about 15% in people aged between 40 and 60 years and more than 40% in higher age groups. Although mostly non progressive, polyps increase the chance of developing CRC [10]. Usually a time window of 5 to 10 years is required for the malignant transformation of these polyps (~95% are non-progressive lesions) [8, 10]. Most if not all cases of CRC arise within polyps, therefore removal of polyps in the transition period significantly reduces the chance of developing colorectal cancer for an individual (70-90%) [20].

### 1.2 Colorectal carcinogenesis

Colorectal tumours are a good model for studying carcinogenesis and the molecular events implicated in the development of cancer [14]. Hereditary forms follow defined stages from normal epithelium through adenoma to cancer [14]. They are the result of accumulation of multiple mutations in tumour suppressor genes and oncogenes that affect the balance between proliferation and apoptosis [14]. This is well represented by the multiple stages pattern "adenoma to carcinoma sequence" described by Vogelstein *et al.* [21].

The pathogenesis of CRC differs according to the genetic or epigenetic changes which are associated with each case. These genetic and epigenetic alterations are directly responsible for a specific event(s) that leads to CRC, by contributing to the "initiation" of neoplastic transformation of healthy epithelium and/or determining the "progression" towards more invasive stages of the disease [19]. Moreover, without a cellular environment that accelerates the accumulation of genetic events, it may be difficult for a cancer to develop during the lifetime of a person. This environment is ensured via the creation of a state of genomic instability that enables the occurrence of strategic mutations at an increasingly greater likelihood [22]. In general, inherited factors may determine the predisposition of an individual to develop an adenoma and cancer; while environmental factors may determine which of the susceptible individuals will develop small adenomas, large adenomas or cancer [23].

Colorectal carcinogenesis is not always the same; there are different pathways which are recognised for their characteristic models of genetic instability, associated clinical manifestations, and pathological behaviours [19]. The most common is the chromosomal instability (CIN) pathway, in which structural chromosomal defects

(aneuploidy) are responsible for the gross genetic abnormalities and wide spread loss of heterozygosity (LOH) [24]. The microsatellite instability (MSI) pathway is another carcinogenesis model in which there is failure to detect and/or repair the mismatched bases at microsatellite sequences of the daughter strand of DNA due to a defect in the mismatch repair system (MMR) [22]. Recently epigenetic factors have also been considered as drivers of carcinogenesis in a certain proportion of colorectal tumours [25]. CpG island methylator phenotype ($CIMP^{+}$) cancers are an example of this, where methylation of promoter sequences is postulated to drive a separate colorectal carcinogenesis pathway, the serrated neoplasia pathway [26].

### 1.2.1 The suppressor pathway (traditional or chromosomal instability)

CIN (figure 1.3) is the most well characterised colorectal carcinogenesis pathway [19]. About 70-85% of CRCs develop following this pathway [27]. The earliest lesion in this pathway is proposed to be the aberrant crypt focus (ACF), a microscopic lesion that precedes polyp formation [28]. Allelic losses are quite common in CRC and CIN is thought to induce carcinogenesis through loss of tumor suppressors and copy number gains of oncogenes [29, 30].

Genetic defects commonly seen in the tumours of this pathway include:

- *APC* mutation and 5q loss of heterozygosity
- *K-ras* mutation and 18q loss of heterozygosity
- *p53* mutation and 17p loss of heterozygosity

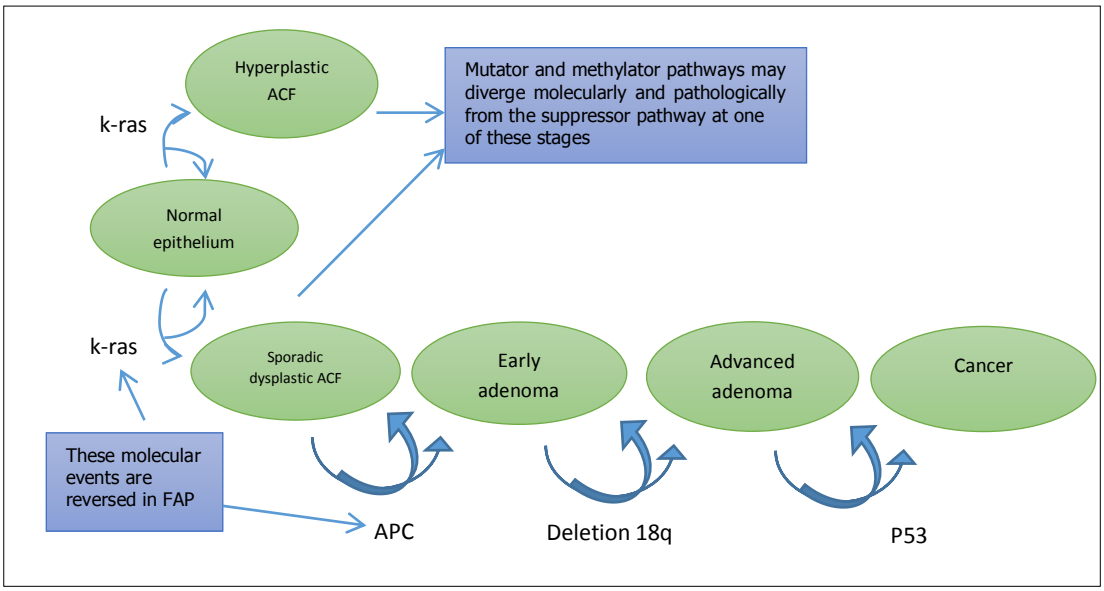


**Figure 1.3 Sporadic/traditional/CIN pathway: sequential pathological stages and molecular events [22] (modified). ACF= aberrant crypt foci.**

Remarkably, only a small minority of CRCs show all of the above mutations together [31].

### *APC* gene (5q21)

In cancer, it is thought that each mutation confers a growth advantage to the affected cell. Therefore, multiple stages of clonal expansion may occur within the same tumour which in turn leads to tumour progression [32]. The majority of hereditary CRCs are due to mutations in tumour suppressor genes [33]. It is has been suggested that tumour suppressors are divided into gatekeepers which directly inhibit tumour growth and promote apoptosis and caretakers which do not directly affect tumour growth but their loss produces genomic instability [34].

The *APC* gene (figure 1.4) is the gatekeeper of cell proliferation in the colonic epithelium. It was identified and characterised in 1991 [35]. It is localised on chromosome 5q21 and is made up of 8535 bp distributed onto 15 exons. It encodes a large protein of 2843 amino acids in its common isoform [36]. Exon 15 occupies more than 75% of the coding sequence of *APC* gene and is the most frequently affected by mutations, both germline and somatic [37].

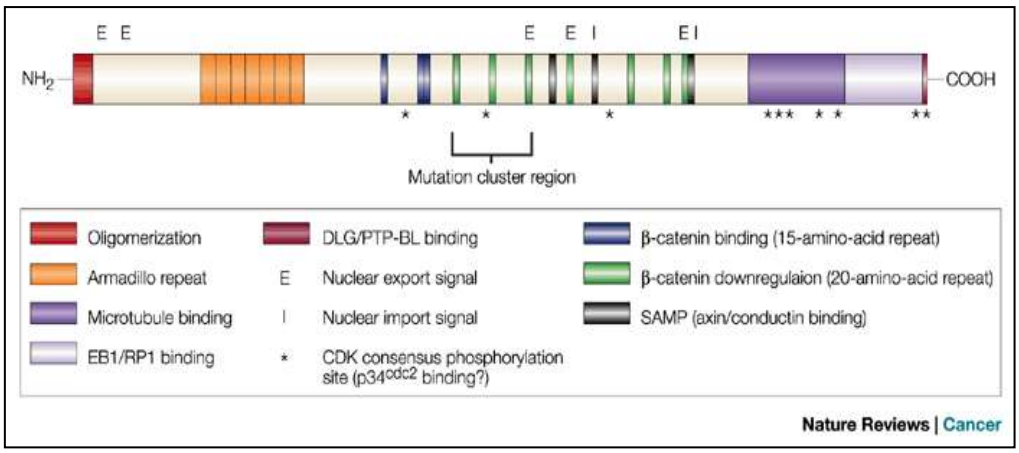


**Figure 1.4 This image is adapted from reference [38] depicting the structure of *APC* gene. EB1 end binding 1, RP1 retinitis pigmentosa 1, DLG discs large, PTP-BL protein tyrosine phosphatase-BL, CDK cyclin-dependent kinase, SAMP small archaeal modifier protein. Reprinted by permission from Macmillan Publishers Ltd: Nature reviews Cancer. APC, signal transduction and genetic instability in colorectal cancer. Copyright (2001).**

The APC protein forms homo-oligomers and is associated with catenins. It is made up of an oligomerisation domain and an armadillo region, 15 and 20 amino acid repetitions in its central portion and a carboxy-terminal end containing a basic domain and union sites for other proteins. Each domain has a defined role in APC activity [39]. The oligomerisation domain allows APC to form homodimers, the active forms of the protein while the armadillo region contributes to the stabilisation and motility of the cytoskeleton and it may not be essential for the tumour suppression function of APC [39]. The 15 and 20 amino acid sites allow the protein to bind Beta catenin [40].

The various functions of APC include regulation of Beta catenin mediated WNT signalling, regulation of cell to cell adhesion via Beta catenin and cadherins, regulation of cell migration via interaction with the microtubules, cell cycle arrest and coordination of cell adhesion and motility [23, 41]. In addition to abnormalities of the above functions, APC's contribution to tumourigenesis involves a deranged mitotic spindle function and a resultant genomic instability [42]. As a result, *APC* deletion is a key early mutation in sporadic CIN and FAP (germline mutation) [43].

The more frequent mutations of *APC* result in the production of truncated inactive proteins. An example of APC dysfunction is FAP, in which all cells of the body lack one copy of the *APC* gene and initiation of the adenoma carcinoma sequence in the

intestine follows the inactivation of the other existing copy, loss of hetrozygosity (LOH) [44]. Therefore, in FAP unlike sporadic adenomas there is *APC* mutation in all associated aberrant crypt foci (ACF) [22].

Due to relevance to this project, APC and the WNT signalling pathway are reviewed in more detail below.

***K-ras* mutation (12p12)**

*K-ras* is a proto oncogene encoding a guanosine-5-triphosphate (GTP)-binding protein and when mutated it causes loss of inherent GTPase activity [22]. It is mutated (activating mutations) in more than 40% of CRCs, driving constitutive signalling for proliferation through BRAF, which in turn activates the mitogen-activated protein kinase (MAPK) pathway [45]. Higher rates of *K-ras* mutations in sporadic dysplastic ACF (63%) than those in CRC and advanced adenomas (35-42%) suggest that despite the growth advantage that mutation of this gene confers, it is neither sufficient nor necessary for driving colorectal carcinogenesis [22].

***SMAD2, SMAD4 &* deleted in colorectal cancer (*DCC*) genes**

SMAD2 and SMAD4 are involved in the transforming growth factor beta (TGFβ) signalling pathway that regulates growth and apoptosis. The *DCC* gene encodes a transmembrane receptor protein that mediates apoptosis in the absence of its ligand, netrin1 [22]. These three genes are located at 18q21.1 and allelic loss at this site is found in up to 60% of CRCs [46]. *SMAD4* mutation is more frequently encountered than *SMAD2* and *DCC* mutations, which are rare in CRC. Moreover, *SMAD4* germ line mutation causes juvenile polyposis, which is associated with an increased risk of developing CRC [22].

***p53* gene (17p13)**

The *p53* gene encodes a tumour suppressor protein that controls the expression of genes regulating apoptosis, angiogenesis, the cell cycle and maintenance of the genome. Approximately half of human cancers contain mutated *p53* genes, and 30–60% of CRCs have mutations in the gene [47, 48]. Normal p53 protein is stabilised by DNA damage and acts as a transcription factor inducing the expression of cell cycle retarding genes. This function allows adequate time after an insult to DNA for the MMR system to repair the resulting defects during cell proliferation [22]. Loss of

*p53* (usually through allelic loss) is a late event in the traditional pathway of colorectal carcinogenesis and adds an invasive trait to the abnormal growth [22].

### 1.2.2 Microsatellite instability (mutator) pathway (MSI)

Another mechanism of genomic instability is the MSI pathway, which is seen in approximately 20% of CRCs (90% of HNPCC and 10-15% of sporadic CRC) [49, 50]. Microsatellites are stretches of short DNA sequences, which contain a motif of 1–5 nucleotides with tandem repeats spread throughout the human genome [51]. A change in microsatellites length (MSI) dramatically increases the chance of genetic errors and several microsatellites are present in genes implicated in CRC such as *TGFβRII, Bax*, *Caspase5*, *MSH3*, *MSH6*, Beta catenin, *APC*, *IGFII* and *E2F4*.

In MSI, genetic defects are in the DNA mismatch repair (MMR) system [52]. There are at least six DNA mismatch repair genes, some of which are implicated in HNPCC aetiology. Any breach in the MMR system will lead to inheritance of DNA defects by daughter cells and accumulation of mutations in genes that control proliferation ending up with the formation of tumours [53].

### 1.2.3 Methylator pathway

Epigenetic processes such as methylation are involved in the regulation of gene transcription [22]. In CRC, there is universal hypo-methylation of the genome, mainly in repeat DNA sequences, while the promoter regions of strategic genes are hyper-methylated [54]. This latter phenomenon disrupts the involvement of a particular gene with the transcription mechanism by inhibiting binding of the transcription factor and changing histone acetylation, thereby interrupting its expression (silencing) [55]. Therefore, CpG island methylation corresponds to inactivation mutations during cancer development causing first and/or second hits (loss of function of vital tumour suppressors) [22].

### 1.3 The Wnt signalling pathway

The Wnt pathway is a highly conserved signalling cascade, which is activated by secreted Wnt proteins. Gene sequencing has revealed 20 Wnt proteins in humans, which are subdivided into 12 conserved subgroups (WNT1 to WNT11 and WNT16) according to their shared functions. The biological significance of Wnt signalling comes from its involvement in all aspects of embryonic development as well as homeostasis and self-renewal in a number of adult tissues such as skin, adipose tissue, haematopoietic tissue and others [40]. Germline mutations in genes of this pathway may cause hereditary diseases and their somatic mutations cause cancer of the intestine and some other organs [56].

Currently one or more of three pathways are believed to be induced when Wnt receptors are activated:

1. Canonical Wnt/ Beta catenin pathway
2. Non canonical planar cell polarity pathway
3. Wnt/Calcium pathway.

The best understood so far is the canonical pathway [56].

### 1.3.1 Canonical Wnt pathway

After their secretion, Wnt proteins bind frizzled (Fz) and LRP trans-membrane receptors activating the canonical pathway [56]. Details of the possible events are illustrated in figure 1.5 below.

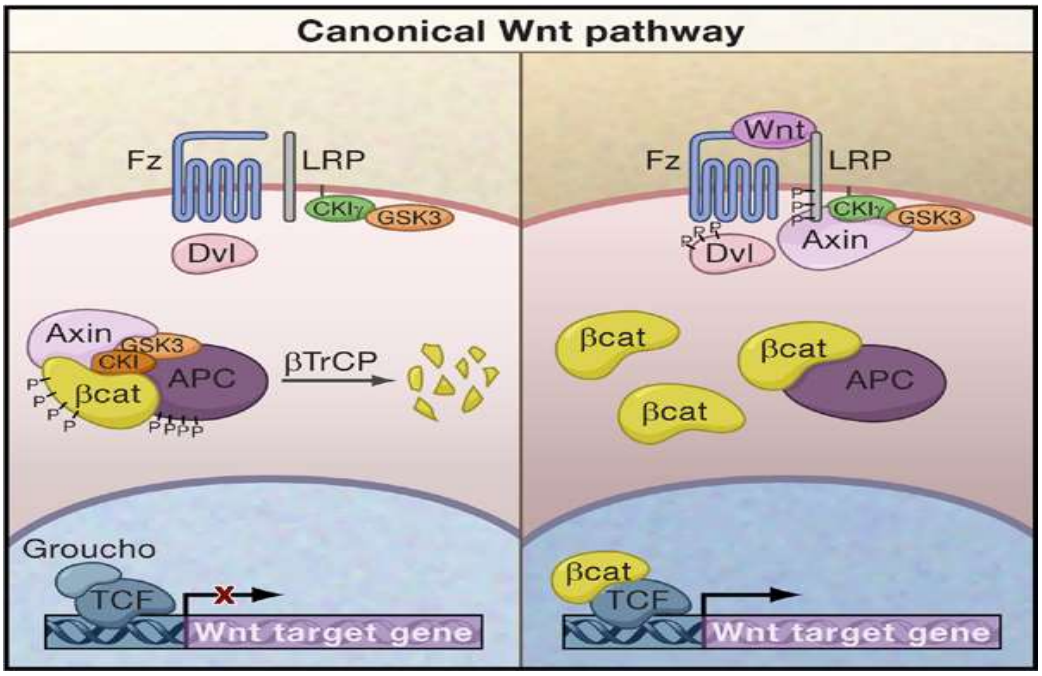


**Figure 1.5 Canonical Wnt Signaling: "(Left panel) When Wnt receptor complexes are not bound by ligands, the serine/threonine kinases, CK1 and GSK3α/β, phosphorylate β-catenin. Phosphorylated β-catenin is recognized by the F box/WD repeat protein β-TrCP, a component of a dedicated E3 ubiquitin ligase complex. Following ubiquitination, β-catenin is targeted for rapid destruction by the proteasome. In the nucleus, the binding of Groucho to TCF (T cell factor) inhibits the transcription of Wnt target genes. (Right panel) Once bound by Wnt, the Frizzled (Fz)/LRP coreceptor complex activates the canonical signalling pathway. Fz interacts with Dishevelled (Dsh), a cytoplasmic protein that functions upstream of β-catenin and the kinase GSK3β. Wnt signalling controls phosphorylation of Dsh. Wnts are thought to induce the phosphorylation of LRP by GSK3β and casein kinase I-γ (CK1γ), thus regulating the docking of Axin. The recruitment of Axin away from the destruction complex leads to the stabilization of β-catenin. In the nucleus, β-catenin displaces Groucho from Tcf/Lef to promote the transcription of Wnt target genes" [56]. CK1 is casein kinase1, GSK is glycogen synthase kinase and LRP is lipoprotein receptor related protein. This article was published in Cell, 127, Clevers H., Wnt/beta-catenin signaling in development and disease. 269-280, Copyright Elsevier (2006).**

A new model of Wnt pathway signalling suggests that even during activation of this pathway, the destruction complex still captures and phosphorylates Beta catenin, but ubiquitination by b-TrCP is blocked [57].

### 1.3.2 Wnt activity and the cytoplasmic destruction complex

The main player in the canonical pathway is Beta catenin which is a multifunctional cytoplasmic protein involved in cellular adhesion and Wnt signalling [56, 58, 59]. Stability of Beta catenin is regulated by the destruction complex [56, 60]. In this complex the tumour suppressor Axin acts as a scaffold as it directly interacts with the other components of the complex. The complex involves Beta catenin, APC, Glycogen synthase kinase 3 (GSK3), and Casein kinase 1 (CK1) [56, 60]. When Wnt receptor complexes are not engaged, CK1 and GSK3 phosphorylate Beta catenin sequentially and Beta catenin is targeted for rapid destruction by the proteosome (figure 1.5) [56, 61].

### 1.3.3 APC role in the Wnt pathway

The main role of APC in the Wnt pathway is negatively controlling its activity via ensuring efficient shuttling as well as loading and unloading of Beta catenin on to the destruction complex [56, 62]. To perform this task, APC has a series (seven) of 15-20 amino acid repeats through which it interacts with Beta catenin [63] and three Axin binding motifs which are interspersed among these amino acid repeats [56].

Beta catenin plays a second role in the simple epithelia as an element of adherens junctions, where APC may also have a role. Beta catenin has binding sites on both APC and E cadherin. E cadherin and Beta catenin interaction is regulated by the phosphorylation of the latter and this phosphorylation only occurs when a complex with the homodimer of APC protein has previously been formed [39]. Moreover, APC contributes to the ordered migration of intestinal cells inside the crypt where Beta catenin has a crucial role [64].

It has been suggested that newly synthesised Beta catenin first saturates the adherens pool and it never becomes available for signalling. Excess cytoplasmic Beta catenin is then efficiently degraded by the APC complex, which means that the second highly unstable pool is regulated by Wnt signalling [56]. It has also been suggested that APC, independent of its role in the cytoplasmic destruction complex, acts on chromatin to facilitate CtBP (transcriptional co-repressor) mediated repression of Wnt target gene transcription in normal but not CRC cells [65].

### 1.3.4 Biological role of Wnt pathway

Loss of one or more components of the Wnt signalling cascade causes dramatic phenotypic changes that vary with different tissues and organs. One important role of the Wnt pathway is its involvement in the maintenance or activation of stem cells [66]. Wnt signals may activate transcriptional programmes, promote cell proliferation and tissue expansion and may control cell cycle as well as fate and terminal differentiation of post mitotic cells [67, 68]. However, the consequences of Wnt pathway activation differ according to the developmental identity of the induced cell rather than the content of the signal [69].

### 1.3.5 Wnt signalling in self-renewing tissues

In addition to developmental processes, Wnt signalling in adult mammals is an essential lifelong tool for self-renewal and maintenance of tissue integrity for many organs. This fact is closely related to several disease states [56].

#### Gastrointestinal tract

It has been demonstrated that Wnt signalling is essential to maintain the stem cell compartment of intestinal crypts [70]. It has been found that approximately six $Lgr5^{+}$ stem cells (crypt base columnar cells, CBC) are located at the bottom of the intestinal crypts; intermingled with Paneth cells in the small intestine and with goblet cells in the colon (figure 1.6) [71, 72]. Colonic epithelium almost constantly renews and it is replaced approximately every six days (2-3 days in human) [73]. In the mouse, around 300 cells are produced in each crypt every day [74]. This is balanced by the loss of cells at the surface by apoptosis and exfoliation. The epithelium forms a two dimensional layer that is in continuous upward movement except for the stem and Paneth cells which escape this flow. These stem cells cycle slowly and continuously producing rapidly proliferating "transit amplifying" cells, which have the capacity to differentiate to all other lineages. This gives them the ability to regenerate the epithelium after injury [66]. Moreover, it has been suggested that Wnt proteins are secreted by the crypt epithelial cells rather than the surrounding mesenchyme, giving the epithelium a self-renewal tool [75]. Committed progenitor cells stop cycling and start to differentiate upon reaching the top one third of the colorectal crypt or the crypt villus boundary in the small intestine. In adenomas, these events are deranged. Newly formed cells maintain their mitotic capacity and do not differentiate and their compartment expands to take up the whole crypt [14].

Also in the intestinal crypt, the Wnt signal gradient mediates the expression of a genetic programme to maintain progenitor cell proliferation [56]. The Wnt gradient also controls the expression of EphB/EphrinB sorting receptors and ligands. The resulting EphB/EphrinB counter gradients determine the crypt villus boundaries and the position of Paneth cells at the bottom of the crypt [76].

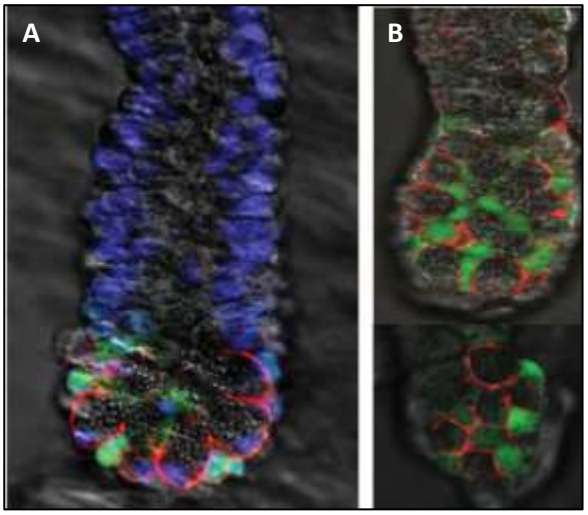


**Figure 1.6 Small intestinal (A) and colonic (B) stem cells. Adapted from [77]. $CD24^+$ staining (red) shows paneth cells (A) and colonic cells (B) while Lgr5-$GFP^+$ stained cells (green) are stem cells. Counter stain: DAPI (4', 6-diamidino-2-phenylindole) (blue). Reprinted by permission from Macmillan Publishers Ltd: Nature. Paneth cells constitute the niche for Lgr5 stem cells in intestinal crypts. Copyright (2011).**

Generally, current evidence suggests that the Wnt pathway is the main force controlling cell fate along the crypt villus axis. For instance in *Tcf4*$^{-/-}$ (transcription factor 4) neonatal mice, the entire crypt progenitor compartment is absent while the villus is unaffected [70].

### 1.3.6 APC and Wnt signalling in intestinal cancer

In many tissues in which the Wnt signalling cascade controls stem cells, cancer develops upon abnormal activation of the Wnt pathway [66]. This indicates the importance of stem cell regulators in cancer [66]. In FAP, following the loss of APC, the large burden of adenomas eventually leads to the development of adenocarcinoma through clonal evolution, which is evident from the accumulation of mutations in additional critical genes such as *K-Ras*, *p53* and *Smad4* [66]. Mutational inactivation of APC leads to an abnormal stabilisation of Beta catenin which seems to play a critical role in transforming epithelial cells. Moreover, increased nuclear

activity of Beta catenin is considered a hallmark of APC loss induced intestinal neoplasia [78]. This is supported by the observation that reporter plasmids containing concatemerized Tcf binding sites such as pTOPFLASH, normally transcribed only upon Wnt signalling, are inappropriately transcribed in APC mutant cancer cells through the action of constitutive Beta catenin–Tcf4 complexes [79]. Further in agreement with this central role of Wnt pathway in colon cancer, in rare instances where APC is not mutated, mutations that also cause inappropriate stabilisation of Beta catenin can be found such as mutations of axin2 or Beta catenin [79, 80].

Interestingly, it has been suggested that the Wnt pathway drives similar genetic programmes in both cancer and stem/progenitor cells [81]. Therefore, APC knockout adenoma cells can represent the transformed counterparts of the proliferative crypt progenitor cells; once the Wnt pathway is mutationally activated, adenoma cells can maintain their progenitor status indefinitely. This allows the adenoma to persist for many years providing a good environment for further mutations to occur. In further support of this, the *in vivo* model described by Sansom *et al.*, in which they conditionally deleted both *Apc* alleles in the adult murine intestine, showed expansion of the crypt progenitor compartment and induction of the Wnt target genes already described in cancer cell lines [44]. Colorectal cancer almost always initiates with an activating mutation in the Wnt pathway, a fact that can be attributed to the dependence of the intestinal progenitor/stem cells on this cascade [66].

It has also been suggested that *APC* mutations are not random and the position of the original mutation in FAP determines the nature and site of the somatic hit [63, 82]. Consistently, it has been reported that over 60% of somatic mutations occur within a mutation cluster region (MCR) between amino acids 1286-1513 [63]. Mostly these mutations lead to the production of a truncated APC protein with the removal of all aixin/conductin binding sites (SAMP repeats), often the Beta catenin inhibitory domain (CID) and most Beta catenin binding 20 amino acid repeats with a common end result of Beta catenin stabilisation. Therefore, one suggested mechanism for selectivity in the occurrence of the second hit, is the level of Beta catenin determined by the first hit [63].

Remarkably, activating mutations of the WNT signalling pathway are not restricted to cancer of the intestine, as loss of function mutations of Axin2 have been found in

hepatocellular carcinoma while oncogenic mutations of Beta catenin have been found in a wide range of solid tumours [83]. Moreover, it has recently been found that *CREPT* (cell cycle-related and expression elevated protein in tumor)/*RPRD1B* (regulation of nuclear pre-mRNA domaincontaining protein 1B) protein elevated in many tumours, regulates Wnt activity. It acts as a co-factor for Beta catenin-Tcf4, engancing the transcriptional activity of this complex particulary for cell growth-related genes such as c-Myc and Cyclin D1 [84].

### 1.4 Mouse models of colorectal cancer

Various mouse models have revealed many aspects about the development, progression and management of colorectal cancer [85]. There have been recent advances in the ability to produce cancer models in mice [86]. One of the important techniques described, involves the ability to manipulate specific genes in defined tissues at a known time, using the Cre loxP system [87].

#### 1.4.1 Apc mutant mice

The mouse homologue of human *APC* is located on murine chromosome 18 [52]. The sequences are 86% and 90% identical in terms of nucleotides and amino acids respectively [88]. The first mouse carrying a mutation in this gene was identified in a colony that was subjected to chemical mutagenesis to induce random mutations (phenotype based detection) and it was called the Min (multiple intestinal neoplasia) mouse as it developed up to thirty neoplasms in the small intestine [89]. The underlying germline mutation involved truncation at codon 850 of the *Apc* gene producing an autosomal dominant $Apc^{Min}$ allele [90]. This mouse has an average life span of 4-6 months after which it dies due to chronic anaemia and intestinal obstruction caused by tumour burden [88].

For further exploration of the role of *Apc* gene in tumourigenesis, several Apc truncation mutation models have subsequently been constructed. For example, $Apc^{\Delta 716}$, $Apc^{1638N}$ and $Apc^{\Delta 14}$ mice showed differences in the number of polyps developing in the small intestine but that were histologically indistinguishable [52]. Moreover, the impact of mutations in other genes has been studied in Apc mutant mice. Examples include; studying the effect of Cox enzymes in Apc mutant mice whose deletion caused great reduction in size and numbers of polyps. In addition, when *Cdx2* was deleted, numerous polyps developed in the distal colon, whereas *Apc*

mutation alone caused polyps to develop mainly in the small intestine [91]. Another example was the introduction of the *BubR1*$^{+/-}$ mutation in the *Apc*$^{Min/+}$ mice, which caused 10 times more polyps to develop in the colon than in small intestine [52].

The roles of many other genes and pathways have also been assessed in intestinal tumorigenesis using mice models such as the role of Beta catenin. One research group used Cre recombinase mediated deletion of exon three (phosphorylation site) of Beta catein in the murine intestine. The expression of the enzyme was put under control of calbindin and either cytokeratin 19 (k19) or fatty acid binding protein gene promoters. Expression of each of these proteins, lead to the deletion of exon three from Beta catenin and rendered it rsistaant to phosphorylation. With calbindin, few polyps developed while the other two proteins caused 700-3000 polyps to develop in the small intestine [92, 93]. This discovery supports the involvement of the Wnt signalling pathway in polyp formation and that it is initiated from the transit amplifying cells in the proliferative zone where K19 and fatty acid binding proteins are expressed significantly, but where only traces of calbindin are found [85]. Calbindin is only expressed by differentiated cells, mainly in the proximal small and large intestine (duodenum and caecum respectivley) [94].

### 1.4.2 MMR (mismatch repair) and Apc mutations

When MMR dysfunction related CRCs (positive for microsatellite instability, MSI) are examined in humans, most are also positive for APC mutations [85]. To further address this synergy, transgenic mouse lines have been constructed having both an Apc mutation (Min mice) and null mutations in different elements of the MMR system such as Msh2, Msh3, Msh6, Mlh1 and Pms2 [85]. These compound mutations caused tumours to develop almost exclusively in the intestine with incidence being related to the severity of MMR defects.

### 1.4.3 Cancer progression & metastasis models

The metastatic potential of a cancer determines its aggressiveness and most of the resulting mortalities. Therefore, mouse models have been constructed to investigate the underlining mechanisms responsible for tumour metastasis [85]. In mice, the Apc mutation alone has not been shown to cause a significant rate of progression of adenomatous polyps to invasive metastatic adenocarcinoma [85]. In the same context introducing the *Smad4* mutation into *Apc*$^{\Delta 716}$ mutant mice results in locally invasive

adenocarcinomas [95]. In addition, when *Tgfbr2* and *Apc*$^{1368N}$ mutations coexist, malignant transformation of the resulting adenomas is accelerated [96].

### 1.4.4 Chemically induced tumour formation

Chemical agents are frequently used to induce tumour formation in the intestine of mice. These agents can either act directly without the need for enzymatic catalysis or indirectly after being changed chemically with the aid of tissue enzymes and sometimes normal bacterial flora [97]. The end results are molecules that react with the DNA to inflict changes that may not be repairable. Thus, after several cell cycles, unrepaired DNA damage occurs and with the accumulation of further changes, neoplasia can ensue. Common agents used in this process include dimethyl hydrazine (DMH) and its metabolites azoxymethane (AOM) and methylazoxy methanol (MAM) [97].

### 1.4.5 Mouse models of inflammatory bowel disease and colorectal cancer

The most common mouse model that has been used to study IBD related CRC is the AOM/DSS (dextran sodium sulphate) model [98]. This model has shown that when mice are only subjected to DSS, prolonged exposures are needed to induce tumours, which have low multiplicity [99]. This suggests that other factors also contribute to neoplasia formation in IBD such as genetic background, changes in crypt cell metabolism, changes in bile salts circulation and even changes in bacterial microbiota (dysbiosis) [100]. Over the last decade, substantial evidence from both basic and clinical research has been obtained that gut microbiota can profoundly affect intestinal inflammation and tumour development. This is particulary true for certain members of the microbiota called the alpha bugs which possess unique virulence traits identified as direct drivers for carcinogensis [101]. For example, *E coli* colibactin (a genotoxin) has been shown to promote CRC development in experiemtal animals. Monoassociation of the adherent-invasive *E. coli* (AIEC) mouse strain NC101, which produces colibactin, enhanced colonic tumor development in azoxymethane (AOM)-treated interleukin-10- knockout (*Il-10−/−*) mice, a mouse model of colitis associated CRC [102]. Interstingly, gentic predisposition was also shown to be essential for colibactin to elicit its carcinogenic effects as observed in *Apc*$^{Min/+}$ mice (altered Apc signalling) versus wild type mice infected with colibactin producing *E. coli* 11G5 [103]. Moreover, it has also been

observed that tumour development in germ free $Apc^{Min/+}$ mice was halved as compared with that in mice housed under specific pathogen-free conditions [104].

### 1.4.6 Cre and loxP mouse strains

The Cre-lox system is an advanced transgenic mouse technology that can produce general knockouts, conditional knockouts and reporter strains. Moreover, insertion, inversion and translocation events can be carried out using this system [105, 106].

Although the Min mouse is a very useful model for studying human diseases, it is limited in its ability to show the early changes that follow *Apc* loss. Moreover, deletion of both *Apc* alleles is lethal *in utero*. For these reasons, researchers have developed a mouse model using the Cre-loxP system to have spatial and temporal control of *Apc* deletion in the small intestine of an adult mouse, the $AhCre^{+}Apc^{fl/fl}$ model [107].

A mouse strain carrying both *Cre* and flanked *Apc* genes within cells of interest was produced by crossing mice with a Cre recombinase transgene with mice carrying *Apc* alleles flanked with *loxP* sites [107]. In the latter, *loxP* sites were inserted into the introns around *Apc* exon 14, and the resultant mutant allele ($Apc^{580S}$) was introduced into the mouse germline [108]. In this system, the orientation of the *loxP* sites is critical for the fate of the intervening DNA sequence (target sequence) upon induction of Cre expression. If they are in same direction, the intervening DNA sequence will be deleted upon induction, otherwise it will only be inverted when the *loxP* sites are inverted [106].

To achieve deletion of *Apc* alleles in small intestinal stem cells, Cre expression was placed under control of the cyp1A1 (cytochrome P450 subfamily1 A1) promoter. By injecting beta naphthoflavone (BNF) into the peritoneal cavity of the mouse, expression of the recombinase enzyme was induced (by activating cyp1A1), which in turn recombined the genome at the *loxP* sites deleting the intervening *Apc* alleles in the intestinal stem cells with nearly 100% efficiency [107].

In the $AhCre^{+}Apc^{fl/fl}$ mouse model, intestinal epithelial changes were observed, including a rapid change in the histological appearance with gross distortion of the crypts (figure 1.7), immediate entrance of cells into S phase (DNA synthesis) of cell cycle and loss of differentiated cells including enteroendocrine cells and goblet cells

[44]. Interestingly, the increased number of cells which entered S phase did not correspond to an increase in mitotic figures, but to increased apoptosis and loss of control over nuclear volume. Among other acute changes following *Apc* loss were aberrant migration along the crypt villus axis and disturbed Paneth cells positioning [107]. Most of these changes can be seen in figure 1.8 below.

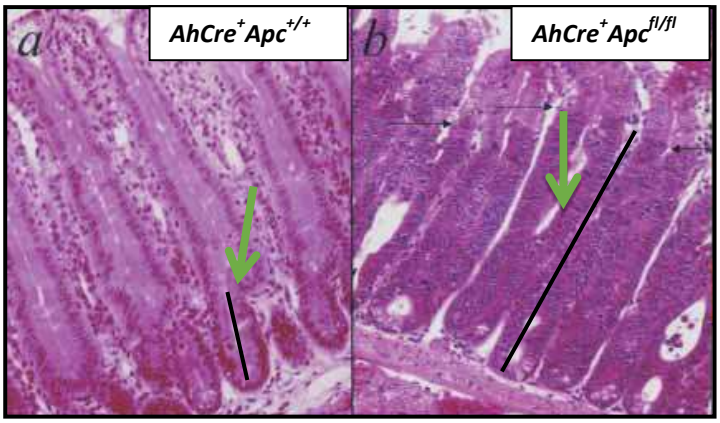


**Figure 1.7 shows control crypt-villus architecture (left) and distorted crypt villus architecture in *AhCre*$^{+}$*Apc*$^{fl/fl}$ mouse (right). The black lines show crypt length in the tissue samples (modified image). Adapted from [44].**

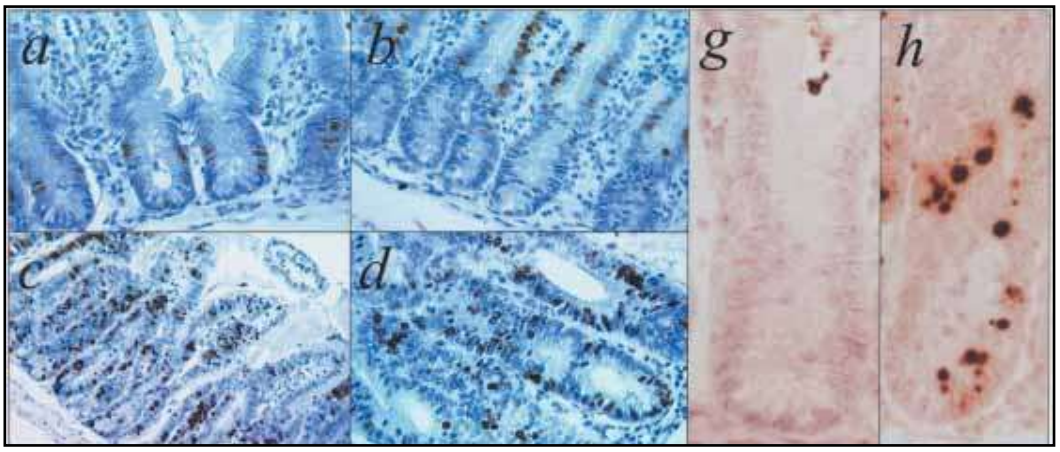


**Figure 1.8 small intestinal sections. Images a, b and g are from the control (*AhCre*$^{+}$*Apc*$^{+/+}$) while c, d and h are from *AhCre*$^{+}$*Apc*$^{fl/fl}$ mouse. a and c are BrdU incorporation of 2 hours duration while b and d are BrdU incorporation for 24 hours where a and b show normal proliferation and migration of cells and c and d show increased proliferation and aberrant migration (evident from presence of new, stained cells all over the crypt) respectively. h shows increased apoptosis compared to g which is the normal pattern as depicted by active caspase3 staining [44]. Reprinted by permission from Cold Spring Harbor Laboratory Press: *Genes and development*. Loss of Apc in vivo immediately perturbs Wnt signaling, differentiation, and migration.Copyright (2004).**

Since the proto-oncogene *c-Myc* has been described as a Wnt target gene in colon cancer cell lines, in normal crypts *in vivo* and in intestinal epithelial cells in the $AhCre^{+}Apc^{fl/fl}$ mouse (constitutively active Wnt pathway) model and because the significance of this was unclear, researchers have simultaneously deleted both Apc and c-Myc in the adult murine small intestine [44, 109, 110]. C-Myc deletion alone had little effect on intestinal epithelial cell proliferation and apoptosis over a five-day time course. However, in the double knockout model ($Apc^{fl/fl}$ $Myc^{fl/fl}$) almost all the phenotypic changes (shown in figures 1.7 and 1.8) associated with *Apc* deletion were rescued [110]. Interestingly, nuclear activity of Beta catenin remained high indicating the critical role of c-Myc in mediating the effects of Apc loss. Moreover, persistent Wnt activity allowed the examination of a number of genes that were shown to be Wnt dependent in the literature. These included 58 genes which were upregulated following *Apc* deletion. Deletion of *c-Myc* blocked the upregulation of 62% of these genes in the double mutant mouse. Furthermore, the few unaffected genes were shown not to be sufficient to mediate the changes induced by *Apc* deletion [110].

## 1.5. Biomarkers and CRC screening

### 1.5.1 Current CRC screening modalities

As described above, CRC is a major health problem that justifies the use of mass screening. Since CRC develops slowly from removable precancerous lesions; therefore, detection of these lesions at an early stage by regular health check-ups can potentially reduce CRC incidence and mortality [111]. Therefore, screening programmes have already been adopted by several countries [112].

So far colonoscopy is the gold standard for diagnosing CRC; however, it is not generally accepted as a screening tool in many countries because of its invasiveness, cost and low compliance [1]. Moreover, evidence for the effectiveness of screening colonoscopy is limited. There are few randomised trials in average risk individuals and few observational studies which have evaluated the effects of screening colonoscopy, in comparison to unscreened controls, on CRC incidence or mortality [113, 114].

By looking at published literature, one can find two different opinions about the efficacy and safety of flexible sigmoidoscopy (FS) as a screening tool for CRC. One suggests that FS is only recommended for individual groups and not mass screening. Flexible sigmoidoscopy has been reported to be as effective as colonoscopy in subjects less than 60 years however, there is a low compliance rate that has been reported to be as low as 15-30% of eligible individuals to undergo regular FS [115]. Although it has been reported that FS reduced CRC incidence by 70% in some series, prospective randomised controlled trials are missing to support this [115]. Moreover, one review from the Cochrane library that involved a meta-analysis of nine randomised controlled trials on more than 300,000 subjects and more than 400,000 controls (FS vs. no screening, FOBT vs. no screening and FS vs. FOBT), demonstrated no clear benefits of FS over FOBT in reducing mortality from CRC. Moreover, the authors reported the need for more studies to better outline the risks associated with FS [116]. The second opinion is more positive; a trial that involved 14 UK centres and 113,195 people for the control group (not offered endoscopy) and 57,237 people for the intervention group. Of the latter group, 71% underwent FS and participants were followed up for a mean duration of 11.2 years. It was reported that incidence of CRC was reduced by 23% in the intervention group and mortality by

31% (33% vs 43% after correction for self-selection bias). Moreover, incidence of distal cancers (rectum and sigmoid colon) was reduced by 50%. Therefore, the conclusion was; "FS is a safe and practical test and when offered once between ages 55 and 64 years, confers a substantial and long lasting benefit" [117].

Computed tomographic colonography (CTC) is another minimally invasive test that can be used for CRC screening. However, it also has limitations such as not being widely available, is costly, and has a false positive rate of 15%. Moreover, those with suspected lesions have to undergo colonoscopy and this has been reported to yield no more than 2% clinical benefit. Furthermore, although its sensitivity for invasive cancer is comparable to that of conventional colonoscopy, the sensitivity is inversely related to the size of lesions in less advanced disease. For example it has been shown to have a sensitivity of 85-93% and specificity of 97% for lesions larger than 1 cm and a sensitivity of 70-86% and specificity of 86-93% for lesions measuring 6-9 mm [115].

DNA testing and molecular screening are becoming an important part of routine patient care [118]. Moreover, it is predicted that whole genome sequencing may replace the practice of only screening at risk individuals for target genes, as this can provide access to vital information that might not be directly related to CRC.

The detection of abnormal DNA in stool from tumour cells shed into the lumen is expected to improve over time with improvements in the panel of mutant DNA being examined and the increase in clinical studies. Faecal DNA testing involves the identification of non-disintegrated human DNA (L-DNA) and mutations of specific genes known to be involved in colorectal carcinogenesis such as *APC*, *KRAS* and *p53* [111, 119]. This DNA comes from tumour cells shed into the colonic lumen. When detected the individual needs to undergo further confirmatory and localisation tests [120]. Very few faecal DNA tests have yet made their way into commercial use [121]. This is because of a lack of quality studies that can demonstrate the diagnostic accuracy of these tests. The existing few studies on the performance of faecal DNA tests demonstrated a sensitivity of 25-50% for cancer detection [122]. At present fecal DNA tests are not widely used and are reserved for those individuals who are not suitable or are unwilling to be screened by other modalities [115]. Other obstacles facing the wide implementation of faecal DNA testing are lack of

standardisation of faecal DNA panels for better sensitivity and specificity, unclear ease of use and acceptability by patients, lack of standard stool collection protocols, no defined intervals for screening individuals, and higher cost than faecal immunochemical testing (FIT) and faecal occult blood testing (FOBT) [118].

FOBT is the most widely available test for CRC screening. This is due to its non-invasiveness, cost-effectiveness and ease of use. It has currently been adopted by several countries as an annual or biyearly examination for average risk individuals. Moreover, it is the only test where several randomised trials have shown its effectiveness in reducing incidence and mortality from CRC by 33% and 15-20% respectively [112, 115, 123]. This is primarily due to early detection of cancers and/or detection and removal of adenomas [124]. However, despite the development of more sensitive tests such as the immunochemical FOBT (iFOBT), the sensitivity of this test is still suboptimal. Immunochemical FOBT has been reported to have a sensitivity of 47-69% and a specificity of 88-97%. Guaiac based FOBTs have even lower sensitivity (37%) and specificity (86%) [115, 125] . Since many adenomas do not bleed, the sensitivity of FOBT is even lower for these lesions (about 10%) [111]. In addition, individuals with false positive tests will unnecessarily go through the discomfort, cost and risks of colonoscopy. Compliance issues and low referral rates further reduce the yields even after positive tests. Moreover, FOBT is ineffective if the patient undergoes one test and does not return for repeat testing or does not undergo colonoscopy after a positive test [115]. These facts are better understood by looking at the outcome of the CRC screening programme in England. Guaiac based FOBT kits are sent every two years to people between the ages of 60-75 years. It has been reported that out of 1000 participants who receive the kit, 20 will have a positive test. Sixteen will undergo colonoscopy: 8 will have nothing abnormal, 6 will have polyps and 2 will have cancer [2].

Despite their low cost and non-invasiveness, sub-optimal sensitivity as well as the low compliance rate with FOBTs, is still preventing satisfactory results in places which have adopted these tests for mass screening [126, 127]. Strong evidence supporting these conclusions comes from the report of the English Bowel Cancer Screening Evaluation Committee. They showed that out of 2.1 million people (60-69 years old) invited to undergo gFOBT between 2006 and 2008, only around 50% returned the test. Moreover, the results agree with what has already been

demonstrated in the initial European studies regarding the sensitivity and specificity of the test. Furthermore, the percentage of cancers that were found in the right colon was lower than expected [128].

Therefore, there is still an urgent need for non- or minimally invasive, cost-effective and accurate tests to detect adenomatous polyps and early CRC. Thus, novel CRC biomarkers that will further enhance the detection of the disease and trigger follow-up colonoscopies when necessary should be developed [111].

### 1.5.2 Biomarkers of colorectal cancer

A biomarker is a characteristic that can be objectively measured and evaluated as an indicator of a physiological or pathological process or of a pharmacological response to a therapeutic intervention [129]. Any specific molecular change in the DNA, RNA, metabolism or proteins is called a molecular biomarker. The different purposes of biomarkers in clinical practice include assessment of disease predisposition, screening, staging and prediction of response to treatment. The criteria for the ideal biomarker include specificity (more true negatives), sensitivity (more true positives), easy access (in serum or urine for instance) and practicality (simple and inexpensive) [129].

Blood based tests are attractive due to their minimal invasiveness and widespread acceptance by patients [1]. Over the past decades, several attempts have been made to detect tumour markers for CRC in the blood; however, validation data from large studies are still not sufficient or the tests showed suboptimal performances [130].

Cancer pathology is complex and is determined by the interaction between cancer cells and epithelial and stromal cells, vasculature, and extracellular matrix in addition to the immune system. Elements of these interactions include cell surface antigens and receptors, secreted enzymes, cytokines and extracellular matrix molecules [131]. Such molecules can pass in to the blood stream supplying the tissue making them potential biomarkers. Therefore, tumour markers in the blood could indicate the release of proteins or nucleic acids by the tumour into the blood stream, the presence of tumour cells in the blood or the existence of a host generated response to tumour derived signals [1]. Interestingly mass spectrometry (MS) profiling has shown that a higher sensitivity and specificity can be obtained when biomarkers involving both cancer cells and reactive cells are analysed together and not separately. Therefore,

the main current direction in biomarker discovery is to seek panels of biomarkers rather than an ideal single cancer specific biomarker (more markers means more details and better judgement). Furthermore, despite decades of efforts, single biomarkers have not made their way into clinical practice for screening purposes, reflecting the complexity of the malignant micro-environment [129].

Many efforts have been focused on protein biomarker discovery over the last decade and the majority of recently discovered biomarkers are based on 2D gels coupled to MS/MS. This is because most of the information reflecting the range of genes that are involved in cancer resides in the proteome [132, 133]. Moreover, proteins are easier to detect, using antibodies for instance in readily accessible samples such as body fluids [8]. Unfortunately, so far, only a limited number of proteins associated with CRC have been validated in the serum for non-invasive testing of CRC [8]. This has been attributed to lack of follow up studies due to technological limitations [133].

Carcinoembryonic antigen (CEA) is a high molecular weight glycoprotein belonging to the immunoglobulin superfamily [111]. CEA is the best-known CRC serum biomarker in current use [8]. However, it is mainly useful to detect disease recurrence after surgery or metastasis, in particular to the liver [134]. It has not been accepted as a screening tool for the early stages of CRC, since less than 25% of patients at this stage have elevated CEA levels [135]. Moreover, advanced cancers may not produce CEA elevation, whereas non-cancerous conditions such as inflammatory conditions (inflammatory bowel disease, hepatitis, pancreatitis and obstructive pulmonary disease) may do so [111]. Furthermore, a study conducted in Birmingham by Shimwell (2010), concluded that currently suggested serum biomarkers for CRC are not useful neither individually nor as panels for the early detection of CRC due to suboptimal sensitivity and specificity [136].

Carbohydrate antigen (CA) 19-9, which is the second most investigated gastrointestinal tumour marker, as well as other members of this family have all been extensively studied and all showed sensitivity lower than that of CEA [137].

Tissue inhibitor of metalloproteinase type (TIMP)-1 is a multifunctional glycoprotein which inhibits most matrix metalloproteinases (MMPs) has been reported to be

mainly elevated in advanced CRC [111]. Studies that suggest use of this protein in the early stages of CRC are lacking.

A panel of five serum markers: spondin-2, tumor necrosis factor receptor superfamily member 6B (DcR3), TRAIL receptor 2 (TRAIL-R2), Reg IV and macrophage inhibitory cytokine 1 (MIC1), have been shown to be elevated in patients with CRC when compared to normal controls and patients with benign diseases in a study that involved 600 serum samples. According to these studies, this five-marker panel may perform better than CEA, a proposal that needs further investigation [111].

Nicotinamide N-methyltransferase (NNMT) and Proteasome Activator Complex Subunit 3 (PSME3) were evaluated in some initial studies involving matched human CRC samples and adjacent normal tissues. PSME3 demonstrated sensitivity similar to that of CEA while NNMT was superior to CEA [138]. Collapsin Response Mediator Protein-2 (CRMP-2) in one series (serum from 201 CRC patients vs. 210 healthy controls) showed a poorer specificity than CEA but superior sensitivity when used alone. The outcome was demonstrated to be better when both markers were interpreted together (77% sensitivity and 95% specificity) [139].

MicroRNAs have recently attracted major attention in the field of cancer research. They are involved in the post-transcriptional regulation of genes. Although not all miRNAs are functionally important, some of them regulate major physiological and pathological events [140]. For example, miRNA alterations have been reported in several cancers including CRC [141]. These are promising biomarkers and therapeutic targets, however they need to be further investigated.

In conclusion, the above biomarkers and those shown in table 1.2 still require, large scale clinical studies to refine and validate their diagnostic accuracy and suitability as biomarkers.

| Clinical use | Subjects | Types | Potential markers |
|---|---|---|---|
| In use | Stool | Protein | Fecal hemoglobin |
| | Serum | Protein | Carcino-embryonic antigen (CEA) |
| | | Carbohydrate | Cancer antigen 19.9 (CA19.9) |
| Clinical validation | Stool | DNA | *K-ras* |
| | | DNA | *APC* |
| | | DNA | Long (L)-DNA |
| | | DNA | *p53* |
| | Serum | Protein | Tissue inhibitor of metalloproteinases 1 (TIMP-1) |
| Preclinical development | Serum | Protein | Spondin-2, Decoy receptor 3, Trail-R2, Reg IV, MIC1 |
| | | Protein | Proteasome activator complex sub-unit 3 (PSME3) |
| | | Protein | Nicotinamide N-methyltransferase (NNMT) |
| | | Protein | Collapsin response mediator protein 2 (CRMP-2) |
| | | Protein | Macrophage migration inhibitory factor (MIF) |
| | | Protein | Macrophage colony stimulating factor (M-CSF) |
| | | Protein | Human neutrophiil peptide 1-3 |
| | | Protein | M2-pyruvate kinase |
| | | Protein | Prolcatin |
| | | Protein | Colon cancer specifc antigen 2, 3, 4 |
| | | Protein | Metalloproteinase 9, 7 |
| | | Protein | Laminin |
| | | Protein | SELDI (apolipoprotein C1, C3a-desArg, α1 antitrypsin, transferring |
| | Plasma | DNA | Septin 9 |
| | WBC | DNA | 5-gene panel (*CDA*, *BANK1*, *BCNP1*, *MS4A1*, *MGC20553* |

**Table 1.2 shows current and potential CRC biomarkers. Adapted modified from [111]. SELDI surface-enhanced laser desorption/ionisation, C3a complement 3a, Trail-R2 TNF (tumour necrosis factor) related apoptosis inducing receptor ligand-receptor 2, MIC1 macrophage inhibitory cytokine 1, Reg IV regenerating islet-derived family member 4, CDA cytidine deaminase, BANK1 B-cell scaffold protein with ankyrin repeats 1, BCNP1 B-Cell Novel Protein 1, MS4A1 membrane-spanning 4-domains, subfamily A, member 1.**

### 1.5.3 Importance of molecular sub-classification of CRC

The growing knowledge about the genetics and epigenetics of the syndromes predisposing to CRC and other cancers has helped to modify the natural history of these syndromes [118]. For example, many studies have shown that shifting the detection of the disease to an earlier stage via mass screening and intervening at early stages can reduce the risk of death from CRC [123].

The treatment for sporadic CRC is primarily surgical [142]. Polyps can be removed during colonoscopy, but larger polyps and early cancers need a surgical approach for cure. An example of the current challenges in the management of CRC is to define

the sub-group of Dukes' B CRC who can benefit from adjuvant chemotherapy like their Dukes' C counterparts. A panel of seven cancer-related genes associated with colon cancer recurrence (*Ki-67*, *c-MYC*, *MYBL2*, *FAP*, *BGN*, *INHBA*, and *GADD45B*) analysed from the tumour specimen via real-time RT-PCR has been validated as a tool to help predict stage II patients whose tumours behave like stage III disease [32, 143]. Another important example of biologically driven clinical decisions is the survival benefit of CRC patients with retained MMR over those with defective MMR when treated with 5 fluorouracil based adjuvant chemotherapy [144, 145]. In the same context, the use of epidermal growth factor receptor targeted therapy requires pre-knowledge of the mutational status of *KRAS* and *BRAF* genes, and phosphatidylinositol-4,5-bisphosphate 3-kinase (*PIK3CA*) mutation may determine the response of CRC patients to aspirin therapy for preventing recurrence [146].

## 1.6 Work leading up to this project

### 1.6.1 The *AhCre$^{+}$Apc$^{fl/fl}$* phenotype

Mutations in the Wnt pathway, particularly Apc, are regarded as the key drivers of sporadic CRC development. Our group have used murine intestinal samples from a novel transgenic mouse model with a conditional *Apc* gene deletion, *AhCre$^{+}$Apc$^{fl/fl}$* mouse [44] as part of our strategy to identify potential biomarkers and to study their roles.

The initial stage of this project involved a proteomic analysis of extracted murine small intestinal epithelial cells in which acute *Apc* deletion was induced *in vivo*. This was carried out to study the changes in the protein profile of these cells immediately following loss of Apc. This is important as it can shed light on the molecular basis of the early changes during colorectal tumourigeneis, and provide the opportunity for identifying potential biomarkers or therapeutic targets for CRC. This work yielded 81 proteins that demonstrated increased expression by at least 1.2 fold in the *AhCre$^{+}$Apc$^{fl/fl}$* mice compared to control *AhCre$^{+}$Apc$^{+/+}$* mice [147]. These were then subjected to Ingenuity pathway analysis (IPA) which further filtered down the candidate proteins to 13 proteins based on the possibility of their detection in the blood/serum. Nine of these proteins were further validated using independent techniques such as western blotting, ELISA and qRT-PCR in the same mouse model.

Moreover, 9 candidate proteins were also assessed for the relative mRNA expression in 15 human subjects (lesions vs. adjacent normal tissue). Four of the candidate proteins demonstrated statistically significant increases in CRC [147]. Furthermore, in separate unpublished work by a previous colleague (Dr. Fei Song) the remainder (5) of the candidate proteins also demonstrated significant mRNA upregulation in CRC compared to normal adjacent tissue.

The candidate proteins described above and that were assessed during the course of this project are:

- High-mobility group protein B1 (HMGB1)
- Nucleolin (NCL)
- Splicing factor, arginine/serine-rich 2 (SFRS2)
- Nucleosome assembly protein 1-like 1 (NAP1L1)
- Fatty acid binding protein6 (FABP6)
- Nucleophosmin (NPM)
- Ribosomal protein L6 (RPL6)
- DEAD box protein 5 (DDX5)
- Prohibitin (PHB)

### 1.7 Overview on the candidate protein biomarkers

Described below are some of the proteins, which have been proposed as candidate CRC biomarkers, based on the work of previous colleagues at the University of Liverpool. The proposal is that, their up-regulation shortly after APC loss is coincident with the early stages of CRC, making them candidate biomarkers for early colon cancer.

#### 1.7.1 Nucleosome Assembly protein1 like1 (NAP1L1)

The exact mechanisms by which NAP1 like proteins function are currently unknown. There are contradicting reports about the sub-cellular localisation of NAP1L1; it has been suggested that NAP1L1 is a nuclear protein in one report [148] and mainly cytoplasmic in another report [149]. In terms of function, NAP1L1 has been suggested to mediate nucleosome formation and disassembly through transporting and depositing histones onto chromatin. Nucleosome assembly is crucial for maintaining genome integrity [149]. In one study that involved 15 CRC patients,

*NAP1L1* mRNA was shown to be overexpressed by 2-9 fold in the tumours compared to normal adjacent tissue in seven patients [150]. Moreover, NAP1L1 has been demonstrated to be overexpressed in foetal liver compared to adult liver and in hepatoblastoma compared to non-diseased liver [151].

### 1.7.2 DEAD Box 5 (DDX5) or p68

DDX5 or P68 is a DEAD box RNA helicase and it is described as a transcriptional co-activator for a number of highly regulated transcription factors such as oestrogen receptor alpha and the tumour suppressor p53 [152]. This family of proteins is involved in RNA processing and export as well as ribosome assembly and translation [152]. In some contexts, DDX5 can also act as a promoter dependent transcriptional repressor [153]. In cancer, the above cellular processes in which DDX5 is involved are commonly deregulated [154]. The role of DDX5 can be context dependent, as it has been reported that DDX5 has pro-proliferative and even oncogenic properties as well as anti-proliferative and tumour co-suppressor roles [154]. DDX5 is also involved in developmental processes such as organ differentiation and maturation. DDX5 has been shown to be over expressed in prostate and in breast cancers where its expression is associated with high-grade tumours and poor prognosis [154]. DDX5 is also over expressed in colonic adenomas and cancers, where it is post-translationally modified [155].

### 1.7.3 Nucleophosmin (NPM)

Nucleophosmin is a ubiquitously expressed multifunctional nucleolar phosphoprotein [156]. It is localised mainly to the nucleolus, but it shuttles in and out of the nucleolus and between the nucleus and cytoplasm [157, 158]. It belongs to the nucleophosmin family of chaperone proteins, which are involved in other cellular processes such as centrosome duplication, ribosome biogenesis and environmental stress responses. It is also involved in the regulation of tumour suppressor proteins such as p53 and $p14^{ARF}$. In addition, NPM has been suggested to play role in maintaining genomic stability [159]. NPM is strongly implicated in cancer pathogenesis, although its role in oncogenesis is not clearly understood. Pathologically NPM is mutated in a number of haematological disorders and it is the most frequently mutated gene in acute myeloid leukaemia (AML). In the latter condition, it has been reported that mutations (35% of patients) of the *NPM* gene causes cytoplasmic displacement of the protein [159].

High levels of NPM could be found in tumour cells due to their rapid proliferation as the amount of NPM rapidly rises in G1 phase of mitosis [160]. However, some studies involving cell lines and mice have suggested a tumour suppressor role for this protein [161].

### 1.7.4 Ribosomal protein like 6 (RPL6)

Ribosomal proteins have extra-ribosomal functions in addition to protein synthesis [162]. RPL6 is located in the cytoplasm of cells. It is a ribosomal protein and a component of the 60s subunit belonging to the L6E family of ribosomal proteins. Increasing data have suggested that dysregulation of RPs occurs during tumourigenesis; for example, RPL19 is over expressed in breast cancer, while RPL7 and RPL37 are increased in prostate cancer. However, their exact role in this process needs further investigation [163]. Consistently, some studies have shown that RPL6 up-regulation may protect cancer cells against multiple chemotherapeutic drugs [164]. In the same context, it has been shown that RPL6 overexpression may correlate with tumour differentiation, promote G1 to S phase transition and up regulate cyclin E (Cyclin E is one of the major players in cell cycle progression from G1 phase to S phase, and its deregulation has been reported in many types of malignant tumours) expression. Conversely, down-regulating RPL6 inhibited cell proliferation, cell cycle progression and cyclin E expression in cancer cells [164]. Additionally, it has been reported that c-Myc's role in murine tumours such as osteosarcomas and lymphomas and in human lymphomas is linked to ribosomal proteins in such a way that its ability to initiate and maintain tumorigenesisis is dependent on its ability to induce the expression of RP genes [165].

### 1.7.5 Fatty Acid Binding Protein 6 (FABP6)

Fatty acid binding proteins are a family of small highly conserved cytoplasmic proteins that bind long chain fatty acids and other hydrophobic ligands. FABP6 and FABP1 (the liver fatty acid binding protein) are able to bind bile acids. The role of these proteins may include uptake, transport and metabolism of fatty acids. They are located in the cytoplasm within cells [166].

FABP6 is a cancer related protein that acts as an intra-cellular transporter of bile acid in the ileal epithelium. Due to the possible role of bile acids in colorectal carcinogenesis especially secondary ones, FABPs may be possible contributing

elements in this process. FABP6 expression has also been correlated with certain clinico-pathological characteristics of CRC. For example, high FABP6 expression was noted in smaller tumours, tumours located in the left colon, and tumours with less serosal invasion (early stages). In addition, a dramatic reduction in FABP6 expression was found in tumours with lymph node metastasis, suggesting that it plays a role in early carcinogenesis [166].

### 1.7.6 Nucleolin (NCL)

Nucleolin is a well-known major non-ribosomal protein consisting of 710 amino acids and which is located in the nucleolus. It is a ubiquitous phospho-protein that plays a role in the regulation of ribosomal biogenesis and maturation. In addition, it controls the transcription of ribosomal DNA (rDNA), pre-ribosome packaging and organisation of nucleolar chromatin [167].

Nucleolin is found at several locations in cells: in the nucleolus, it controls many aspects of DNA and RNA metabolism, in the cytoplasm, it shuttles proteins into the nucleus and provides a post-transcriptional regulation of strategic mRNAs and on the cell surface it serves as an attachment protein for several ligands such as midkine, lactoferrin, endostatin and HIV particles. Furthermore, NCL levels are highly elevated in rapidly proliferating cells including cancer cell lines [167].

Surface NCL does not bind to all commercial antibodies, suggesting that a specific posttranslational modification in the conformation is gained during this re-localisation [167]. Moreover, surface and cytoplasmic NCL levels change independently of those in nucleus [168].

It has been suggested that NCL binds to c-Myc G-quadreplex structures regulating the transcription of c-Myc and overexpression of nucleolin can significantly inhibit c-Myc promoter-driven transcription [169].

### 1.7.7 Splicing factor, arginine/serine-rich 2 (SFRS2) or Serine/arginine rich splicing factor 2 (SRSF2) or SC35

SFRS2 belongs to the serine rich (SR) family of proteins, which are critical regulators of constitutive and alternative pre-mRNA splicing. The molecular functions of this protein include protein binding, RNA binding, nucleotide binding, transcription co-repressor activity and it is mainly located in the nucleus [170].

Studies have shown that alterations in splicing regulators are involved in the development of malignancy, since cancer cells often take advantage of this flexibility in protein synthesis to produce proteins that promote growth and survival. Examples include SFRS2, which is one of the genes that is up-regulated in primary and metastatic pancreatic cancer in which c-Myc is also overexpressed [171].

### 1.7.8 High mobility group box 1 (HMGB1)

HMGB1 acts as a chromatin binding protein that bends DNA and facilitates access to transcriptional protein assemblies on specific DNA targets [172]. In addition, it acts as an extra-cellular signalling molecule during inflammation, cell differentiation, cell migration and tumour metastasis. HMGB1 is implicated in disease states including sepsis, ischaemia re-perfusion, arthritis, meningitis, neuro-degeneration, aging and cancer. It is constitutively expressed in the nucleus of both normal and cancer cells. HMGB1 overexpression and/or aberrant location are associated with all main hallmarks of cancer [172]. Both the extracellular and intracellular/nuclear forms of HMGB1 are implicated in cancer development, progression and resistance to treatment. HMGB1 is found at increased levels in a number of solid tumours such as cancers of the colon, breast, pancreas, prostate, skin (melanoma) and others [173].

In colon cancer, HMGB1 overexpression is associated with reduced apoptosis, which is thought to be due increased expression of the anti-apoptotic molecule-IAP2 [174]. Also it has been found that HMGB1 is expressed in CRC regardless of tumour stage, but tumour invasiveness increases when HMGB1 and the receptor for advanced glycation end products (RAGE) are co-expressed [175].

### 1.7.9 Prohibitin (PHB)

PHB is a pleotropic protein, which has been shown to be involved in cellular proliferation, differentiation and apoptosis [176]. In the cell it localises to the inner membrane of the mitochondria, where it acts as a chaperone protein [177], but it is also found in the nucleus where it is involved in the negative regulation of transcription [178]. PHB has been shown to be upregulated in tumour cells compared with normal cells [179]. Moreover, recent studies have reported overexpression of PHB in different cancers such as liver, uterine and gastric cancers. In addition, it has been shown that PHB interacts with certain tumour suppressors to mediate apoptosis [180]. For example, in a Glutathione S-transferase (GST) pull-down assay, PHB was

shown to directly interact with p53, c-Myc and Bax in HaCaT (immortalised human epidermal ) cells [181]. Moreover, this PHB, c-Myc and p53 co-localisation was suggested as a mechanism to regulate apoptosis. However, despite the above observations, the functions and sub-cellular localisation of PHB still need to be better understood [181].

## 1.8 Hypothesis, aims and objectives

### 1.8.1 Hypothesis

**Proteins, which are upregulated at early time points following *Apc* deletion, are involved in intestinal tumourigenesis and represent potential CRC biomarkers**

### 1.8.2 Aims

The main purpose of the project is to identify a panel of clinically valid human biomarkers for improved diagnosis and treatment of CRC as well as to understand the role of these proteins in the carcinogenesis process.

- To verify intestinal overexpression of the candidate biomarker proteins in $AhCre^{+}Apc^{fl/fl}$ mice.
- To investigate the expression patterns of the same candidate biomarker proteins during colorectal tumourigenesis in $Apc^{Min/+}$ mice.
- To understand the molecular mechanisms and biological functions mediated by these candidate biomarker proteins.
- To investigate the expression of the candidate biomarker proteins in human CRC samples.

### 1.8.3 Objectives

- Optimise the immunohistochemistry (IHC) experimental conditions for each of the candidate proteins in $AhCre^{+}Apc^{fl/fl}$ mice.
- Investigate protein expression in established neoplastic lesions in $Apc^{Min/+}$ mice aged 1, 3 and 6 months using the optimised IHC conditions.
- Assess the abundance of the candidate biomarker proteins using western blots in the same mouse models that were used for IHC.
- Perform siRNA knockdown of selected candidate proteins in CRC cell lines to study their possible biological roles.
- Apply the optimised assays to human colorectal tumour samples to assess the expression of selected candidate proteins using IHC.

# Chapter two

## Materials and Methods

# 2. Methods

## 2.1 Tissue samples

### 2.1.1 Animal models

All animal handling procedures were carried out in line with the UK Home Office regulations. Animal breeding, drug injections and tissue collection were conducted under supervision of Dr Karen Reed (University of Cardiff, project license numbered 30/2737- awarded to Professor Alan Clarke). The experimental mice had access to food and water at all times. All *AhCre*$^{+}$*Apc*$^{fl/fl}$ mice used were of an outbred background and were genotyped to establish that they were carrying the correct alleles [44]. Ahcre-positive mice were intercrossed with mice carrying a LoxP flanked *Apc* allele: *Apc580s* [108] and the *Rosa26R* reporter allele. Progeny from this cross were intercrossed to derive an outbred colony, segregating for the C57BL6/J, 129/Ola, and C3H genomes at a ratio of 75%, 12.5%, and 12.5%, respectively [44]. *Apc*$^{Min/+}$ mice were maintained on an inbred C57BL/6J background [90]. *AhCreER*$^{T+}$*Apc*$^{fl/+}$*Pten*$^{fl/fl}$ mice were maintained on an outbred background. Control (*AhCreER*$^{T+}$*Apc*$^{fl/+}$*Pten*$^{+/+}$) mice were derived from the same colony as experimental mice but they were not always littermates [182]. Cre enzyme was induced using combined intraperitoneal injection of 80 mg/kg β-naphthoflavone and tamoxifen (Sigma), dissolved together in corn oil, for four consecutive days [183].

### 2.1.2 Clinical samples

Samples were collected by Mr Paul Sutton, Countess of Chester Hospital NHS Foundation Trust under REC number 12/NW/001 IRAS reference: 88870. Patients were recruited from a population presenting to secondary care with abdominal/bowel symptoms warranting endoscopic evaluation and those attending for colon resection surgery in the above hospital. Tissues samples were assessed and colon cancer was diagnosed and staged by Dr Bushra Hamid, Consultant Pathologist, Pathology Department, Countess of Chester Hospital NHS Foundation Trust. Normal colon was established as not having colorectal carcinoma; high risk adenomas (greater than 1 cm, ≥3 adenomas and/or villous structure) or low risk adenomas (less than 1 cm, less than 3 adenomas and/or no villous structure) as confirmed by endoscopy. Normal colon samples were mainly from patients who had a range of other conditions including; IBD, haemorrhoids, diverticultis and nothing detectable. Fixed tissue samples were obtained from the Countess of Chester NHS Trust, under a material

transfer agreement, (samples were, fixed and embedded following standard NHS protocols).

## 2.2 Immunohistochemistry

### 2.2.1 Tissue preparation

Following sacrifice of the animals, the intestine was removed and flushed with PBS to remove the luminal contents. Sections of intestine (QF sections, figure 2.1) were fixed in formalin at 4 ºC for no more than 24 hours [44] then processed and embedded in paraffin wax. This work was also carried out in Cardiff. Epithelial cell extracts (ECEs) were harvested by centrifugation and pellets of total intestinal epithelaial samples were prepared (in Cardiff) [147]. We used these cells to assess relative expression of candidate biomarkers in the mouse models by western blotting. Small intestinal sections from the $AhCreER^{T+}Apc^{fl/+}Pten^{fl/fl}$ and colonic sections from six month old $Apc^{Min/+}$ mice were bundled using surigal tape and fixed overnight. Longitudinal whole colon sections were used from one and three month old $Apc^{Min/+}$ mice.

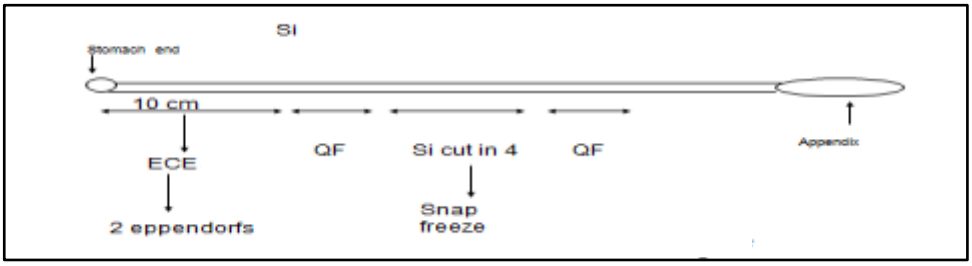


**Figure 2.1 shows how the small and large intestine of mice used in this project was processed. SI, ECE and QF stand for small intestine, epithelial cell extract and quick fix respectively.**

### 2.2.2 Immunohistochemistry methods and materials

Using a microtome, 4 µm sections were cut from the tissue blocks and put onto 3-aminopropyltriethoxysilane (APES, Sigma) coated or free glass slides which were then incubated overnight at 37°C to be used in immunohistochemistry or haematoxylin and eosin (H and E) staining experiments respectively.

#### Tissue de-waxing and rehydration

Tissue slides were immersed into xylene twice, each time for 5 minutes and 100% industrial methylated spirit (IMS) twice, each time for 3 minutes. At this point endogenous peroxidase activity was blocked using 3% $H_2O_2$-Methanol solution for

10 minutes. Then the slides were further rehydrated using 90% IMS for 2 minutes and 70% IMS for another 2 minutes. Sections were then immersed in distilled water (D/W) for 5 minutes while on an orbital shaker. Sections were then washed in Tris buffered saline/0.1%Tween twenty (TBST) twice on the orbital shaker, for 5 minutes each time.

**Antigen retrieval**

Heat induced antigen retrieval was performed by immersing the sections in pre-prepared citric buffer solution pH 6 and putting them into a domestic microwave at full power, 800 Watts for two 10 minutes sessions. Then sections were left to cool down for 10 minutes before washing them under running tap water for a further 10 minutes. Sections were again washed in TBST three times, for 5 minutes each while moving on the orbital shaker.

**Blocking**

To prevent background staining resulting from secondary antibody binding to other antigens in the tissue, 10% normal goat serum in TBST was applied to the tissue sections for 45 min at room temperature. At this stage, the tissue sections on the slides were demarcated using a liquid blocker pap pen (Sigma).

**Primary antibody incubation**

The sections were incubated overnight with predetermined primary antibody dilutions in a humid box at 4°C in a refrigerator. The blocking serum was first removed using a piece of tissue. The optimal primary antibody dilution was determined in a preceding experiment, the range of dilutions for each antibody and the optimal one used are shown in table 2.1 (below).

**Secondary antibody incubation**

Next day, the sections were washed in TBST twice, each time for 5 minutes. Then a biotinylated secondary antibody, goat anti-rabbit or goat anti-mouse polyclonal (according to the species in which the primary antibody was developed) was applied to the tissues and the slides were incubated in a humid box for 30 minutes at room temperature. The secondary antibody solution was diluted to 1:200 for all experiments in 5% normal goat serum in TBST.

**Stain development**

The sections were then washed in TBST solution two times, for 5 minutes each while moving them on the orbital shaker. Pre-prepared Vecta stain (details in table 2.2) was then applied bridging the secondary antibodies with peroxidase enzymes via avidin molecules. This was performed in the humid box for 30 minutes at room temperature. Then the sections were washed in TBST solution twice, for 5 minutes each time and the pre-prepared diaminobenzidine (DAB)-substrate solution (Sigma) was applied to the sections for 3-5 minutes again in the humid box and at room temperature to visualise the reaction.

**Haematoxylin counter staining**

The slides were then washed using de-ionized water to remove excess DAB and block further colouring. Then the slides were rinsed in TBST and for counter staining, Gills number 1 haematoxylin (Sigma) was used and slides were immersed in this solution for 3-5 minutes. Then the slides were placed under running slightly warm tap water for 5-10 minutes to deoxidize the haematoxylin (bluing).

**Dehydration and mounting**

The slides were then dehydrated by sequential immersion in 70% and then 90% IMS (dipping them at least 20 times). Then the slides were put in to 100% IMS twice for 2 minutes each time. Lastly, sections were immersed in xylene twice for 5 minutes each time. At this stage the slides were cover slipped and left in the fume hood to dry prior to visualisation under a light microscope.

### 2.2.3 Immunohistochemistry staining assessment

**$AhCre^{+}$ $Apc^{fl/fl}$ mice IHC assessment:**

For each primary antibody, a series of dilutions were assessed and at least 3 mice (from a cohort of 5-10 mice) were included in each experiment. Each slide examined, contained 3-6 small intestinal (SI) cross sections and each cross section had 20-30 crypt-villus structures (allowing significant repetition of staining patterns).

Sections were assessed visually under a light microscope (Leica, DM1000) and the optimal dilution was determined based on maximum staining contrast between the crypts and villi in $AhCre^{+}Apc^{fl/fl}$ mice compared to those in control mice. This comparison was based on information provided by other groups in published work

[44]. In addition, we used Beta catenin nuclear localisation as an indicator of *Apc* deletion and Wnt pathway activation. Following the detemintation of the optimal primary antibody dilution, one slide (as described above) per mouse (n3) was assessed fully and representative images were taken using a Leica laser capture micro-dissection microscope.

**$Apc^{Min/+}$ mice IHC assessment:**

Tissue blocks from these mice were initially assessed for presence of adenomatous lesions using H and E and Beta catenin staining (as described below). Using predetermined IHC conditions for the selected primary antibodies, tissues were then stained and maximum DAB colour contrast between the lesions and the surrounding as well as the wild type tissues was used as a criterion for differential expression. The mice numbers were as follow;

6 month old mice - sections were used from a cohort of 5-10 mice

3 month old mice - sections were used from a cohort of 5-10 mice

1 month old mice - sections were used from a cohort of 10-15 mice

Following full assessment of one or more lesions per section per mouse (n3), representitaive images were taken using a Leica laser capture micro-dissection microscope.

Tables 2.1 and 2.2 show details of the materials used in IHC;

| Primary Ab | Host & clonality | Tested dilutions | Optimal primary Ab dilution | Secondary Ab | Secondary Ab dilution | Blocking agent |
|---|---|---|---|---|---|---|
| HMGB1, abcam, ab18256 | Rabbit polyclonal | 1:100-10000 | 1:4000 in 10% GS in TBS | Goat anti-Rabbit, polyclonal, Dako | 1:200 in 5% GS in TBS | Normal Goat serum, Dako |
| HMGB1, MBL, M137-3 | Rabbit polyclonal | 1:50-1600 | 1:50 in 10% GS in TBS | Goat anti-Rabbit, polyclonal, Dako | 1:200 in 5% GS in TBS | Normal Goat serum, Dako |
| NCL, abcam, ab16940 | Rabbit polyclonal | 1:100-2000 | 1:500in 10% GS in TBS | Goat anti-Rabbit, polyclonal, Dako | 1:200 in 5% GS in TBS | Normal Goat serum, Dako |
| NCL, abcam, ab22758 | Rabbit polyclonal | 1:250-4000 | 1:4000 in 10% GS in TBS | Goat anti-Rabbit, polyclonal, Dako | 1:200 in 5% GS in TBS | Normal Goat serum, Dako |
| RPL6, Proteintech, 15387-1-AP | Rabbit polyclonal | 1:25-1600 | 1:200 in 10% GS in TBS | Goat anti-Rabbit, polyclonal, Dako | 1:200 in 5% GS in TBS | Normal Goat serum, Dako |
| RPL6, abcam, ab50907 | Rabbit polyclonal | 1:50-800 | 1:200 in 10% GS in TBS | Goat anti-Rabbit, polyclonal, Dako | 1:200 in 5% GS in TBS | Normal Goat serum, Dako |
| NAP1L1, Proteintech, 14898-1-AP | Rabbit polyclonal | 1:25-1600 | 1:100 in 10% GS in TBS | Goat anti-Rabbit, polyclonal, Dako | 1:200 in 5% GS in TBS | Normal Goat serum, Dako |
| NAP1L1, abcam, ab33076 | Rabbit polyclonal | 1:125-4000 | 1:4000 in 10% GS in TBS | Goat anti-Rabbit, polyclonal, Dako | 1:200 in 5% GS in TBS | Normal Goat serum, Dako |
| NPM, abcam, ab10530 | Mouse monoclonal | 1:250-8000 | 1:6000 in 10% GS in TBS | Goat anti-Mouse, polyclonal, Dako | 1:200 in 5% GS in TBS | Normal Goat serum, Dako |
| SFRS2, abcam, ab11826 | Mouse monoclonal | 1:125-2000 | 1:250 in 10% GS in TBS | Goat anti-Mouse, polyclonal, Dako | 1:200 in 5% GS in TBS | Normal Goat serum, Dako |
| SFRS2, Sigma, S2320 | Rabbit polyclonal | 1:100-1600 | 1:100 in 10% GS in TBS | Goat anti-Mouse, polyclonal, Dako | 1:200 in 5% GS in TBS | Normal Goat serum, Dako |
| FABP6, abcam, ab911841 | Rabbit polyclonal | 1:25-1600 | 1:50 in 10% GS in TBS | Goat anti-Rabbit, polyclonal, Dako | 1:200 in 5% GS in TBS | Normal Goat serum, Dako |
| DDX5, abcam, ab21696 | Rabbit polyclonal | 1:250-40000 | Not found | Goat anti-Rabbit, polyclonal, Dako | 1:200 in 5% GS in TBS | Normal Goat serum, Dako |
| Prohibitin, abcam, ab75771 | Rabbit monoclonal | 1:100-1600 | 1:200 in 10% GS in TBS | Goat anti-Rabbit, polyclonal, Dako | 1:200 in 5% GS in TBS | Normal Goat serum, Dako |
| Cyclin E, Santa cruz, Sc481 | Rabbit polyclonal | 1:25-1:800 | 1:600 in 10% GS in TBS | Goat anti-Rabbit, polyclonal, Dako | 1:200 in 5% GS in TBS | Normal Goat serum, Dako |
| CDC5L, Epitomics,, 5761-1 | Rabbit monoclonal | 1:125-1:10000 | 1:10000 in 10% GS in TBS | Goat anti-Rabbit, polyclonal, Dako | 1:200 in 5% GS in TBS | Normal Goat serum, Dako |
| Beta catenin, BD, 610154 | Mousse monoclonal | 1:50-1:800 | 1:50 in 10% GS in TBS | Goat anti-Mouse, polyclonal, Dako | 1:200 in 5% GS in TBS | Normal Goat serum, Dako |
| Lysozyme, Dako, EC3.2.1.17 | Rabbit polyclonal | 1:100-1:800 | 1:200in 10% GS in TBS | Goat anti-Rabbit, polyclonal, Dako | Normal Goat serum, Dako | Normal Goat serum, Dako |

**Table 2.1 shows the individual primary and secondary antibodies used in the IHC experiments with their supplier, origin, clonality and optimal dilutions. Ab = antibody, GS= goat serum.**

| Material | Composition | Remarks |
|---|---|---|
| Tris buffered saline (TBS) | NaCl (Sigma) 6.05g, Tris-base (Sigma) 8.76g | Completed to one litre by adding $dH_2O$ and pH adjusted to 7.5 by adding HCl |
| Citric acid buffer | Citric acid (Sigma) 1.92 g | Completed to one litre by adding $dH_2O$ and pH adjusted to 6 by adding HCl |
| 10% Goat serum (GS) | Normal GS (Dako) | To make up one ml; 100µl normal GS is added to 900 µl of TBS and allowed to stand at room temperature (RT) for 45 minutes |
| 5% GS | Normal GS (Dako) | To make up one ml; 50 µl normal GS is added to 950 µl of TBS and allowed to stand at RT for 45 minutes |
| Vectastain, (Vector labs) | Agents A and B | To 5 ml TBS 2 drops agent A and 2 drops of agent B were added and allowed to stand at RT for 30 minutes |
| DAB Tablet (Sigma fast) | 3,3-Diaminobenzidine | One tablet was added to 5 ml TBS and 5 µl hydrogen peroxide and kept in the dark until use (best within one hour) |
| Haematoxylin, (Sigma Aldrich) | Haematoxylin Solution, Gill No. 1 | Slides were immersed in undiluted solution for 3-5 minutes. Solution was returned to the container after use. |

**Table 2.2 shows the different solution compositions and methods of preparation**

### 2.3 Haematoxylin and Eosin staining methods

The pre-prepared tissue sections were processed by de-waxing and rehydration using xylene (x2, five minutes each), reducing concentrations of ethanol (100%, 95%, twice in each concentration and for 5 minutes each time) and lastly deionised water (x1 for 5 minutes) in the fume hood. Sections were then immersed in haematoxylin (3-5 minutes) and placed under running tap water (10 minutes) followed by eosin staining (2.5 minutes) and then a single dip in water. Sections were then dehydrated in increasing concentrations of ethanol (95% and 100%, twice in each concentration and for 15 seconds each time) followed by two immersions in xylene, for 5 minutes each. At this point slides were mounted and left in the fume hood to dry.

## 2.4 Tissue culture

### 2.4.1 Maintaining cell lines

HT29 (kindly provided by professor Barry Campbell, Henry welcome Labortory, University of Liverpool), HCT116 and HCT116 $p53^{(-/-)}$ ( kind gifit from professor B Vogelstein, The John Hopkins Medical Institutions, Baltimore, MD, USA) [184] human colon adenocarcinoma cell lines [185] were stored in the cell bank in liquid nitrogen by a previous colleague (Dr Ann McNamara, Henry Wellcome Laboratory, University of Liverpool). Cells were taken out in aliquots of 1-1.5 million cells in cryo-vials and partially thawed down in the water bath. Cells were then added to the relevant complete media, Dulbecco's Modified Eagle Medium (DMEM) for HT29 and McCoy's 5A modified for HCT116 cells. The growth media were supplemented with foetal calf serum (FCS) (Gibco) 10% (v/v), 0.4% (v/v) penicillin/streptomycin (Sigma) and 0.5% (v/v) L-glutamine (Sigma) to 2mM final concentration. Cells were grown as mono-layers in T75 flasks (Appleton Woods Ltd.). After 24 hours of incubation at 37°C and 5% CO2 (standard incubation conditions for all tissue culture work) the media was replaced to reduce toxicity from the freezing media. Cells were allowed to reach 80-90% confluence before sub-culturing. Two passages were allowed before the newly thawed cells were included in any experiment. Trypsin (50µg/ml, Sigma) was used for detaching cells during maintenance. Cells were maintained thereafter by sub-culturing at 80-90% confluence. Cells reaching high passage numbers (above 20) were discarded.

HT29 (APC is deleted at the carboxyl terminus at residue 1555) [186] and HCT116 (HCT116 cells have one allele of wild type Beta catenin and one allele of mutated Beta catenin that has a deletion at Ser-45 [187]) cells were used as induced WNT pathway models. HT29 and HCT116 cells have American type culture collection (ATCC) numbers of HTB-38 and CCL-247 respectively.

**Storage of cells**

Cells were stored as aliquots of 1-1.5 $x10^6$ cells per cryo-vial in the freezing media in the cell bank. The freezing media was made up of 10% dimethyl sulphoxide (DMSO, 50% w/w aqueous solution, Ben Venue laboratories, Inc.), 80% relevant complete media and 10% FCS.

### 2.5 Protein extraction

For the purpose of detection and quantification by different techniques, proteins were extracted from:

#### 2.5.1 Cell lines

Cells were allowed to grow to 60-70% confluence. The growth medium was then discarded and cells were washed with sterile PBS. Cells were detached from the flask by incubation with Trypsin (50 µg/ml., Sigma) for 5-10 minutes at 37°C. The action of Trypsin was then blocked by adding relevant complete media. Cells were collected by centrifugation at 1000 RPM (Sorvall Heraeues 3 S-R, rotor radius 145 mm) and 4°C for 5 minutes. The supernatant was discarded and cell pellets were re-suspended in one ml PBS, then transferred to 1.5 ml eppendorf tubes and centrifuged at 3000 RPM (microcentaur/Sanyo, rotor radius 50 mm) and 4°C for 5 minutes. The supernatant was again discarded and the cells were lysed by incubation with RIPA lysis buffer (50 mM Tris-HCl pH 8, 425 mM NaCl, 1% v/v Igepal CA 630, 0.5% v/v Deoxycholic Acid, 0.1% w/v SDS, 1 mM EDTA, 10 mM Sodium Fluoride and 0.5 mM sodium Orthovanadate in ultra-pure water) on ice for 40 minutes. Protease inhibitor (Calbiochem) (10 µl/ml RIPA buffer) and 2 Beta-Mercaptoethanol (0.7 µl/ml RIPA buffer) were added prior to use. Then the cells were centrifuged again at 13000 RPM (microcentaur/Sanyo, rotor radius 50 mm) and 4°C for 15-20 minutes. Proteins suspended in the supernatant were collected (at this stage samples were sometimes stored at -80°C for future work) for total protein estimation.

#### 2.5.2 Tissues

**Animal tissues**

Snap frozen small intestinal and colonic tissues from the mouse models were provided by our collaborators from the University of Cardiff and stored in our laboratory at -80ºC. A tissue sample or a piece of it was transferred into a 1.5 ml eppendorf tube and left to defrost on ice. Then RIPA lysis buffer was added and a homogenizer was used to disintegrate the tissue using short pulses to prevent unwanted heating of the sample. The tissue fragments were left on ice with the lysis buffer for 40 minutes. The sample was then centrifuged at 13000 RPM (microcentaur/Sanyo, rotor radius 50 mm) and 4°C for 15 minutes. The supernatant was collected and used for total protein estimation or stored in a -80°C freezer.

**An alternative method for protein extraction from tissues**

For smaller tissue samples, an alternative extraction method was needed. The tissue of interest was placed in a mortar with liquid nitrogen and left to freeze dry while the nitrogen evaporated. A pestle was then used to smash the tissues into a fine powder which was then collected in an eppendorf tube. RIPA lysis buffer was then added, and steps similar to those described above were followed to extract the proteins.

### 2.5.3 Total protein estimation

**Bradford assay**

This method involves the binding of Coomassie Brilliant Blue G-250 to amino acids. The binding of the dye to proteins causes a shift in the absorption spectrum of the dye from 465 to 595 nm, and it is the increase in absorption at 595 nm which is monitored. The Bradford assay is rapid, with the dye binding process being almost complete in approximately 2 minutes with good colour stability being maintained for 1 hour. Cations such as sodium or potassium and carbohydrates such as sucrose have little or no effect on the test. However, large amounts of detergents such as sodium dodecyl sulfate, Triton X-100, and commercial glassware detergents may significantly interfere with the results [188].

Extracted proteins were stored in lysis buffer at -80°C. A standard curve was made from a series of known concentrations of bovine serum albumin (BSA) solution (1mg BSA/1ml ddH2O); 0, 10, 20, 30, 40 and 50 µl in one ml of ddH2O. The protein sample being tested was made from 5 µl protein suspension (lysate) and 995 µl ddH2O. Then 200 µl of the Bradford reagent was added to each of the BSA and the protein samples and mixed thoroughly. To quantify the proteins in the samples 200 µl from each of the standard and the protein samples were loaded onto a 96 well plate and absorbance was read at 595 nm in a Tecan Sunrise micro-plate reader using XRead Plus v4.30 software. Once plotted against the standard curve, results from the protein samples represented the amount of total protein present in 5 µl of the original extracted protein sample. The standard curve showed optimum linearity between 10 and 40 µg BSA.

**Alternative method**

When RIPA buffer was used with high Igepal content (undiluted form), all protein samples displayed a dark blue colour resulting in falsely high protein content estimation by Bradford assay. Since these samples were from a successful siRNA transfection experiment, we decided to estimate the total protein in these samples using an alternative method that was not affected by the high Igepal content.

**Bicinchoninic acid (BCA) assay (Sigma, Catalog Numbers BCA1 AND B9643)**

The BCA assay is more sensitive than either Biuret or Lowry procedures. In addition, it has less variability than the Bradford assay (manufacturer's instructions, Sigma). Moreover, it is not affected by a range of interfering compounds including the various detergents that are sometimes used during protein extraction.

BCA is a Copper-based assay which comprises protein–copper chelation followed by secondary detection of reduced copper [189]. Proteins reduce alkaline Cu (II) to Cu (I) in a concentration dependent manner. Bicinchoninic acid is a highly specific chromogenic reagent for Cu (I) and forms a purple complex with an absorbance maximum at 562 nm (540-590 nm). The results can be interpreted by comparing them to known concentrations of a protein such as BSA.

**The BCA assay procedure:**

The working reagent (WR) was made by adding 50 parts of reagent A (a solution containing 1% w/v bicinchoninic acid, 2% w/v sodium carbonate, 0.16% w/v sodium tartrate and 0.95% w/v sodium bicarbonate in 0.1N NaOH, pH 11.25) to one part of reagent B (4% w/v $CuSO_4.5H_2O$) and mixing these well until a light green colour was seen. To get a linear concentration range, one part of each protein sample was added to 20 parts of the WR (standard assay) or one part of each protein sample was added to 8 parts WR (micro assay).

BCA micro assay (working concentration range 5-25 µg total protein):

A standard curve was made using BSA dilutions 0, 5, 10, 15, 20 and 25 µg in 25 µl $ddH_2O$. Protein samples were made by adding 5 µl of the extracted protein to 20µl of $ddH_2O$. Also two controls were prepared from 25 µl $ddH_2O$ (blank) and 5 µl of RIPA buffer in 20 µl of $ddH_2O$. Twenty five µl of each test tube were mixed with 200 µl working reagent in a 96 well plate (samples were loaded first to facilitate good mixing) and this was incubated at 37ºC for 30 minutes. The samples were then left to

cool down to room temperature and absorbance was read at 570 nm in a Tecan Sunrise micro-plate reader. The colour complex was stable for more than one hour at room temperature.

### 2.6 Western Blotting (WB)

In this thesis, WB was used to detect and/or quantify a certain protein in a total protein sample. It was also used to determine the specificities of various primary antibodies that were used in IHC, to compare levels of candidate biomarker proteins between models and their wild type counterparts, and to show the success and degree of knockdown of proteins after siRNA transfection experiments.

#### SDS-Polyacrylamide Gel Electrophoresis (SDS-PAGE)

After estimating the total protein content of a sample as described above, 20 µg proteins in 20 µl of RIPA lysis buffer were used per lane. Each sample was mixed with 5 µl sample buffer (2% SDS, 0.125 M Tris-base HCl pH 6.8, 0.001% w/v bromophenol blue, 10% v/v glycerol) and β-mercaptoethanol (one quarter volume of loading sample buffer), vortexed briefly and heated at 100°C for 2 minutes. The samples were centrifuged briefly before loading them onto the gel.

The denatured protein samples were separated by SDS-PAGE using MINI PROTEAN$^{TM}$ (BioRAD) gel casts. Ten percent gels were prepared by mixing 4.2 ml of dd$H_2O$, 3.3 ml polyacrylamide (30%, Sigma), 2.5 ml 1.5M Tris-base HCl pH 8.8, 100 µl of 10% w/v SDS, 50 µl of 10% w/v APS (ammonium persulphate) and 5 µl TEMED (Sigma). TEMED was added just before loading the mixture into the gel cassette. Saturated butanol (1:9 parts dd$H_2O$: butanol) was overlaid and the gel allowed to set for about 45 minutes. Butanol was washed off with water and any excess water was then removed using blotting paper. A 4% stacking gel (10 ml final volume) was made up of 6.6 ml dd$H_2O$, 1.3 ml 30% acrylamide (Sigma), 2.5 ml of 0.5M Tris-base HCl pH 6.8, 100 µl of 10% w/v SDS, 50 µl of 10% w/v APS (ammonium persulphate) and 10 µl TEMED (Sigma). The mixture was poured immediately over the resolving gel. A multiwell comb was inserted carefully and the gel was allowed to set for 20-30 minutes.

The comb was removed and the protein samples were carefully loaded into the wells, avoiding any loss or spillage into adjacent lanes. The proteins were first allowed to penetrate through the stacking gel by running at a low voltage (50 V) for 30 minutes

in running buffer (14.4 g glycine (Sigma), 3.03 g Tris-base (Sigma) and 10 ml 10% w/v SDS (Sigma) in one litre dd$H_2O$). Immediately thereafter the running voltage was increased to 100-150 V in order to separate the proteins according to their molecular weight.

**Western blotting:**

The separated proteins were transferred to a Protran® nitrocellulose membrane (Shneiller and Shneider) in a transfer buffer (14.4 g glycine (Sigma), 3.03 g Tris-base (Sigma) and 200 ml MeOH in one litre dd$H_2O$) using a 100 V current for one hour.

Successful transfer was tested by soaking the membranes in Ponceau S solution (5% w/v in glacial acetic acid, Sigma) for few minutes. The membranes were then washed with PBS.

For blocking non-specific antibody binding, the membranes were incubated in 1-5% non-fat dried milk in PBS/0.05% Tween 20 (or 1% w/v bovine serum albumin (Sigma) in PBS/0.05% Tween20) for 20-30 minutes with constant agitation on a roller. The membranes were then incubated with a primary antibody (at a dilution recommended by the manufacturer) (table 1) in the blocking solution for either 2 hours at room temperature or overnight at 4°C with constant agitation. The membranes were then washed three times, for 5 minutes each in 0.1% v/v Tween20 in PBS with constant agitation. Then they were incubated with the appropriate HRP-conjugated secondary antibody (Dako) at a dilution of 1:1000-1:3000 in the blocking solution for one hour at room temperature again with constant agitation. The membranes were then washed three times, for 5 minutes each with agitation.

For development, SuperSignal® West Dura Extended Duration Substrate (Pierce) was used. Then images were captured using a Bio-Rad ChemiDoc™XRS+System with Image Lab™software.

As a loading control, membranes were re-probed with 1:1000 mouse monoclonal anti-Pan actin antibody in the blocking solution for one hour at room temperature. Pan actin has a molecular weight of 42 kDa.

| Antibody | Company | Dilution, final | M.WT, kDa | Host | Reactivity |
|---|---|---|---|---|---|
| Nap1l1 | abcam | 1:1000 | 45-52 | Rabbit polyclonal | Hu. |
| Nap1l1 | Proteintech | 1:800 | 45-52 | Rabbit polyclonal | Hu., Ms. |
| RPL6 | Proteintech | 1:1000 | 34 | Rabbit polyclonal | Hu., Ms. |
| RPL6 | abcam | 1:400 | 33 | Rabbit polyclonal | Hu. |
| SFRS2 | abcam | 1:1000 | 35 | Mouse monoclonal | Hu., Ms. |
| SFRS2 | abcam | 1:2000 | 26-30 | Rabbit polyclonal | Hu. |
| CDC5L | Epitomics | 1:1000 | 100 | Rabbit monoclonal | Hu., Ms., Rat |
| PHB | abcam | 1:1000 | 30 | Rabbit monoclonal | Hu., Ms., Rat |
| Cyclin E | Santa cruiz | 1:500 | 53 | Rabbit polyclonal | Hu., Ms. |
| Beta catenin | BD | 1:1000 | 92 | Mouse monoclonal | Hu. |
| NCL | abcam | 1:1000 | 76 | Rabbit polyclonal | Human |
| FABP6 | abcam | 1:50 | 14 | Rabbit polyclonal | Ms., Rat |
| Pan actin | abcam | 1:1000 | 42 | Mouse monoclonal | Ms., Rat., Hu. |

**Table 2.3 Primary antibodies used in western blotting experiments. M.WT. = molecular weight, Hu= human, Ms= mouse, BD= Becton Dickinson.**

For most of the primary antibodies a range of dilutions was tested before adopting the optimal one. Moreover, with some antibodies such as those to SFRS2, RPL6, Beta catenin, Cyclin E and others many modifications to the protocols including varying the secondary antibody dilutions were tried to improve the results. Details of the specific modifications tried can be found in chapter three (section 3.5.2).

## 2.7 siRNA transfection

Discovered in 1998 by Fire *et al.*, RNA interference (RNAi) has now become an established way for inhibiting gene expression both *in vitro* and even *in vivo* [190]. Elbashir *et al.* described RNAi in mammalian cell lines [191]. RNAi involves double-stranded small interfering RNAs (siRNAs) approximately 21–23 nucleotides base pairs long that trigger a sequence-specific cleavage of primary transcripts leading to their subsequent degradation [192]. These siRNAs are generated intracellularly through the cleavage of longer double-stranded RNAs [193] or are introduced into the cell as chemically synthesized siRNA molecules [191]. However, the naked siRNA molecule, with negative charges, is susceptible to serum nucleases, renal clearance, and non-targeted bio-distribution, making cellular target sites more difficult to access [190]. These factors may render poor efficiency to RNAi due to short half-life and low stability [190]. Virus vectors are efficient delivery systems for nucleic acids; however, the potential for mutagenicity, limited loading capacities, high production costs, and most importantly, safety risks limit their uses [190]. Therefore, the need for alternative delivery methods led to the introduction of chemical modification of siRNA, nano-particles for delivering siRNA, liposomes, cell penetrating peptides, and targeted delivery [190].

### 2.7.1 Liposome siRNA delivery

Liposomes represent the most commonly used siRNA delivery method. The phospholipid bilayer of these particles enables them to fuse with a cellular membrane to deliver a drug [190]. siRNA can either attach to the lipid surface or be enclosed in a lipid core to pass through the cell membrane [194, 195]. Neutral liposomes tend to be less toxic to mammalian cells but are less efficient, whereas cataionic liposomes have good biocompatibility, but can cause significant toxicity such as cell contraction and mitotic inhibition [196].

It is worth highlighting that this method of gene knock down is limited by a number of factors that can affect the length of the time to reach peak silencing and the duration of silencing. These include the time cells take to double their numbers, the role of the target gene in regulating cell proliferation and the half-life of the target protein. For example cells that double within 24 hours may take 72 hours to show maximum silencing, but this can change with the above factors. Moreover, with certain cycles of doubling the pool of the siRNA in a cell will drop below the

effective threshold. Although generally resistant to degradation, siRNA degradation may also dilute their pool and reduce their efficiency.

### 2.7.2 Mechanism of silencing

The basic principle underlying RNA interference (RNAi) involves the disruption of mRNA by the use of homologous double stranded RNA (dsRNA) [197]. Small interfering RNAs are produced within cells from endogenous and exogenous longer ds-RNA molecules by the cleaving activity of Dicer, aribonuclease III-type protein [193, 198]. A dsRNA is cut by Dicer into short 19–21 duplexes with two symmetric nucleotide overhangs at the 3′ end and a 5′ phosphate along with a 3′ hydroxyl group that are known as siRNAs [197]. Alternatively, exogenous siRNAs may be delivered in to the cells (figure 2.2). The siRNAs are recognised by a nuclease-containing multiprotein complex known as the RNA-induced silencing complex (RISC). The helicase domain of RISC binds to one end of the duplex and unwinds the siRNA in an ATP-dependent manner. RISC is activated when the antisense strand (template, also complementary for the target mRNA) of the siRNA enters into the complex. The activated RISC guided by the antisense strand finds the target mRNA and induces cleavage of the mRNA within the target site with subsequent degradation of the whole mRNA molecule [192].

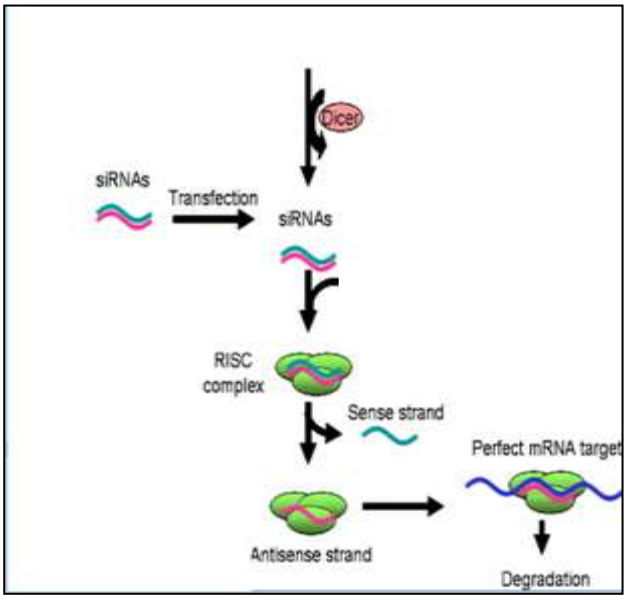


**Figure 2.2 Mechanism of siRNA mediated mRNA degradation, adapted from [199]. Reprinted by permission from Macmillan Publishers Ltd: Gynaecologic Oncology. The genesis of RNA interference, its potential clinical applications, and implications in gynecologic cancer. Copyright (2005).**

### 2.7.3 Transfection procedure

Specific and non-targeting (control) siRNAs, transfection reagents (TRs) and siRNA buffers were all purchased from Dharmacon, Inc. siRNA work was started based on recommendations made by the manufacturer for the cell lines used. The following table explains Dharamcon, Inc. volume recommendations for the plate format and the cells that we used:

| Plate format-well number | Surface area $cm^2$/well | Vol. of 5 µM siRNA (µl) | Serum free medium (µl) | Vol. of DharmaFECT reagent (µl) | Serum free medium (µl) | Complete medium (µl/well) | Total transfection medium |
|---|---|---|---|---|---|---|---|
| 6 | 10 | 10-50 | 150-190 | 4-10 | 190-196 | 1600 | 2000 |

**Table 2.4 The different materials used in each experiment and their volumes**

siRNAs were re-suspended according to the manufacturer's guidelines. siRNAs were stored in 20 µM aliquots, and upon transfection were diluted to 5 µM solutions. Optimised volumes (chapter four, section 4.2.1) of the transfection reagents (TRs) were used in the experiments conducted. Six well plates were used throughout the transfection work.

We used three types of media during this work. Both cell types needed the same categories of media (refer to section 2.4.1 for concentrations).

- Complete media (described for each cell line in cell culture section, 2.4.1) was used to maintain the cells before transfection.
- Antibiotic free media (cells become vulnerable to antibiotic toxicity during transfection due to increased cell permeabilisation) was used 24 hours before actual transfection. This media was also used to maintain untransfected cells used as controls during this work. Moreover, this media was also used to complete the transfection media to the required volumes.
- Serum free media was used to prepare and dilute the siRNAs before adding them to the antibiotic free media to make the final solutions.

The predetermined cell densities were allowed to attach for 24 hours in 2 ml antibiotic free media per well and these were incubated at 37ºC with $CO_2$ supply in a humid environment.

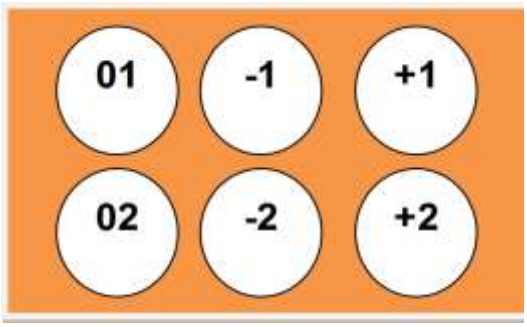


**Figure 2.3 Six well plate format in the siRNA work. 0 = untrasfected cells, - = cell transfected with non-targeting siRNA and + = cells transfected with a specific siRNA, 1 and 2 represent duplicate samples.**

At each time point per cell line, target proteins were knocked down using treatment groups set up as shown in figure 2.3. Samples were run in duplicates. Initially, cells were allowed to attach in the antibiotic free media. The next day, before taking the cells out of the incubator, the required volumes of transfection media were prepared based on the number of samples (wells) to be treated. Each well required 2 ml of the total transfection media that replaced the antibiotic free media. The constituents of the final transfection media are shown in table 2.4. The same steps were duplicated for the non-targeting siRNA throughout the process. Due to possible losses during pipetting, an extra 0.15% was added to the calculated volume of each reagent, hence the final volumes per experiment were calculated.

The transfection media was prepared in a sterile tissue culture hood. The predetermined siRNA volume was added to a volume of serum free media to make up 10% of the total transfection media and this was mixed thoroughly. This solution was left at room temperature for 5 minutes. At the same time, the predetermined volume of the TR was added to a volume of the serum free media to again make up 10% of the total transfection media and this too was mixed well and left at room temperature for 5 minutes. Then the siRNA media was added to the TR medium and this was mixed well by pipetting, before leaving it at room temperature in the tissue culture hood for 20 minutes. Finally, this mixture was made up to 2 ml/well with antibiotic free media.

At this point, the media for untransfected cells was replaced with 2 ml/well of fresh antibiotic free media to rule out lack of nutrients as an interfering factor when interpreting experimental results. The media for the cells to be transfected was replaced with 2 ml/well of the corresponding siRNA media. Finally cells were re-incubated at 37°C for the given duration of each time point.

### 2.7.4 Assessing siRNA knockdown efficiency

At the end of each time point floating and attached cells were counted and knockdown efficiency was assessed by western blotting and/or qRT-PCR (sections 2.6 and 2.8).

#### Cell counting

The media in each well was collected into labelled tubes. Since dead cells detach and float, the number of the floating cells in this media was used as an approximate indication of the amount of apoptosis [200]. Moreover, as the total number of cells was changing, the percentage of floating cells to total cells per well was used to represent these results.

After trypsinisation (400 µl/well), samples (50-100 µl) of attached cells were collected into labelled tubes. These were used as an approximate indication of the amount of cell proliferation per well. To ensure that significant numbers of cells were not left in the wells, 600 µl of media was added first and the cells were detached and separated from each other by thorough up and down pipetting. After collecting this, each well was washed with another 1 ml of media to collect any remaining cells.

#### Cell harvesting

At each time point, cells were trypsinised and collected as described above. Thereafter, the tubes were immediately put on ice. When cells from all wells had been collected, tubes (15 ml) were spun at 1000 RPM (Sorvall Heraeus, Multifuge 3 S-R, rotor radius 145 mm) for 5 minutes at 4ºC to pellet the cells. The cells were then re-suspended in one ml PBS and transferred to 1.5 ml eppendorf tubes and spun at 3000 RPM (microcentaur/Sanyo, rotor radius 50 mm) at 4ºC for 5 minutes. After discarding the supernatant, dry cell pellets were either stored at -80ºC for later use or were immediately used for protein extraction.

After estimating the total protein content of cells from each well, WB was used to estimate the relative expression of the appropriate target protein in each cell group.

### 2.8 Quantitative real time polymerase chain reaction (qRT-PCR)

RT-PCR was used as an alternative technique to assess knockdown efficiency for proteins that did not show conclusive results by WB.

After harvesting, cells were stored at -80ºC before being used for RNA extraction.

#### 2.8.1 RNA extraction

RNA extraction was carried out using RNeasy Mini Kit-QIAGEN. Since each sample contained less than 5 million cells, 350 µl of RTL (Guanidine Isothiocyanate) lysis buffer was added to disrupt cells and the suspension was pipetted up and down several times. Then a qia-shredder was used to homogenise the samples. Qiashredders were fitted to 2 ml collection tubes and centrifuged at full speed for 2 minutes. The volume of the samples was measured and an equal volume of 70% ethanol was added and mixed well by pipetting the solution up and down. Up to 700 µl of the samples were then used (including any precipitates) in an RNeasy mini column (RSC) placed in a 2 ml collection tube. The samples were then centrifuged at ≥10000 RPM (Hawk 15/05 microcentrifuge/rotor radius 75 mm was used throughout the extraction process) for 15 seconds. The flow through was discarded (if the sample size was more than 700 µl, this step was repeated using the same collection tube provided the flow through was discarded each time so as not to contaminate the RSC). 700 µl of buffer RW1 (guanidine salt and ethanol) were added to the RSC from the previous step and centrifuged at ≥10000 RPM for 15 seconds. Flow through was discarded and 500 µl of RPE washing buffer were added to the RSCs and spun at ≥10000 RPM for 15 seconds. Then 500 µl of RPE buffer were again added to each RSC and centrifuged at ≥10000 RPM for 2 minutes. Finally the RSC was placed in a new 1.5 ml collection tube and 30-50 µl RNase free water was added directly in to the spin column membrane and this was spun at ≥10000 RPM for one minute to elute RNA. The latter step was repeated if the RNA volume was expected to be more than 30 µg using RNase free water or the elute itself. A Nanodrop-spectrophotometer was used to quantify the eluted RNA.

### 2.8.2 1st strand cDNA synthesis (reverse transcription)

The main purpose of PCR in this project was to measure the relative expression of a target mRNA. Reverse transcription was used to synthesise a complementary DNA (cDNA) from the target mRNA because DNA is more stable than RNA.

The following table shows the reagents (Roche) for a single reaction of reverse transcription. The reagents that were prepared as a master mix are denoted with an *.

| **Reagents** | Vol/sample | Final conc. |
|---|---|---|
| 10x reaction buffer | 2 µl | 1x * |
| 25 mM $MgCl_2$ | 4 µl | 5 mM * |
| Deoxynucleotide mix | 2 µl | 1 mM * |
| Primer, oligo p(dT)15 | 2 µl | 0.75-1 µM * |
| RNase inhibitor | 1 µl | 50 units * |
| AMV RT | 0.8 µl | ≥20 units |
| Sterile water | 7.2 µl | |
| RNA sample | 1 µl | |
| Total | 20 µl | |

**Table 2.5 Recipe for a single reaction of reverse transcription. RNA amount used in each reaction was ≤ 1 µg. AMV RT = Avian Myeloblastosis Virus Reverse Transcriptase.**

When all components were added, the tube was briefly vortexed and centrifuged to collect the solution at the bottom of the tube. Then the reaction was first incubated at +25ºC (using a bench heating block) for 10 minutes then at +42ºC for 60 minutes (for cDNA synthesis). Then AMV RT was denatured by incubating the samples at 99 ºC for 5 minutes and then cooling them down at +4ºC (on ice) for another 5 minutes.

The synthesised cDNA was then stored at -15 to -25ºC for later use in qRT-PCR experiments. However, for shorter storage periods (1-2 hours) cDNA was stored at +2 to +8 ºC.

### 2.8.3 qRT-PCR

RT-PC was performed using LightCycler 480 (Roche, Burgess Hill, UK). A primer and probe technique was used. Probes were from the Universal Probe Library (Roche) and labled with fluorescein (FAM) at the 5'-end with a dark quencher dye near the 3'-end.

Each gene tested required a stock of left and right primers mix (Roche). The latter was made up of 20% left (20 µM), 20% right (20 µM) and 60% RNase free water. The number of samples per gene per experiment determined the total volume required. Each sample was run in triplicate. Each well in the plate was loaded with 20 µl of the reaction mixture. Each well contained 5 µl of the selected primer-probe mix (0.4 µl primers mix, 0.4 µl probe (10 µM) and 4.2 µl water). The remaining 15 µl in each well was made up of 10 µl 2x probe master (Roche), predetermined cDNA volume and water. Each run incorporated control wells, without cDNA (to rule out contamination) and without primers.

**Running PCR reactions**

Assays were designed and were run according to the conditions shown below in table 2.6.

| Cycle description | Temperature, $^{o}C$ | Duration, seconds | Cycles |
|---|---|---|---|
| Pre-incubation | 95 | 600 | 1 |
| Amplification | 95 | 10 | 45 |
| | 60 | 30 | |
| | 72 | 1 | |
| Cooling | 40 | 30 | 1 |

**Table 2.6 Conditions of qRT-PCR reactions**

### 2.9 Sulforhodamine B (SRB) assay

The SRB assay is a widely used cytotoxicity assay that involves the determination of cellular density based on the total protein content of cells. SRB is a bright pink aminoxanthene dye that binds basic amino acid residues under mild acidic conditions and dissociates under basic conditions [201].

Cell groups transfected with either a target siRNA or a control non-targeting siRNA along with non-transfected cells were incubated for 48 hours in 6 well plates (as described above). After 48 hours, cells were harvested by trypsinisation. Cells from the attached monolayer in each well were counted using a haemocytometer and then adjusted to 1000 cells/100 µl of complete media for each cell.

100 µl of cell suspension from each of the treatment categories above were loaded as 6 replicates into 96 well plates. The format was set as untransfected, non-targeting siRNA, and target siRNA in adjacent columns for each protein. Seven plates were used for each protein and cells were allowed to grow from 1 to 7 days. Each day, one plate was stained with the SRB dye. The media was discarded and cells were fixed at room temperature in 100 µl/well glacial acid-methanol solution (3:1 vol/vol) for 5 minutes. After discarding this fixative, the cells were gently washed with water and stained with 100 µl/well SRB dye (0.4% wt/vol in 1% glacial acid) at room temperature for 30 minutes. Then the wells were washed with 1% glacial acid at least three times with care being taken not to leave any excess dye on the walls of the wells. The plates were then left to dry overnight. Then the dye was re-suspended in 100 µl/well 10 mM Tris-HCl solution pH 10.5 and mixing was achieved using an orbital shaker for 10-15 minutes at high speed. Then the plate was loaded in to a Sunrise Tecan micro-plate reader and the optical density in each well was determined at 572 nm.

### 2.10 Clonogenic survival assay

The clonogenic survival assay is based on assessing the ability of an individual cell to survive by forming a colony under given experimental conditions. A colony is generally defined as cluster of 50 cells or more [202].

The same cells used in the SRB assay were also used for clonogenic survival assay. 1000 cell/well and 500 cells/well were used for HT29 and HCT116 cells respectively. Again cells transfected with the target siRNA or the two control groups

were seeded in 2 ml of the relevant complete media in 6 well plates and allowed to grow for 10 days in a $CO_2$ supplied and humid incubator at 37ºC. Then the cells were fixed in 4% formaldehyde for 5 minutes at room temperature. The fixative was then discarded and colonies were stained with 5% crystal violet for 5 minutes. The plates were gently washed under tap water and left to dry overnight before counting the visible colonies.

### 2.11 Fluorescence activated cell sorting (FACS) analysis

FACS involves staining single-cell suspensions prepared from cell culture or tissues with fluorochrome labelled antibodies. The stained cells are then analysed using a flow cytometer. A flow cytometer uses a small nozzle to produce a tiny stream of fluid. The stream takes individual cells past a laser. Part of the light will be detected as front scatter and some as side scatter to give representations of cell size and complexity (cytoplasmic granules, membrane size etc.) respectively. Further sub-classification of cells is possible using the fluorescence emitted from the fluorophores used to stain the cells as a result of excitation by the laser beam. A set of filters and mirrors (photo-multiplying tubes, PMTs) inside the cytometer will split the scattered light into defined wavelengths such that each sensor will detect fluorescence only at a specified wavelength. Examples of these sensors are the Fluorescein isothiocyanate (FITC) and Phycoerythrin (PE) channels which detect light at or near 519 and 575 nm respectively.

Among the issues encountered with this technique are dealing with intracellular antigens, secreted antigens and the overlap that happens between the fuorophores that have a close range of wavelengths in multi-colour analysis. Therefore, successful analysis will depend on the optimisation of experimental conditions through choosing the right dilutions for the antibodies, use of suitable controls to set up the flow cytometer properly, and optimised fixation and permeabilisation procedures [203].

Optimisation steps were performed with untreated HCT116 cells to determine the best acquisition settings for dual staining. This mainly included determining the compensation setting required to avoid overlap between channels with a close range of wavelengths. For example channel one bleeds into channel two and the latter bleeds into channels 1 and 3.

For each individual protein, the same optimised siRNA conditions were applied prior to harvesting the cells at a pre-defined time point (section 2.7). Cells were harvested as described in section 2.7.4.

**Fixation and permeabilisation**

Harvested cells (from untreated, scrambled siRNA and target siRNA groups) were first re-suspended in 1 ml PBS. Formaldehyde (Sigma, methanol free) was then added to a final concentration of 2-4%. Cells were then incubated for 10 minutes at 37ºC, followed by chilling on ice for one minute. The fixative was then removed after pelleting the cells by centrifugation. Then the cells were re-suspended and permeabilised by adding 90% methanol and incubating them on ice for 30 minutes. At this point, cells were used for staining or stored at -20ºC for later use.

**Caspase 8 and propidium iodide (PI) staining**

Approximately one million cell aliquots were used per sample. Two samples were included from each treatment group. Two to three mls of the incubation buffer (0.5 g BSA in 100 ml PBS) were added to each tube and cells were rinsed by centrifugation (repeated 2-3 times). Cells were then re-suspended in 100 µl incubation buffer and blocked for 10 minutes at room temperature. Primary (Cell Signalling-Asp391, anti-caspase 8, rabbit monoclonal IgG, # 9496) antibody was added to the tubes to make a dilution of 1:100 (recommended by the manufacturer) and cells were incubated for one hour at room temperature. After this step, cells were rinsed again in the incubation buffer 2-3 times. Then cells were re-suspended in 1:100 solution of the fluorochrome (FITC) conjugated secondary antibody (abcam, goat polyclonal to rabbit IgG, diluted in the incubation buffer) and incubated for 30 minutes at room temperature (in the dark). After rinsing in the incubation buffer 2-3 times, cells were re-suspended in 40 µl of a 100 µg/ml solution of Ribonuclease A (Sigma) in 10 mM Tris-HCl pH 7.5/15 mM NaCl (Sigma) and incubated for 15 minutes at room temperature. After this step, cells were counter stained with 500 µl of 500 µg/ml PI (Sigma) in PBS. Cells were stored at 4ºC for later analysis (cells could be analysed immediately or after overnight incubation protected from light). Prior to analysis, cells were filtered through 40 micron cell strainers (Falcon). Cells were then processed using a BD FACSCalibur cytometer and CellQuest software and the acquired data were analysed using the free version of "FCSexpress 4 flow research edition" software.

## 2.12 Immunocytochemistry

Cells were grown in 6 well plates following the same steps that were described above in section 2.7. The only difference was the addition of glass cover slip to the bottom of each well in the plate to allow the attachment of cells. The transfection procedure for each protein was the same as described in section 2.7.

At a defined time point (section 2.7), culture media was discarded and the cells were washed twice in PBS. Then the cells were fixed by adding 2% paraformaldehyde (Sigma) and incubated for 20-30 minutes at room temperature. Thereafter, the cells were washed in PBS three times and permeabilised with 0.2% Triton X-100 (Sigma) in PBS for 30 minutes at room temperature. Cells were again washed in PBS three times and blocked with 10% normal goat serum (Dako) in PBS for 45 minutes at room temperature. Cells were then incubated with a predetermined optimal dilution of the target primary antibody (diluted in 10% normal goat serum in PBS) for 1-2 hours at room temperature and in a humid box. Cells were washed twice in PBS by gentle shaking over an orbital shaker for 2-3 minutes each time. Then cells were incubated with the appropriate secondary antibody (Dako) in 5% normal goat serum in PBS for 30 minutes at room temperature. The cells were again washed in PBS as described above. Cells were then incubated with VECTASTAIN (Vector Laboratories, elite ABC kit) for 30 minutes at room temperature. The latter was prepared according the steps described in table 2.2. Again, cells were washed in PBS and then incubated with DAB (preparation details in table 2.2) for 5 minutes in the dark and at room temperature. Then DAB was blocked by the addition of distilled water. Cells were then counter stained using Gills number 1 haematoxylin (Sigma) for 3-5 minutes. The cells were then washed under gently running tap water for 5-7 minutes. Finally, the cover slips were mounted on glass slides using DPX mountant.

### 2.13 Statistical analysis

Most of the data (expressed as means ±SD unless otherwise stated) shown in this thesis were of the continuous numerical type and were divided into two groups with one dependent variable. Using Sigma plot software version 12, data were first checked for normality (by Shapiro-Wilk test) and equality of variance (using Levenes test). A two tailed t test was used for normally distributed data and a Mann Whitney U test was used for data that were not normally distributed or that had unequal variances. A p value of 0.05 was used as a threshold for statistical significance.

For data that were divided into more than two groups but with one dependent variable; one way analysis of variance was used for data which had a normal distribution and equal variances, otherwise the Kruskal-Wallis test was used to assess the significance of any difference between the groups. Dunnett's method was used to perform multiple comparisons with a control group.

In the various figures in this thesis asterisks represent p values as follows:

* p value of less than 0.05; ** p value of less than 0.01; *** p value of less than 0,001 and **** p value of less than 0.0001.

N stands for number of experiments performed while n indicates the number of replicate samples in each comparison group.

# Chapter three

# Validation of upregulation of candidate biomarker proteins in animal models of CRC

## 3. Validation of candidate biomarker proteins upregulation in animal models of CRC

### 3.1 Introduction and aims

If we accept the hypothesis that *APC* (adenomatous polyposis coli) gene mutation is an early key event in most cases (80%) of CRC [10] and that APC negatively regulates the activity of the WNT signalling pathway [204], then it would be rational to study the elements of the latter, when this relationship has been disturbed. This may provide a better understanding of mechanisms that are involved in colorectal carcinogenesis (the early stages in particular).

The WNT signalling pathway is a major regulator of intestinal homeostasis; proliferation, self-renewal, cell cycle and apoptosis [205, 206]. For example, it has been suggested that the WNT pathway is part of the niche involved in maintaining the stem cells and the proliferative compartment located at the base of the intestinal crypt [60]. Moreover, it is now widely accepted that the few signalling pathways (including the WNT pathway) that orchestrate key developmental processes can also be involved in the development of major pathologies such as cancer [207]. However, deregulation of WNT signalling has only been clearly documented to be involved in a small number of tumours. Since, WNT derangement is observed in a wide range of carcinogenesis processes, but without clear and specific associations, it is critical to investigate this connection between WNT signalling and neoplasia [68]. This critical role of the WNT pathway in the pathogenesis of different cancers and CRC in particular provides a good opportunity for identifying biomarkers or therapeutic targets that can improve the outcome of screening and treatment respectively.

As described in the introduction chapter, using iTRAQ/LC-MS, the following candidate proteins NAP1L1, RPL6, SFRS2, FABP6, PHB, NCL, NPM, HMGB1 and DDX5 were identified together with many other proteins that showed up regulation in the acute intestinal *Apc* deletion mouse model ($AhCre^{+}Apc^{fl/fl}$). Moreover, based on initial data from bioinformatics analysis carried out by our team, it has been suggested that the selected proteins are linked to cellular processes that are critical during tumourigensis such as cellular proliferation, cell cycle regulation and apoptosis. Furthermore, these candidate proteins have not been extensively studied in

the context of colorectal tumourigenesis. Therefore, there is a possibility that one or more of these could be potential biomarkers of CRC or even therapeutic targets.

In this chapter, using immunohistochemistry (IHC), the expression and localisation of the above proteins were assessed in *AhCre*$^{+}$*Apc*$^{fl/fl}$ and *Apc*$^{Min/+}$ mice. For the *Apc*$^{Min/+}$ mice 1, 3 and 6 month old mice were used to map possible changes in protein expression and correlate these with the histological progression of lesions during the average life span (6 months) of these mice by the end of which most of them develop numerous adenomas throughout the intestine (mainly the small intestine) [208].

**Aims**

- Confirmation of upregulation of the candidate proteins at early time points after *Apc* deletion in the intestine (*AhCre*$^{+}$*Apc*$^{fl/fl}$ mice).
- Investigation of the expression of the same candidate proteins in established intestinal neoplastic lesions in *Apc*$^{Min/+}$ mice aged 1, 3 and 6 months.

### 3.2 IHC validation of Wnt pathway activation in *AhCre*$^{+}$*Apc*$^{fl/fl}$ mice

Beta catenin, is a key player in mediating an induced Wnt signalling pathway [206]. Moreover, nuclear translocation of this pivotal molecule is regarded as a surrogate maker for activity of the Wnt signalling pathway [80]. Therefore, we used this latter observation to confirm and locate *Apc* deletion induced Wnt derangement in tissues from both mouse models.

As the whole small intestinal epithelium from the *AhCre*$^{+}$*Apc*$^{fl/fl}$ mouse was the source of the proteomic results, small intestinal sections from *AhCre*$^{+}$*Apc*$^{fl/fl}$ mice and their control counterparts were stained with anti-Beta catenin mouse monoclonal antibody (Becton Dickinson) to assess the state of the Wnt pathway. Several dilutions of the primary antibody were tested (1:25-1:800) of which 1:50 was thought to be optimal (shown below in figure 3.1). IHC protocols (described in methods section) were optimised in our laboratory. Moreover, the primary antibody was the same used by Sansom *et al*. [44] and our results (figure 3.1) were consistent with what they had previously described.

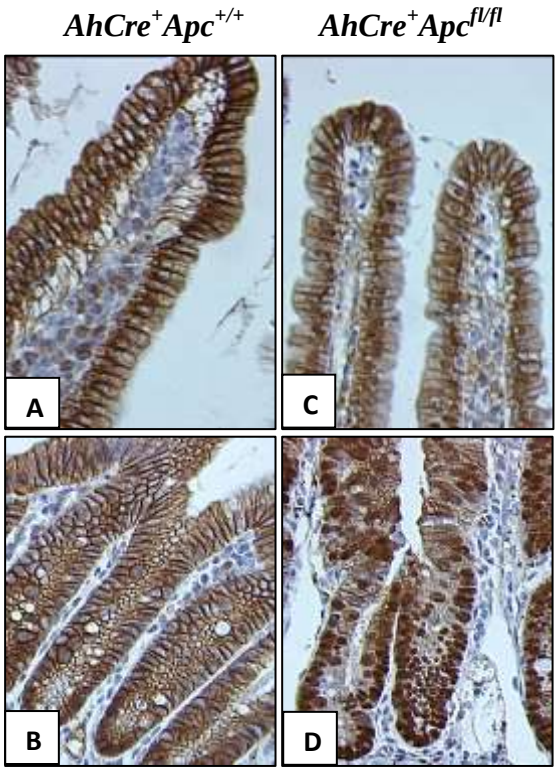


**Figure 3.1 Small intestinal sections stained for Beta catenin protein. A) & B) images are from *AhCre*$^{+}$*Apc*$^{+/+}$ mouse while C) and D) images show *AhCre*$^{+}$*Apc*$^{fl/fl}$ mouse tissue sections. All images are X40 objective (original magnification). Images in the upper panel are villi and those in the lower panel are crypts. N= 3-5 mice in each group.**

*AhCre*$^{+}$*Apc*$^{fl/fl}$ mice were sacrificed five days after the first Beta Naphthoflavone (BNF) injection. Within this period, only the small intestinal crypts were shown to exhibit constitutively active Wnt pathway (figure 3.1D), the hallmark of which is nuclear localisation of beta catenin [80].

### 3.3 Detection of "Apc loss" driven lesions in *Apc*$^{Min/+}$ mice

Unlike the *AhCre*$^{+}$*Apc*$^{fl/fl}$ mouse in which *Apc* deletion is present in nearly all epithelial cells across the small intestine, *Apc*$^{Min/+}$ mice develop scattered neoplastic lesions throughout the intestine. Therefore, it was not practical to stain random sections from tissue blocks as there was a high chance of not cutting through any neoplasm, and this would have been a waste of time and resources. Moreover, although intestinal segments with polyps were fixed and then paraffinised in labelled blocks, it was still not possible to identify lesions within an individual block without cutting through and staining it. Even after identifying lesions, the possible number of lesion positive sections was random, especially in younger animals.

To identify lesions in a cost effective way, Haematoxylin and Eosin (H and E) staining was therefore used initially. However, it was found that H and E was not very useful (as described below). Beta catenin staining (described below) was then used for this purpose based on observations from other separate experiments.

**Haematoxylin and Eosin (H and E) staining in *Apc*$^{Min/+}$ mice**

In initial studies, we assessed tissue sections from *Apc*$^{Min/+}$ mice for the presence of neoplastic lesions with H&E staining. Serial sections with lesions were then used in IHC experiments.

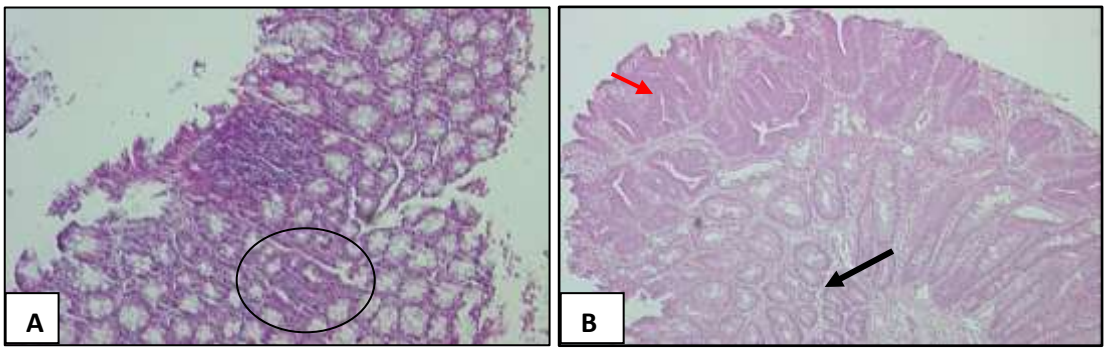


**Figure 3.2 H and E staining of colonic tissue sections from 3 month old (A) and 6 month old (B) *Apc*$^{Min/+}$ mice. A) Shows abnormal crypts (encircled) while B) shows a polyp, exophytic with a stalk and hyperplastic crypts. The red arrow points to the dysplastic part and the black arrow to the normal part. Both images are x10 magnification.**

The abnormal crypts in the 3 month old *Apc*$^{Min/+}$ mouse (A) showed the same changes as the polyp tissue in image (B). The dysplastic areas generally showed an increase in the number of cells, loss of goblet cells and larger nuclei compared to the normal adjacent tissue. Unfortunately, H and E was not as useful especially in younger mice because there were fewer lesions which were small and difficult to recognise due to similar colour patterns to normal tissue.

**Beta catenin staining in *Apc*$^{Min/+}$ mice**

As described above, H and E staining was not very convenient for detecting small lesions especially in 1 and 3 month old *Apc*$^{Min/+}$ mice. On the other hand, we observed that even in a single abnormal cell, Beta catenin staining demonstrated obvious colour contrast (due to dramatic early changes in expression after Apc dysfunction) compared to normal surrounding cells. Therefore, Beta catenin staining was used to identify possible small neoplastic lesions in younger mice.

Below (figure 3.3) are examples of neoplastic lesions in the three age groups of *Apc*$^{Min/+}$ mice detected using Beta catenin staining.

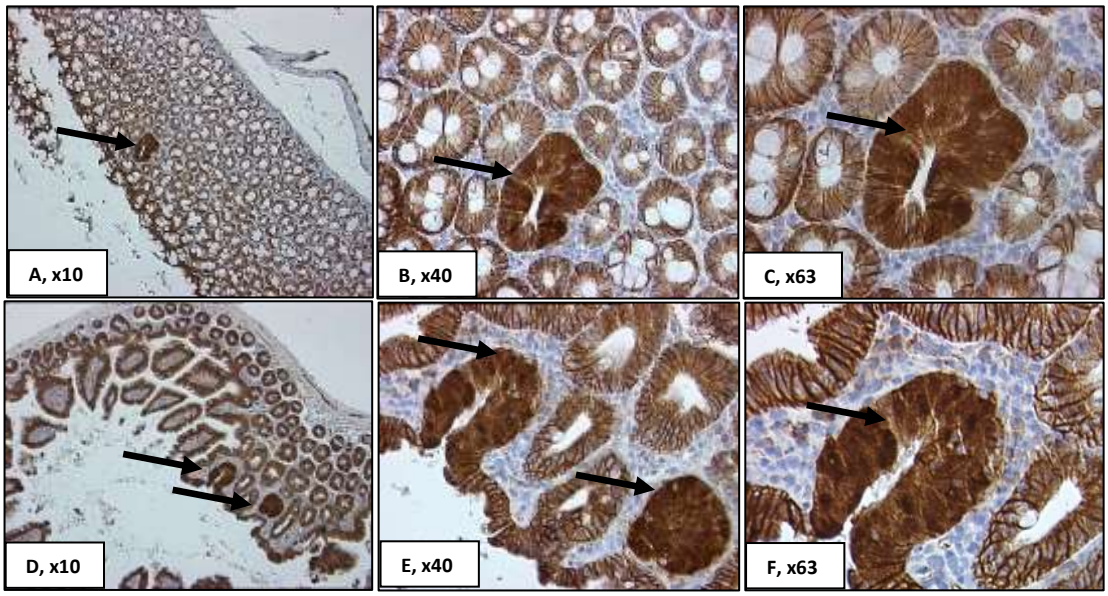


**Figure 3.3 Intestinal sections stained with anti-Beta catenin mouse monoclonal antibody (1:50). A), B) and C) images show colonic sections from a one month old *Apc*$^{Min/+}$ mouse. D), E) and F) images show small intestinal sections from a three month old *Apc*$^{Min/+}$ mouse. Arrows point to neoplastic lesions where cellular Beta catenin expression is increased compared to normal surrounding tissue. Magnification used to capture the images is indicated with the labels.**

In one and three month old mice, lesions showed increased cellular expression of Beta catenin with more intensity in the nuclei, suggesting increased nuclear localisation of this protein. The latter observation was even more prominent with the advancement of tumourigeneis and the development of more advanced adenomas in six month old mice as shown below in figure 3.4.

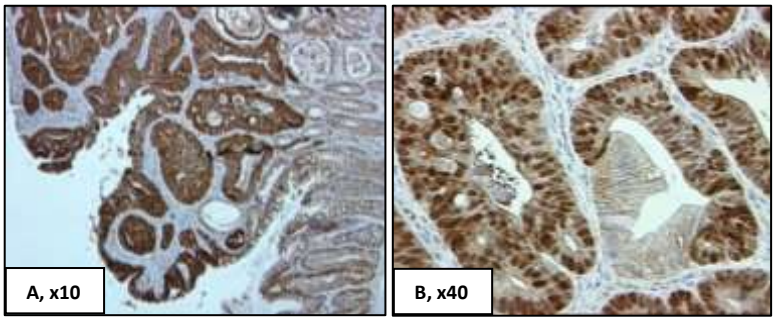


**Figure 3.4 Colonic polyp from a six month old *Apc*$^{Min/+}$ mouse stained with Beta catenin (same conditions described for figure 3.1). A) is x10 and B) is x40 magnification.**

### 3.4 Work overview

The following section describes the assessment of nine proteins (NAP1L1, RPL6, SFRS2, FABP6, PHB, NCL, HMGB1, NPM and DDX5) in the *AhCre*$^{+}$*Apc*$^{fl/fl}$ mouse model five days after *Apc* deletion and in a time course in *Apc*$^{Min/+}$ mice (1, 3 and 6 month old animals). As the lesions in *Apc*$^{Min/+}$ mice included here are thought to be Apc mutation driven, we tried to analyse changes in expression of the candidate proteins in correlation with the histological progression of lesions over a six month period. All experiments were carried out according to the protocols described in the methods section. Samples were from cohorts of 5-10 mice each. In each IHC experiment at least three target and three age matched control mice were included. In *Apc*$^{Min/+}$ mice, the blocks that had lesions were mainly from the colon. Although non-intentional, working on murine colonic lesions may provide a pathophysiologic environment that is closer to that associated with human CRC. All images included in this chapter are representative and the number of sections examined and the mice used are described in the methods chapter, section 2.2.3.

#### 3.4.1 IHC assessment of NAP1L1 expression

NAP1L1 is one of the candidate proteins that showed upregulation shortly after *Apc* deletion in the proteomics studies performed in the *AhCre*$^{+}$*Apc*$^{fl/fl}$ mice. There are contradicting reports in the literature about the subcellular localisation of NAP1L1: it has been reported that NAP1L1 is mainly located in the cytoplasm by one paper and in the nucleus by another [148, 149]. NAP1L1 is linked to nucleosome assembly (chaperoning), chromatin modulation and cell proliferation [149]. Below are images showing IHC assessment of this protein in *AhCre*$^{+}$*Apc*$^{fl/fl}$ and *Apc*$^{Min/+}$ mice. The primary antibody was commercially available (Proteintech) and was tested using different dilutions (1:25-1:1600). We found a dilution of 1:100 to be optimal as it produced observable differential staining (figure 3.5).

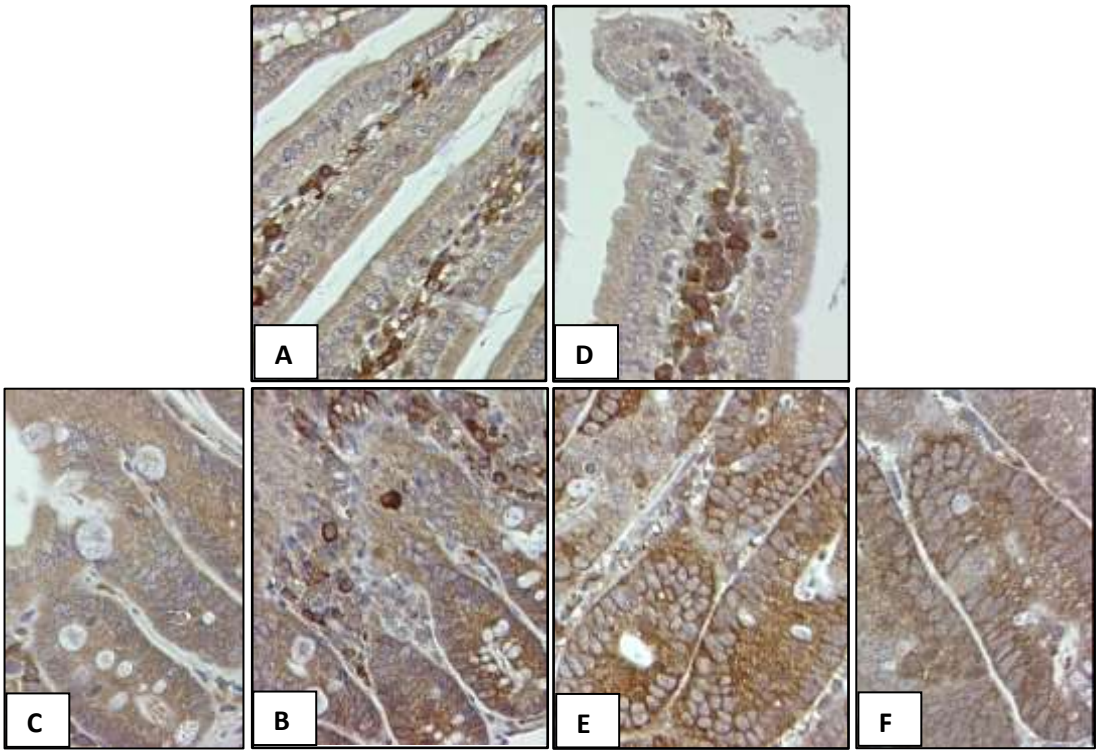


**Figure 3.5 Small intestinal tissues from a control mouse (A, B and C) an *AhCre*$^{+}$*Apc*$^{fl/fl}$ mouse (D, E and F) stained with anti-NAP1L1 rabbit polyclonal antibody at a dilution of 1:100 and the secondary antibody was from Dako, used at a dilution of 1:200. A), B), D) & E) are X40 (original magnification) while C) & F) are X63 (original magnification). Images A and D are villi while the rest are images of small intestinal crypts.**

There was increased staining intensity in the cytoplasm of the crypt cells in the *AhCre*$^{+}$*Apc*$^{fl/fl}$ mouse, compared to the villi of the same mouse and also compared to both crypts and villi of the control mouse.

### IHC assessment of NAP1L1 expression in *Apc*$^{Min/+}$ mice

The same experimental conditions used to assess the expression of NAP1L1 in *AhCre*$^{+}$*Apc*$^{fl/fl}$ mice were then applied to intestinal tissue samples from *Apc*$^{Min/+}$ mice aged 1, 3 and 6 months and their wild type control counterparts.

**One month old *Apc*$^{Min/+}$ mice**

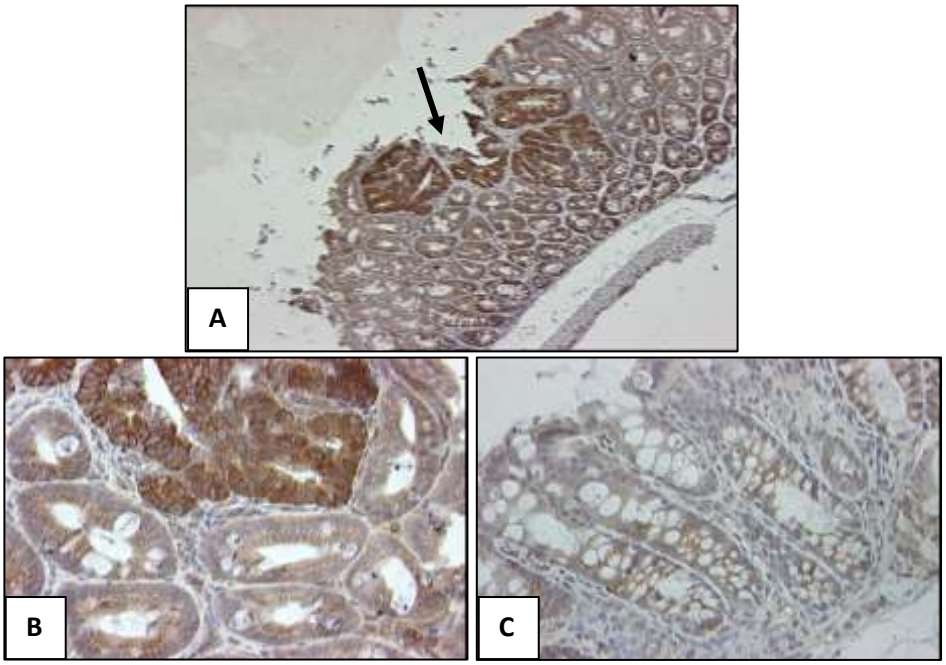


**Figure 3.6 Colonic sections from 1 month old *Apc*$^{Min/+}$ (A and B) and *Apc*$^{+/+}$ (C) mice stained with anti-NAP1L1 antibody. A) Shows a dysplastic lesion (arrow) X10, B) shows the same dysplastic lesion (X40) and C) shows wild type tissue (X40).**

The dysplastic lesion showed an obvious increase in brown staining in the cytoplasm when compared to the surrounding histologically normal mucosa or wild type tissue.

**Three month old *Apc*$^{Min/+}$ mice**

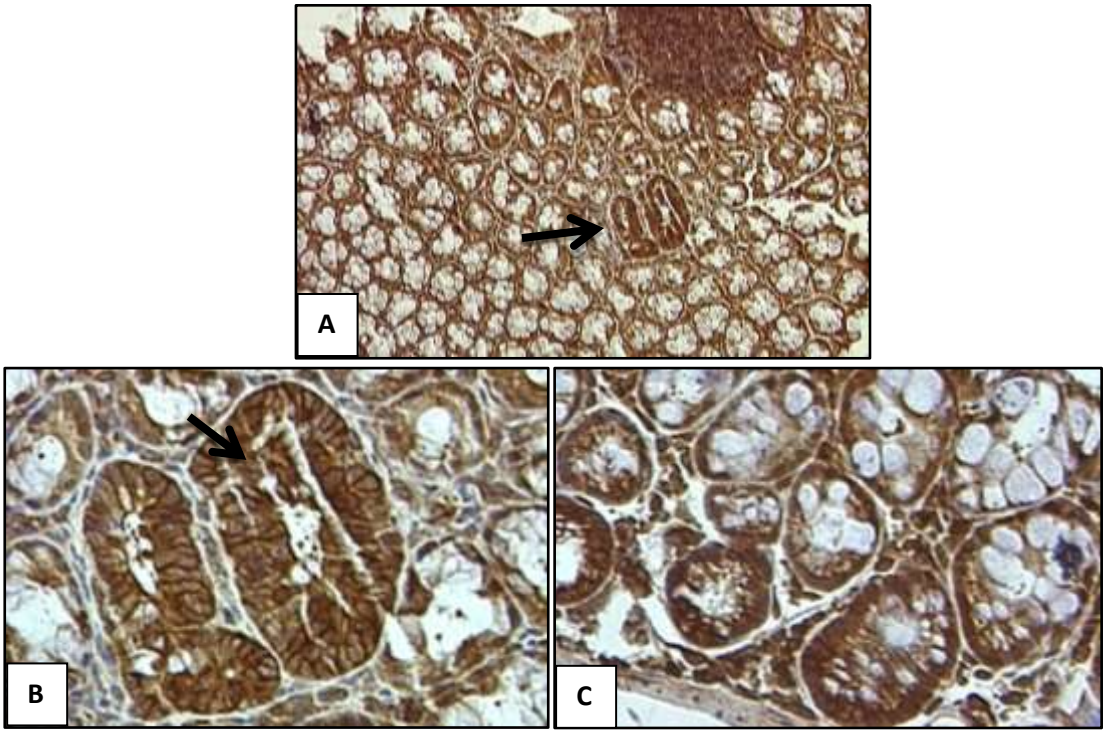


**Figure 3.7 Colonic sections from 3 month old *Apc*$^{Min/+}$ (A and B) and *Apc*$^{+/+}$ (C) mice stained with anti-NAP1L1 antibody. A) shows two dysplastic crypts (arrow) X10. B), the same dysplastic crypts X40 and C), wild type tissue.**

The dysplastic crypts (A and B) showed increased numbers of cells, loss of goblet cells and larger nuclei. The cells within the dysplastic crypts showed more NAP1L1 staining in the cytoplasm compared to the surrounding normal appearing tissue, but the difference in staining was less obvious when compared to wild type tissue. Repeating the experiment on other tissue sections from this age group may demonstrate better differential staining. However, lack of suitable tissues prevented this.

**Six month old *Apc*$^{Min/+}$ mice**

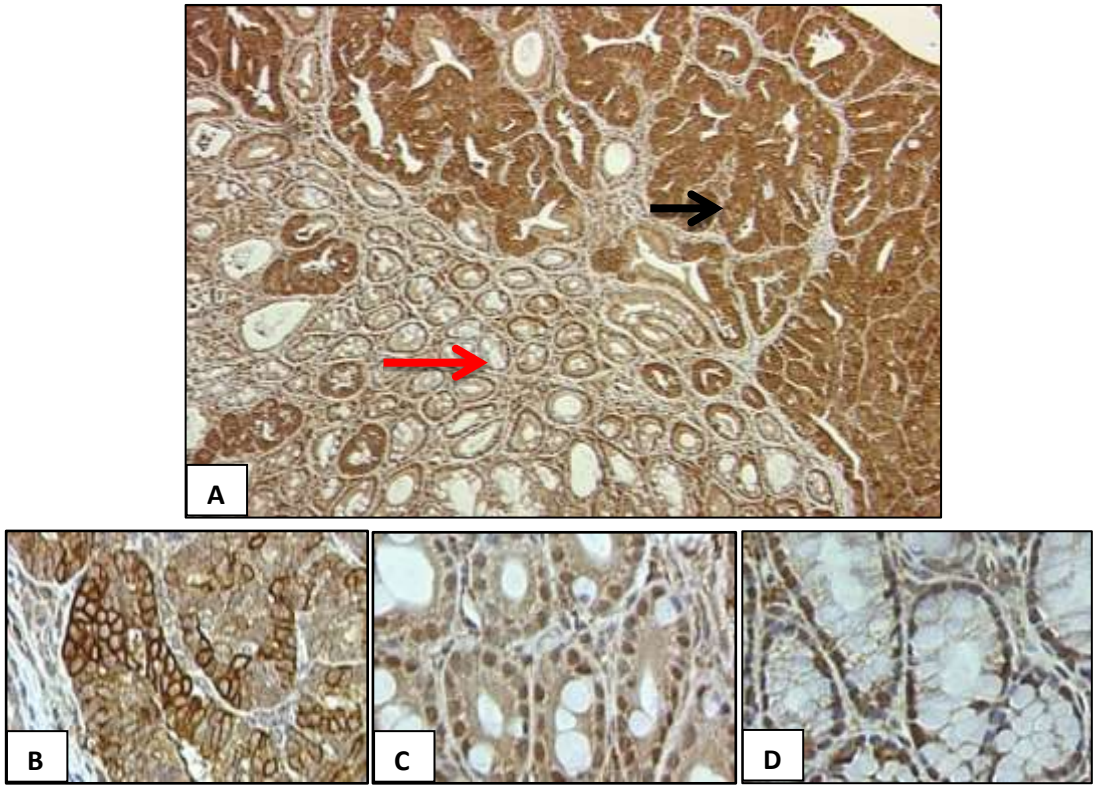


**Figure 3.8 Six month old *Apc*$^{Min/+}$ (A-C) and *Apc*$^{+/+}$ (D) mice colonic tissue sections stained with anti-NAP1L1 antibody. A) shows a colonic polyp (black arrow) and normal appearing tissue (red arrow) X10, B) shows magnified section from the same polyp (X40), C) shows magnified section from the tissue adjacent to the polyp (X40) and D) shows section from the colon of a matched wild type mouse (X40).**

The increase in NAP1L1 staining seen within the polyp was mainly cytoplasmic and the intensity of staining within the polyp was again more than that observed in normal appearing adjacent and wild type tissues. Interestingly, sub-cellular re-localisation was more obvious in these older *Apc*$^{Min/+}$ mice (figure 3.8).

### 3.4.2 IHC assessment of NAP1L1 expression, using an independent antibody

### *AhCre*$^{+}$*Apc*$^{fl/fl}$ mice

In an attempt to validate our results observed above, an antibody (abcam, ab33076) that was reactive to a different epitope of NAP1L1 protein was also used. This antibody was initially assessed at different dilutions (1:125-1:4000) on small intestinal sections from *AhCre*$^{+}$*Apc*$^{fl/fl}$ mice and their control counterparts. The dilution 1:4000 demonstrated the best differential staining as shown below (figure 3.9):

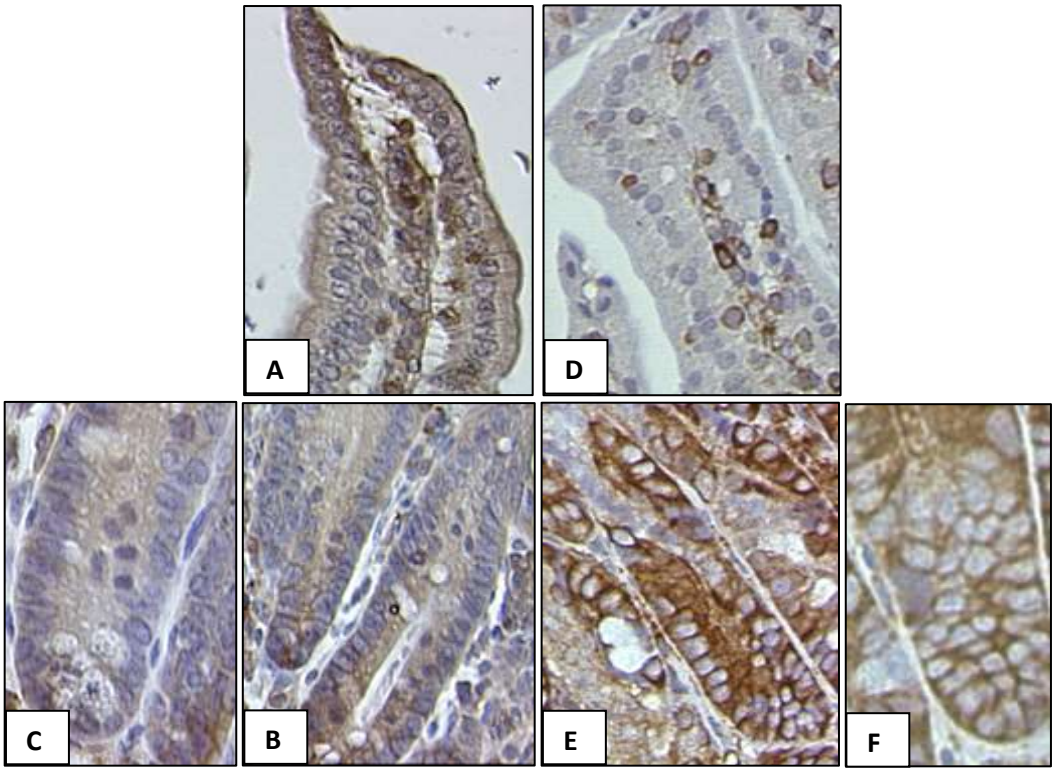


**Figure 3.9 Small intestinal tissues from a control mouse (A, B and C) and an *AhCre*$^{+}$*Apc*$^{fl/fl}$ mouse (D, E and F) stained with anti-NAP1L1 rabbit polyclonal antibody (abcam, ab33076) at a dilution of 1:4000 and a secondary antibody from Dako, used at a dilution of 1:200. A), B), D) & E) are X40 objective (original magnification) while C) & F) are X63 objective (original magnification). Images A and D are villi while the rest of the images are crypts.**

With the second primary antibody, there was again the same cytoplasmic over expression of NAP1L1 in the crypt epithelial cells of the *AhCre*$^{+}$*Apc*$^{fl/fl}$ mice compared to *AhCre*$^{+}$*Apc*$^{+/+}$ control mice. A point worth highlighting is that this antibody showed more obvious staining than the previous one (figure 3.3).

### *Apc*$^{Min/+}$ mice

To further validate our results for NAP1L1 staining observed using the first primary antibody, lesions from the three age groups of *Apc*$^{Min/+}$ mice were also stained with the second NAP1L1 antibody under the same conditions used for the *AhCre*$^{+}$*Apc*$^{fl/fl}$ mice.

### One month old *Apc*$^{Min/+}$ mice

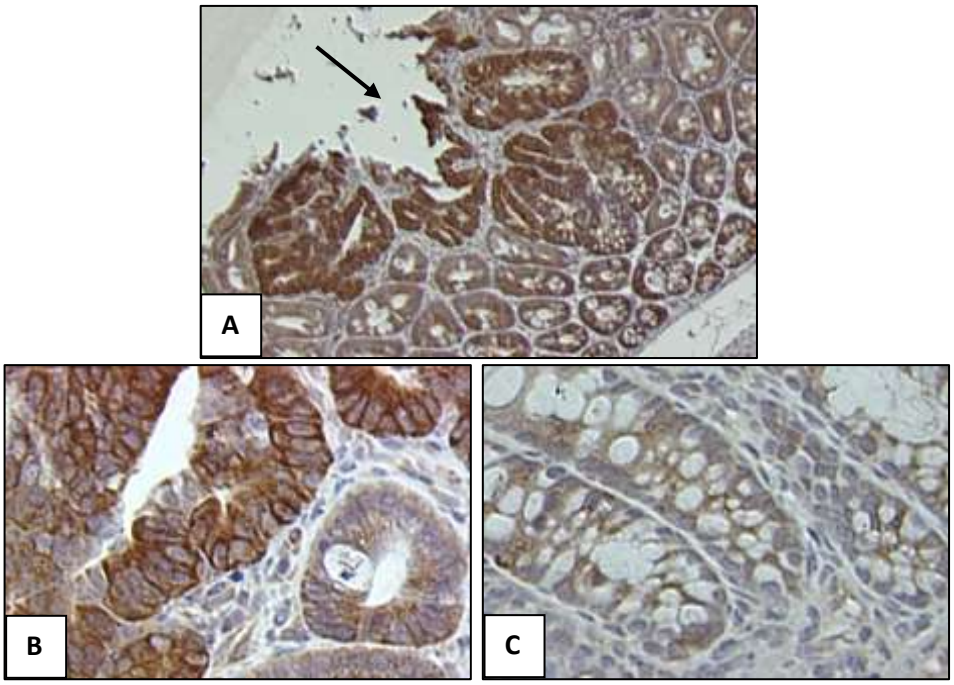


**Figure 3.10 Colonic sections from 1 month old *Apc*$^{Min/+}$ (A and B) and *Apc*$^{+/+}$ (C) mice stained with anti-NAP1L1 antibody (second antibody). A) Shows a dysplastic lesion (arrow) x10, B) shows the same dysplastic lesion (X40 objective) and C) shows wild type tissue (x40 objective).**

A similar pattern of staining was seen using the second NAP1L1 antibody as with the first one. There was increased cytoplasmic expression of NAP1L1 in the neoplastic lesions.

**Three month old *Apc*$^{Min/+}$ mice**

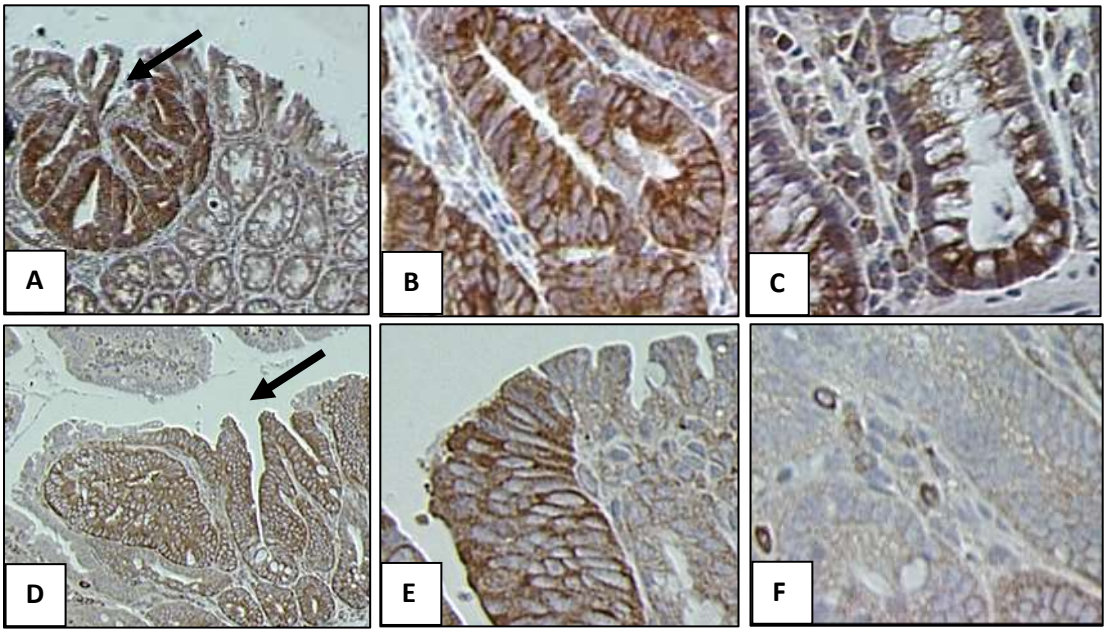


**Figure 3.11 Intestinal sections stained with anti-NAP1L1 Rabbit polyclonal antibody (1:4000). A) and B) images show colonic sections from a three month old *Apc*$^{Min/+}$ mouse. D) and E) images show small intestinal sections from a three month old *Apc*$^{Min/+}$ mouse. Images (A and D) are X10 magnification while (B and E) are magnified sections (X40) from (A and D) respectively. Images (C and F) are age matched WT tissues. Arrows point to neoplastic lesions where NAP1L1 expression is increased compared to the normal surrounding and wild type tissue.**

The differential staining (more cytoplasmic staining) was more obvious in the small intestine (images E vs. F) than in the colon (images B vs. C), an observation that needs more experiments to confirm. Lack of suitable tissue sections for this age group of mice was the reason not to do so.

**Six month old *Apc*$^{Min/+}$ mice**

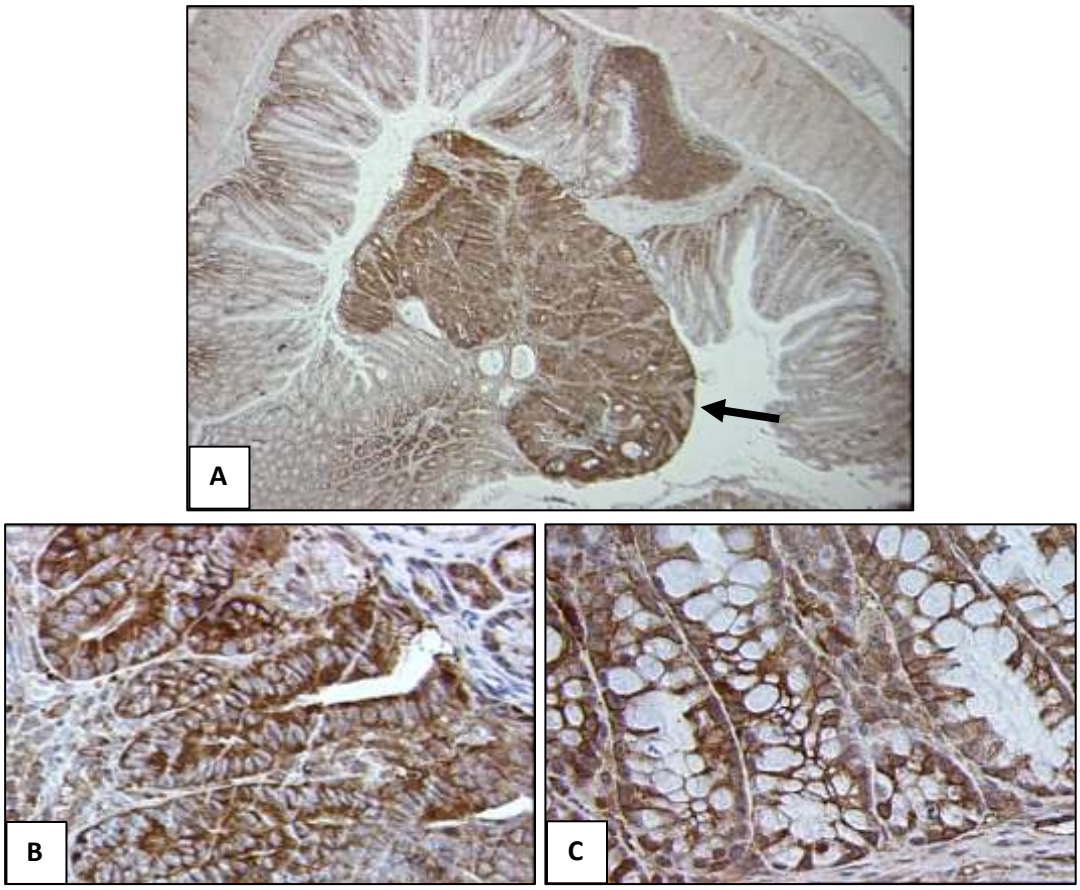


**Figure 3.12 Six month old *Apc*$^{Min/+}$ (A and B) and *Apc*$^{+/+}$ (C) mice colonic tissue sections stained with anti-NAP1L1 antibody (2nd NAP1L1 antibody). A) Shows a colonic polyp (arrow) X10, B) shows magnified section from the polyp (X40) and C) shows a section from the colon of a matched wild type mouse (X40).**

A similar staining pattern was again observed with this second NAP1L1 antibody as observed with the first antibody. This finding further supported our results for this protein in *Apc*$^{Min/+}$ mice.

**Co-expression of Beta catenin and candidate proteins**

Interestingly, some lesions from six month old *Apc*$^{Min/+}$ mice showed mixed lineage crypts upon staining for the different proteins. Although normal crypts are thought to be monoclonal in adult mice and polyclonal only during the first few weeks of life [209, 210], the above observation agrees with the concept of loss of differentiation as part of the tumourigenesis process. These lesions (figure 3.13) were used as examples to show expression of candidate proteins in correlation with WNT activity as indicated by nuclear Beta catenin localisation.

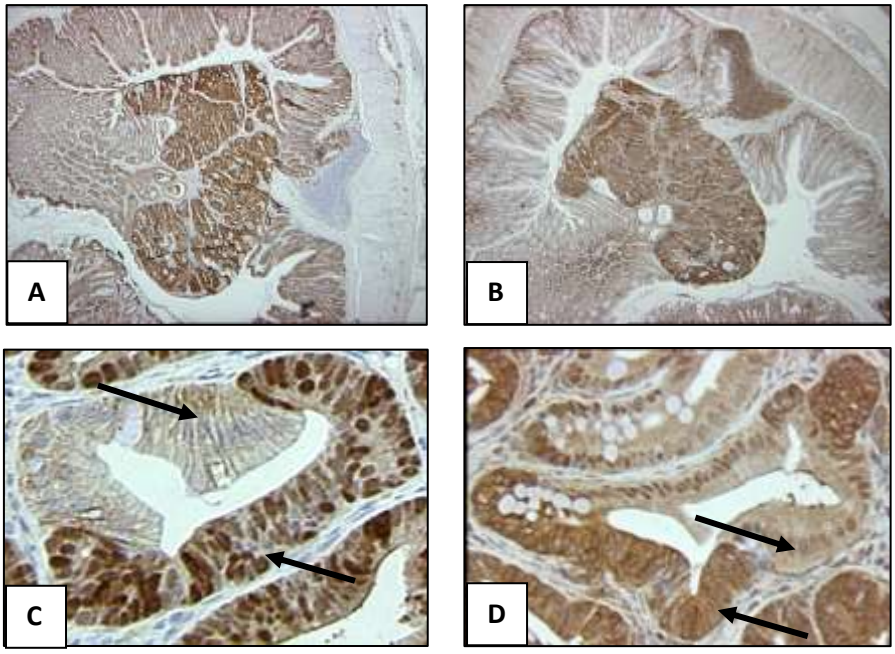


**Figure 3.13 Colonic lesions in six month old old *Apc*$^{Min/+}$ mice. A) and B) show the same polyp stained with anti-Beta catenin and anti-NAP1L1 antibodies. C) Beta catenin staining, showing nuclear translocation in one part and normal membranous expression in the other part (arrows). D) Shows a similar differential staining (arrows) for NAP1L1 protein in a subsequent section from the same crypt. Images A and B are X5 magnification and images C and D are X40 magnification.**

The above images (figure 3.13) represent visual evidence for the co-expression of Beta catenin and one of our candidate proteins. Histologically, the same crypt (figure 3.13, C and D) (arrows) showed both normal and abnormal cells in terms of number, organisation and shape of nuclei. Moreover, the presence of differential staining within the same crypt supported the findings found in other sections. Moreover, co-expression of NAP1L1 with Beta catenin indicated that this protein and other candidate proteins which showed the same staining pattern are over expressed in the

setting of an activated WNT pathway. Further in agreement with these findings is co-expression of this candidate protein and Beta catenin in the same tissue compartment in *AhCre*$^{+}$*Apc*$^{fl/fl}$ mice.

**Comments on NAP1L1 expression following *Apc* deletion**

NAP1L1, although acting on chromatin as a chaperone protein, appeared to have cytoplasmic localisation in both *AhCre*$^{+}$*Apc*$^{fl/fl}$ and *Apc*$^{Min/+}$ animal models. This is consistent with the way this protein is proposed to function, where it is thought to shuttle essential molecules (such as histone proteins) into the nucleus upon demand in situations such as proliferation and DNA replication and that it remains mainly cytoplasmic throughout the cell cycle [149]. In our work, NAP1L1 seems to play a role in the hyperproliferation that results from Apc loss in these mice. This is because NAP1L1 showed an early increase in expression as evident from the *AhCre*$^{+}$*Apc*$^{fl/fl}$ mice and the small lesions that were observed in one month old *Apc*$^{Min/+}$ mice. Furthermore, previous reports have shown marked over expression of NAP1L1 in T cells after induction with Phorbol 12-myristate 13-acetate (PMA)/ionomycin and a reduction by 50% in T cell proliferation after treatment with NAP1L1 antisense oligonucleotides. Therefore, NAP1L1 has been proposed as a therapeutic target in view of its possible role in promoting cell proliferation [211].

### 3.4.3 IHC assessment of RPL6 expression

#### *AhCre*$^{+}$*Apc*$^{fl/fl}$ mice

RPL6 is the second candidate protein that was found to be upregulated in the proteomic analysis performed using the *AhCre*$^{+}$*Apc*$^{fl/fl}$ mouse model [147]. It has been reported that RPL6 is a cytoplasmic protein and it is involved in protein synthesis and modulation of the cell cycle [162]. Below is an IHC assessment of its expression in the *AhCre*$^{+}$*Apc*$^{fl/fl}$ and *AhCre*$^{+}$*Apc*$^{+/+}$ (control) mice. The first anti-RPL6 primary antibody (abcam) that was used, although it was tested at various dilutions, did not show any conclusive staining. The second anti-RPL6 primary antibody from Proteintech was again tested at different dilutions (1:25-1:1600). The dilution 1:200 demonstrated the most clear differential staining pattern, as shown below (figure 3.14):

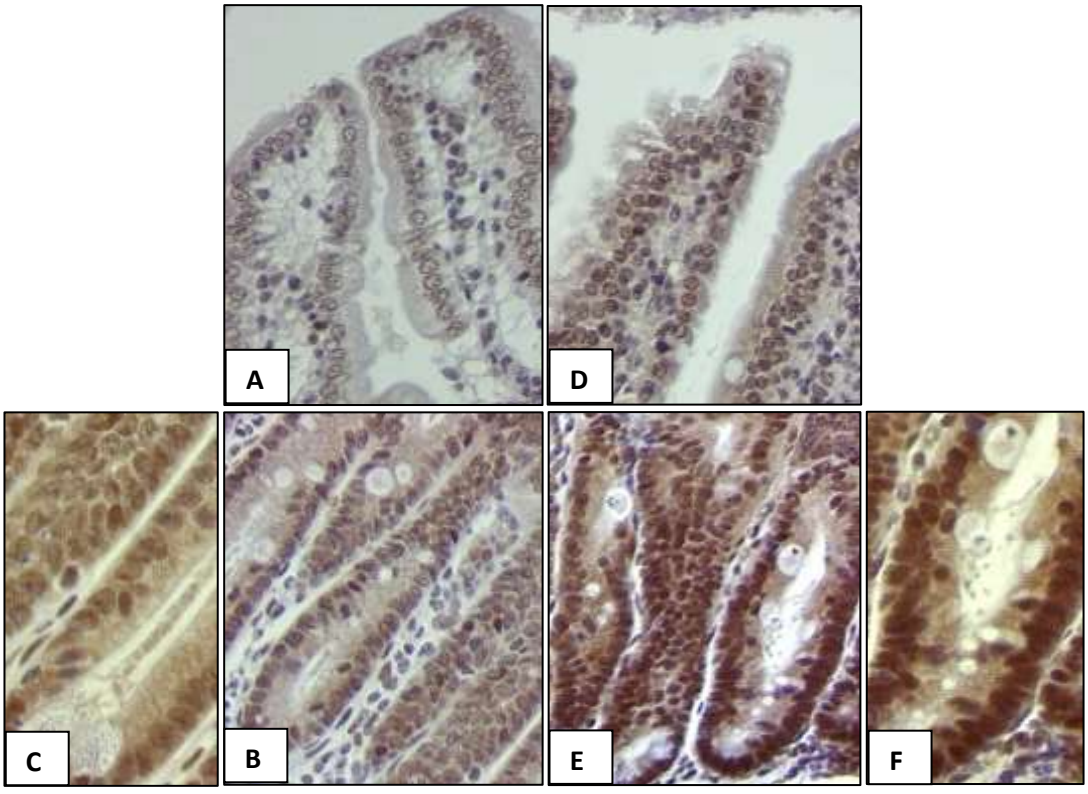


**Figure 3.14 Small intestinal tissues from an *AhCre*$^{+}$*Apc*$^{+/+}$ control mouse (A, B and C) and an *AhCre*$^{+}$*Apc*$^{fl/fl}$ mouse (D, E and F) stained with anti-RPL6 rabbit polyclonal antibody at a dilution of 1:200 with the secondary antibody being from Dako and used at a dilution of 1:200. A), B), D) & E) are X40 (original magnification) while C) & F) are X63 (original magnification). Images A and D are villi and the rest of the images are crypts.**

In the *AhCre*$^{+}$*Apc*$^{fl/fl}$ mouse, crypt cells showed increased expression of RPL6 protein as depicted by increased brown staining in the nuclei and to a lesser extent in the

cytoplasm of these cells compared to the villi of the same mouse and the whole crypt villus axis in wild type control tissue.

### IHC assessment of RPL6 expression in *Apc*$^{Min/+}$ mice

The same experimental conditions used to assess expression of RPL6 in *AhCre*$^{+}$*Apc*$^{fl/fl}$ mice were applied to intestinal tissue samples from *Apc*$^{Min/+}$ mice aged 1, 3 and 6 months and wild type control mice.

### One month old *Apc*$^{Min/+}$ mice

Difficulty in finding dysplastic lesions in this age group prevented us from assessing RPL6 expression in *Apc*$^{Min/+}$ and wild type mice at this stage. Unfortunately, this was the case for all the other proteins described in the rest of this chapter.

### Three month old *Apc*$^{Min/+}$ mice

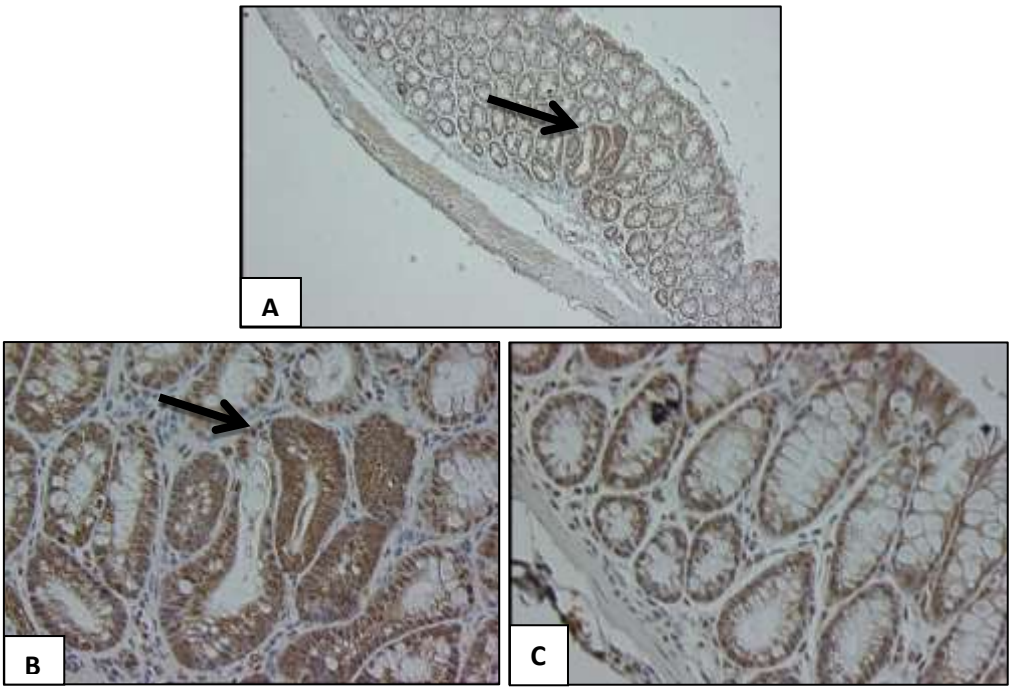


**Figure 3.15 Colonic tissue sections from 3 month old *Apc*$^{Min/+}$ (A and B) and *Apc*$^{+/+}$ (C) mice, stained with anti RPL6 antibody. A) Shows dysplastic crypts (arrow) X10, B) shows the same dysplastic crypts X40 and C) shows wild type tissue (X40).**

The cells within dysplastic crypts (indicated by black arrows) showed more staining; this was mainly in the cytoplasm compared to the surrounding histologically normal mucosa and also wild type tissues.

**Six month old *Apc*$^{Min/+}$ mice**

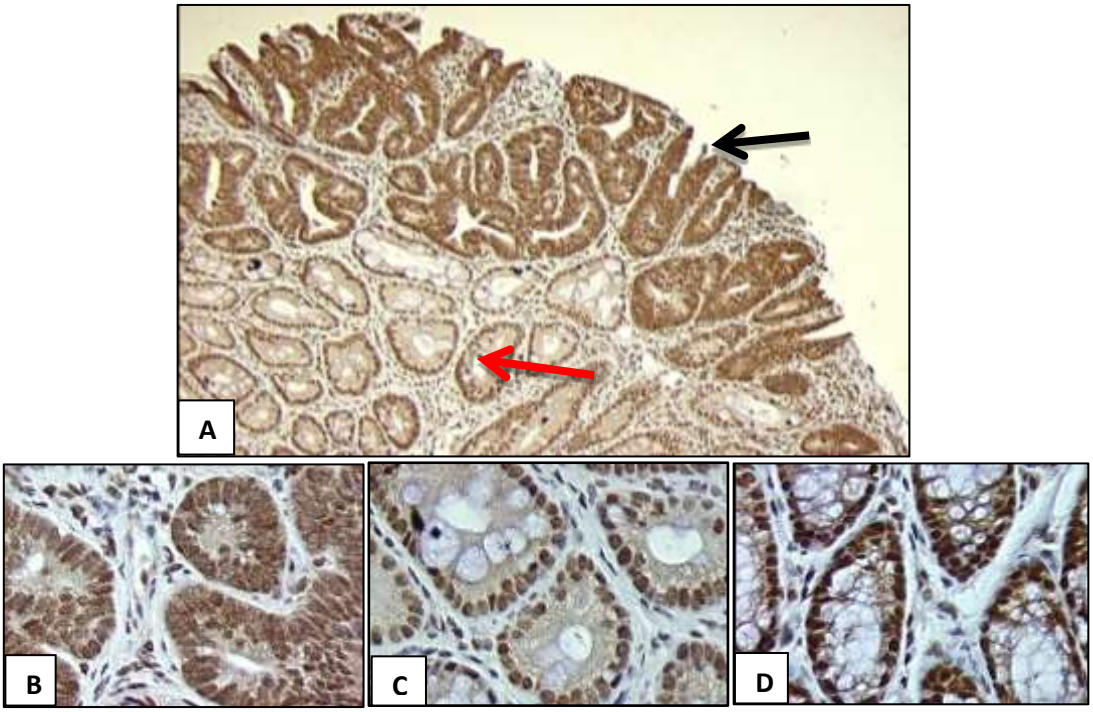


**Figure 3.16 Six month old *Apc*$^{Min/+}$ (A-C) and *Apc*$^{+/+}$ (D) control mice colonic tissue sections stained with anti-RPL6 antibody. A) shows a polyp (black arrow) and normal appearing tissue (red arrow) X10, B) shows magnified section from the polyp (X40), C) shows magnified section from the tissue adjacent to the polyp (X40) and D) shows section from the colon of a matched wild type mouse (X40).**

RPL6 protein expression was again increased in the nuclei (mainly) and the cytoplasm of cells in the polyp tissue compared to the adjacent histologically normal tissue, but less obvious differences were observed when compared to wild type control tissue.

Similar to NAP1L1, RPL6 also demonstrated co-expression with Beta catenin in the same tissue compartment (crypts) in *AhCre*$^{+}$*Apc*$^{fl/fl}$ mice and in *Apc*$^{Min/+}$ mice (figure 3.17).

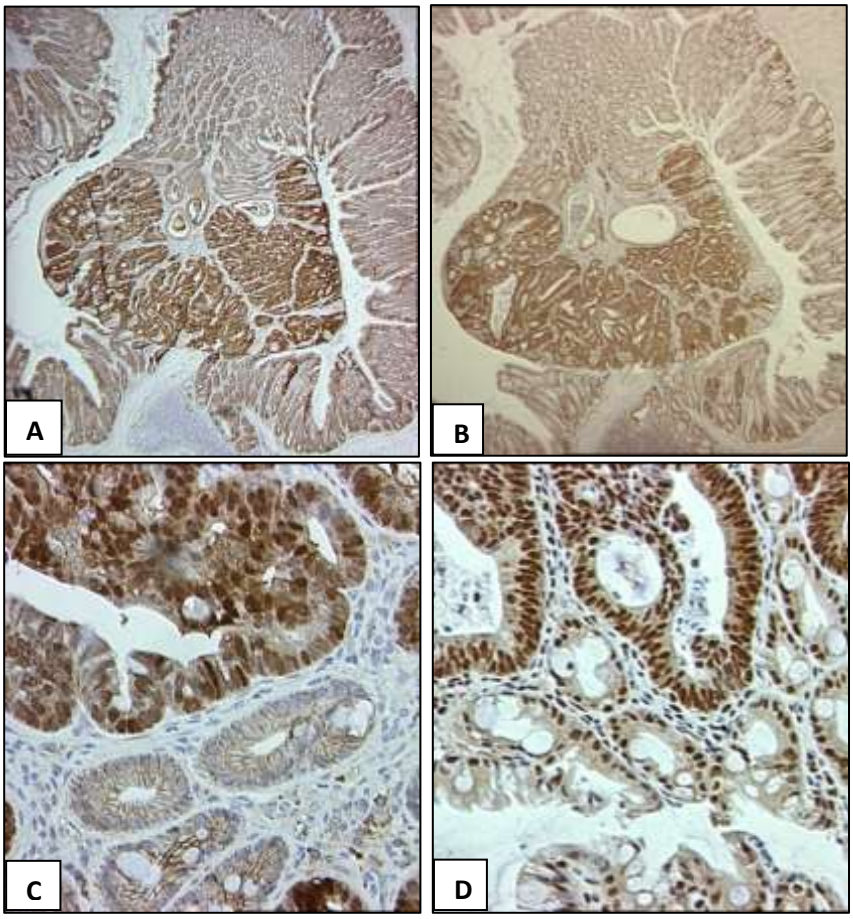


**Figure 3.17 Co-expression of Beta catenin and RPL6 in the same tissue compartments in *Apc*$^{Min/+}$ mice. A and B) show a colonic polyp (X10) from a six month old mouse stained with anti-Beta catenin and anti-RPL6 antibodies respectively. C and D) show magnified sections (X40) from the same polyp in (A) and (B) respectively.**

**Comments on RPL6 expression following *Apc* deletion**

RPL6 showed initial cytoplasmic over expression in lesions from three month old *Apc*$^{Min/+}$ mice, but interestingly this protein showed a predominant nuclear over expression in more advanced adenomas from six month old *Apc*$^{Min/+}$ mice. This nuclear localisation of RPL6 was also observed in the *AhCre*$^{+}$*Apc*$^{fl/fl}$ mice, suggesting a correlation between the severity of the phenotype and the sub-cellular location of this protein.

### 3.4.4 IHC assessment of SFRS2 (Sc35) expression

SFRS2 is the third candidate protein that showed upregulation in the proteomic studies performed using the *AhCre*$^{+}$*Apc*$^{fl/fl}$ mouse model [147]. It is a member of the serine rich (SR) family of proteins which is involved mainly with pre-mRNA splicing. Normally, it is a component of the spliceosome units in the nuclei [170].

SFRS2 expression was again initially assessed in *AhCre*$^{+}$*Apc*$^{fl/fl}$ and their *AhCre*$^{+}$*Apc*$^{+/+}$ control mice: the first antibody from Sigma was tested at different dilutions but it did not show any clear staining patterns. The second antibody was from abcam and after testing it at different dilutions (1:125-1:2000), a dilution of 1:250 was selected as optimal as shown below (figure 3.17).

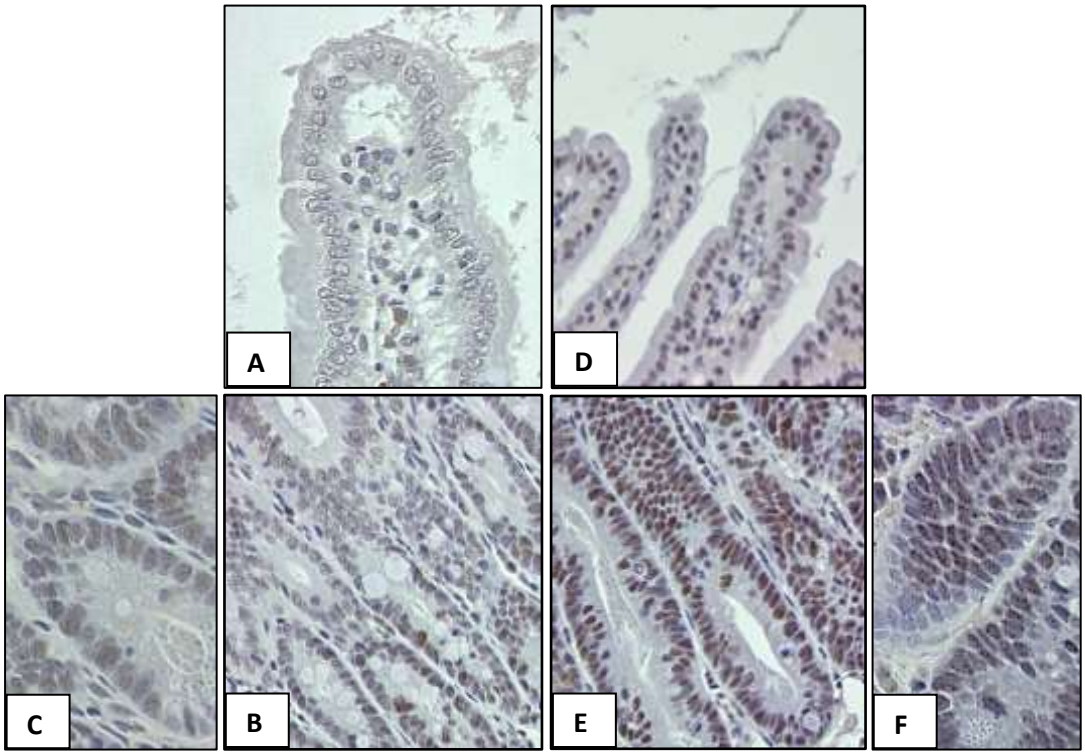


**Figure 3.18 Small intestinal tissues from *AhCre*$^{+}$*Apc*$^{+/+}$ (A, B and C) and *AhCre*$^{+}$*Apc*$^{fl/fl}$ (D, E and F) mice stained with anti-SFRS2 mouse monoclonal antibody (abcam, ab11826) at a dilution of 1:250 and a secondary antibody from Dako at a dilution of 1:200. A), B), D) & E) are X40 (original magnification) while C) & F) are X63 (original magnification). Images A and D are villi and C, B, E and F are crypts.**

The *AhCre*$^{+}$*Apc*$^{fl/fl}$ mouse sections showed increased nuclear staining manifest as dark dots (speckles) in the nuclei. This can be seen in images (E) and (F) in the crypts compared to the villi from the same mouse (D) and to the control tissue (A-C).

**IHC assessment of SFRS2 expression in *Apc*$^{Min/+}$ mice**

The same experimental conditions used to assess expression of SFRS2 in *AhCre*$^{+}$*Apc*$^{fl/fl}$ mice were then applied to intestinal tissue samples from *Apc*$^{Min/+}$ mice aged 3 and 6 months and *Apc*$^{+/+}$ control tissues.

**Three month old *Apc*$^{Min/+}$ mice**

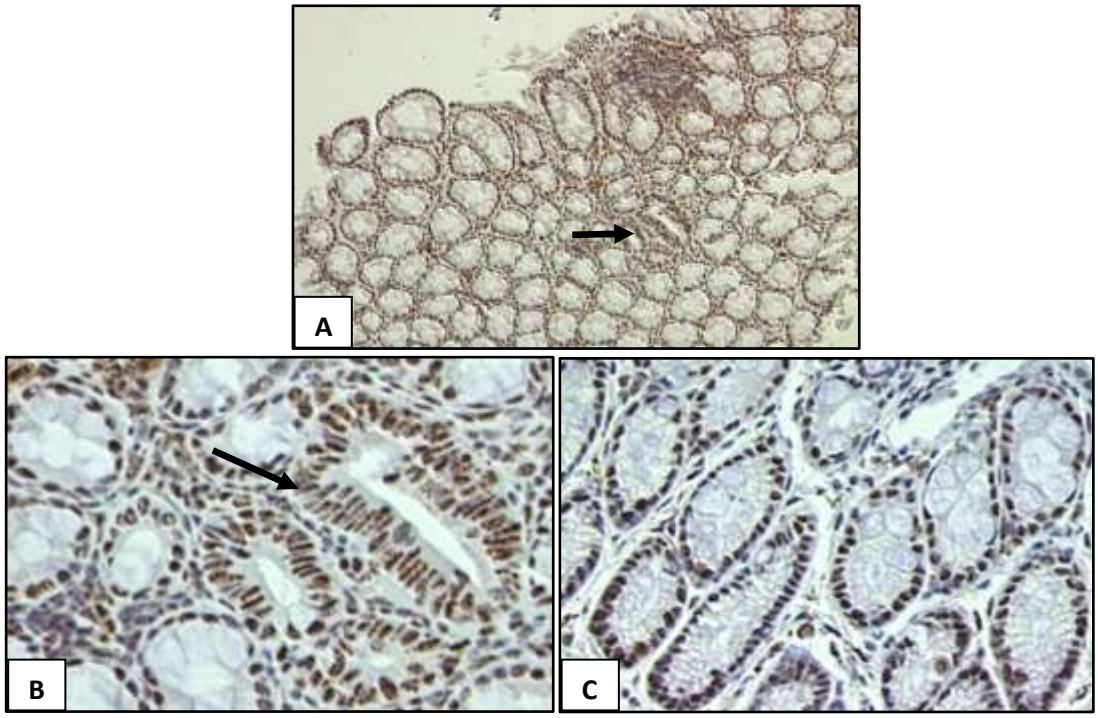


**Figure 3.19 Colonic tissue sections from 3 month old *Apc*$^{Min/+}$ (A and B) and *Apc*$^{+/+}$ (C) mice stained with anti-SFRS2 antibody. A) Shows two dysplastic crypts (arrow) X10. B) shows the same dysplastic crypts X40 and C) shows *Apc*$^{+/+}$ tissue (X40).**

The cells within these dysplastic crypts showed more SFRS2 staining in nuclei compared to surrounding histologically normal tissue and wild type tissue.

**Six month old *Apc*$^{Min/+}$ mice**

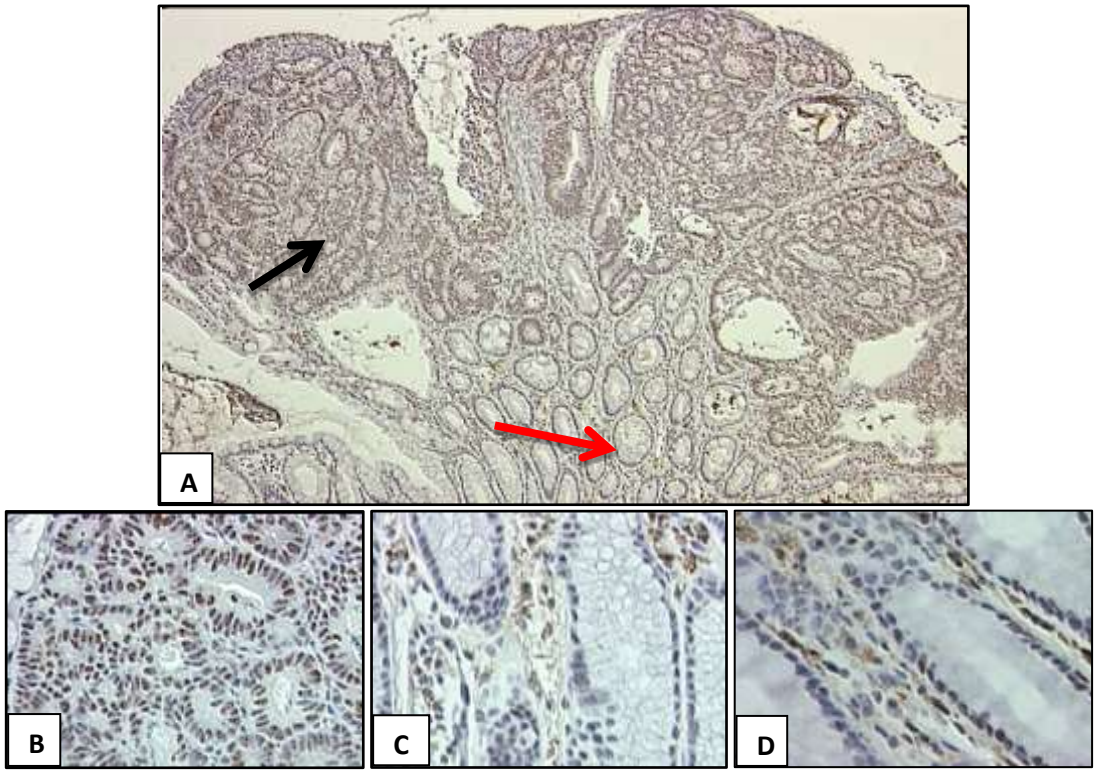


**Figure 3.20 Six month old *Apc*$^{Min/+}$ (A-C) and *Apc*$^{+/+}$ (D) mice tissue sections stained with anti-SFRS2 mouse monoclonal antibody. Image A) is a colonic polyp X10 (original magnification). Image B) is a magnified section from the polyp (X 40 original magnification). Image C) is normal appearing tissue adjacent to the polyp (X40, original magnification). Image D) is a colonic tissue section from a matched *Apc*$^{+/+}$ mouse (X40).**

The polyp tissue (black arrow) showed a clear increase in SFRS2 staining in the nuclei compared to adjacent normal tissue (red arrow) and *Apc*$^{+/+}$ tissue.

Co-expression of SFRS2 and Beta catenin was also noted in the crypts of *AhCre*$^{+}$*Apc*$^{fl/fl}$ mice following *Apc* deletion. Also, *Apc*$^{Min/+}$ mice showed co-expression of these two proteins in the same tissue compartment (figure 3.21). This again indicated that SFRS2 overexpression is related to the activity of the WNT signalling pathway.

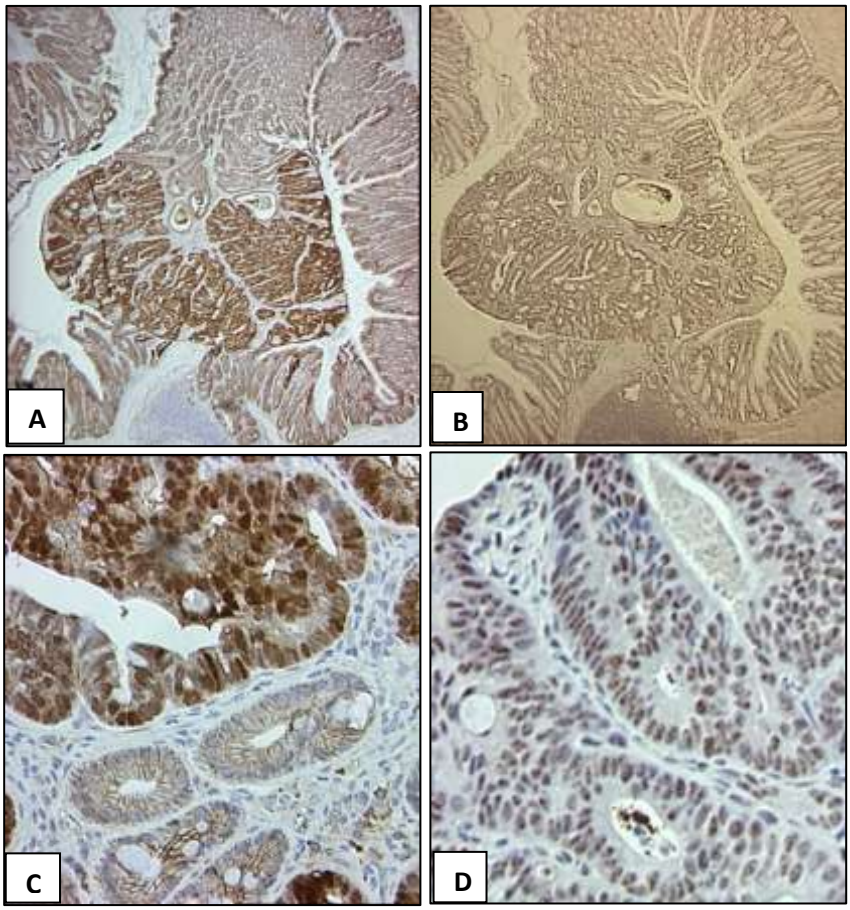


**Figure 3.21 Co-expression of SFRS2 and Beta catenin in *Apc*$^{Min/+}$ mice. A and B) show colonic polyp (X10) from a six month old mouse stained with anti-Beta catenin and anti-SFRS2 antibodies respectively. C and D) show magnified sections (X40) from the same polyp in (A) and (B) repectively.**

**Comments on SFRS2 expression following *Apc* deletion**

SFRS2 is a component of the chromatin associated dynamic structures, the spliceosomes [212]. Early following *Apc* deletion in *AhCre*$^{+}$*Apc*$^{fl/fl}$ mice, SFRS2 showed increased nuclear expression, an observation that was also found in three and six month old *Apc*$^{Min/+}$ mice. Interestingly, SFRS2 staining was observed in a speckling pattern and was associated with increased Wnt activity.

### 3.4.5 IHC assessment of FABP6 expression

FABP6 was also upregulated in the proteomic analysis carried out on *AhCre*$^{+}$*Apc*$^{fl/fl}$ mice [147]. It is normally cytoplasmic in localisation and is mainly involved with bile salt metabolism [166]. FABP6 expression was assessed in *AhCre*$^{+}$*Apc*$^{fl/fl}$ mice as shown below: the primary antibody from abcam was tested at different dilutions (1:25-1:1600) and the dilution 1:50 demonstrated the best differential staining as shown below in figure 3.22.

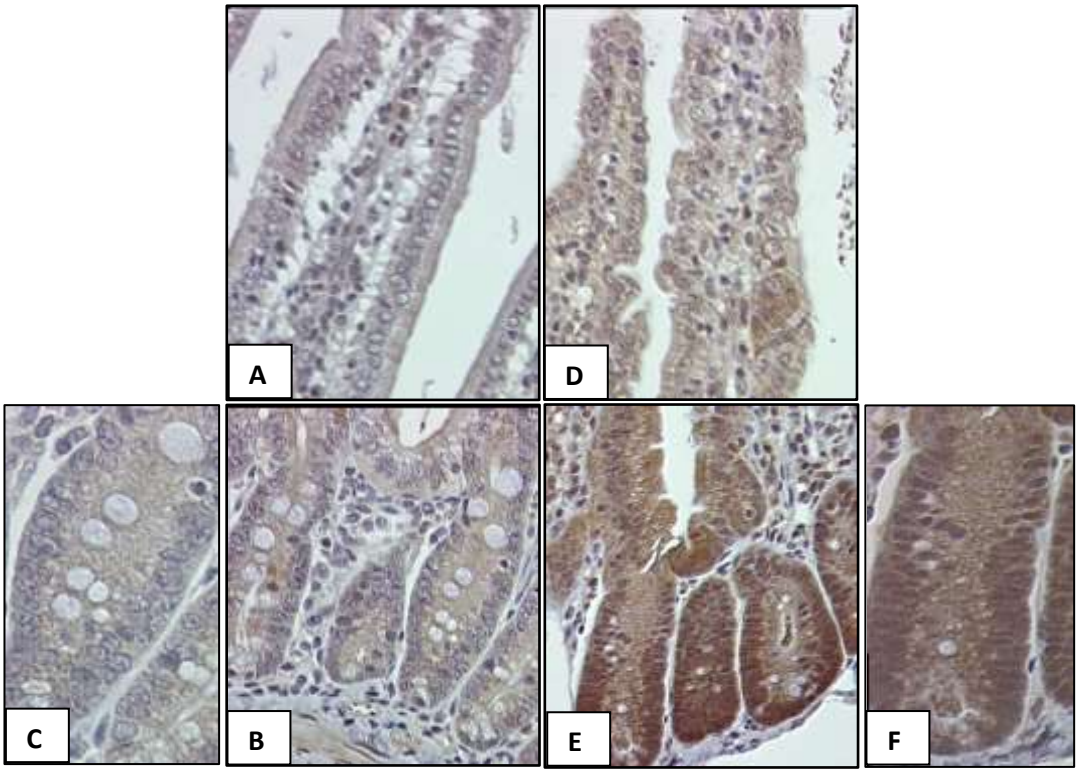


**Figure 3.22 Small intestinal tissues from a control mouse (A, B and C) and an *AhCre*$^{+}$*Apc*$^{fl/fl}$ mouse (D, E and F) stained with anti-FABP6 Rabbit polyclonal antibody at a dilution of 1:50 while the secondary antibody was from Dako (1:200 dilution). A), B), D) & E) are X40 (original magnification) while C) & F) are X63 (original magnification). Images A and D are villi while the rest are crypts.**

In the *AhCre*$^{+}$*Apc*$^{fl/fl}$ mouse, small intestinal crypt cells showed increased expression of FABP6 protein as depicted by increased brown staining in the cytoplasm and in the nuclei of these cells compared to the villi of same mouse and the whole crypt villus axis of control mice.

**IHC assessment of FABP6 expression in *Apc*$^{Min/+}$ mice**

The expression of FABP6 was also assessed in intestinal tissue samples from *Apc*$^{Min/+}$ mice aged 3 and 6 months and their wild type control tissues using the same experimental conditions that had been developed in the *AhCre*$^{+}$*Apc*$^{fl/fl}$ mice.

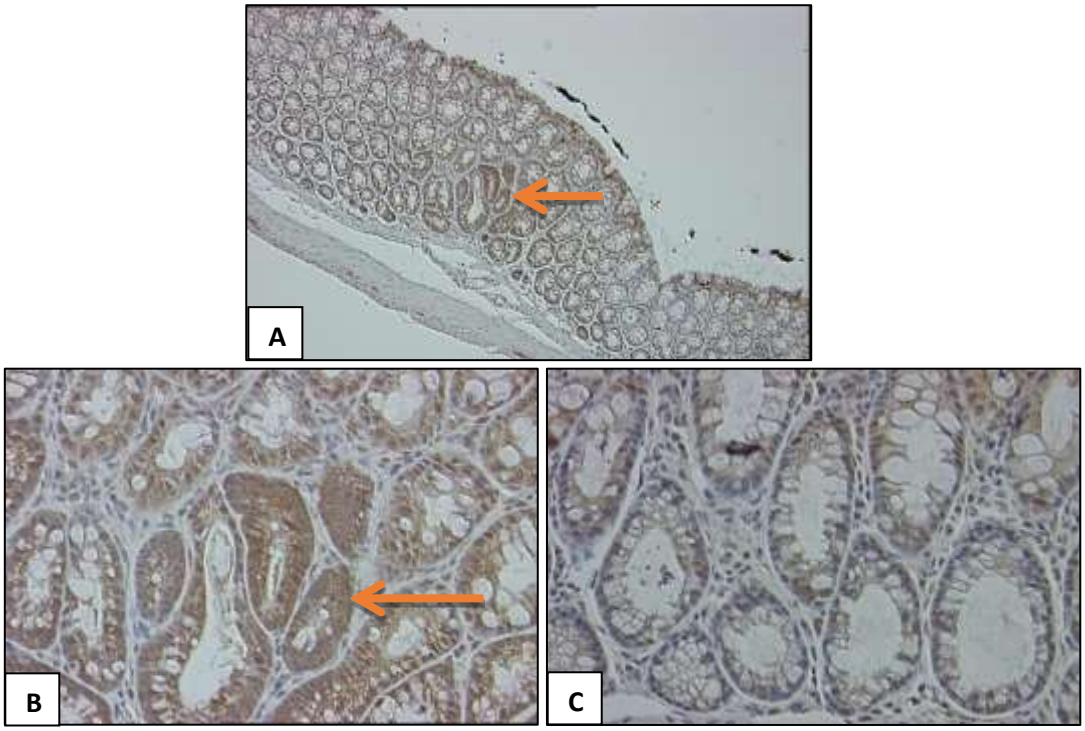


**Figure 3.23 Colonic sections from 3 month old *Apc*$^{Min/+}$ (A and B) and *Apc*$^{+/+}$ (C) control mice stained with anti-FABP6 rabbit polyclonal antibody. A), shows dysplastic crypts (arrow) X10, B) shows the same dysplastic crypts X40 and C) shows wild type tissue (X40).**

The cells within the dysplastic crypts showed more FABP6 staining in the cytoplasm compared to the surrounding histologically normal and wild type tissues. This indicates a role for FABP6 early in colorectal tumourigenesis. This observation is consistent with the findings in *AhCre*$^{+}$*Apc*$^{fl/fl}$ mice.

**Six month old *Apc*$^{Min/+}$ mice**

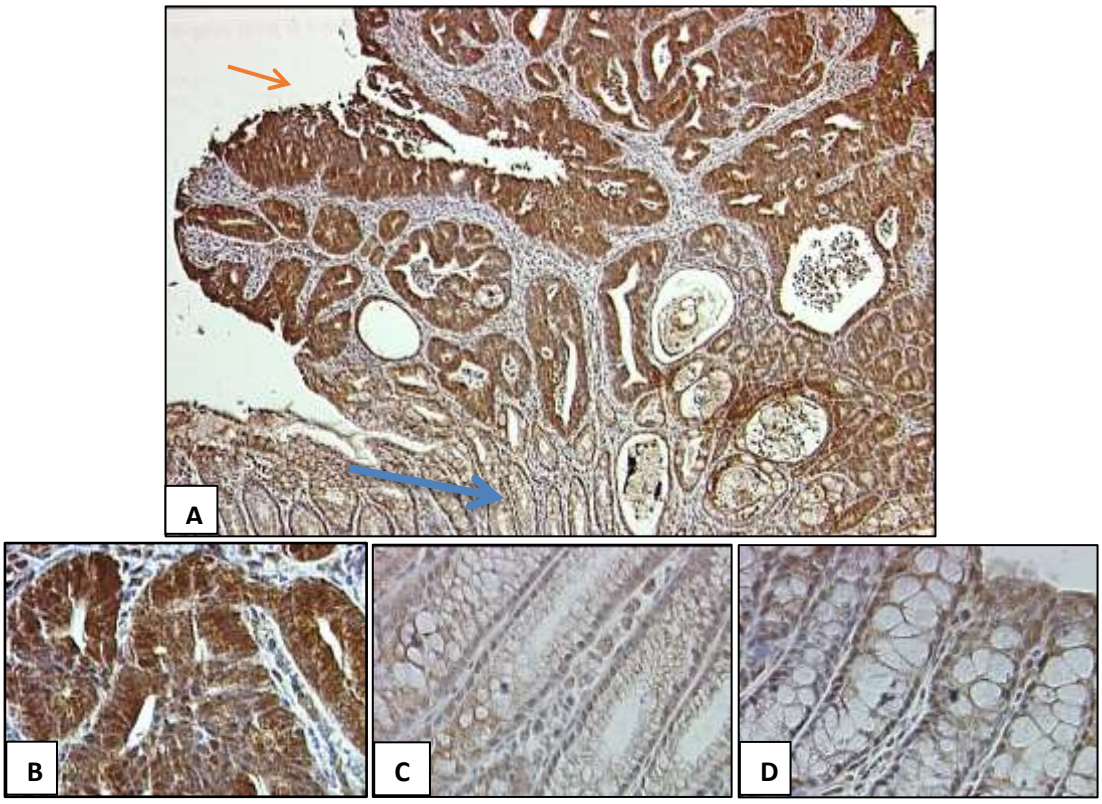


**Figure 3.24 Six month old *Apc*$^{Min/+}$ (A-C) and *Apc*$^{+/+}$ (D) control mice colonic tissue sections stained with anti-FABP6 antibody. A) shows polyp tissue (red arrow) and normal appearing tissue (blue arrow) X10, B) shows magnified section from the polyp (X40), C) shows a magnified section from the tissue adjacent to the polyp (X40) and D) shows a section from the colon of a matched *Apc*$^{+/+}$ mouse (X40).**

FABP6 expression was increased; mainly in the cytoplasm within polyp tissue when compared to adjacent histologically normal tissue and the wild type control tissue**.**

Similar to all other candidate biomarkers already examined, FABP6 was also over expressed in the setting of an active WNT pathway as indicated by its co-expression with Beta catenin in crypts of *AhCre*$^{+}$*Apc*$^{fl/fl}$ mice. Moreover, FABP6 also demonstrated co-expression in the same tissue compartments as Beta cateinin in *Apc*$^{Min/+}$ mice (figure 3.25).

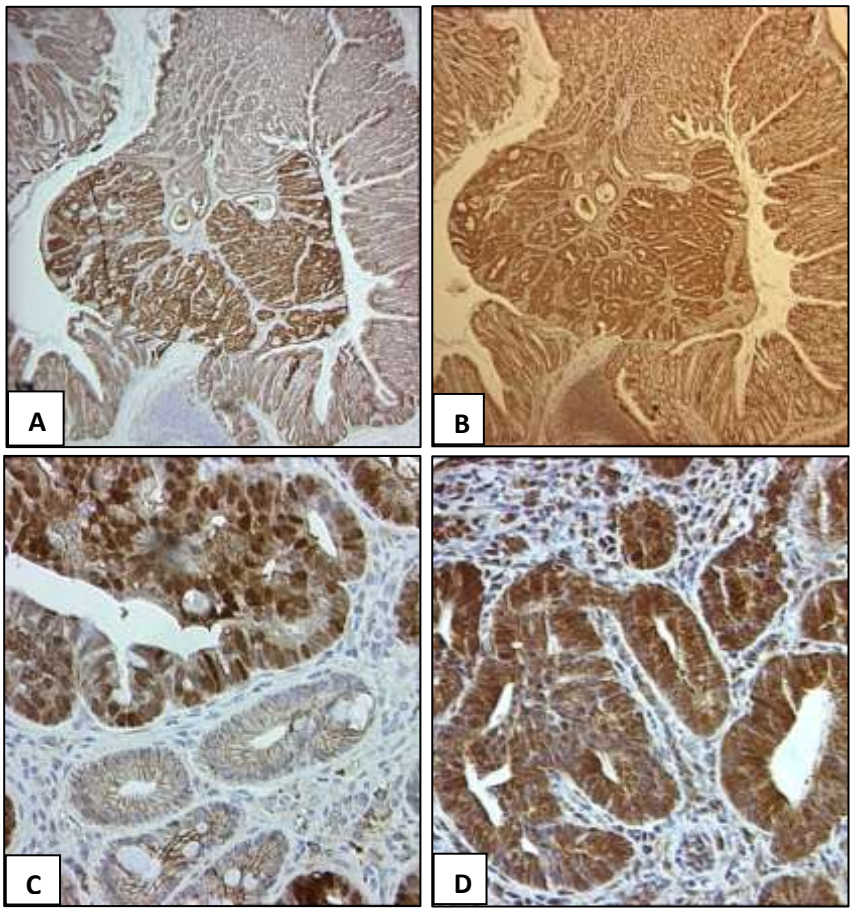


**Figure 3.25 Co-expression of Beta catenin and FABP6 in *Apc*$^{Min/+}$ mice. A and B) show colonic polyp (X10) from a six month old mouse stained with anti-Beta catenin and anti-FABP6 antibodies respectively. C and D) show magnified sections (X40) from the same polyp in (A) and (B) respectively.**

**Comments on FABP6 expression following *Apc* deletion**

Increased expression of FABP6 in dysplastic lesions from *Apc*$^{Min/+}$ mice and in *AhCre*$^{+}$*Apc*$^{fl/fl}$ mice is supported by other studies that have reported similar findings in humans where FABP6 expression was significantly increased in colonic adenomas versus normal adjacent tissue and in colonic cancer versus adenoma but decreased dramatically after nodal metastasis [166]. Therefore, FABP6 may also be involved in the early stages of colorectal tumourigenesis.

### 3.4.6 IHC assessment of Prohibitin (PHB) expression

PHB was also upregulated after deletion of both *Apc* alleles in the intestinal epithelium of *AhCre*$^{+}$*Apc*$^{fl/fl}$ mice as shown by the proteomics studies [147]. PHB is a mitochondrial protein, but its functions are not fully understood [213]. PHB expression was assessed in the *AhCre*$^{+}$*Apc*$^{fl/fl}$ mice and their *AhCre*$^{+}$*Apc*$^{+/+}$ control mice: the primary antibody (abcam) was tested at dilutions 1:50-1:1600. The dilution 1:200 was optimal as shown below. The staining was in general faint despite varying the duration of incubation with DAB and using different secondary antibody dilutions.

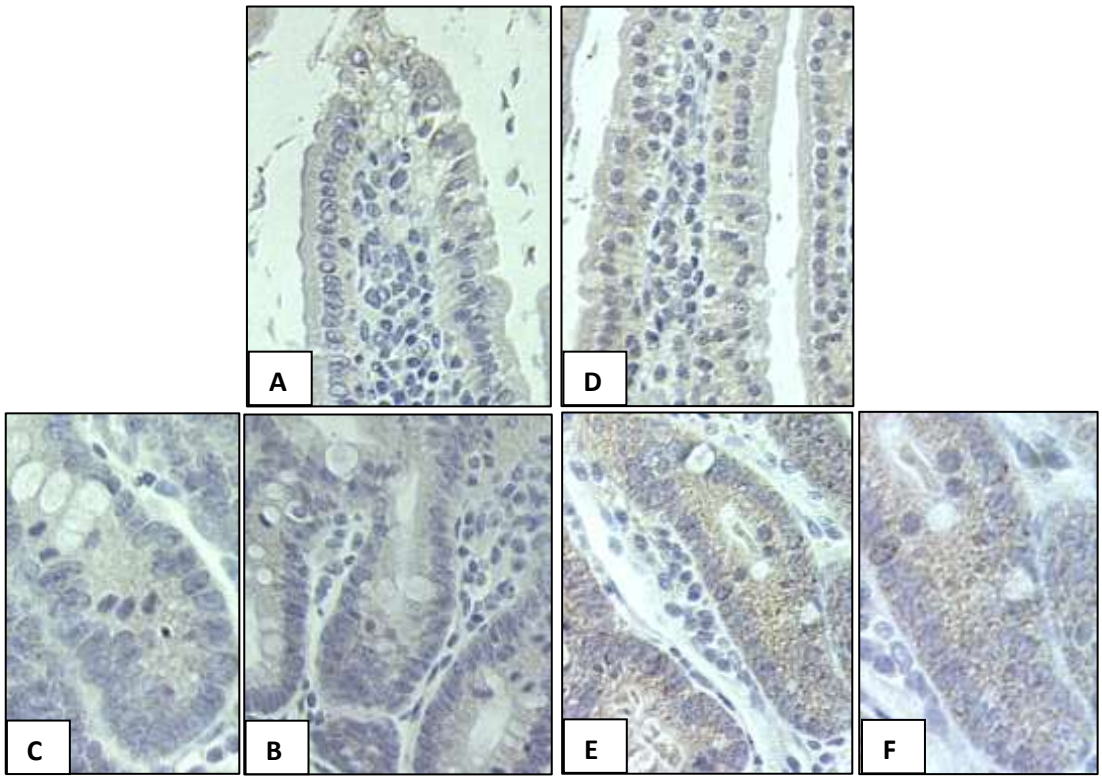


**Figure 3.26 Small intestinal tissues from a control mouse (A, B and C) and an *AhCre*$^{+}$*Apc*$^{fl/fl}$ mouse (D, E and F) stained with anti-PHB Rabbit monoclonal antibody at a dilution of 1:200 and a secondary antibody from Dako (1:200 dilution). A), B), D) & E) are X40 (original magnification) while C) & F) are X63 (original magnification). A and D= villi and B, C, E and F = crypts.**

In the *AhCre*$^{+}$*Apc*$^{fl/fl}$ mouse, crypt epithelial cells showed more brown staining in the cytoplasm compared to those in the *AhCre*$^{+}$*Apc*$^{+/+}$ mouse. This suggests increased PHB expression following *Apc* deletion.

**IHC assessment of PHB expression in *Apc*$^{Min/+}$ mice**

As with other candidate proteins, the same experimental conditions used to assess expression of PHB in *AhCre*$^{+}$*Apc*$^{fl/fl}$ mice were applied to intestinal tissue samples from *Apc*$^{Min/+}$ mice aged 3 and 6 months and wild type control tissues.

**Three month old *Apc*$^{Min/+}$ mice**

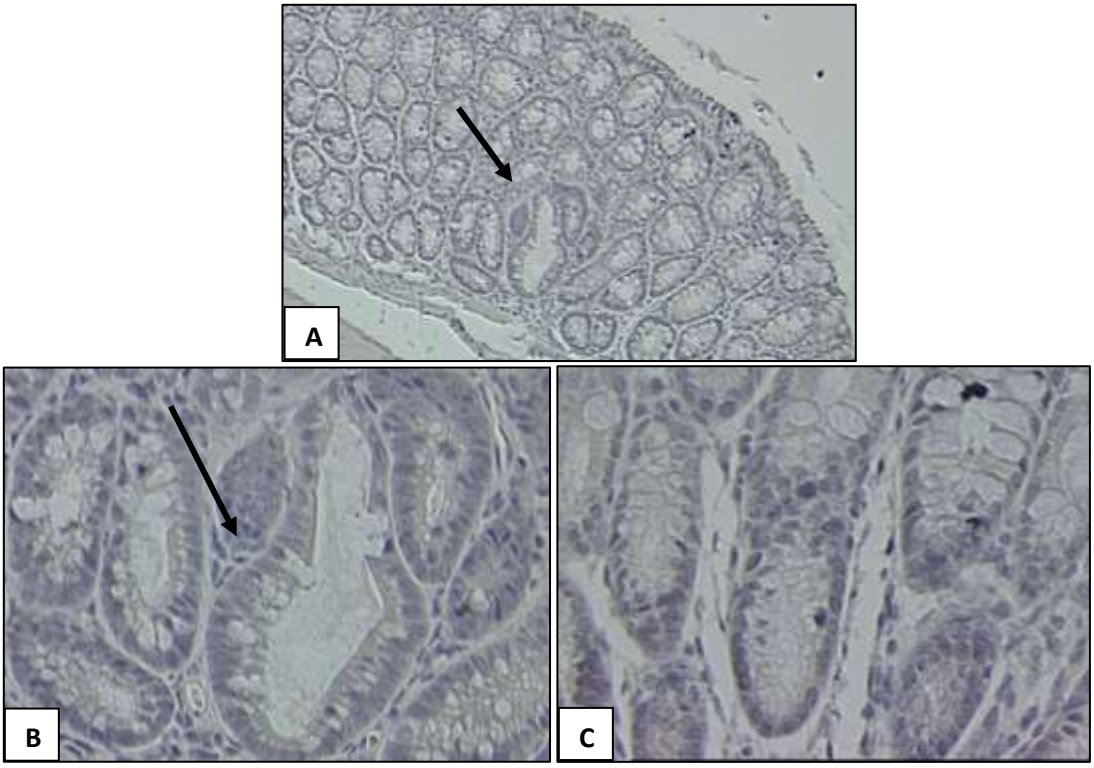


**Figure 3.27 Colonic tissue sections from 3 month old *Apc*$^{Min/+}$ (A and B) and *Apc*$^{+/+}$ (C) mice, stained with anti PHB antibody. A) Shows dysplastic crypts (arrow) x10. B) Shows the same dysplastic crypts X40 and C) shows wild type tissue (X40).**

Unlike *AhCre*$^{+}$*Apc*$^{fl/fl}$ mice, we observed only a very weak PHB staining in lesions from three month old min mice.

**Six month old *Apc*$^{Min/+}$ mice**

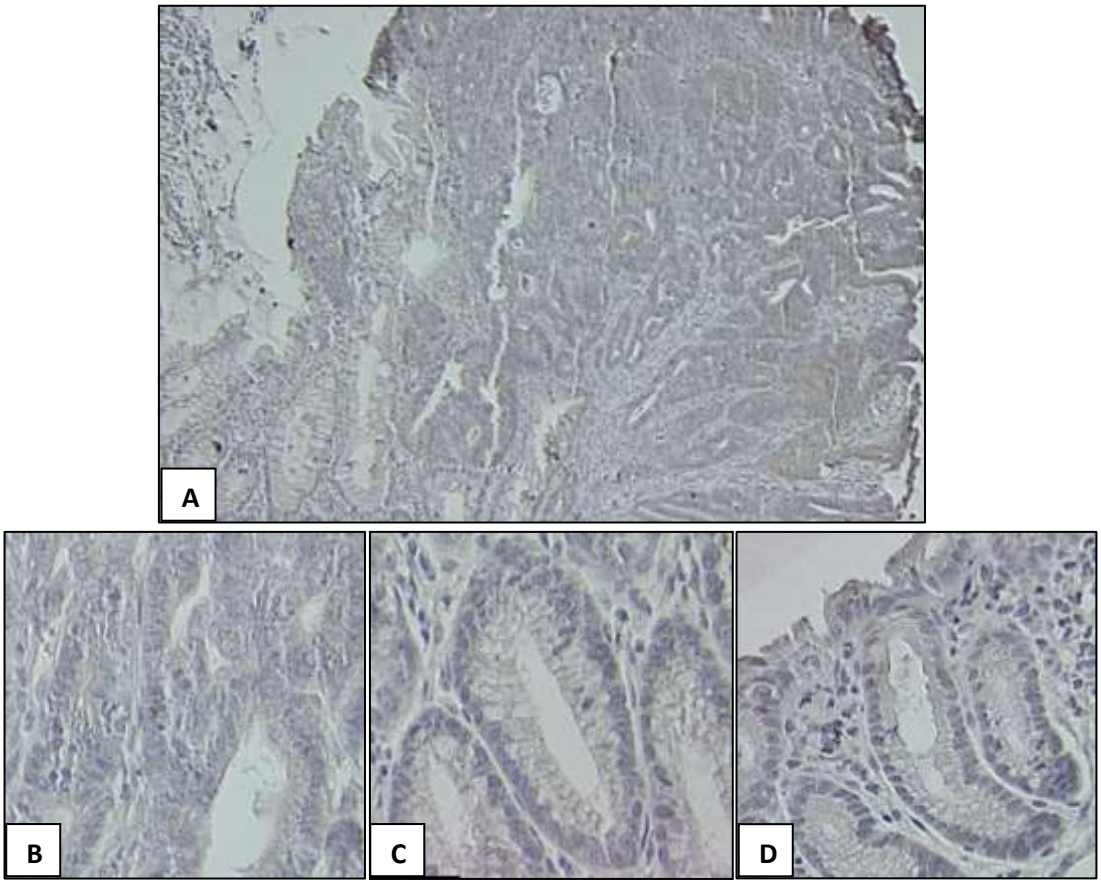


**Figure 3.28 Six month old *Apc*$^{Min/+}$ (A-C) and wild type (D) control mice colonic tissue sections stained with anti-PHB antibody. A) Shows a section from a polyp X10, B) shows magnified section from the polyp (X40), C) shows an adjacent histologically normal tissue (X40) and D) shows section from the colon of a matched wild type mouse (X40).**

Similar to three month old mice, the staining was also weak in lesions from six month old mice. The staining was observed mainly in the cytoplasm of cells in the polyp area in comparison to the histologically normal adjacent and wild type tissues.

PHB also exhibited changes in expression in the same tissue compartments as Beta catenin in both *AhCre*$^{+}$*Apc*$^{fl/fl}$ and *Apc*$^{Min/+}$ mice. Figure 3.29 shows co-expression of the two proteins in a polyp from a six month old *Apc*$^{Min/+}$ mouse.

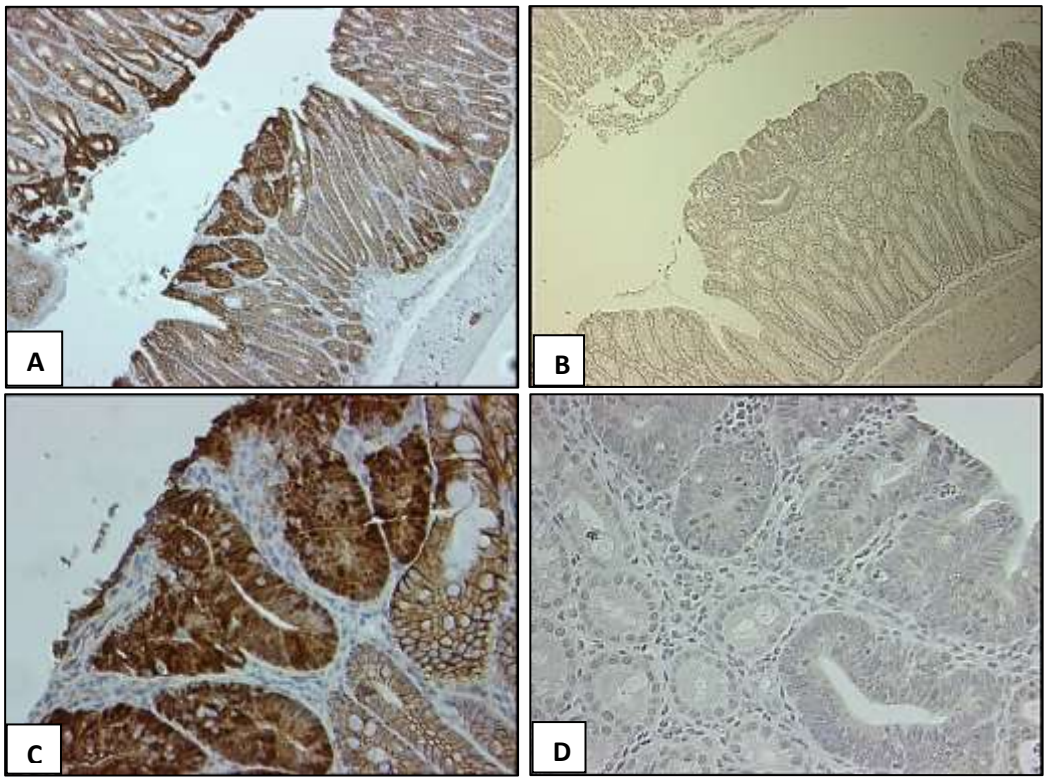


**Figure 3.29 co-expression of Beta catenin and PHB in *Apc*$^{Min/+}$ mice. A and B) show colonic polyp (X10) from a six month old mouse stained with anti-Beta catenin and anti-PHB antibodies respectively. C and D) show magnified sections (X40) from the same polyp in (A) and (B) respectively.**

**Comments on PHB expression after *Apc* deletion**

PHB showed a probable weak over expression in lesions from three month old *Apc* $^{Min/+}$ mice, but more clear differential staining was observed in more advanced adenomas from six month old *Apc*$^{Min/+}$ mice. These observations are consistent with those observed in the *AhCre*$^{+}$*Apc*$^{fl/fl}$ mice, suggesting a possible role for this protein in *Apc* deletion driven colorectal tumourigenesis.

### 3.4.7 IHC assessment of Nucleolin (NCL) expression

NCL is a nucleolar phosphoprotein that was also upregulated in the proteomic analysis performed on the *AhCre*$^{+}$*Apc*$^{fl/fl}$ mice [147]. It is found in the cytoplasm and on the cell surface [167]. NCL expression was assessed in the *AhCre*$^{+}$*Apc*$^{fl/fl}$ mice and their *AhCre*$^{+}$*Apc*$^{+/+}$ counterparts as shown below: the first primary antibody (abcam) tested showed a lot of nonspecific staining. The second primary antibody (abcam) was again initially tested at different dilutions (1:250-1:4000). This showed more specific staining and the best dilution was 1:4000 as shown below.

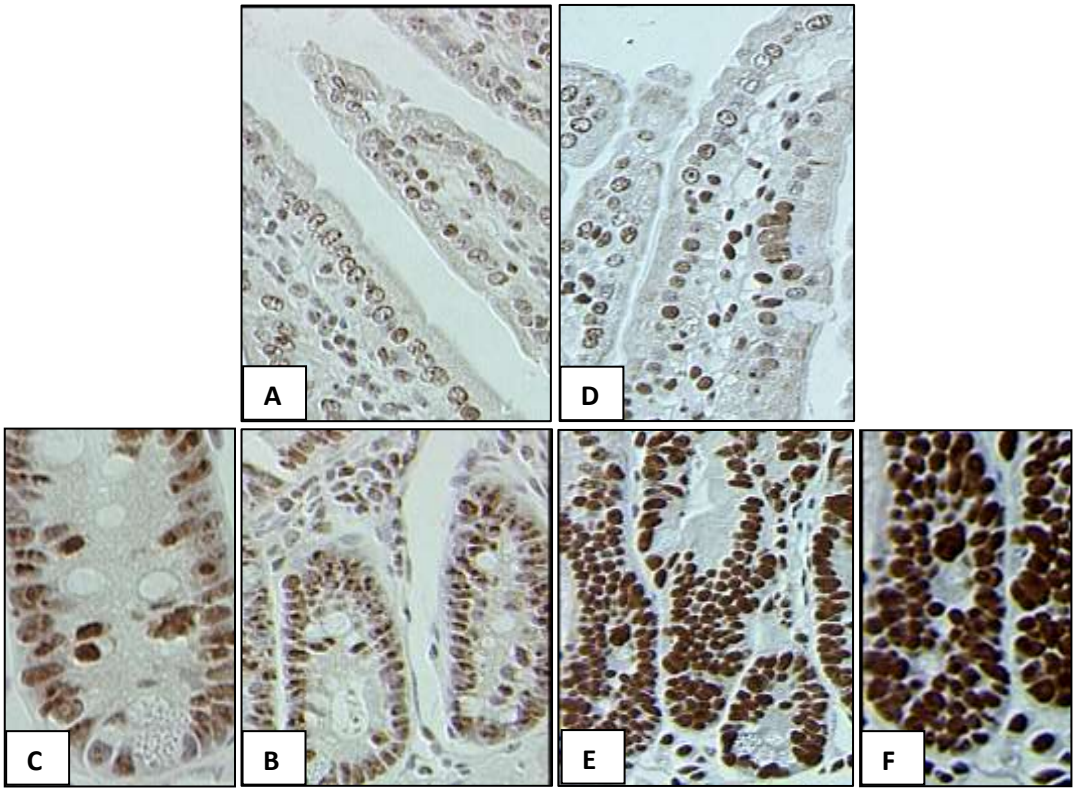


**Figure 3.30 Small intestinal tissues from *AhCre*$^{+}$*Apc*$^{+/+}$ (A, B and C) and *AhCre*$^{+}$*Apc*$^{fl/fl}$ (E, D and F) mice stained with anti-NCL Rabbit polyclonal antibody at a dilution of 1:4000 and a secondary antibody from Dako used at a dilution of 1:200.. A), B), D) & E) are X40 (original magnification) while C) & F) are X63 (original magnification). A and D = villi and B, C, E and F = crypts.**

Nucleolin showed increased nuclear (and nucleolar) staining in the crypt epithelial cells of *AhCre*$^{+}$*Apc*$^{fl/fl}$ mice compared to those in the *AhCre*$^{+}$*Apc*$^{+/+}$ mice.

**IHC assessment of NCL expression in *Apc*$^{Min/+}$ mice**

To validate the observations in *AhCre*$^{+}$*Apc*$^{fl/fl}$ mice, the same experimental conditions used to assess expression of NCL in these mice were applied to intestinal tissue samples from *Apc*$^{Min/+}$ mice and wild type control tissues. No neoplastic lesions from one and three month old mice were available at this stage. Therefore, NCL expression was only assessed in six month old *Apc*$^{Min/+}$ mice.

**Six month old *Apc*$^{Min/+}$ mice**

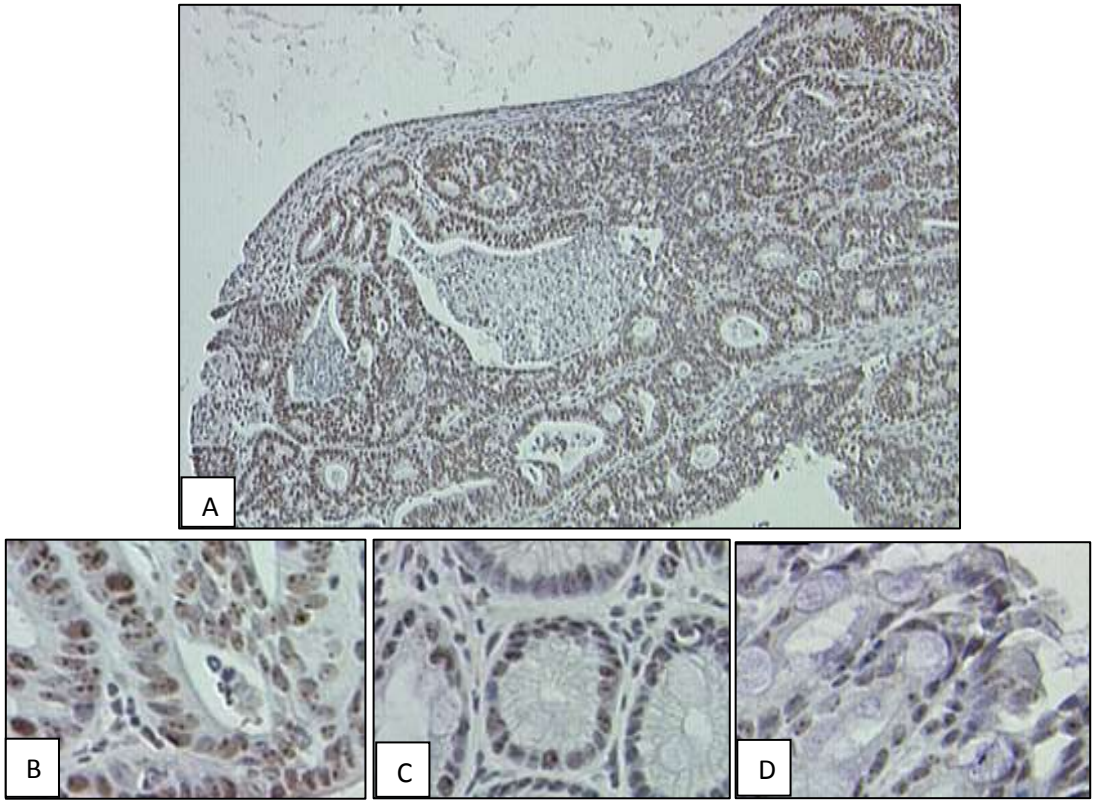


**Figure 3.31 Six month old *Apc*$^{Min/+}$ (A-C) and *Apc*$^{+/+}$ (D) mice colonic tissue sections stained with anti-NCL Rabbit polyclonal antibody (abcam, 1:4000) and a secondary antibody from Dako (1:200). A) is a colonic polyp X10, B) is a magnified section from the polyp (X40), C) is normal appearing tissue adjacent to the polyp (X40) and D) is colonic tissue section from a matched *Apc*$^{+/+}$ control mouse (X40).**

Polyp tissue (A and B) showed a clear increase in NCL staining intensity which was mainly nuclear (nucleolar) in location compared to adjacent normal tissue (C) and wild type tissue (D).

By examining the expression of NCL in the context of a deranged Wnt pathway, it was obvious that NCL and Beta catenin co-express. This was evident in the crypts of *AhCre*$^{+}$*Apc*$^{fl/fl}$ mice and the neoplastic lesions in *Apc*$^{Min/+}$ mice (figure 3.32).

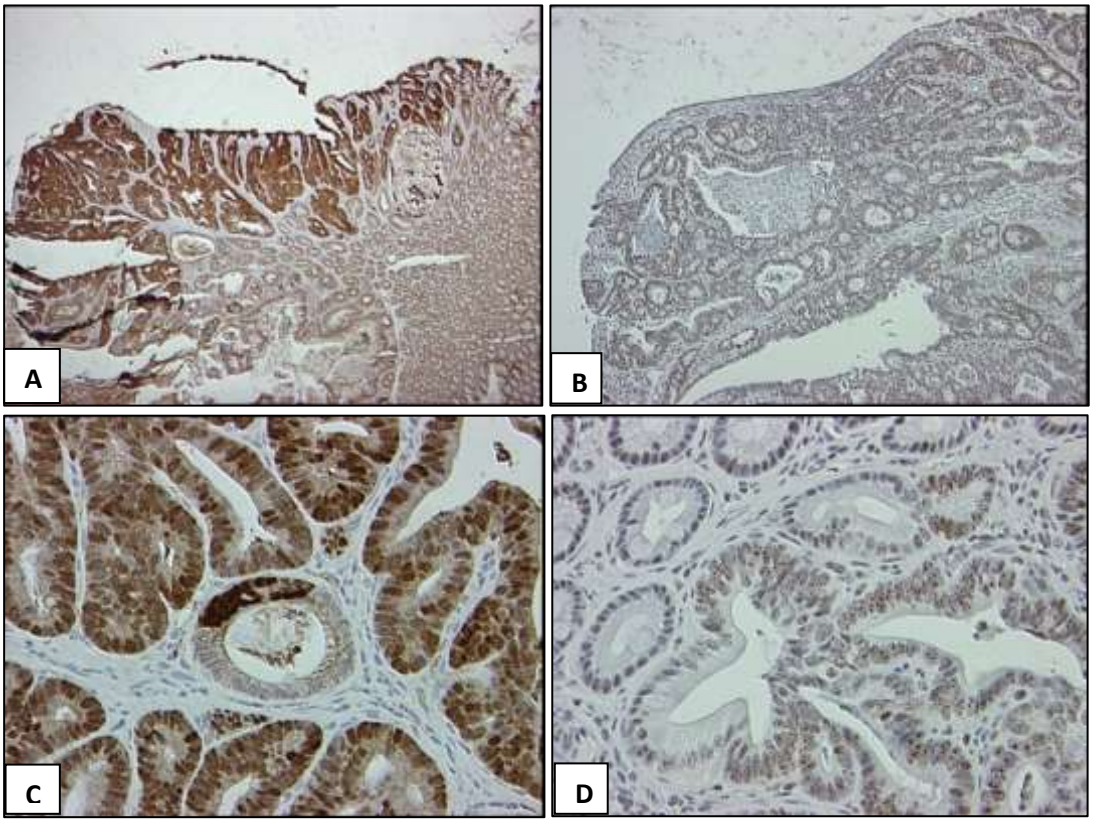


**Figure 3.32 Co-expression of Beta catenin and NCL in the same tissue compartments in *Apc*$^{Min/+}$ mice. A and B) show colonic polyp (X10) from a six month old mouse stained with anti-Beta catenin and anti-NCL antibodies respectively. C and D) show magnified sections (X40) from the same polyp in (A) and (B) respectively.**

This co-expression again supports the proposal that candidate proteins demonstrated changes in expression in the setting of Apc loss induced activation of the Wnt pathway.

### Comments on NCL expression after *Apc* deletion

Nucleolin, a ubiquitous nucleolar phosphoprotein is involved in diverse cellular functions such as ribosome biogenesis, transcription, G-quadreplex binding and apoptosis [169]. *c-Myc*, a Wnt target gene and a key molecule in cellular proliferation and growth, has been suggested to have a G-quadreplex structure that negatively regulates its expression [169]. Interestingly NCL has been reported to bind to this G-quadreplex structure, stabilising it. Therefore, Nucleolin may play a controlling role in high proliferation states (including cancer) by regulating c-Myc

activity [169]. This is supported by observations that NCL is highly expressed in rapidly dividing cells and rapidly degrades when cells become quiescent [214].

### 3.4.8 IHC assessment of HMGB1 expression

HMGB1 is another candidate protein that showed up-regulation in the initial proteomics studies using the *AhCre*$^{+}$*Apc*$^{fl/fl}$ mouse model [147]. It is a nuclear chromatin binding protein and an extracellular signalling molecule that mediates inflammation as well as cell differentiation and migration [172]. Its expression was assessed in *AhCre*$^{+}$*Apc*$^{fl/fl}$ and *AhCre*$^{+}$*Apc*$^{+/+}$ mice using optimised IHC experimental conditions: the first primary antibody (EBL) was tested at different dilutions with varying DAB incubation times and secondary antibody dilutions, but it caused strong staining in control tissues from various mice. The second antibody (abcam) also gave rise to similar staining patterns, as shown below.

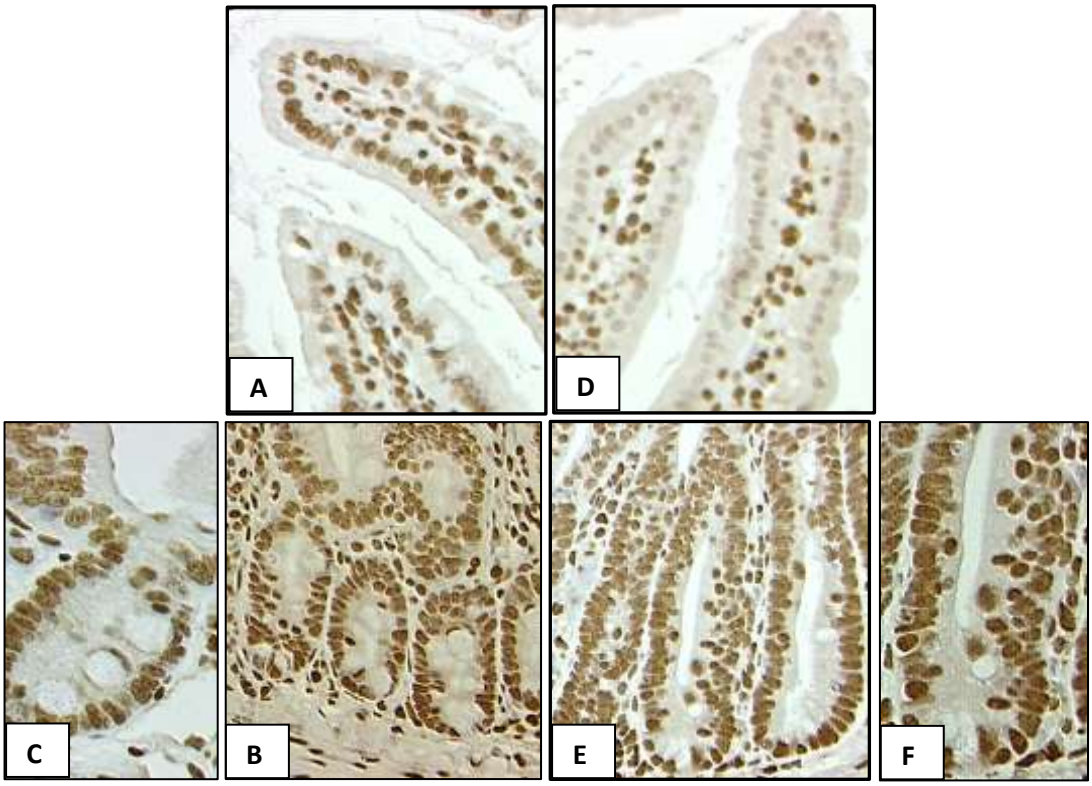


**Figure 3.33 Small intestinal tissues from *AhCre*$^{+}$*Apc*$^{fl/fl}$ and *AhCre*$^{+}$*Apc*$^{+/+}$ mice stained with anti-HMGB1 Rabbit polyclonal antibody (abcam, dilution of 1:4000). The secondary antibody was from Dako at a dilution of 1:200. Images A), B) and C) are from *AhCre*$^{+}$*Apc*$^{+/+}$ mouse and D), E) and F) are from *AhCre*$^{+}$*Apc*$^{fl/fl}$ mouse. A), B), D) & E) are X40 (original magnification) while C) & F) are X63 (original magnification). A and D= villi and B, C, E and F = crypts.**

The epithelial cells of the villi of the *AhCre*$^{+}$*Apc*$^{fl/fl}$ mouse showed no observable nuclear staining whilst those of the crypts in the same mice did show a staining intensity similar to that observed in the crypt cells of *AhCre*$^{+}$*Apc*$^{+/+}$ mice. This suggests less HMGB1 protein in the villi of *AhCre*$^{+}$*Apc*$^{fl/fl}$ mouse relative to the crypts of the same mice or the villi of control mice. We cannot currently provide an explanation for the loss of HMGB1 from the villi of the knockout mice, but a structural modification of this protein or a subtle change in its expression may cause retention of abnormal cells within the crypts.

**IHC assessment of HMGB1 expression in *Apc*$^{Min/+}$ mice**

HMGB1 expression was also assessed in tissue samples from *Apc*$^{Min/+}$ mice aged 3 and 6 months along with their wild type counterparts.

**Three month old *Apc*$^{Min/+}$ mice**

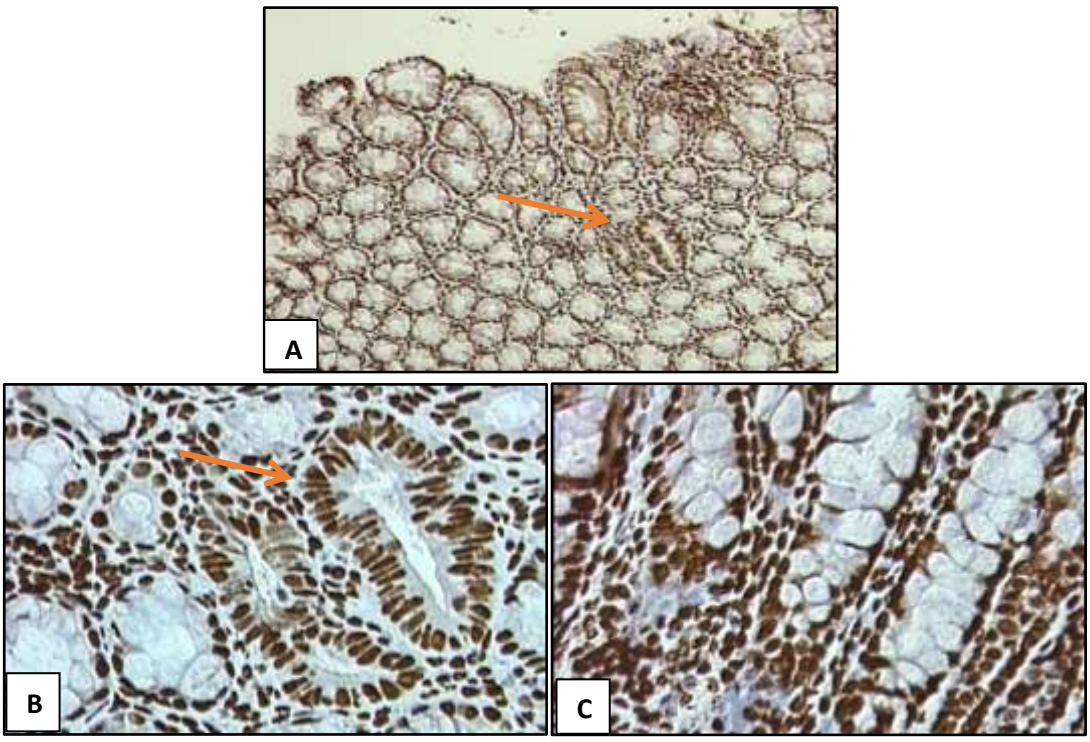


**Figure 3.34 Colonic sections from 3 month old *Apc*$^{Min/+}$ (A and B) and *Apc*$^{+/+}$ (C) mice stained with anti-HMGB1 antibody (abcam, 1:4000) and a secondary antibody from Dako (1:200). Image A) shows two dysplastic crypts (arrow), X10 original magnification. Image B) shows the same dysplastic crypts and C) shows wild type tissue sample (X40 original magnification).**

Dysplastic crypts showed increased number of cells, loss of goblet cells and larger nuclei. The above mentioned changes made dysplastic crypts stand out; otherwise the

intensity of HMGB1 staining in these crypts was similar to that of the surrounding normal and wild type control tissues.

**Six month old *Apc*$^{Min/+}$ mice**


**Figure 3.35 Six month old *Apc*$^{Min/+}$ (A-C) and *Apc*$^{+/+}$ (D) mice intestinal tissue samples stained with anti-HMGB1 rabbit polyclonal antibody (1:4000). The secondary antibody from Dako was used at a dilution of 1:200. A) is a colonic polyp showing dysplastic features in the form of increased number of cells and larger nuclei (black arrow) and normal adjacent tissue (red arrow). B), C) and D) are magnified (X40, original magnification) sections from the polyp, the normal appearing tissue adjacent to the polyp and crypt area from a matched wild type control mouse respectively.**

More intense staining was obviously seen in the polyp area relative to the normal adjacent tissue but this was slightly greater than that observed in the wild type control tissue. The other parts of the colonic epithelium in the same *Apc*$^{Min/+}$ tissue section, showed staining patterns similar to that observed in wild type tissue (not shown). Morphological changes such as the increase in the size of nuclei and number of cells and loss of goblet cells in the polyp area may thus have contributed to the apparent difference in staining intensity between polyp and wild type tissues.

**Comments on HMGB1 expression following *Apc* deletion**

HMGB1 is a nuclear protein involved in the regulation of gene expression without sequence specificity [215]. It is also found in the cytoplasm and as a secretory molecule with cytokine properties [216]. The latter form of the protein has been shown to be present in several cancers including colon cancer [217]. Furthermore, HMGB1 secretion by cancer cells has been suggested to mediate proliferation, migration and invasion by these cells [218]. In this piece of work, HMGB1 did not show a noticeable change in expression in the areas of the tissue where the WNT pathway was constitutively active, namely in the crypts of the $AhCre^{+}Apc^{fl/fl}$ mice and the neoplastic lesions of the $Apc^{Min/+}$ mice. However, in $AhCre^{+}Apc^{fl/fl}$ mice, villi showed less HMGB1 expression compared to villi in the control mice. Moreover, due to retention of new cells in the crypts fowlloing *Apc* deletion in $AhCre^{+}Apc^{fl/fl}$ mice [44], cells in the villi might not be shed normally and get older than they should be.

### 3.4.9 IHC assessment of Nucleophosmin (NPM) expression

NPM is another protein that was detected by iTRAQ/MS-MS as being upregulated in the intestinal epithelium of *AhCre*$^{+}$*Apc*$^{fl/fl}$ mice after deletion of both *Apc* alleles [147]. It is a ubiquitous protein that is mainly localised to the nucleus [156]. It has multiple functions including ribosome biogenesis and regulation of cellular proliferation and transcription of some tumour suppressors [159]. Its expression was assessed in *AhCre*$^{+}$*Apc*$^{fl/fl}$ mice and *AhCre*$^{+}$*Apc*$^{+/+}$ control mice as shown below: the primary antibody was initially tested at different dilutions (1:50-1:6000). The dilution 1:6000 showed the best differential staining as shown below.

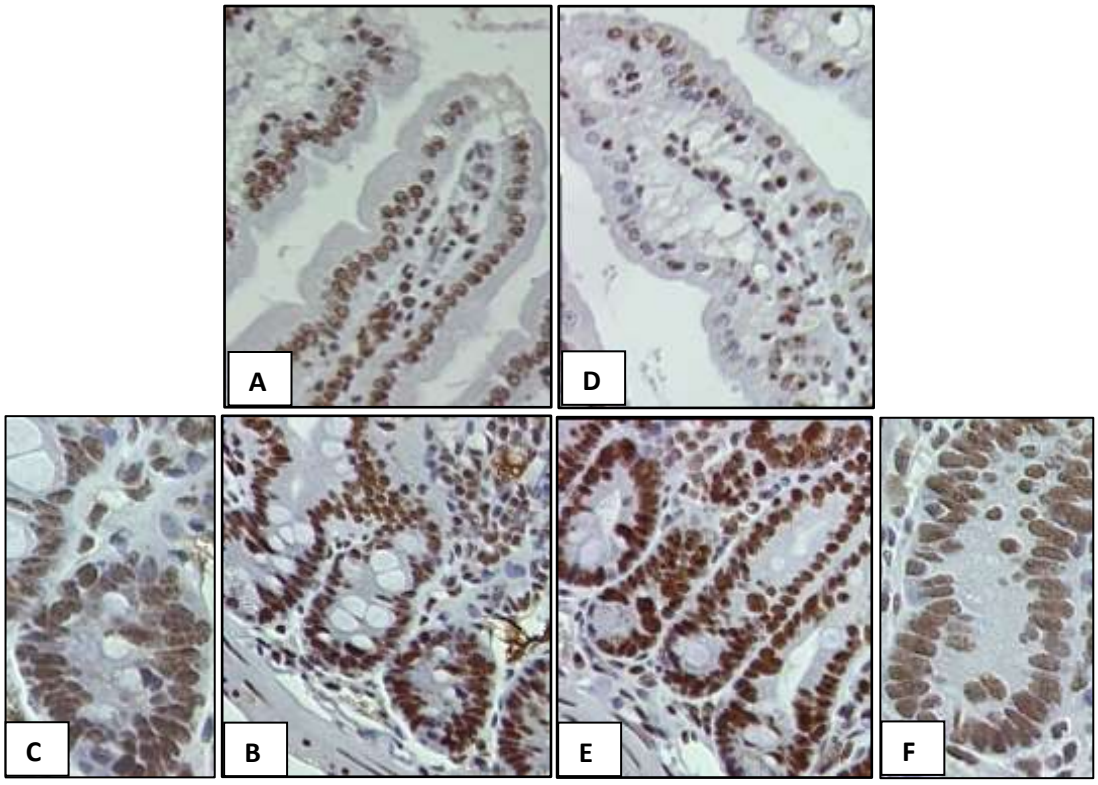


**Figure 3.36 Small intestinal tissues from an *AhCre*$^{+}$*Apc*$^{+/+}$ control mouse (A, B and C) and an *AhCre*$^{+}$*Apc*$^{fl/fl}$ mouse (D, E and F) stained with anti-NPM mouse monoclonal antibody at a dilution of 1:6000 with a secondary antibody from Dako at a dilution of 1:200. A), B), D) & E) are X40 (original magnification) while C) & F) are X63 (original magnification). A and D= villi and B, C, E and F = crypts.**

In the *AhCre*$^{+}$*Apc*$^{fl/fl}$ mouse, villus epithelium showed less nuclear NPM staining than that observed in the crypts. At the same time, there was no observable difference in the intensity of NPM staining between the crypts of *AhCre*$^{+}$*Apc*$^{fl/fl}$ and control mice. Similar to HMGB1, NPM may contribute to the retention of cells within the abnormal crypts following deletion of *Apc*.

**IHC assessment of NPM expression in *Apc*$^{Min/+}$ mice**

The same experimental conditions used in *AhCre*$^{+}$*Apc*$^{fl/fl}$ mice were applied to intestinal tissue samples from *Apc*$^{Min/+}$ mice to assess NPM expression in established neoplastic lesions.

**Three month old *Apc*$^{Min/+}$ mice**

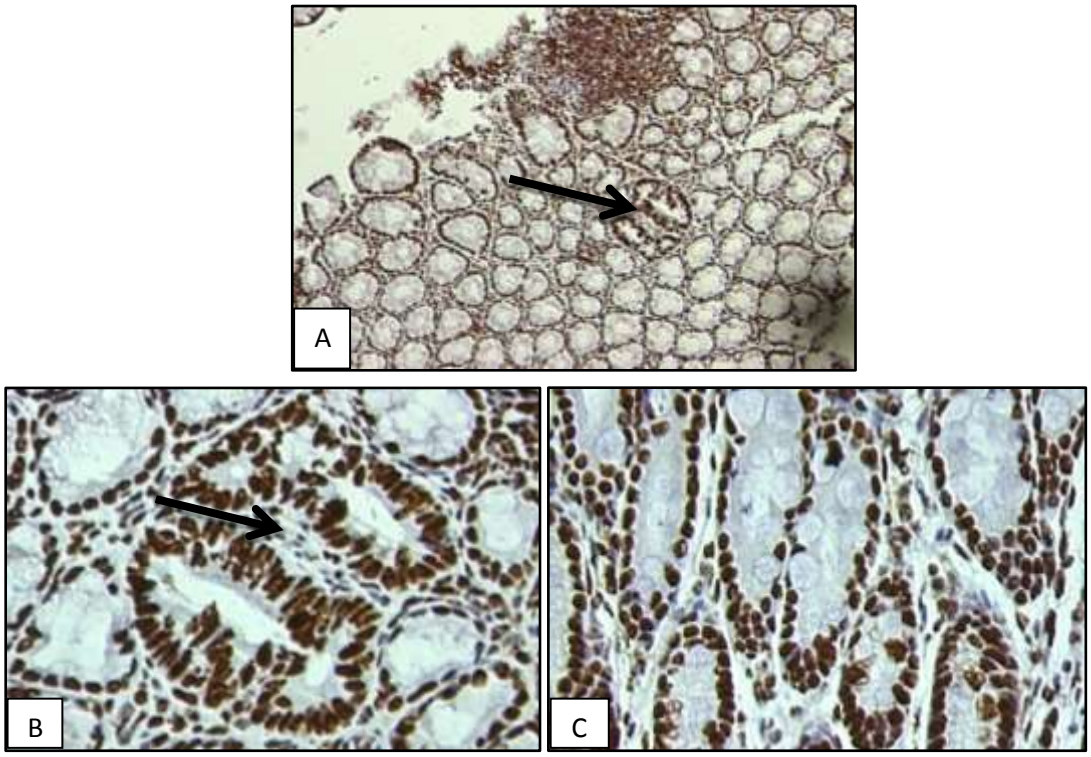


**Figure 3.37 Colonic tissue sections from 3 month old *Apc*$^{Min/+}$ (A and B) and *Apc*$^{+/+}$ (C) mice stained with anti-NPM antibody. A) shows two dysplastic crypts (arrow) x10, B) shows the same dysplastic crypts X40 and C) shows wild type tissue control.**

NPM staining intensity in the lesion was not clearly different from that observed in the histologically normal adjacent or wild type tissues.

**Six month old *Apc*$^{Min/+}$ mice**

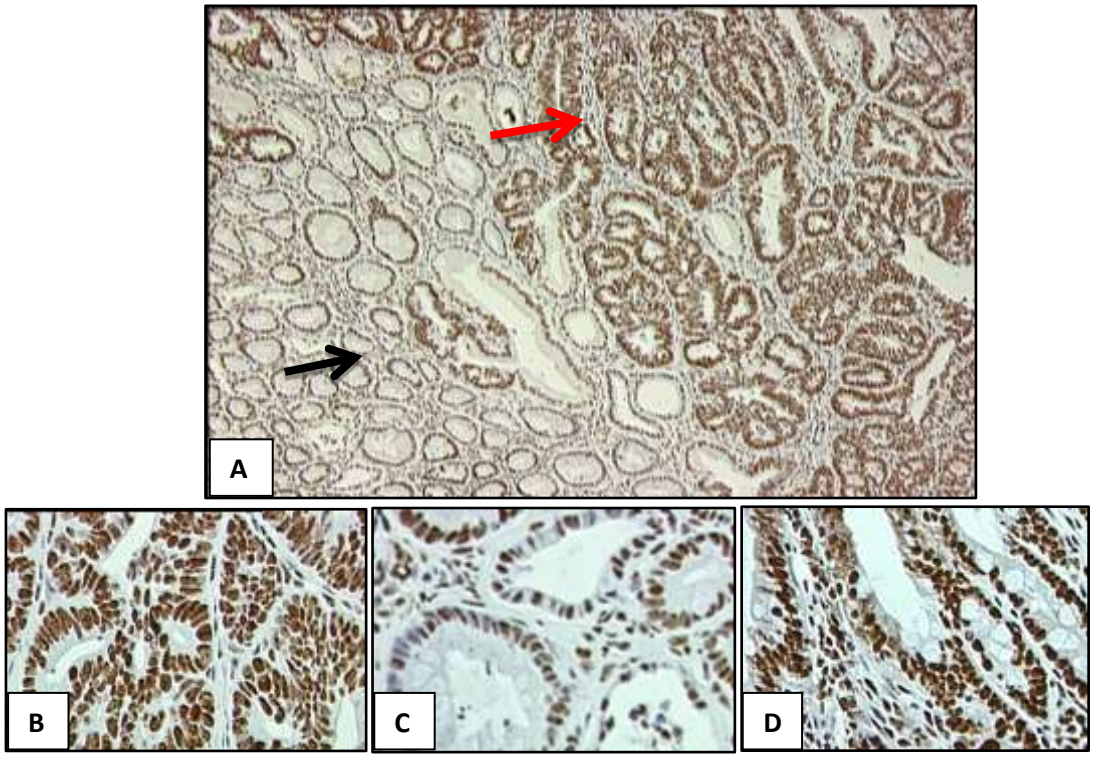


**Figure 3.38 Six month old *Apc*$^{Min/+}$ (A-C) and *Apc*$^{+/+}$ (D) control mice colonic tissue sections stained with anti-NPM antibody. A) shows a section from a polyp (red arrow) and adjacent normal appearing tissue (black arrow) X10, B) shows magnified section from the polyp (X40), C) shows magnified section from the tissue adjacent to the polyp (X40) and D) shows section from the colon of a matched *Apc*$^{+/+}$ mouse (X40).**

NPM protein expression was increased mainly in the nuclei (nucleoli prominently) of cells in the polyp area compared to the histologically normal adjacent tissue. Less obvious differences in staining intensity were observed when polyp tissue was compared to wild type control tissue.

**Comments on NPM expression after *Apc* deletion**

Nucleophosmin is a multifunctional nucleolar phospho-protein which is suggested to shuttle constantly between the nucleus and the cytoplasm [219]. In addition to ribosome assembly and transportation of ribosomal proteins to the cytoplasm, NPM is reported to play an essential role in cellular proliferation and growth by regulating cell cycle progression and centrosome duplication [220]. Moreover, NPM may also regulate the activity of tumour suppressors such as p53 and retinoblastoma protein (Rb) by direct binding and may interact with transcription factors such as c-MYC and NF-κB [221, 222]. In this current work, a clear change in the expression of NPM was not observed during colonic adenoma development. This may be explained by

suggestions made by other groups that NPM is mainly involved in the later stages of carcinogenesis, namely invasion and migration [219].

### 3.4.10. IHC assessment of DDX5 expression

DDX5 also showed upregulation in the intestinal epithelium of *AhCre*$^{+}$*Apc*$^{fl/fl}$ mice as detected by iTRAQ-LC/MS analysis [147]. Normally it is a multifunctional nuclear protein [154]. We assessed its expression in *AhCre*$^{+}$*Apc*$^{fl/fl}$ and control mice as shown below: the primary antibody (abcam) was initially tested at dilutions 1:500-1:40,000.

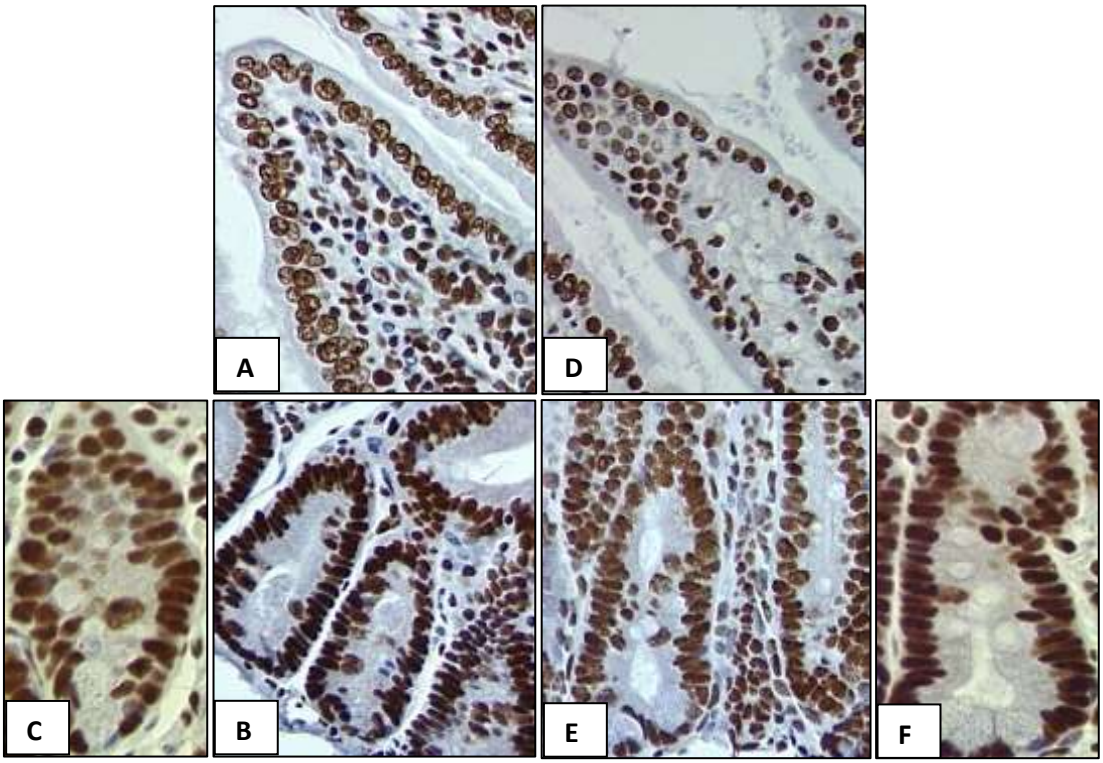


**Figure 3.39 Small intestinal tissues from an *AhCre*$^{+}$*Apc*$^{+/+}$ control mouse (A, B and C) and an *AhCre*$^{+}$*Apc*$^{fl/fl}$ mouse (D, E and F) stained with anti-DDX5 mouse monoclonal antibody at a dilution of 1:40000 with a secondary antibody from Dako at a dilution of 1:200. A), B), D) & E) are X40 (original magnification) while C) & F) are X63 (original magnification). A and D= villi and B, C, E and F = crypts.**

This antibody was diluted to concentrations of up to 1:40000 and still no differential staining was observed between cells in the crypts and villi nor when *AhCre*$^{+}$*Apc*$^{fl/fl}$ tissue was compared to control tissue. Therefore we decided to stop IHC work on this protein at this stage.

**Comments on DDX5 expression following *Apc* deletion**

DDX5 was the only protein among those studied not to show any observable change in small intestinal tissues following *Apc* deletion. However, DDX5 has previously been reported to be over expressed in a number of cancers including CRC [155]. Moreover, DDX5 has been suggested to be over expressed in colorectal tumourigenesis even in pre-invasive adenomas in humans [155]. Either experimental conditions or species differences may have been responsible for seeing no change in DDX5 expression in our mouse models following *Apc* deletion.

### 3.5 Western blot analysis of candidate protein expression

Although immunohistochemistry is a good and commonly used technique to study protein expression and provides information about the amount, subcellular localisation and even post-translational modifications of proteins, it still can be criticised as some antibodies show non-specific staining patterns and quantification can sometimes be difficult.

Western blot analysis can support IHC results by further characterising the proteins under investigation. For example a more reproducible quantification of proteins can be achieved using western blots. Moreover, by showing antibody specificity, western blots can give more credibility to IHC results.

In this section, the aims of performing western blots were to assess the specificity of the primary antibodies that were used in the IHC work described above. They were also used as a semi-quantitative analysis of changes in the expression of candidate proteins in the two animal models used in the IHC work.

Guided by the results described above, western blot experiments were focused on those proteins that demonstrated clear differential staining patterns by IHC.

#### 3.5.1 Assessment of specificity of primary antibodies used in IHC work

A criticism of IHC as described above is how genuine or specific are the results. This can be judged primarily based on the specificity of the primary antibodies used. Therefore, the western blot images shown in figure 3.35 demonstrate the corresponding bands for some of the primary antibodies that showed differential staining in the IHC part of the study.

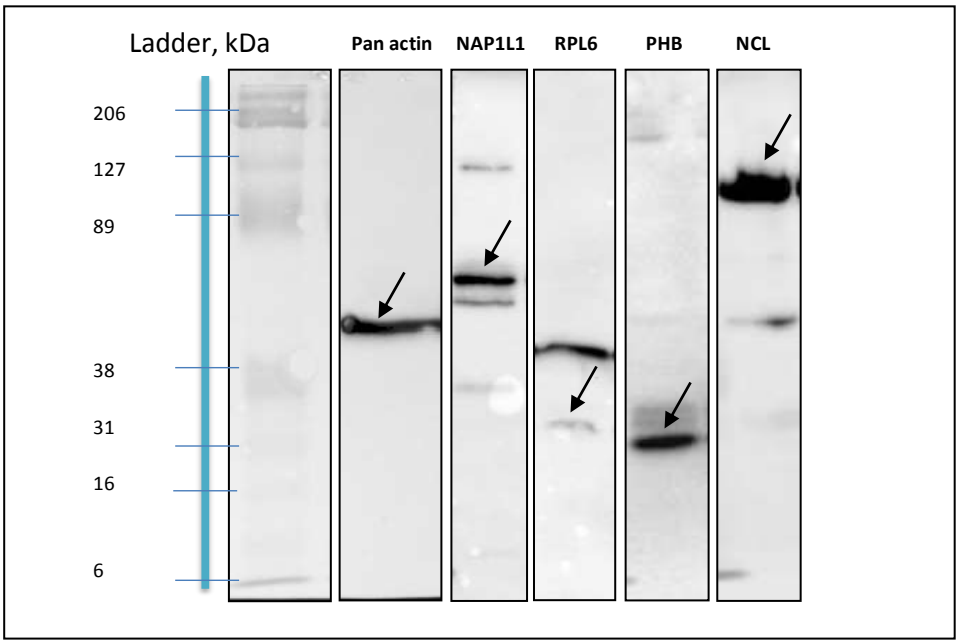


**Figure 3.40 Representative Western blot images. Each column represents whole cell protein extracts from HT29 cells. Full length blots are shown with the relevant candidate protein band indicated by an arrow. SFRS2, FABP6 and Beta catenin blots are not shown.**

The presence of more than one band in some of the blots might have been due to the presence of isoforms/post-translationally modified forms of the relevant protein however, no information could be found to support this neither in the company data sheets nor in literature.

The table below shows details that assist in the interpretation of figure 3.35.

| Protein | Molecular weight (kDa)-data sheet | Primary antibody dilution | Used dilution | Secondary antibody dilution |
|---|---|---|---|---|
| NAP1L1 | 45 | 1:250-1000 | 1:1000 | 1:1000 |
| RPL6 | 33 | 1:500-5000 | 1:500 | 1:1000 |
| SFRS2 | 35 | 1:1000 | | 1:1000 |
| PHB | 30 | 1:500-1000 | 1:1000 | 1:1000 |
| FABP6 | 14 | 1:50 | | 1:1000 |
| NCL | 76 | 1:1000 | 1:1000 | 1:1000 |
| Beta catenin | 92 | 1:500-2000 | | 1:1000 |
| Pan actin | 42 | 1:1000 | 1:1000 | 1:1000 |

**Table 3.1 Details of the reagents used to produce the images in figure 3.40 and the other western blot analyses.**

As seen in the above table, the specificity of six candidate proteins in addition to Beta catenin was assessed. SFRS2, FABP6 and Beta catenin antibodies did not show any conclusive results (nonspecific background signal) in the western blot experiments. The anti-FABP6 antibody used was not reactive to human protein according to the manufacturer. This could explain the lack of specific bands in

proteins extracted from HCT116 and HT29 cells. For SFRS2 and Beta catenin, several modifications of the protocols (details can be found below) were tried to detect better bands. Unfortunately despite all variations, antibodies to these proteins did not work in western blotting.

### 3.5.2 Western blot quantification of candidate proteins in *AhCre*$^{+}$*Apc*$^{fl/fl}$ and *Apc*$^{Min/+}$ mice

To further validate the IHC results, the levels of candidate proteins that showed differential staining were examined using western blot analysis. All measurements made were relative the abundance of pan actin, enabling a comparison of expression for the individual proteins in *AhCre*$^{+}$*Apc*$^{fl/fl}$ and *Apc*$^{Min/+}$ mice with their wild type counterparts to be made.

**Relative expression of NAP1L1 in *AhCre*$^{+}$*Apc*$^{fl/fl}$ and *Apc*$^{Min/+}$ mice**

IHC analysis of NAP1L1 demonstrated cytoplasmic overexpression in *AhCre*$^{+}$*Apc*$^{fl/fl}$ and *Apc*$^{Min/+}$ mice in the Wnt active areas. Epithelial cell extracts from *AhCre*$^{+}$*Apc*$^{fl/fl}$ mice and colonic tissues from one, three and six month old *Apc*$^{Min/+}$ mice were used to extract whole proteins as described in the methods section. The whole cell lysates were then used in the western blot analyses of NAP1L1 expression as shown below.

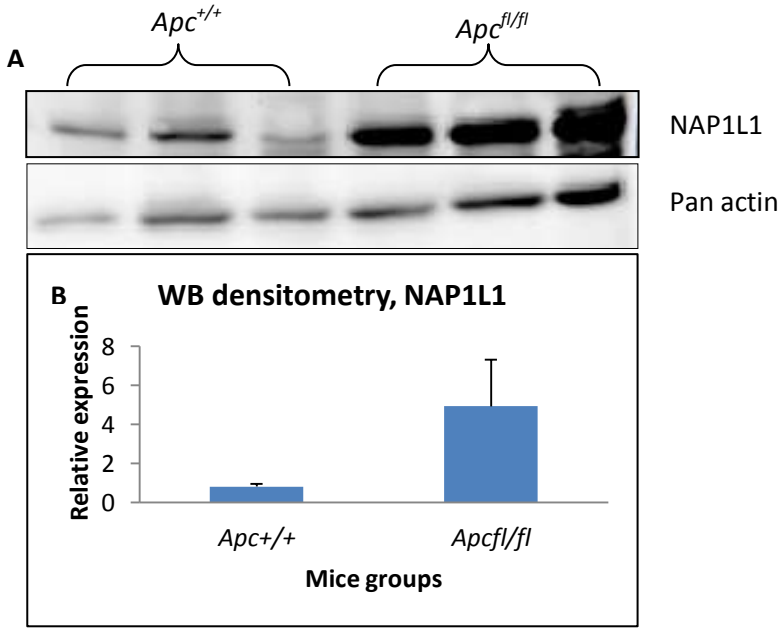


**Figure 3.41 Western blot analysis of NAP1L1 expression in whole cell lysates obtained from small intestinal epithelial cell extracts of *AhCre*$^{+}$*Apc*$^{+/+}$ and *AhCre*$^{+}$*Apc*$^{fl/fl}$ mice (A). B) Shows fold change in NAP1L1 expression in *AhCre*$^{+}$*Apc*$^{fl/fl}$ mice relative to its level in *AhCre*$^{+}$*Apc*$^{+/+}$ mice (N2, 3 mice per group).**

The observed increase in NAP1L1 expression following *Apc* deletion in *AhCre*$^{+}$*Apc*$^{fl/fl}$ mice supported the IHC results for this protein. This indicated that NAP1L1 is directly or indirectly involved in the observed events and that the visual cytoplasmic overexpression of NAP1L1 after *Apc* deletion was associated with an increase in total expression of this protein. Unfortunately, lack of good quality tissue samples prevented the production of a sufficient number of experiments to show statistical significance. This is despite the use of different protein extraction methods (as outlined in the methods section) to improve protein quality and quantity.

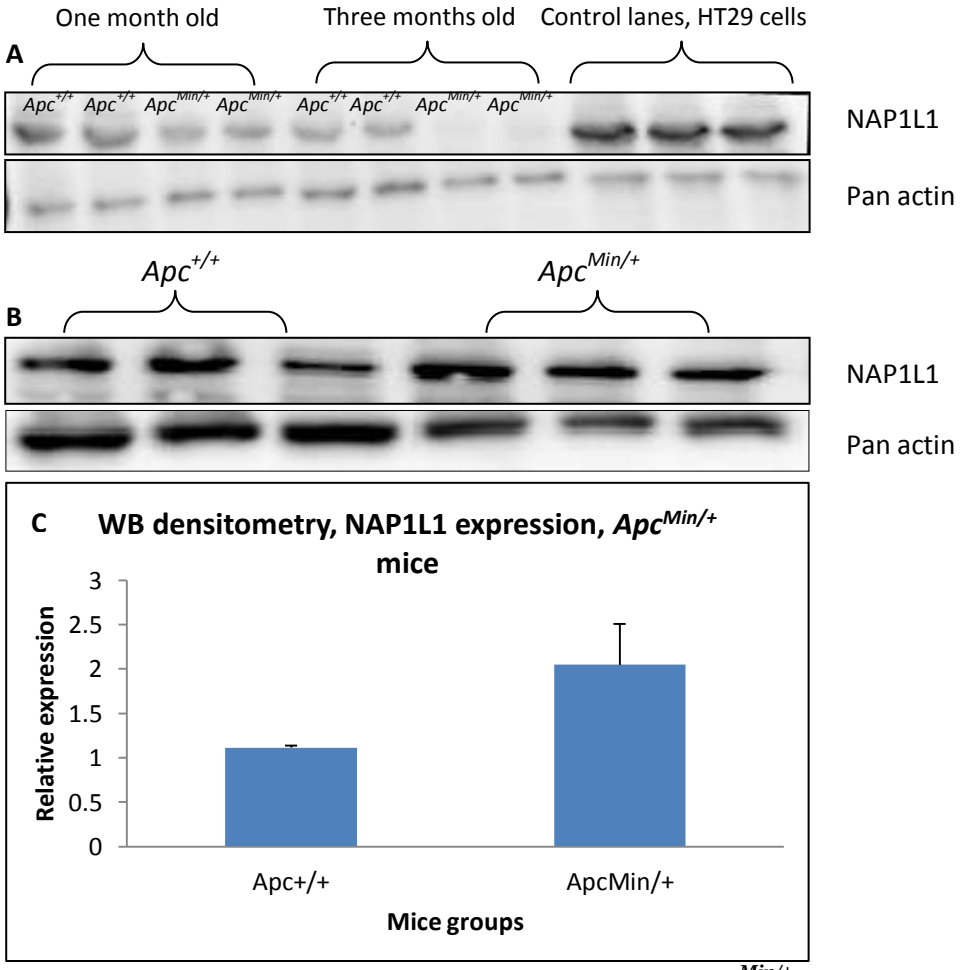


**Figure 3.42 Western blot analysis of NAP1L1 expression in *Apc*$^{Min/+}$ mice and their wild type counterparts. A) shows NAP1L1 expression in one and three month old *Apc*$^{Min/+}$ mice. B) Shows NAP1L1 expression in six month old *Apc*$^{Min/+}$ mice and wild type counterparts. C) Shows densitometry analysis of NAP1L1 expression in six month old *Apc*$^{Min/+}$ mice. N=2, n=3.**

Similar to *AhCre*$^{+}$*Apc*$^{fl/fl}$ mice, *Apc*$^{Min/+}$ mice showed increased relative expression of NAP1L1 in polyps from the heterozygous group of the six month old mice (figure 3.42 B and C). Again lack of sufficient tissue samples was an obstacle for producing enough data from one, three and six month old *Apc*$^{Min/+}$ mice.

Similar studies were also attempted to evaluate the expression of PHB and NCL (figures 3.38 and 3.39) in both animal models using western blotting as shown below.

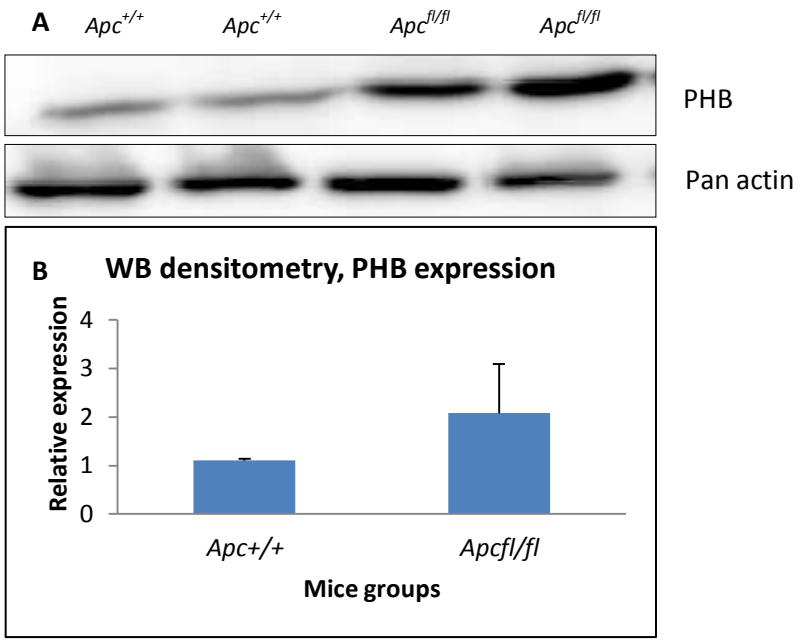


**Figure 3.43 Western blot analysis of PHB expression in whole cell lysates from intestinal epithelial cell extracts of *AhCre*$^{+}$*Apc*$^{+/+}$ and *AhCre*$^{+}$*Apc*$^{fl/fl}$ mice. A) shows PHB bands in both mice groups. B) Shows densitometry analysis of relative PHB expression in both mouse models. N=2, n2.**

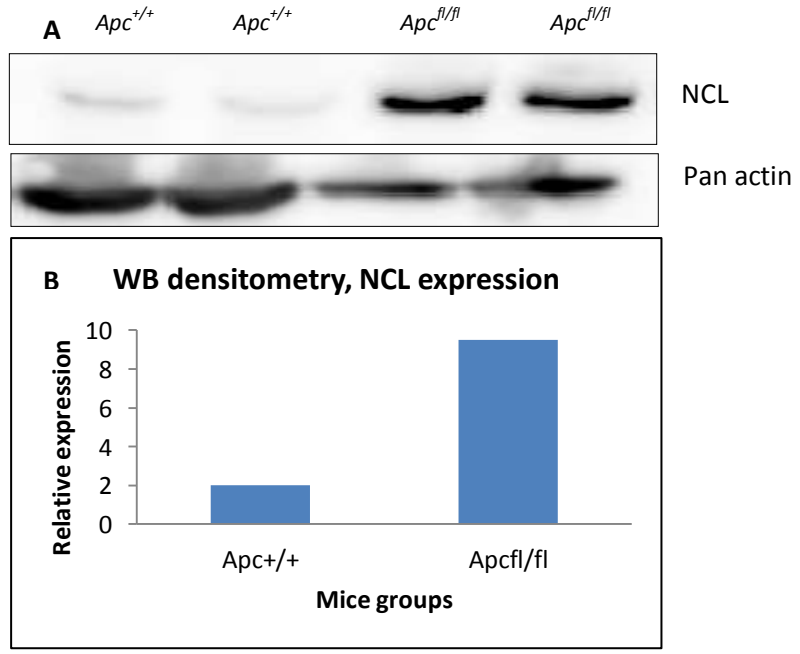


**Figure 3.44 Western blot analysis of NCL expression in *AhCre*$^{+}$*Apc*$^{+/+}$ and *AhCre*$^{+}$*Apc*$^{fl/fl}$ mice. A) is a blot showing NCL bands in both mice groups (two samples each). B) Shows densitometry analysis of relative NCL expression in both mouse models. N=1, n2.**

Again, western blot results for PHB and NCL were in agreement with the IHC results observed in *AhCre*$^{+}$*Apc*$^{fl/fl}$ mice. Due to the reasons mentioned before, the number of experiments carried out was less than that required to show significance. Moreover, western blot experiments in *Apc*$^{Min/+}$ mice did not yield conclusive results for these two proteins. This was mainly due to inability to proceed with the optimisation process because of a lack of sufficient good quality tissue samples.

Furthermore, SFRS2, RPL6, FABP6 and Beta catenin did not show bands good enough to assess their relative expression in the above two mouse models. This is despite the use of various troubleshooting strategies as listed below.

- The use of protein lysates from two cell lines as controls
- The use of different blocking agents (BSA in PBS and milk in PBS, both with and without Tween20) with various incubation periods and concentrations.
- The use of different primary antibodies with varying dilutions and incubation periods and temperatures
- Varying the concentration of the diluent (blocking solution) of the primary antibody
- Varying the concentration of the secondary antibody
- Varying the incubation period with super signal reagents
- Varying washing times
- Using fresh samples from *AhCre*$^{+}$*Apc*$^{fl/fl}$ mice and polyps from *Apc*$^{Min/+}$ mice
- Various exposure times during development
- Making sure that antibodies recognise denatured proteins

It is worth mentioning that, the primary antibodies described in this chapter were primarily chosen on the basis that they were appropriate for IHC. However, according to the data sheets they could also be used in western blot experiments.

## 3.6 Discussion

Unlike many other techniques, IHC provides the opportunity of assessing the localisation of any potential change in protein expression that might occur following *Apc* deletion. Moreover, simultaneous histological assessment may help in correlating any expression changes in protein abundance or position with coincident histological changes. However, as this is at best a semi-quantitative technique, interpretation of findings is sometimes challenging and conclusions may be influenced by the experimental conditions employed.

### 3.6.1 Acute *Apc* deletion mouse model, *AhCre$^{+}$ Apc$^{fl/fl}$*

As a result of acute deletion of both *Apc* alleles in all intestinal epithelial cells, the *AhCre$^{+}$Apc$^{fl/fl}$* mouse model provides insights into the early events following *Apc* deletion in the intestine. Almost all tissue sections from *AhCre$^{+}$Apc$^{fl/fl}$* mice showed morphological changes in comparison to *AhCre$^{+}$Apc$^{+/+}$* mice. These took the form of longer crypts with increased number of cells and larger nuclei, reduced or absent goblet cells and aberrantly positioned Paneth cells. These findings are consistent with the original descriptions of this model [44]. Additionally, independent work by other groups has also shown similar phenotypic changes in a mouse model with constitutive Beta catenin activation [223]. This observation adds evidence to the concept that Apc mutation perturbs the Wnt signalling pathway in the intestine.

In agreement with the above findings, all *AhCre$^{+}$Apc$^{fl/fl}$* small intestinal sections examined showed nuclear localisation of Beta catenin (a hallmark of an active Wnt cascade) [80] in the crypts but not in the villi. Consistently, the latter finding was absent in the whole crypt villus axis in the *AhCre$^{+}$Apc$^{+/+}$* mice. This provided a good platform to study "whether or not" our candidate proteins were involved in these events.

All proteins tested except DDX5 showed observable increased staining in the small intestinal crypts versus villi of *AhCre$^{+}$Apc$^{fl/fl}$* mice. This observation that can be attributed to the failure of Apc deficient cells to migrate upwards and their retention within crypts [107]. The sustained high EphB/EphrinB levels resulting from the abnormal activation of the WNT signalling pathway in Apc deficient cells have been suggested as an explanation for this defective migration [44, 76].

NAP1L1, RPL6, SFRS2, FABP6, NCL and PHB all showed observable differential staining in *AhCre*$^{+}$*Apc*$^{fl/fl}$ mice in comparison to their control counterparts. This suggests that these proteins may be involved in the histological changes that are observed in the intestine after *Apc* deletion. The proteins that showed less clear observable changes were HMGB1 and NPM. The proteins showed reduced expression in the villi of *AhCre*$^{+}$*Apc*$^{fl/fl}$ mice in comparison to the villi of *AhCre*$^{+}$*Apc*$^{+/+}$ mice. We considered these changes outside our area of focus, since they were not in the area where the Wnt cascade was suspected to be activated (the crypts).

### 3.6.2 *Apc*$^{Min/+}$ mice

Genotypic and phenotypic similarities between *Apc*$^{Min/+}$ mice and familial adenomatous polyposis (FAP) patients, have made this mouse an excellent model to investigate intestinal tumourigenesis [208]. *Apc*$^{Min/+}$ mice have a germ line autosomal dominant nonsense mutation of one *Apc* allele [208]. In this mouse model, as well as in FAP patients, all cells of the body carry only one functional *Apc/APC* allele, albeit very few cells progress to neoplasia. This indicates that there are other factors (genetic and/or environmental) which are needed for tumour development to begin [224]. Moreover, the intestinal predilection to Apc related tumours may be due to the constantly active and relatively tough environment involved, which in turn needs faster cell cycling and turnover rates with a higher chance for genetic instability and hence tumour development.

It has been suggested in previous studies that in *Apc*$^{Min/+}$ mice, most neoplastic lesions develop in the first month of life and progress to larger adenomas toward the end of the mouse's average life span [208]. This allowed us to follow the progression of lesions and changes in protein expression chronologically, by sampling a six month time course at only three points (1, 3 and 6 months). Moreover, in a previous study the genetic profiles of normal epithelium, intestinal adenomas and intestinal carcinomas were compared, and the latter two were very similar [225]. This further supports the adenoma carcinoma progression sequence that we have also adopted as our model for this work.

More obvious differential staining intensities were observed for most proteins in the more advanced adenomas, consistent with the more apparent nuclear localisation of

Beta catenin in these lesions. A similar finding has been shown by another research group who concluded that higher levels of nuclear Beta catenin are associated with high grade dysplasia rather than low grade dysplasia or metaplasia in Barrett's oesophagus [223]. Therefore these observations together suggest a causative or correlative role in tumourigenesis for the candidate proteins that showed similar patterns of staining.

Although it was difficult to find dysplastic lesions in one month old $Apc^{Min/+}$ mice, and thus suitable samples were not available for analysis in many cases, we could confirm that most of the proteins we studied started to show changes in expression as early as three months of age.

In general, the proteins studied in this mouse model showed consistent results with those obtained from the $AhCre^{+}Apc^{fl/fl}$ mouse model. NAP1L1 protein showed a clear differential staining pattern using two independent primary antibodies while RPL6 showed changes in staining intensity and localisation (younger vs. older mice). SFRS2, PHB and FABP6 also showed increases in expression in dysplastic lesions but no changes in the sub-cellular location of these proteins were observed. Similar to the findings in $AhCre^{+}Apc^{fl/fl}$ mice, HMGB1 and NPM did not show any clear differences in expression in the neoplastic lesions that we studied in $Apc^{Min/+}$ mice.

As described above six proteins showed consistent results in both mouse models therefore, they will be the focus of the following discussion. The other four proteins have already been briefly discussed at the end of their relevant results sections.

The WNT pathway is critical in regulating embryonic development and maintaining adult tissues. It is therefore not surprising that this pathway is involved in stem cell homeostasis. Moreover, our candidate proteins are proposed to be WNT targets; they showed up-regulation in the setting of a deranged WNT pathway as demonstrated by the proteomics studies in $AhCre^{+}Apc^{fl/fl}$ mice in addition to co-localisation with Beta catenin in both $AhCre^{+}Apc^{fl/fl}$ and $Apc^{Min/+}$ mice as demonstrated by the IHC work shown in this chapter. Therefore, it would not be surprising to find that these proteins were involved in the wide range of cellular processes which are thought to be mediated by the WNT signalling pathway. These processes include maintaining stem cells, promoting differentiation, proliferation, cell cycle progression, apoptosis and response to different kinds of stress outside the normal range of cell functions [226].

NAP1L1 belongs to a family of proteins that include at least five proteins in mammals [227]. This family has been shown to be involved with nucleosome assembly, histone transport, transcriptional regulation and cell cycle progression [228]. NAP1L1 has been shown to be ubiquitously expressed and has been characterised as a histone chaperone [149]. Although there is little information on the role of NAP1L1 in colorectal tumourigenesis, there are contradictory reports about its expression in CRC. For example, one report based on serological identification of antigens by recombinant expression cloning (SEREX) identified NAP1L1 as a potential antigen that can be used as a marker of progression or a therapeutic target for CRC [150]. On the other hand, another report comparing *NAP1L1* mRNA expression in small intestinal carcinoids, CRC and gastric cancer suggested no difference in NAP1L1 expression between CRC and normal adjacent tissue [148]. Our work supports a possible role for NAP1L1 in colorectal tumourigenesis due to its over expression within five days of Apc loss in $AhCre^{+}Apc^{fl/fl}$ mice and its upregulation in the early and advanced neoplastic lesions from $Apc^{Min/+}$ mice as demonstrated by IHC and western blot analysis.

RPL6 is a member of the ribosomal family of proteins (RPs) that are mainly involved in ribosome biosynthesis and protein translation [229]. Several reports are now pointing to abnormalities of protein translation in different malignancies and the possible involvement of RPs [230]. Moreover, RPs have also been suggested to act as oncogenes in various human tumours [231]. Several members of this family have been shown to be expressed in different cancers such as RPL19 in breast cancer and RPL15 in oesophageal cancer [232, 233]. Although these reports are increasing, the exact role of these proteins in tumourigenesis currently remains unclear [229]. This is also true for RPL6, however relatively recent work has suggested a possible role for RPL6 in promoting cell cycle progression (G1 to S) and cellular proliferation in human gastric cancer cell lines [163]. This may explain the early over expression of RPL6 in both mouse models that we studied and its translocation into the nucleus when neoplastic growth was more advanced in six month old $Apc^{Min/+}$ mice.

SFRS2 belongs to the serine rich (SR) family of proteins that have been linked to both constitutive and alternative pre-mRNA splicing [234]. Pre-mRNA splicing is a critical process, since more than 74% of human genes undergo alternative splicing, resulting in the production of different isoforms; sometimes with changes in radical

functional characteristics. A well-known example in this setting is the pro-apoptotic and anti-apoptotic isoforms of caspases [235]. Such changes can have dramatic effects on tumourigenesis [170]. There are many reports of the role of SFRS2 in haematological malignancies, but there are very few publications about its role in solid tumours especially colon cancer. However, there are reports that have suggested a role for SFRS2 in cell cycle control and induction of apoptosis [236]. In this setting, a recent study demonstrated that following treatment of cell lines with cisplatin, SFRS2 induced cell cycle G2M arrest and modulation of caspase 8 pre-mRNA splicing to increase the apoptosis of defective cells [237]. In the light of these observations, SFRS2 over expression in neoplastic lesions from $Apc^{Min/+}$ mice in our work could be a response to mediate apoptosis of defective cells. This observation may also explain the increased intestinal epithelial apoptosis rates that are observed in $AhCre^{+}$ $Apc^{fl/fl}$ mice [44].

Fatty acid binding proteins are a family of small highly conserved cytoplasmic proteins that bind long chain fatty acids and other hydrophobic ligands. FABP6 and FABP1 (the liver fatty acid binding protein) are able to bind bile acids. The role of these proteins includes uptake, transport and metabolism of fatty acids [166]. FABP6 expression has also been correlated with certain clinico-pathological criteria of CRC. For example, high FABP6 expression was noted in smaller tumours, tumours located in the left colon, and tumours with less serosal invasion (early stages of tumour development). In addition, a dramatic reduction in FABP6 expression was found in lymph node metastases suggesting that it plays a role in early carcinogenesis [166]. Our results showed a relatively early change in the level of this protein, an observation that supports the above suggestions. However, data to inform whether FABP6 is a direct or indirect factor in the tumourigenesis process are still limited.

PHB is a mitochondrial protein whose functions are not yet clearly understood [213]. However, it has been reported that the PHB proteins in coordination with Rb protein can suppress E2F-mediated transcription and cell growth [213]. Reports from human CRC studies have shown over expression of PHB, with the most obvious increase in expression being observed in poorly differentiated cancers. The same study adopted the notion that PHB is a tumour suppressor and this paradoxical over expression may be due to its role in cell senescence [238] or to susceptibility of its promoter to c-Myc actions [239]. Consistently, overexpression of PHB has been reported in

different solid tumours such as bladder [240] and stomach [179] cancers and cancer cell lines such as breast [241] and osteosarcoma [242]. Our results are consistent with the above observations, and suggest that PHB may be more important at the stage after cellular transformation.

Nucleoloin, a nucleolar phosphoprotein, has been shown to be involved in critical cellular functions such as ribosomal biogenesis and maturation, RNA and DNA metabolism and cellular response to stress [167]. Therefore, it is not surprising that we found NCL to be upregulated in the context of an activated Wnt signalling pathway. NCL was upregulated in both $AhCre^{+}$ $Apc^{fl/fl}$ and $Apc^{Min/+}$ mice. As with some of our other candidate proteins, NCL may be involved in maintaining the state of cellular un-differentiation. This is supported by reports that have shown high expression of NCL in embryonic stem cells (ESCs) as part of the stemness mechanism. Moreover, NCL blockade by specific short hairpin RNAs in these cells caused a dramatic reduction in proliferation, increased apoptosis and G1 phase accumulation [214]. Furthermore, NCL down-regulation led to differentiation of ESCs and reduced their self-renewal ability. p53 up-regulation has been suggested as a mechanism which mediates these effects of NCL down-regulation [214]. It is also reported that NCL is highly expressed by rapidly dividing cells while it undergoes inactivation by auto-cleavage in quiescent cells [243]. These observations can help to explain the role of NCL in the hyperprolifertive state that is associated with a deranged Wnt signalling pathway.

### 3.7 Conclusion

Despite the interpretation challenges involved with IHC, our results have added extra support to the preliminary data which were obtained in a previous study involving these proteins. Therefore, in the light of the previous data which were obtained using different techniques such as Western Blotting and qRT-PCR in mice and human subjects, we should further investigate those proteins that showed clear differential staining patterns in the setting of *Apc* deletion induced Wnt derangement, namely NAP1L1, RPL6, SRSF2, PHB, NCL and FABP6.

Published data suggest possible roles for the above proteins during intestinal tumourigenesis. These involve critical cellular functions such as proliferation, cell cycle progression, apoptosis, chromatin modulation, transcription, pre-mRNA splicing, protein synthesis and others. Our next task will be to attempt to understand the role of the selected proteins in colorectal tumourigenesis by investigating the cellular functions that they mediate and their main partners in this setting.

# Chapter four

## Mechanistic studies on the functions of NAP1L1 and RPL6 and their possible roles in colorectal tumourigenesis

## 4. Studying potential roles of selected candidate biomarker proteins in colorectal tumourigenesis

### 4.1 Introduction and aims

Due to the importance of APC as a Gatekeeper protein in protecting against the initiation of intestinal tumourigenesis, understanding the biology underlying the changes that follow *APC* deletion may have important implications for the management of CRC. Loss of APC function has been shown to be a key early event in most if not all cases of sporadic colorectal cancer [10]. However, the molecular changes that follow this loss have not yet been fully uncovered [44].

The previous chapter (3) involved studying 9 candidate biomarker proteins. At the end of these studies we demonstrated that the proteins nucleosome assembly protein 1 like 1 (NAP1L1), ribosomal protein like 6 (RPL6), serine/arginin rich splicing factor 2 (SFRS2), prohibitin (PHB), nucleolin (NCL) and fatty acid binding protein 6 (FABP6) exhibited significant changes in their level of expression and/or sub-cellular localisation as assessed by IHC in the $AhCre^{+}Apc^{fl/f}$ mouse model at five days after *Apc* deletion. Our working hypothesis is that these proteins are part of the immediate derangement that occurs following the deletion of *Apc* and that ultimately leads to malignant transformation. To test this hypothesis, we examined the expression of these proteins in a cohort of $Apc^{Min/+}$ mice, a model that involves a more extended period (six months) of APC dysfunction and which leads to tumour formation. The candidate proteins showed consistent results in the established neoplastic lesions in $Apc^{Min/+}$ mice and the crypts of $AhCre^{+}Apc^{fl/fl}$ mice.

Based on the results of the previous chapter, data from previous stages of this project and the previously published literature, the focus of the studies in this chapter will be upon NAP1L1 and RPL6. In addition, published observations by other groups have identified a strong correlation between RPL6 and Cyclin E [229] as will be shown later in this chapter. Therefore, Cyclin E was also included in the mechanistic studies described below.

The S phase of the cell cycle is a critical stage in which cells replicate their DNA. Cyclin E together with its cyclin dependent kinase (CDK) partners regulates the S phase [244]. The Cyclin E/CDK2 complex mediates its effects on G1-S phase via phosphorylation and inactivation of the retinoblastoma protein (Rbp)-E2F complex

[245-247]. E2F then induces the transcription of genes needed for the S phase of the cell cycle including Cyclin E itself [248]. In addition, monomeric Cyclin E has been shown to perform cell cycle related functions independent of the CDKs [249].

The exact role of Cyclin E is still under investigation; it has been shown that mouse embryos lacking Cyclin E develop normally until day 10 [250], however they then develop severe placental defects, suggesting a critical role for Cyclin E in the endoreplicative cell cycles of trophoblast giant cells [251]. It has been suggested that Cyclin A is sufficient for DNA replication, whereas Cyclin E is required for cells restarting cycling following quiescence [250]. Despite this controversy, there is no doubt about the catastrophic outcomes of abnormal Cyclin E expression; high levels of Cyclin E have been shown to correlate with more advanced stages and grade of a critical number of breast cancers as well as a number of other tumour types [252].

**Aims**

1. To study possible roles of the proteins NAP1L1 and RPL6 in regulating cellular processes that are known to be critical during intestinal tumourigensis.
2. To assess possible partner molecules for these candidate proteins that may mediate their roles during intestinal tumourigenesis.

### 4.2 siRNA mediated silencing of candidate proteins

Based on data from the previous chapter and from published work by other research groups [44], we propose that the upregulations observed in the expression of selected candidate proteins following *Apc* deletion *in vivo* are Wnt pathway dependent. Therefore, human colon cancer cell lines such as HCT116 and HT29 cells which harbour an induced WNT pathway are valid *in vitro* systems to assess the roles of these proteins during colorectal carcinogenesis. For this purpose, we have used siRNA mediated gene silencing to knock down the expression of candidate proteins and to study the impact of these changes on cellular functions. Details about the process of siRNA mediated gene knockdown can be found in the methods chapter. For this study we used liposome mediated siRNA transfection which included a number of elements that first needed optimisation as described below.

#### 4.2.1 Optimisation of siRNA protocols

To establish efficient siRNA mediated protein knockdown protocols, a number of experimental conditions had to be optimised. These included the following:

- **Optimal cell density for a given time point**

The time point at which a given gene demonstrates maximum knockdown varies from one gene to another. Changes in the protein level are more accurate than changes in RNA abundance when correlating effects with cellular functions. Therefore, knockdown efficiency was initially assessed at the level of protein expression. The manufacturers recommend that maximum knockdown at the protein level can be observed between days 1 and 3 following siRNA treatment.

Before testing these time points, the optimal seeding cell densities also needed to be determined. To do so, the following criteria were adopted:

1. Ensuring the largest number of cells in the log phase during the siRNA incubation time. This was achieved by avoiding very low cell densities.
2. Avoiding over confluence: this was achieved by avoiding very high cell densities. Slowness in growth due to over-confluence can interfere with data interpretation.

A number of seeding densities were tested for both cell lines in six well plates. The densities ranged from 50,000 to 1,600,000 cells in a total volume of 2 mls per well. The cell densities that were finally chosen are shown in table 4.1.

| Cell line | 24 hr time point-cells/well | 48 hr time point-cells/well | 72 hr time point-cells/well |
|---|---|---|---|
| HCT116 | 700,000 | 300,000 | 100,000 |
| HT29 | 800,000 | 600,000 | 400,000 |

**Table 4.1 Cell line density based on the target time point in 6 well plate format. N3, n2.**

- **siRNA concentrations and time points**

From previous experience in our laboratory, we knew that HT29 cells are relatively difficult to transfect. Therefore, these were made a priority during the optimisation process.

The manufacturer recommended an siRNA final concentration between 5 and 50 nM. However, previous experiments using HT29 cells in our laboratory have needed to utilise siRNA concentrations above 50 nM to produce observable effects [200]. Therefore, we decided to start the experimental series using a 25 nM final siRNA concentration. This concentration did not cause any observable effect (figure 4.1A), consequently the siRNA concentration was increased to 40 and then 50 nM per well (figure 4.1A). Each of the above concentrations was tested using the seeding densities identified in table 4.1 over three time points, 24, 48 and 72 hrs.

Knockdown efficiency was assessed by western blot analyses for the selected proteins. Initially an observable reduction in expression was only seen with NAP1L1 using this technique. A number of modifications in the western blotting conditions (as shown later in this chapter) were tried in an attempt to detect RPL6; however convincing bands were not observed. Therefore, we tested the knockdown efficiency for this protein by assessing mRNA expression using qRT-PCR (shown in the respective section for this protein). The efficiency assessment by qPCR was carried out at the 72 hr time point only. This is because, by the time this technique was used, results from other measurements (data shown in detail later in this chapter) had suggested that the 72 hr time point was the optimum time required for maximum knockdown of the proteins under investigation.

Below is an example of the optimisation process for NAP1L1 knockdown.

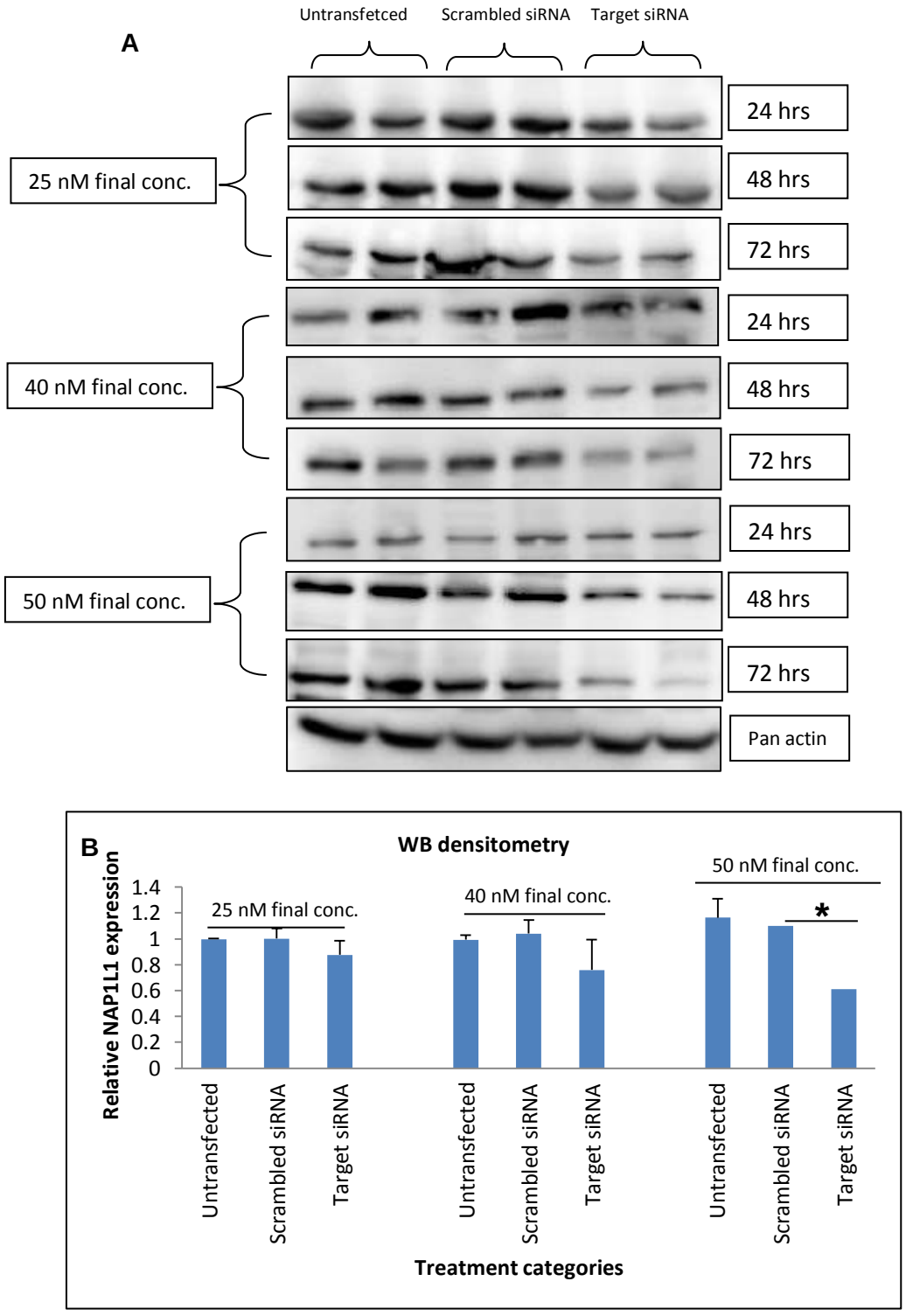


**Figure 4.1 Representative results of the optimisation process for NAP1L1 knockdown in HT29 cells. A) Shows NAP1L1 WB bands for each siRNA concentration over three time points. B) Shows densitometry quantification for the knockdown level for the 72 hr time points. The comparison groups were untransfected, scrambled siRNA and target siRNA transfected HT29 cells (duplicates). Pan actin was used as a loading control. * p value < 0.05. N3, n2.**

Protein levels are shown as fold changes relative to untransfected cells, but results from cells transfected with the scrambled siRNA were used as the basal cellular response for interpretation of results and statistical analysis.

This detailed optimisation was only carried out in HT29 cells. The bands shown in figure 4.1A are representative bands from three or more experiments. Although the Pan actin bands shown in figure 4.1A are from one 72 hr time point only however, there were no changes in the actin levels compared to untreated controls for the other time points, concentrations and duplexes. Densitometry analysis of the bands from the 72 hr time points (figure 4.1B) showed a maximum reduction in NAP1L1 abundance (48%, p value 0.04) with the 50 nM target siRNA concentration. Densitometry analyses from the other time points are not shown because they showed no significant change as assessed by WB images (figure 4.1A).

Based on the above optimisation process, we chose 50 nM as our final siRNA concentration and 72 hours as our target time point for maximum knockdown of protein expression.

- **Selecting the optimal DharamaFECT reagent and type**

Dharmacon recommends one or more DharmaFECT reagents (1-4) for each cell line. Reagents 1 and 2 were suggested as first choices for HT29 and HCT116 cells respectively. Initially DharmaFECT reagent 2 was chosen for both cell lines, since it was recommended for both HT29 (6 µl/well) and HCT116 (4 µl/well) cells. However, when work on HCT116 cells was started, the knockdown level was significantly greater than that obtained with HT29 cells (as shown below) for the selected proteins. Moreover, although the cell background plays role in the sensitivity to transfection, choosing the right experimental tools may also improve the outcome. Therefore, it was decided to test DharmaFECT reagent 1 on HT29 cells. For this set of experiments the volumes 6 and 8 µl/well were used while the other optimised conditions remained the same. Figure 4.2 shows the results from these experiments.

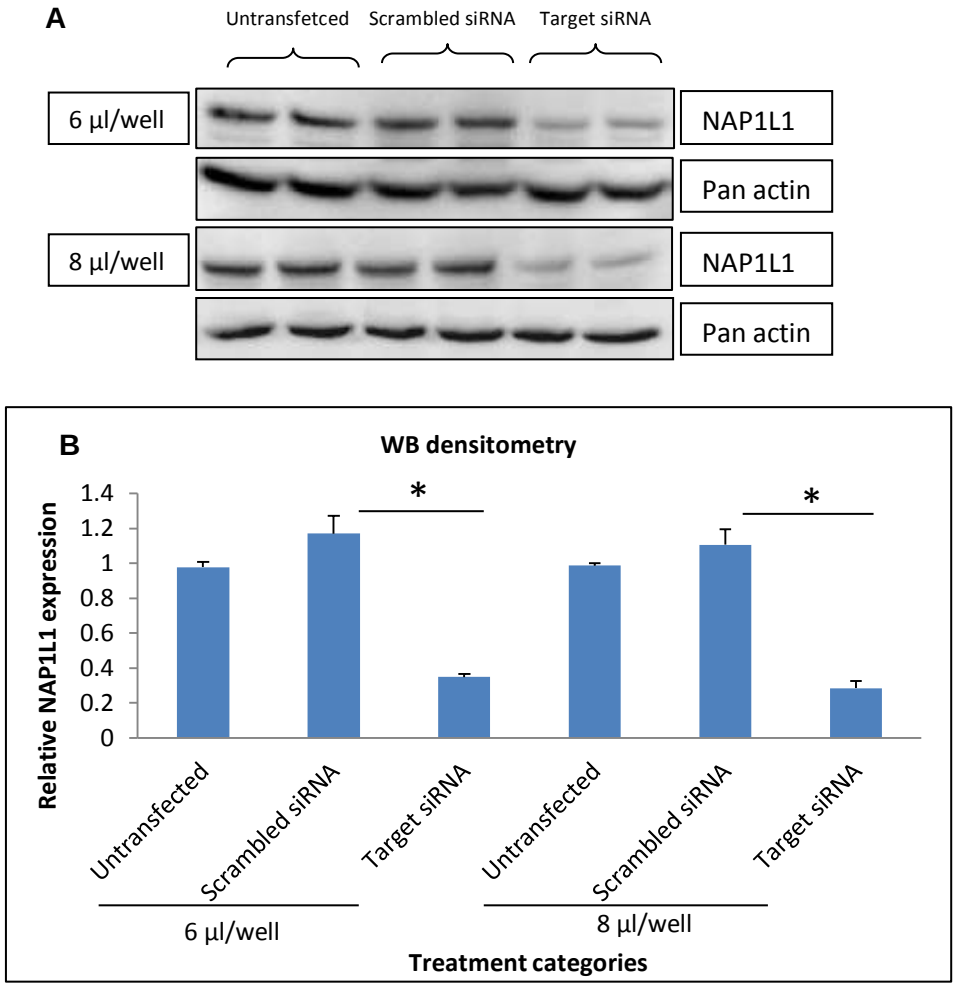


**Figure 4.2 Using DharamFECT reagent 1 instead of reagent 2 for HT29 cells to knockdown NAP1L1. A) Shows WB bands from HT29 whole cell lysates. The three comparison groups were run in duplicates. B) Shows densitometry analysis of the relative expression of NAP1L1 protein in the three groups. This reagent was tested at the 72 hr time point. N3, n2.**

Changing DharmaFECT reagent improved the efficiency of the knockdown process. Also increasing the transfection reagent volume within the recommended range improved the knockdown efficiency (6 µl/well, 70% reduction, p value 0.04 vs. 8 µl/well, 75% reduction, p value 0.02).

### 4.2.2 Haemocytomter based cell counting

Haemocytometer based cell counting was used as a preliminary tool for:

- Assessing the toxicity effect of reagents other than the target siRNA in the transfection process.
- Assessing the knockdown efficiency during the optimisation stage.

A minimum of 80% viability (as recommended by the manufacturer) in the cells transfected with scrambled siRNA was used to rule out any significant nonspecific toxicity.

### 4.2.3 Optimisation of the siRNA mediated knockdown of the candidate proteins in HCT116 cells

As mentioned above, HCT116 cells were much more sensitive to the transfection process than HT29 cells. Optimal knockdown of the selected proteins in these cells was assessed by cell counting at the end of each time point (24, 48 and 72 hrs). Similar to HT29 cells, results in HCT116 cells clearly suggested that 72 hrs was the time point where maximum knockdown occurred (figure 4.3). Therefore, this time point was used to assess the knockdown efficiency in these cells (by WB or qRT-PCR). Assessment of knockdown was carried out for each experiment, but to avoid repetition, subsequent examples of knockdown results will be shown in the related section for each protein.

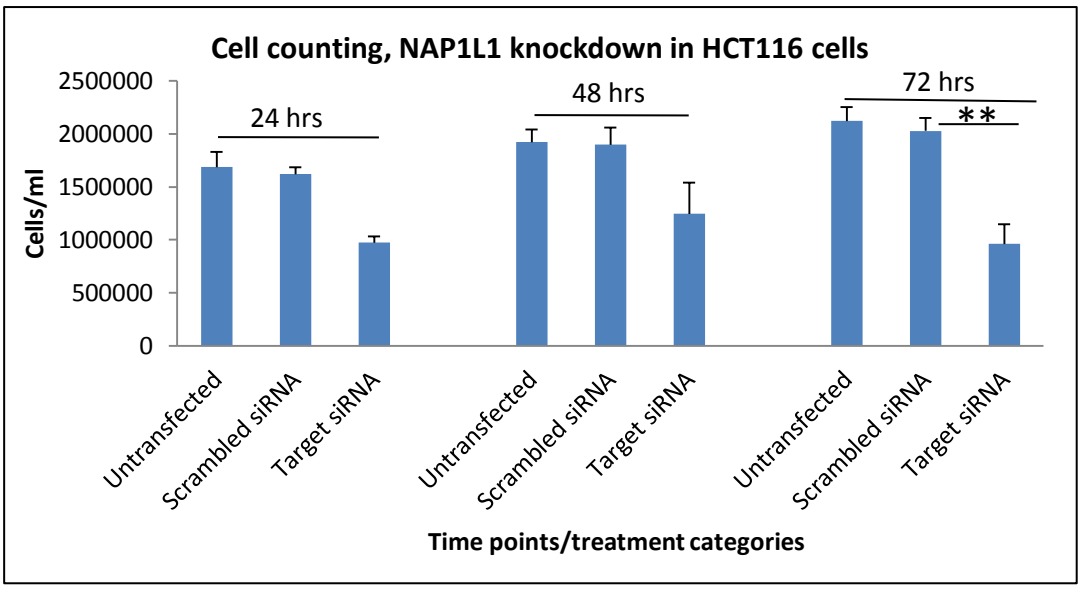


**Figure 4.3 Haemocytometer based cell counting following NAP1L1 knockdown in HCT116 cells over three time points. N3, n2. Error bars represent standard deviation from the mean. **p value < 0.01.**

Consistent with the results from HT29 cells, counting of HCT116 cells demonstrated a maximum reduction in proliferation after 72 hrs incubation with the target siRNA. The target siRNA group showed 53% (p value 0.002) reduction at the 72 hr time point versus 40% and 35% reduction at 24 and 48 hr time points respectively.

Based on results from the above experiments, the table below summarises the optimal conditions for each cell type and the siRNA concentrations as well as the transfection reagent type and volumes used.

| | Plate format-well number | Final siRNA conc. (nM/well) | Volume of DharmaFECT reagent (µl/well) | Time point | Cell density per well |
|---|---|---|---|---|---|
| HCT116 | 6 | 50 | 4 (TR2) | 72 hours | 100,000 |
| HT29 | 6 | 50 | 8 (TR1) | 72 hours | 400,000 |

**Table 4.2 Optimal experimental conditions for the siRNA treatment of HCT116 and HT29 cells. NB. The total volume in each well was 2 ml.**

## 4.3 Effect of NAP1L1 knockdown on cellular proliferation and apoptosis in cultured HCT116 and HT29 cell lines

NAP1L1 has been shown to be involved with nucleosome assembly, histone transport, transcriptional regulation and cell cycle progression [228]. Moreover, NAP1L1 was one of the upregulated proteins in $AhCre^{+}Apc^{fl/fl}$ mice as demonstrated by the proteomic analysis carried out by previous colleagues using this model. Furthermore, NAP1L1 showed cytoplasmic overexpression in the crypts of $AhCre^{+}Apc^{fl/fl}$ mice and colonic adenomatous lesions from $Apc^{Min/+}$ mice compared to their wild type counterparts (as shown in chapter 3).

To assess the significance of NAP1L1 upregulation in transformed cells in which Wnt signalling pathway is active, we used siRNA to knockdown NAP1L1 expression in HT29 and HCT116 cells and studied the impact of this on cell proliferation and survival as well as on apoptosis. WB was used to assess the knockdown efficiency.

Shown below are the results of NAP1L1 knockdown in HCT116 and HT29 cells using various assessment techniques. The experiments were carried out under the optimised conditions described above.

### 4.3.1 NAP1L1 knockdown in HCT116 cells

After 72 hours incubation with a NAP1L1 specific siRNA, western blot analysis of HCT116 whole cell extracts showed more than 95% reduction in NAP1L1 expression relative to that from the scrambled siRNA group (p value 0.02) (figure 4.4b).

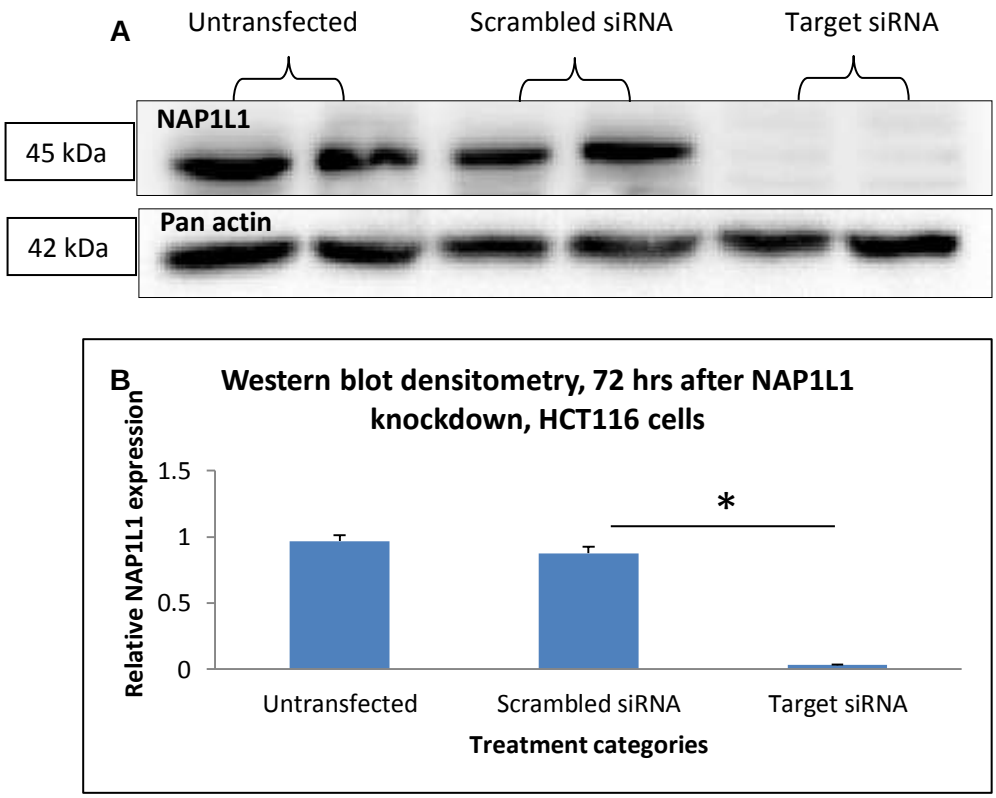


**Figure 4.4 A) Western blot (representative of 3 experiments) of HCT116 whole cell proteins probed with anti-NAP1L1 antibody. Pan actin was used as loading control. B) Densitometry analysis of NAP1L1 expression relative to untransfected cells (N3, n2). Error bars represent standard deviation from the mean. * p value is < 0.05.**

### 4.3.2 Impact of NAP1L1 knockdown on proliferation and apoptosis in HCT116 cells

The effect of knocking down NAP1L1 expression in HCT116 cells was preliminarily assessed using haemocytometer based cell counting. A hundred thousand cells were plated in duplicates into 6 wells plates. Twenty four hours later, media were replaced with equal volumes of fresh antibiotic free media or transfection media accordingly. After 72 hours incubation at 37 ºC, floating cells (indicative of the apoptosis rate) in the media and attached cells (indicative of the proliferation rate) were counted using the haemocytometer method (figure 4.5).

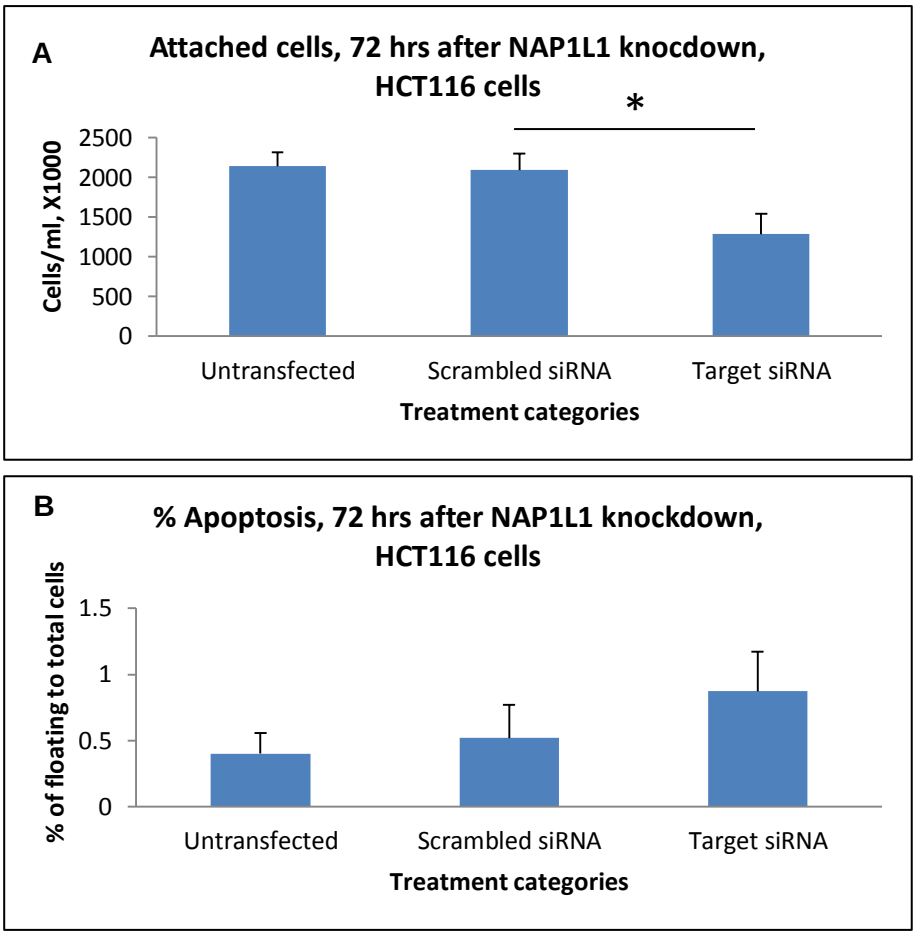


**Figure 4.5 Haemocytometer based cell counts. NAP1L1 knockdown in HCT116 cells, 72 hr time point. A) Change in attached cell number. B) Percentage of apoptotic cells to total cells per sample. Error bars represent standard deviation from the mean. (N3, n2) and * p value < 0.05.**

Cells transfected with the scrambled siRNA did not show significant toxicity relative to untransfected cells. However, cells transfected with NAP1L1 specific siRNA showed a significant reduction in cell number (figure 4.5A, p value 0.02). Cells floating in the media from each well were counted and are shown as a percentage relative to total cells per well. Absolute numbers might be misleading due to the reduction in the total number of cells in the transfected group. An increase in apoptosis was observed concomitant with the reduction in proliferation after NAP1L1 knockdown, but this was not significant (figure 4.5B).

### 4.3.3 NAP1L1 knockdown in HT29 cells

The above experiment was repeated with HT29 cells as shown below:

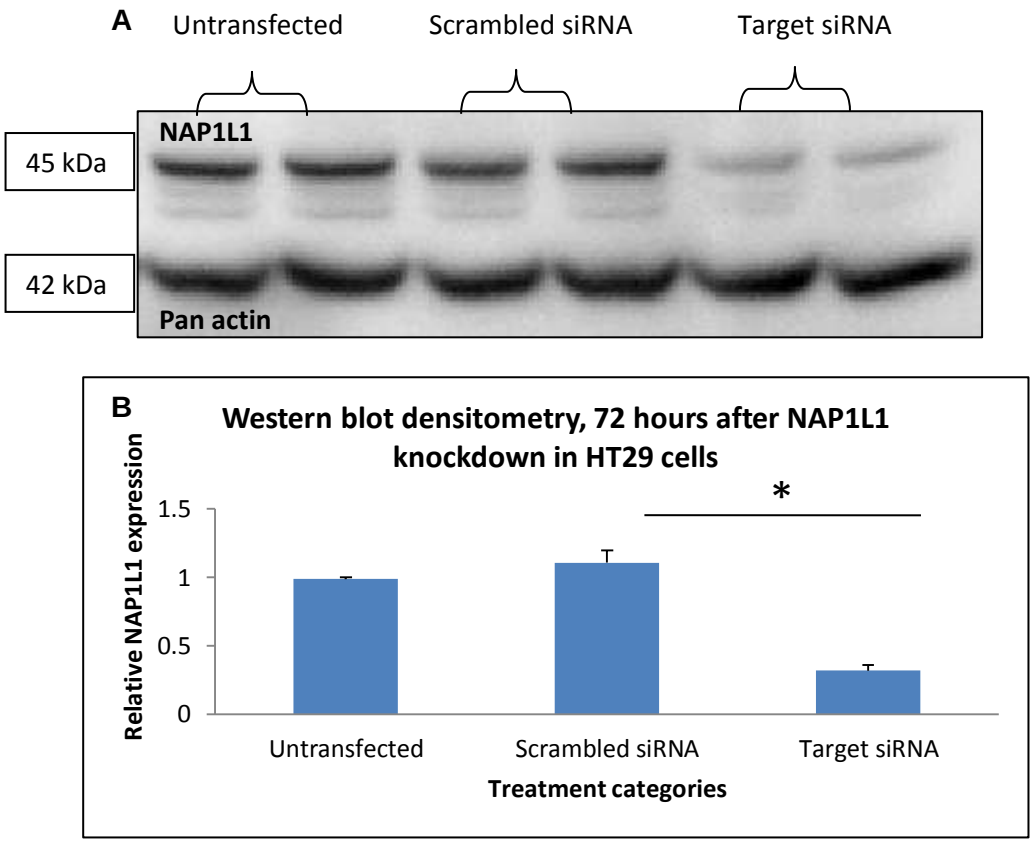


**Figure 4.6 A) Western blot (representative of 3 experiments) of HT29 whole cell proteins probed with anti-NAP1L1 antibody. Pan actin was used as loading control. B) Densitometry analysis of NAP1L1 expression relative to untransfected cells (N3, n2).*p value < 0.05.**

HT29 cells were more resistant to transfection than HCT116 cells; hence the degree of knockdown was not as great as in HCT116 cells. This was further reflected in cell counts as shown below:

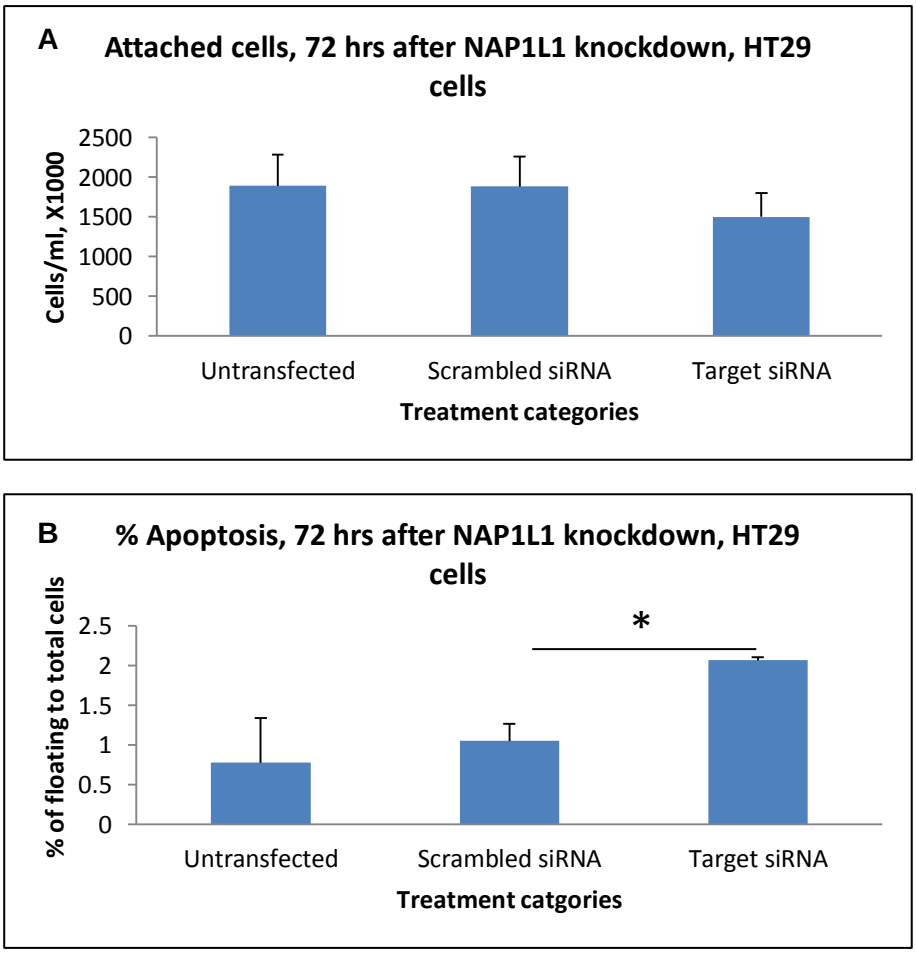


**Figure 4.7 Haemocytometer based cell counts. NAP1L1 knockdown in HT29 cells, 72 hr time point. A) Change in attached cell number. B) Percentage of apoptotic cells to total cells per sample. Error bars represent standard deviation from mean (N3, n2). * P value 0.01.**

The transfection conditions were the same as those for HCT116 cells except for the transfection reagent. Attached cells in the transfected group were reduced in number after 72 hours relative to the control cells (figure 4.7A) with a concomitant increase being observed in the number of apoptotic cells (figure 4.7B). Whilst the trend was the same, the magnitude of the effect (proliferation inhibition) was less in HT29 cells compared to HCT116 cells.

### 4.3.4 Independent assessment of cellular proliferation and cell survival after NAP1L1 knockdown in HCT116 and HT29 cells

Whilst the haemocytometer based cell counting method provided a good preliminary assessment for proliferation and cell survival, we also assessed these parameters using more accurate and objective Sulphrhodamine B (SRB) and clonogenic survival assays. These two assays involve a measurement of cell growth over longer periods of time, and therefore allow better and less subjective demonstration of any sustained changes following transfection.

**SulphorhodamineB (SRB) and Clonogenic assays**

The optimised transfection conditions outlined above were used. However, we used the 48 hour time point as the starting point for these assays. This was done to balance the level of transfection with the avoidance of dilution of samples with newly dividing untransfected cells.

Previous SRB studies on HCT116 and HT29 cells in our laboratory have established a seeding density of 1000 cells/well to be optimal for 96 well plates [253]. Untransfected cells, cells transfected with a scrambled siRNA and cells transfected with the target siRNA were seeded in adjacent columns in 6 replicate wells. Seven plates were used to allow cells to grow for 1-7 days. Each day a plate was fixed and stained with the SRB dye and the optical density for each sample was determined using a micro plate reader at 572 nm wave length.

For clonogenic assays, as again established previously in our laboratory, HCT116 (500 cells/well) and HT29 (1000 cells/well) cells were seeded in 6 well plates using the above comparison groups in triplicates [254]. Cells were grown in the respective complete media (methods section) for 10 days. Then they were fixed and stained with crystal violet before manually counting colonies.

Below are shown the results for the 7 day SRB assays following NAP1L1 knockdown in both HCT116 and HT29 cells (figure 4.8).

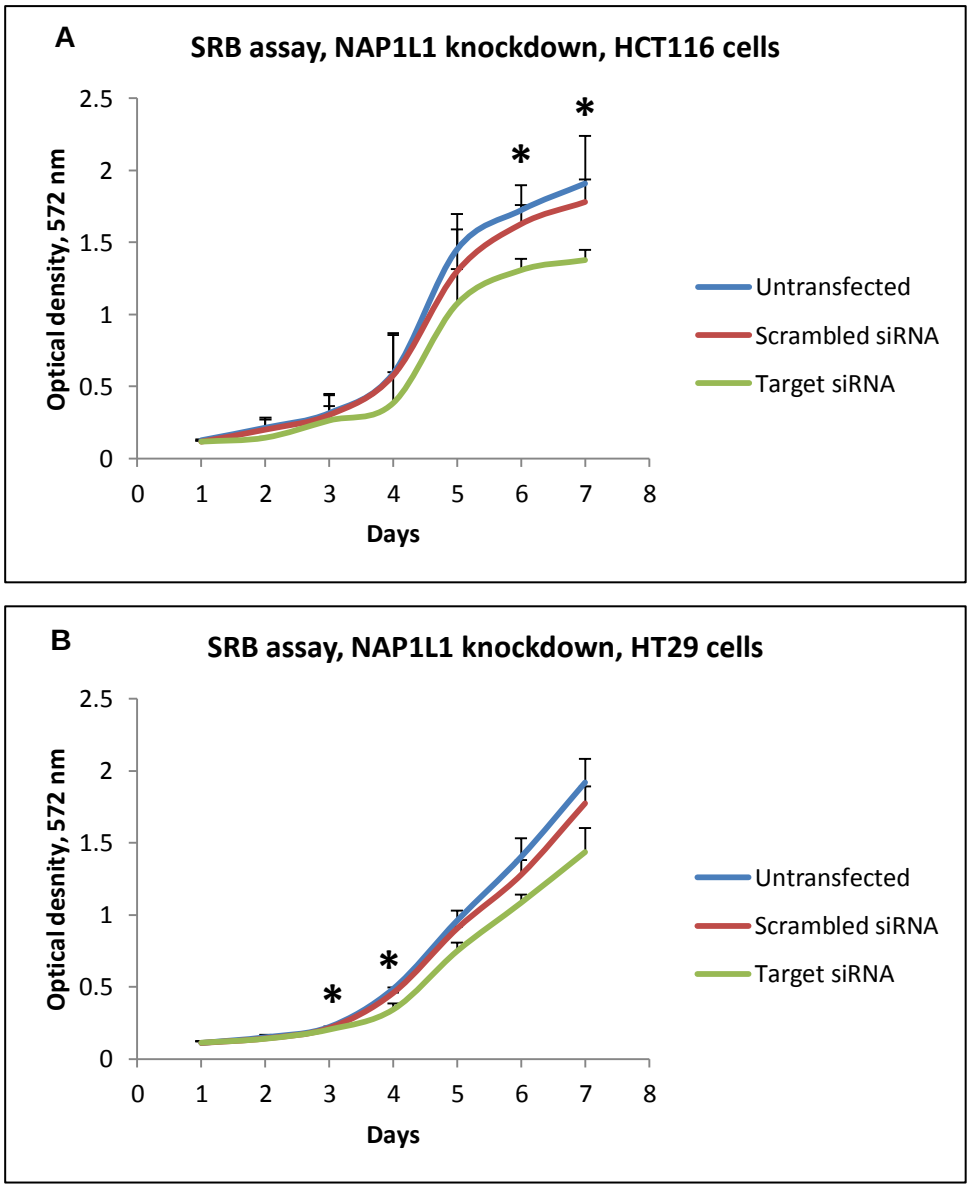


**Figure 4.8 SRB assays following proliferation for 7 days: (A) HCT116 and (B) HT29 cells showed reduced cellular density after knocking down NAP1L1. Error bars represent standard deviation from the mean (N3, n6). *p value < 0.05.**

NAP1L1 knockdown caused the transfected cells to be less capable of increasing their numbers compared to the control cells, in both cell lines. This was apparent after day 3 and became significant at days 6 (p value 0.02) and 7 (p value 0.01) in HCT116 cells and days 3 (p value 0.04) and 4 (p value 0.03) in HT29 cells.

**Clonogenic survival assay following NAP1L1 knockdown in HCT116 and HT29 cells**

To further evaluate the effect of NAP1L1 knockdown on cellular viability we also performed clonogenic survival assays in both cells lines, as shown below.

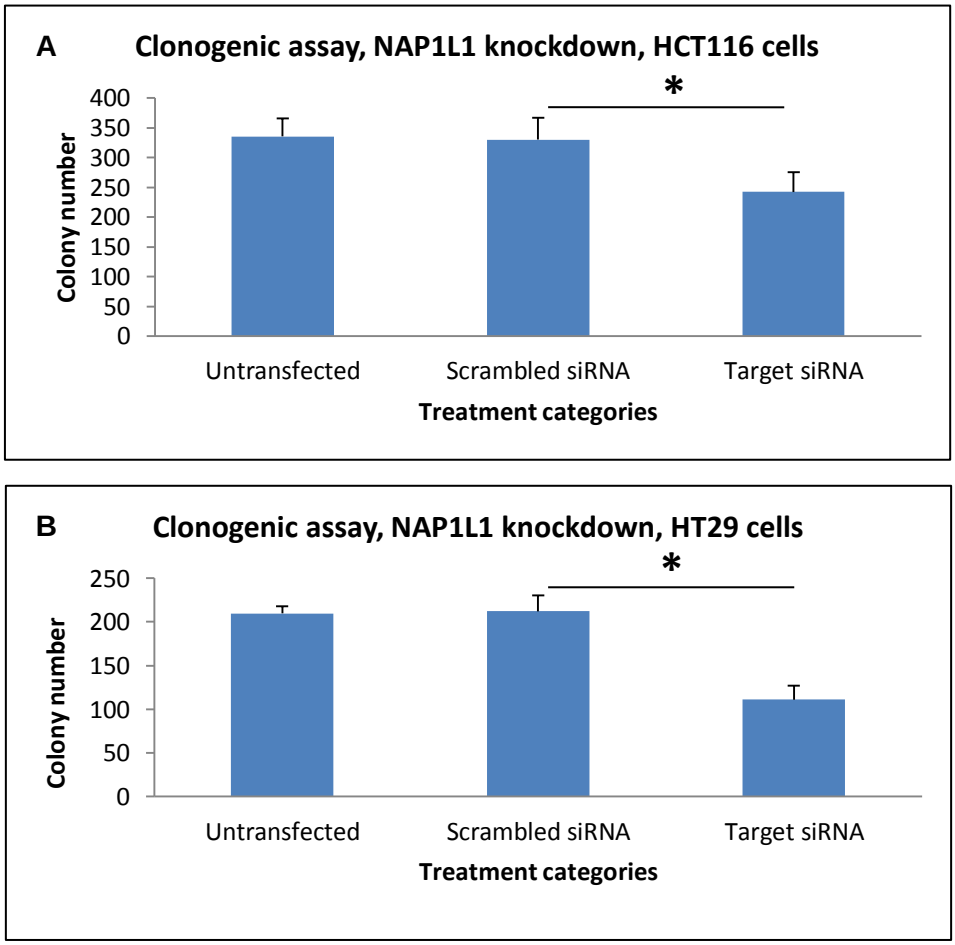


**Figure 4.9 Clonogenic survival assay. Both HCT116 cells (A) and HT29 cells (B) showed a significant reduction in survival and colony forming ability after NAP1L1 knockdown (* p value <0.05). Error bars represent standard deviation from the mean (N3, n3).**

NAP1L1 knockdown significantly affected the ability of both HCT116 and HT29 cell lines to survive and form colonies. Consistent with the SRB assay, cells were not able to compensate for the growth defect that was caused by the initial reduction in NAP1L1 expression.

### 4.4 Effect of siRNA mediated knockdown of RPL6 on proliferation and apoptosis in HCT116 and HT29 cell lines

RPL6 protein is a member of the ribosomal family of proteins (RPs) that are mainly involved in ribosome biosynthesis and protein translation [229]. The role of RPL6 is not yet fully understood in cancer development. However, recent work has suggested a possible role for RPL6 in promoting cell cycle progression (G1 to S) and cellular proliferation in human gastric cancer cell lines [163].

#### 4.4.1 RPL6 knockdown in HCT116 cells

The optimisation process and final experimental conditions were as described previously.

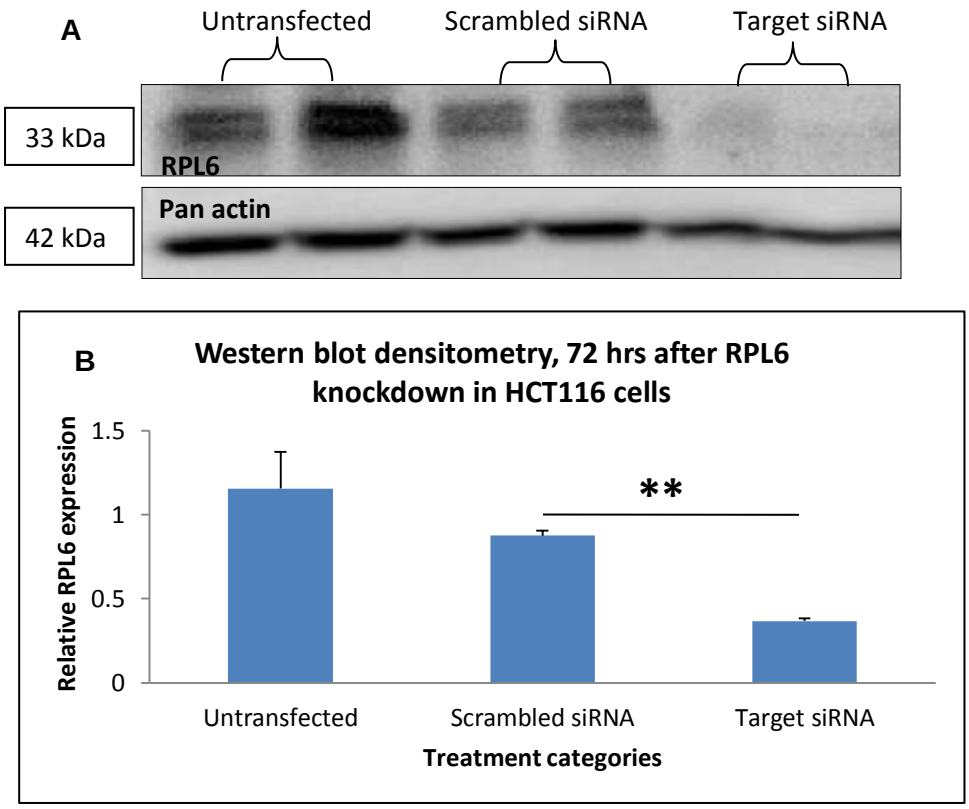


**Figure 4.10 A) Western blot (representative of 3 experiments) of HCT116 whole cell proteins probed with anti-RPL6 antibody. Pan actin was used as loading control. B) Densitometry analysis of RPL6 expression relative to untransfected cells (N3, n2).**p value < 0.01.**

HCT116 cells showed a significant reduction in RPL6 level (by 57%, p value < 0.01) 72 hrs after transfection (figure 4.10B).

As the results of knockdown assessment by WB were variable across the different experiments despite the use of several modifications in the protocols as described on page 47 in the previous chapter, we decided to also assess this at the level of mRNA.

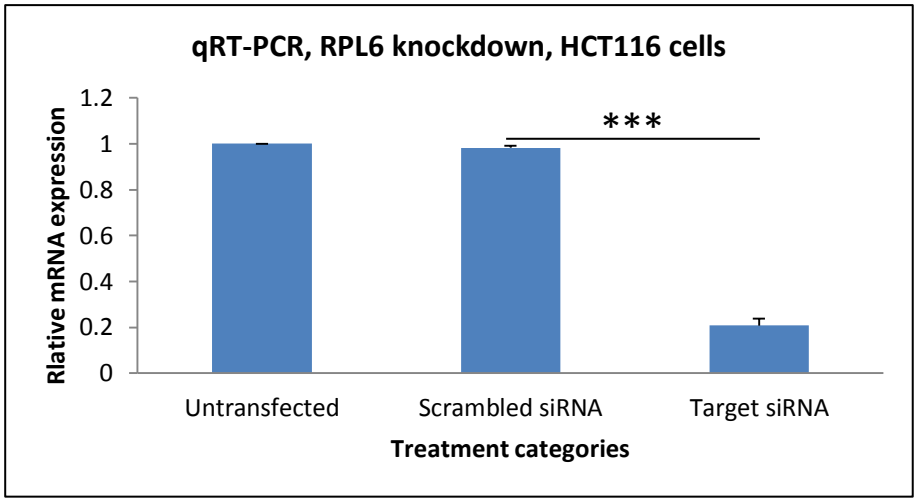


**Figure 4.11 qRT-PCR analysis of relative RPL6 expression in HCT116 cells 72 hrs following RPL6 knockdown. Error bars represent standard deviations from means. N3, n3. *** p value < 0.001.**

There was an approximately 80% (p value <0.001) reduction in RPL6 mRNA abundance relative to that from cells transfected with the scrambled siRNA.

Cell counting was performed post-tranasfection for the preliminary assessment of proliferation and apoptosis as shown below:

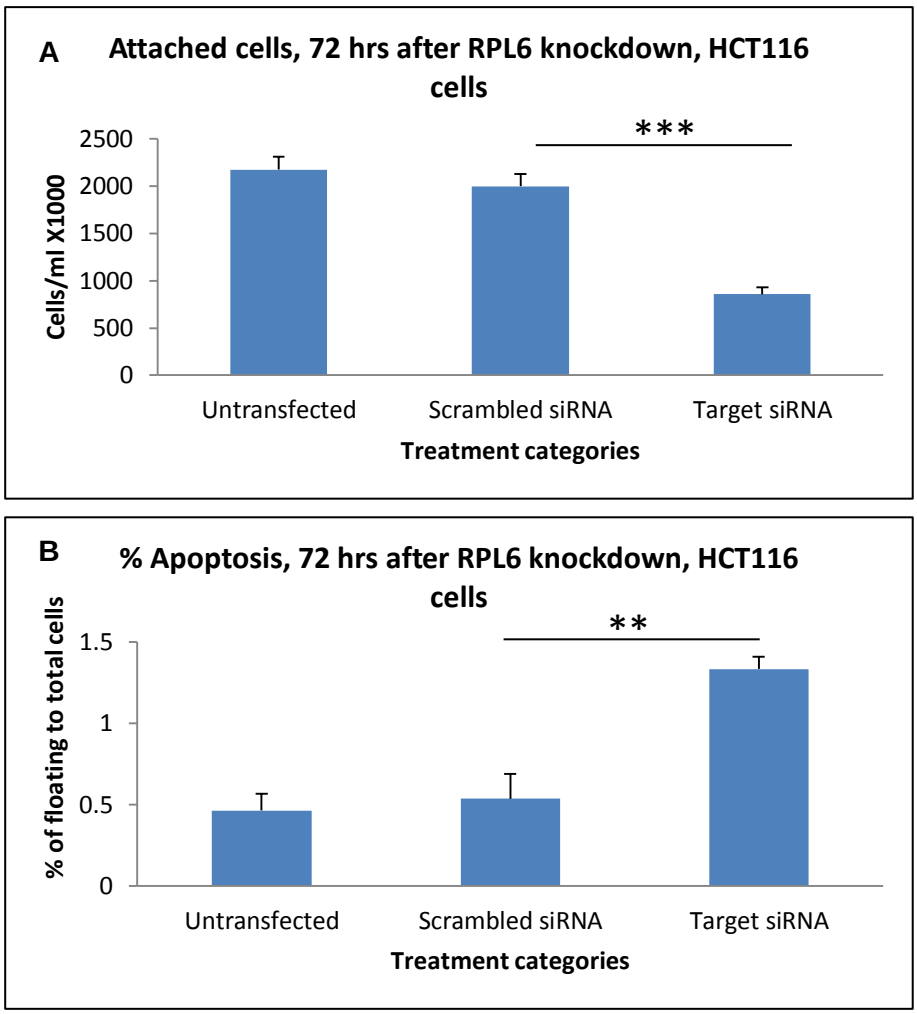


**Figure 4.12 Haemocytometer based cell counts. RPL6 knockdown in HCT116 cells, 72 hrs time point. A) Change in attached cell number. B) Percentage of apoptotic cells to total cells per sample. Error bars represent standard deviation from mean (N3, n2). *** & ** P values <0.001 and <0.01 respectively.**

HCT116 cells showed an obvious and significant inhibitory effect on proliferation following RPL6 knockdown peaking at 72 hrs after transfection. This was associated with a concomitant increase in the number of apoptotic cells (figure 4.12B).

### 4.4.2 RPL6 knockdown in HT29 cells

In HT29 cells, due to inability to demonstrate RPL6 knockdown by WB, we used RT-PCR to determine the efficiency of the mRNA knockdown as shown below (figure 4.13A).

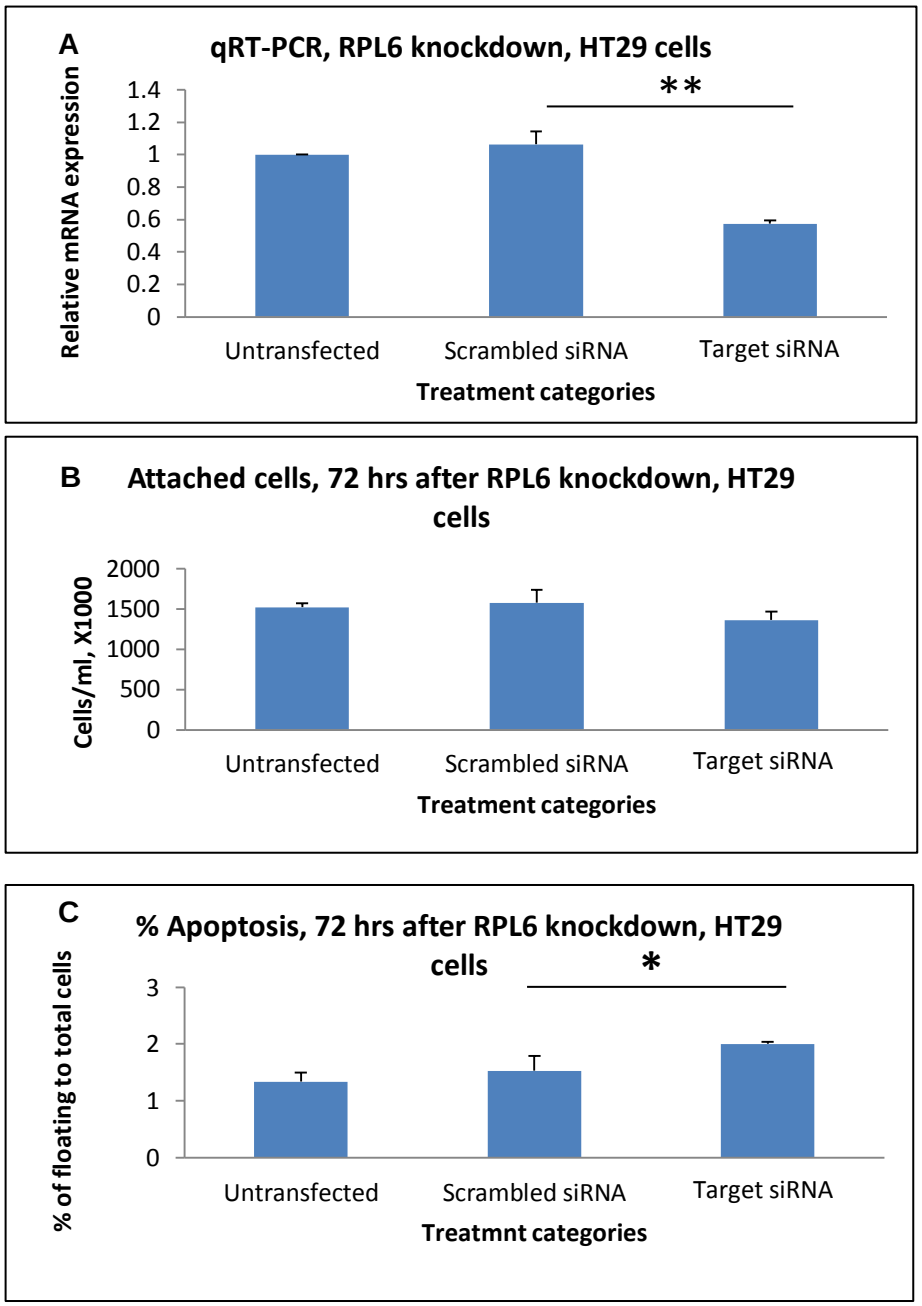


**Figure 4.13 RPL6 knockdown in HT29 cells, 72 hrs time point. A) Relative RPL6 mRNA expression (N3, n3). B) Change in attached cell number. C) Percentage of apoptotic cells to total cells per sample. Error bars represent standard deviation from the mean (N3, n2).*p value < 0.05.**

The significant reduction (40%, p value <0.01) in RPL6 mRNA level (figure 4.13A) was not associated with a concomitant effect on cellular proliferation (figure 4.13B). However, there was a significant increase in apoptosis percentage (figure 4.13C).

Again SRB and clonogenic assays were used to more accurately investigate the effects of RPL6 knockdown in HCT116 and HT29 cells (figures 4.14 and 4.15).

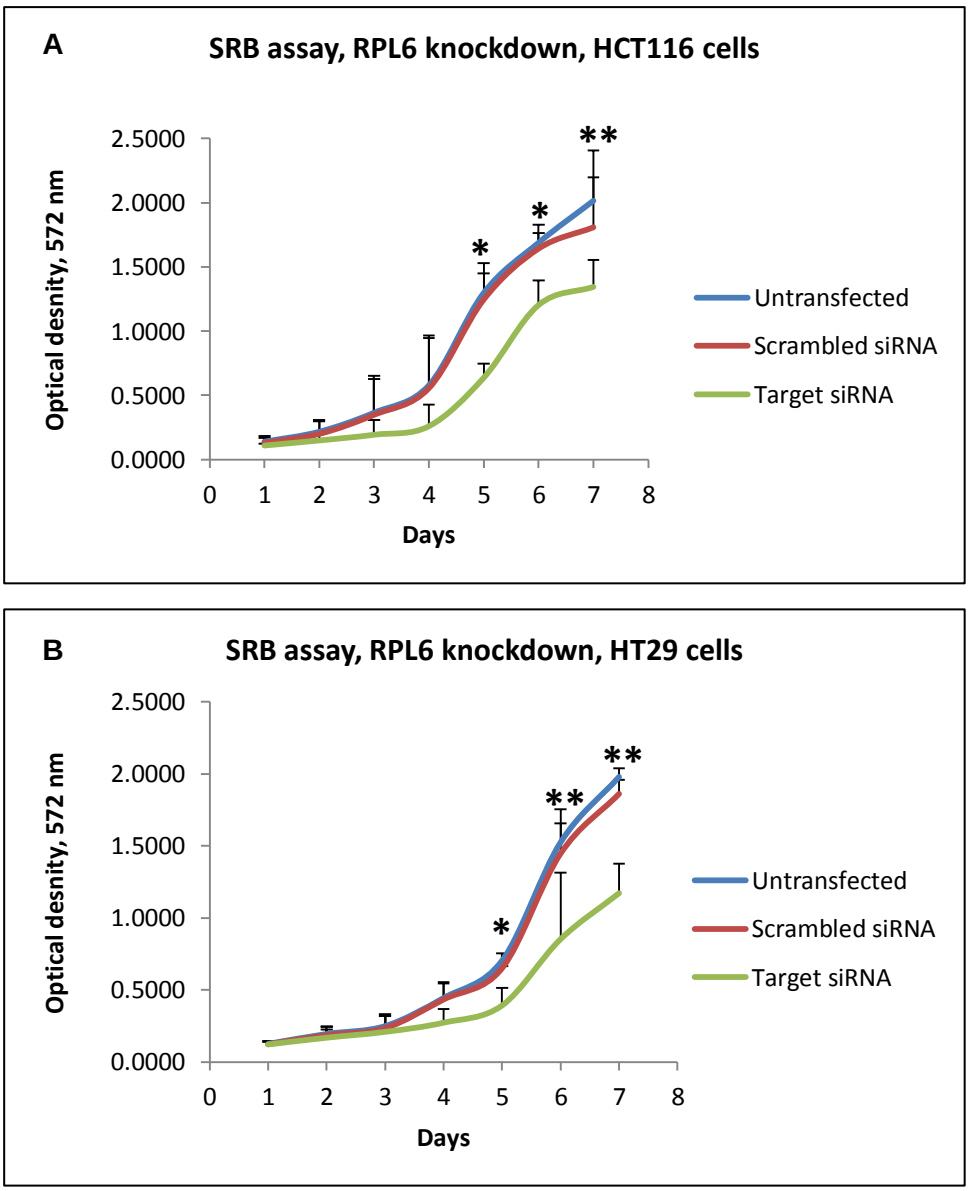


**Figure 4.14 SRB assay, HCT116 (A) and HT29 (B). Cells showed reduced proliferation after knocking down RPL6. Error bars represent standard deviation from the mean (N3, n6). P value * <0.05, ** < 0.001**

Consistent with the findings obtained by the haemocytometer method, the SRB assays identified a statistically significant (at days 5-7 in both cell lines) reduction in cell proliferation.

Again cell viability following RPL6 knockdown in both cells lines was also assessed using colonogenic survival assays as shown below.

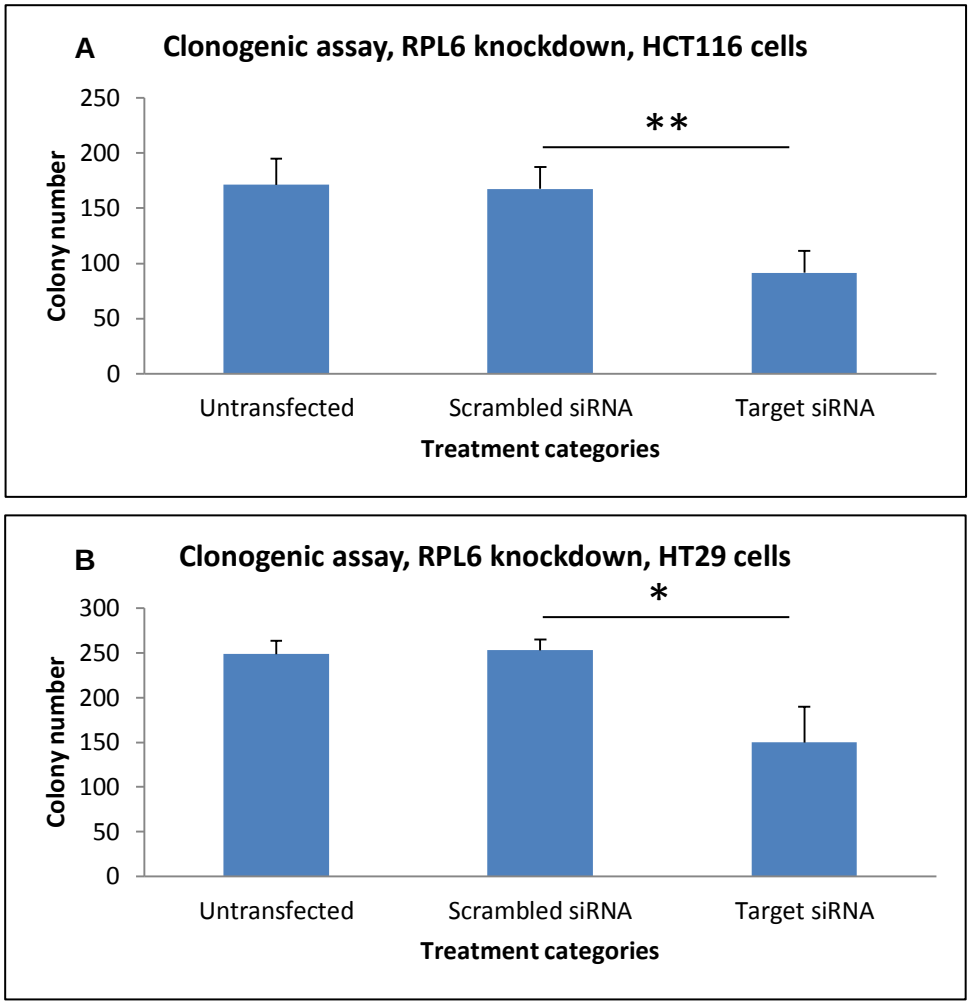


**Figure 4.15 Clonogenic survival assay. Both HCT116 cells (A) and HT29 cells (B) showed a significant reduction in survival and colony forming ability after RPL6 knockdown (* p value <0.05 and ** < 0.01). Error bars represent standard deviation from the mean (N3, n3).**

The results are in agreement with the cell counting technique, identifying a statistically significant inhibition of cell survival following RPL6 knockdown.

## 4.5 Assessment of RPL6 and Cyclin E expression and relationship in murine models of CRC

Ribosomal protein like 6 (RPL6) has been mainly linked to ribosome biosynthesis and protein translation [229]. There is increasing evidence that Ribosomal proteins are involved in different cancer processes [231, 255]. However, not much can be found on the involvement of RPL6 in cancer, particularly in CRC. One recent study on gastric cancer cell lines suggested that RPL6 up-regulation mediated tumour growth as well as tumour resistance to drug induced apoptosis. Moreover, they suggested Cyclin E as a possible partner molecule [229]. Furthermore, they were able to show co-localisation or RPL6 and Cyclin E in human gastric cancer samples.

Here were tried to study the relationship between RPL6 and Cyclin E in our models of colorectal tumourigeneis. Using IHC, the expression of these two proteins was studied in $AhCre^{+}Apc^{fl/fl}$ and $Apc^{Min/+}$ mice which represent the immediate stage and a more extended period following the deletion of *Apc*, respectively.

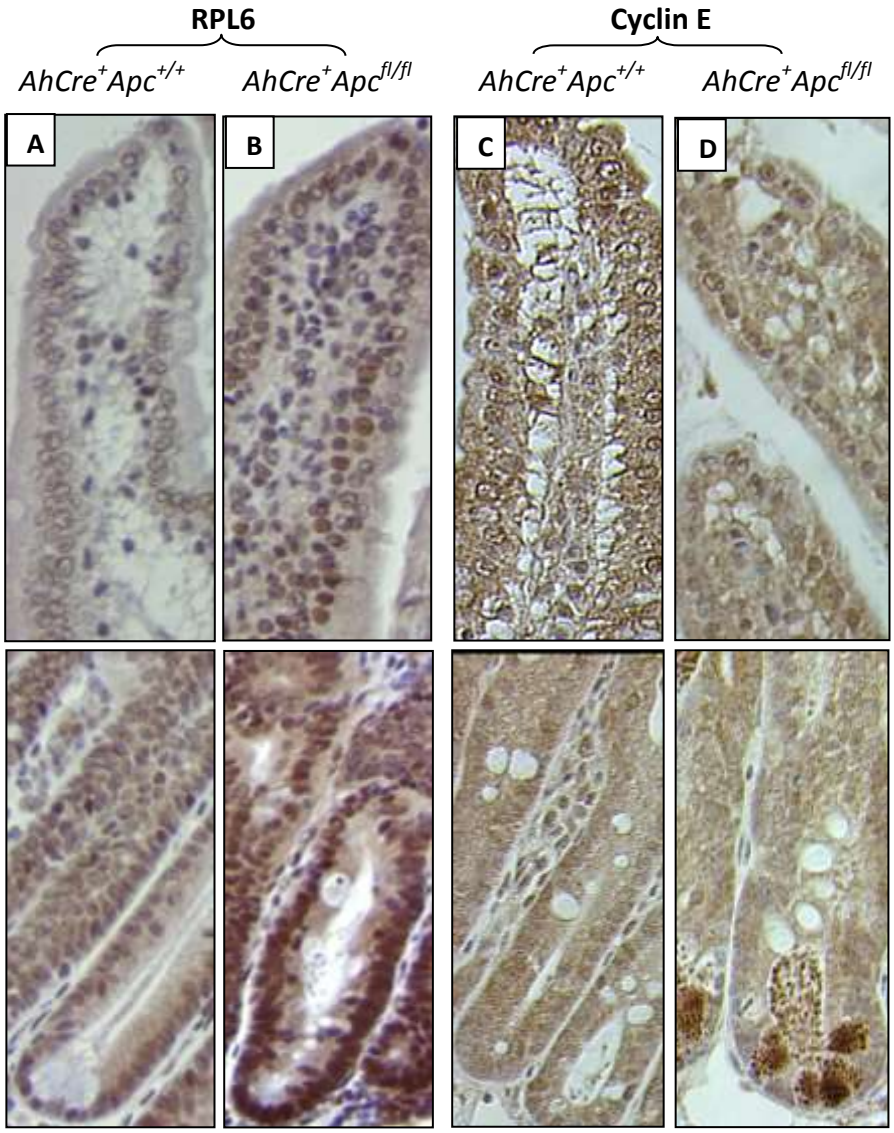


**Figure 4.16 Small intestinal sections (villi-upper panel and crypts-lower panel) from the *AhCre$^{+}$Apc$^{+/+}$* (A and C) and *AhCre$^{+}$Apc$^{fl/fl}$* (B and D) mice. A & B show RPL6 expression (Proteintech, dilution of 1:200) and C & D show Cyclin E (Santa Cruz, dilution of 1:600) staining. The secondary antibody was from Dako (dilution of 1:200). All images were taken with an X40 objective. A cohort of 3-5 mice was used for each group.**

Within only 5 days there was nuclear overexpression of RPL6 in the Wnt active areas of the *AhCre$^{+}$Apc$^{fl/fl}$* (figure 4.16B) mice in comparison to their wild type counterparts (figure 4.16A). On the other hand Cyclin E, although mentioned to be overexpressed following the same pattern as RPL6 [229]; did not show nuclear overexpression. Cyclin E showed intense granular staining at the crypt bases in the *Ahcre$^{+}$Apc$^{fl/fl}$* mice (figure 4.16D). At this stage we thought that these were most likely to be Paneth cell granules. To test the latter assumption we also stained sections from the above models with an anti-Lysozyme antibody as shown below.

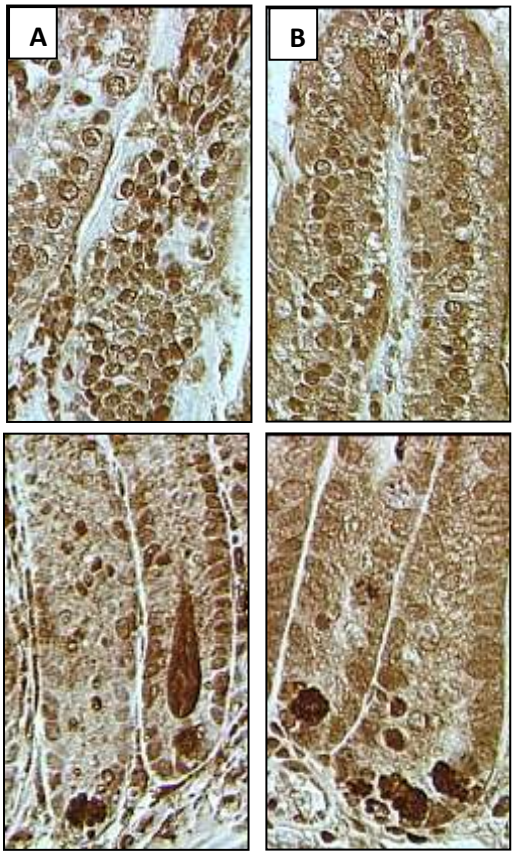


**Figure 4.17 Small intestinal sections (villi-upper panel and crypts-lower panel) from *the Ahcre$^{+}$Apc$^{+/+}$* (A) and *Ahcre$^{+}$Apc$^{fl/fl}$* (B) mice. These are stained with anti-Lysozyme antibody (Dako, dilution of 1:200). The secondary antibody was also from Dako (dilution of 1:200). All images were taken with an x40 objective. A cohort of 3-5 mice was used from each group.**

Staining with anti-Lysozyme antibody is one of the ways of staining Paneth cells [44]. The staining confirmed that those granules at the base of the crypts in the *AhCre$^{+}$Apc$^{fl/fl}$* (figure 4.16D) mice and that demonstrated intense Cyclin E staining were actually Paneth cell granules.

After making this interesting observation with RPL6 and Cyclin E in the *AhCre$^{+}$Apc$^{fl/fl}$* mice, we used the same IHC conditions to study the same proteins in the second mouse model, the *Apc$^{Min/+}$* mouse. The results are shown below.

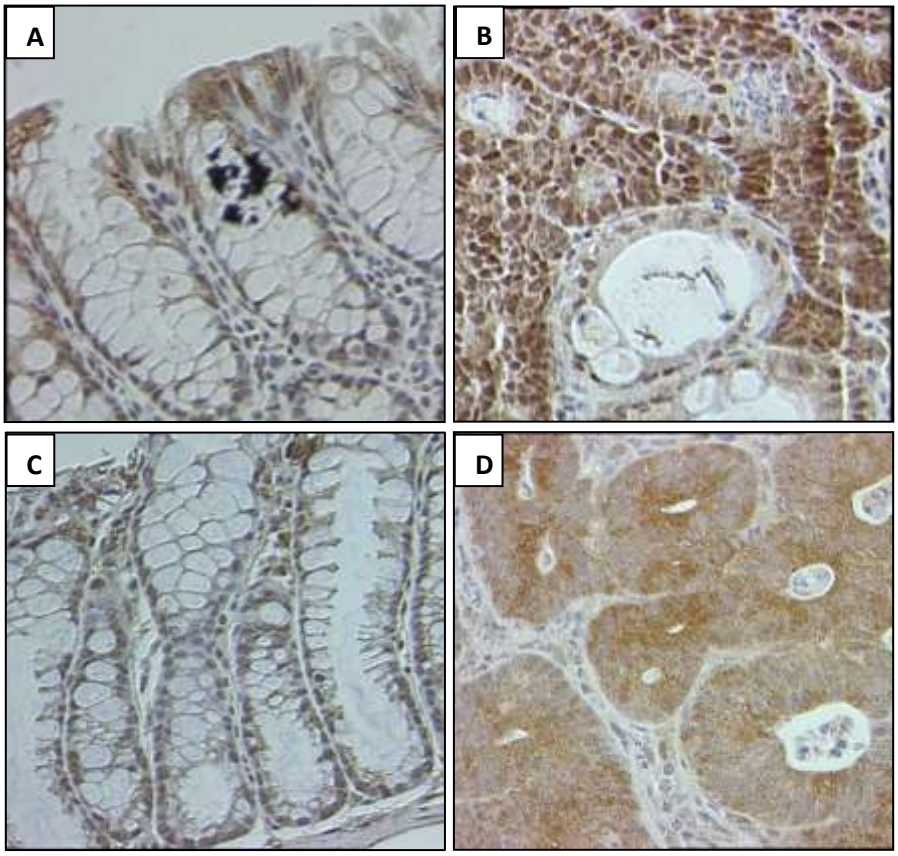


**Figure 4.18 Colonic sections from six month old *Apc*$^{+/+}$ (A & C) and *Apc*$^{Min/+}$ mice (B & D). These were stained with anti-RPL6 antibody (Proteintech, dilution of 1:200) (A & B) and anti-Cyclin E antibody (Santa Cruz, dilution of 1:600) (C & D). The secondary was from Dako (dilution of 1:200). Images were taken with X40 objective. A cohort of 3-5 mice were used from each group.**

The results in *Apc*$^{Min/+}$ mice were in agreement with those from the *Ahcre*$^{+}$*Apc*$^{fl/fl}$ mice. RPL6 showed increased nuclear expression in the colonic adenoma (figure 4.18B). Cyclin E was excluded from the nuclei and was mainly over expressed in the cytoplasm in the polyp tissue (figure 4.18D). Western blot analysis was tried to further assess the changes in Cyclin E expression in these mouse models, however results were too non-specific to be interpreted.

## 4.6 Discussion

In chapter three, we demonstrated that a number of our candidate proteins showed clear differential staining in the context of *Apc* deletion *in vivo*. Therefore, we decided to investigate the role of those proteins that showed the most consistent changes and which represented novel areas for better understanding the development of CRC. For this reason we chose to study NAP1L1 and RPL6.

RNA interference is an effective method for studying the functions of target proteins through regulating their mRNA expression [256]. However, particularly transient siRNA inhibition is limited by a number of factors. These include the time cells take to double their numbers, the significance of the target gene in proliferation and the half-life of the target protein [256].

Moreover, the outcome of RNA interference (RNAi) may vary according to cell type due to variation in their susceptibility to transfection. In an attempt to understand the response of HCT116 and HT29 cells to the protein knockdown process, it is important to understand their genetic backgrounds. Both HCT116 and HT29 cells have a genetic profile that suggests the presence of an induced WNT pathway. However, the level of derangement may have a critical role in cell behaviour and the underlying protein networks. Unlike HCT116, HT29 cells are defective at the level of APC, therefore there might be other mechanisms that may inhibit the WNT pathway such as PTEN (phosphatase and tensin) protein [257]. By contrast in HCT116 cells, the defect is at the level of Beta catenin, rendering it resistant to any degradation. This may partly explain the more aggressive phenotype exhibited by these cells. There are reports that support this concept; one paper suggested that the level of Beta catenin activity has critical effects on tumour development. This notion has been validated in different *Apc* mutant mice which showed different levels of Beta catenin activity and different tumour phenotypes [63]. To complicate the matter further, some cell lines are inherently more resistant than others to siRNA transfection.

In humans and mice, the NAP1 family consists of at least five members, NAP1L1, NAP1L2, NAP1L3, NAP1L4, and NAP1L5. Interestingly, three of the NAP1-like proteins (NAP1L2, NAP1L3, and NAP1L5) are almost exclusively found in the brain. However, NAP1L1 and NAP1L4 are expressed ubiquitously in all vertebrates

[258]. Some publications have described NAP1L1 as a cancer-related protein [148, 259]. NAP1L1 and NAP1L4 serve as cytoplasmic anchors for Diacylglycerol kinase (DGK) and have potential protective effects against conditions of stress [260]. DGK is involved in the regulation of lipid mediated signal transduction through the metabolism of the second messenger diacylglycerol. Moreover, a recent study has shown that knocking down NAP1L1 in P19CL6 cells induced them to differentiate into cardiomyocytes [260].

In this thesis, knocking down NAP1L1 expression in HCT116 and HT29 human CRC cell lines caused a moderate effect on cellular proliferation as demonstrated by the various techniques employed. HCT116 cells were more sensitive to NAP1L1 inhibition than HT29 cells. This observation may be attributed to differences between the two cell lines or the resistance to transfection exhibited by the latter. Moreover, this result may support the suggestion that NAP1L1 is involved in the state of cellular de-differentiation [260]. Therefore, knocking down NAP1L1 expression in HCT116 cells in particular may contribute to the reduction in their aggressive behaviour.

Changes in the tightly regulated process of ribosomal biogenesis have been implicated in a number of human pathologies [261]. Therefore, it is important to study the elements involved in this process including ribosomal proteins [262]. RPL6 is another protein that was upregulated in the $AhCre^{+}Apc^{fl/fl}$ mouse intestine and that is also relatively new to the field of colorectal carcinogenesis. However, the role of the ribosomal family of proteins has been increasingly suggested in different cancers such as breast and oesophageal cancers [232, 233]. A recent study evaluating RPL6 in gastric cancer lines suggested a possible role for RPL6 in promoting cell cycle progression (G1 to S), cellular proliferation and mediating resistance against drug induced apoptosis [163].

RPL6 knockdown in HCT116 and HT29 cells caused a marked inhibition of cell proliferation. Again the effect was more noticeable in HCT116 cells. This finding supports a role for RPL6 in mediating cell cycle progression and cellular proliferation. Moreover, RPL6 inhibition in both cell lines caused reduced viability and colony forming ability. This agrees with the observation that RPL6 upregulation causes enhanced colony forming abilities in gastric cancer cell lines [229].

Furthermore, the observed increased rate of apoptosis following RPL6 knockdown, agrees with the notion that RPL6 up-regulation mediates resistance to apoptosis by tumour cells. These findings make RPL6 a potential prognostic biomarker and even a therapeutic target at least in a subset of tumours.

As we and others have shown, loss of APC function in the intestine is associated with a constitutively active Wnt pathway, and this leads to a state of hyperproliferation and the expression of a range of genes such as those involved in regulating the cell cycle including c-Myc and Cyclin D2 [263]. Recent work has shown that the Cyclin D2-cyclin dependent kinase 4/6 (CDK4/6) complex induces hyperproliferation in Apc deficient intestinal tissue and $Apc^{Min/+}$ adenomas [263]. Moreover, this same work showed that the hyperproliferative state is partly attributed to Cyclin D2. By inhibiting the latter the authors were able to suppress the hyperprolifertive state and the adenoma cells. This is a good example of the importance of finding alternative therapeutic targets for undruggable molecules such as Beta catenin and c-Myc in CRC. In a similar context, Cyclin E has also been shown to be part of the tumourigenesis process in gastric cell lines [229]. Cyclin E was also shown to be linked to RPL6 in these cell lines and in human gastric cancer samples [229]. Therefore, we decided to study Cyclin E expression in the same Wnt active areas that showed RPL6 overexpression in our CRC mouse models. This might help to open new opportunities to find more suitable therapeutic targets in CRC management.

The normal cell cycle is tightly controlled such that cells are only allowed to divide in a timely and scheduled manner. The control machinery involves two classes of proteins: the cyclin dependent kinases (CDKs) and their activators, the cyclins [264]. The G1/S phases of the cell cycle are mediated primarily by retinoblastoma susceptibility protein (Rb). Rb protein binds to the E2F family of transcription factors and acts as a repressor for genes required to mediate the S phase [263]. In early G1 phase, Cyclin D activates CDK4/6. The resultant complex leads to the phosphorylation of Rb, which in turn releases the E2F factor. The latter in turn induces the expression of genes needed for DNA replication and promotion of the G1/S phase of the cell cycle including Cyclin E [248].

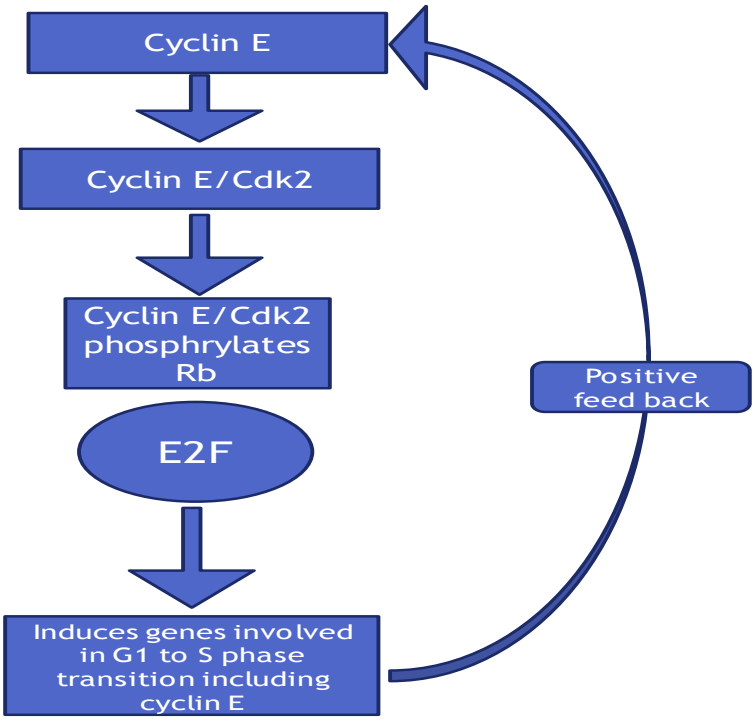


**Figure 4.19 The mechanism by which Cyclin E mediates its function in cell cycle regulation.**

The Cyclin E/Cdk2 complex is required for the phosphorylation and inactivation of Rb releasing E2F factor (figure 4.19). Interestingly, Cyclin E can induce its own expression in a positive feedback loop. Not surprisingly, normal cells maintain strict control of Cyclin E activity and Cyclin E has been reported to be upregulated in many tumours including CRC. Not only that, but Cyclin E deregulation is thought to play a fundamental role in tumorigenesis [265]. Cyclin E has also been shown to be associated with high grade tumours and poor prognosis in CRC patients and therefore it is a potential prognostic marker [264]. The most common means of activating Cyclin E expression in cancers involve mutations in regulatory pathways, rather than within Cyclin E itself.

We have shown that, in the setting of acute Apc loss in the small intestine of *AhCre*$^{+}$*Apc*$^{fl/fl}$ mice, Cyclin E showed intense staining in Paneth cell granules (figure 4.16). At the same time, there was no obvious differential staining in other epithelial cell types relative to their wild type counterparts. To confirm this observation, an anti-lysozyme antibody was used to stain Paneth cells (figure 4.17). This showed the same granular staining pattern that was seen with the anti-Cyclin E antibody.

Moreover, the absence of similar staining in the Paneth cells of control animals ruled out any nonspecific staining.

To explain this observation, we need to explore the role of Paneth cells in the stem cells niche in the small intestine. The location and direction of Paneth cell migration, their high density and long residency time at the crypt base, and the nature of their secreted gene products, suggest that they may influence the structure and/or function of the stem cell niche [266]. For example, it has been shown that Paneth cells regulate the numbers of intestinal stem cells *in vivo* and that CD24 positive Paneth cells express EGF, TGF-a, Wnt3 and the Notch ligand Dll4, all of which are essential signals for stem-cell maintenance in culture [77]. Moreover, it has also been shown that the ability of stem cells to form organoids improves by co-culturing them with Paneth cells [77]. In addition, genetic deletion of Paneth cells results in the loss of Lrg5 stem cells. These observations indicate that Paneth cells at least feed a subgroup of stem cells with the essential signals for their sustainability. Cyclin E could be involved in this complex relationship between Paneth cells and stem cells. This may explain the observed increased level of Cyclin E in Paneth cells in the setting of a deranged Wnt pathway following the loss of Apc.

In $Apc^{Min/+}$ mice, Cyclin E showed cytoplasmic staining in the colonic adenomas of six month old mice. To further highlight the role of Cyclin E in colorectal tumourigenesis, WB analysis was also used to study its expression in $AhCre^{+}Apc^{fl/fl}$ and $Apc^{Min/+}$ mice as well as in HT29 and HCT116 cells following RPL6 knockdown. This is because Cyclin E upregulation in the setting of Apc loss induced Wnt activation could further support the role of this protein in the events observed. Moreover, the level of Cyclin E following RPL6 knockdown could provide a more objective indication about the relationship between these two proteins. However, unfortunately, due to the lack of sufficient samples and availability of good quality antibodies, it was not possible to produce blots that were good enough for quantification purposes. Moreover, lack of time did not allow the use of an alternative quantification technique such as qRT-PCR.

Therefore, based only on IHC alone, a firm conclusion cannot be drawn about the relationship between RPL6 and Cyclin E in the setting of *Apc* deletion, apart from their concomitant overexpression.

In conclusion, it appears that NAP1L1 and RPL6 both play roles in mediating the hyper-proliferative state that is associated with activation of the Wnt pathway following *Apc* deletion. This was evident by the techniques used to assess proliferation (cell counting and SRB assay) and to assess cell viability and colony forming ability (clonogenic assay). Although, other work (not shown) by our group has demonstrated a similar pattern of expression between NAP1L1 and RPL6 in the serum of patients at different stages of CRC by ELISA (Dr. Fei Song), and it has been mentioned that *RPL6* is one of the genes that has an expression profile closely related to NAP1L1 (G2SBC data base, breat cancer) [267], more specific tools such as immunoprecipitation and upregulation studies are needed to investigate whether there is any direct interaction between these proteins.

Some studies have suggested a role for Beta catenin in the control of G1/S transition [268]. In this context, the candidate proteins RPL6 and NAP1L1 could therefore be possible mediators of this function of Beta catenin.

# Chapter five

# Mechanistic studies on the functions of SFRS2 and its possible roles in colorectal tumourigenesis

## 5. Mechanistic studies on the function of SFRS2 and its possible roles in colorectal tumourigenesis

### 5.1 Introduction

SFRS2 was among the proteins that showed upregulation in the proteomics analysis performed in the *AhCre*$^{+}$*Apc*$^{fl/fl}$ mice by a previous colleague in our department [147]. Also in chapter three, using IHC, it was shown that SFRS2 was upregulated in the intestine in the setting of acute *Apc* deletion and in colonic adenomas from six month old *Apc*$^{Min/+}$ mice. Moreover, preliminary work by our team at a previous stage of this project showed upregulation of SFRS2 in human CRC samples (blood and tissue). Therefore, we decided to further analyse the role of this protein in colorectal tumourigenesis.

SFRS2 belongs to the serine rich (SR) family of proteins, one of the most important regulators of pre-mRNA splicing [234]. Pre-mRNA splicing is a critical process, because it is an important mechanism of genetic diversity [269]. Although SR proteins have well been documented to be linked to mRNA splicing *in vitro*, less is known about their role *in vivo*. However, SR proteins have been shown to be involved in critical biological functions such as cell viability and animal development [234].

In an attempt to expand our knowledge about SFRS2, it was important to find a partner molecule with which it may directly or indirectly interact. We therefore carried out a literature search. A paper published in 2002 demonstrated that CDC5L (cell division cycle 5 like) overexpression displaced SFRS2 into the cytoplasm in cell lines [270]. This is even more interesting as both molecules are involved in the same spectrum of cellular functions such as pre-mRNA splicing and cell cycle progression. Therefore, we hypothesised that there may be some kind of antagonistic relationship between SFRS2 and CDC5L in mediating these functions.

For the above reasons we decided to study the possible interconnected roles of SFRS2 and CDC5L in colorectal tuomourigenesis using animal and human cell line models of CRC.

**Aims**

- To study the roles of SFRS2 and CDC5L in colorectal tumourigenesis
- To compare the results of the above studies to investigate whether there are any possible functional interactions between these two proteins

## 5.2 Comparison of SFRS2 and CDC5L expression in colorectal tumourigensis using IHC

From our observations and evaluation of the published literature, there appears to be an important interaction between SFRS2 and CDC5L. Therefore, the expression of SFRS2 and CDC5L was initially investigated by IHC in three mouse models representing critical stages during colorectal tumourigenesis.

### 5.2.1 SFRS2 and CDC5L expression in *AhCre$^{+}$Apc$^{fl/fl}$* mice

As described in chapter three, the *AhCre$^{+}$Apc$^{fl/fl}$* mouse model allows the evaluation of events that occur in the intestine immediately after *Apc* deletion. Below are representative images showing the expression of SFRS2 and CDC5L in paraffin embedded sections of small intestinal epithelium from *AhCre$^{+}$Apc$^{fl/fl}$* mice.

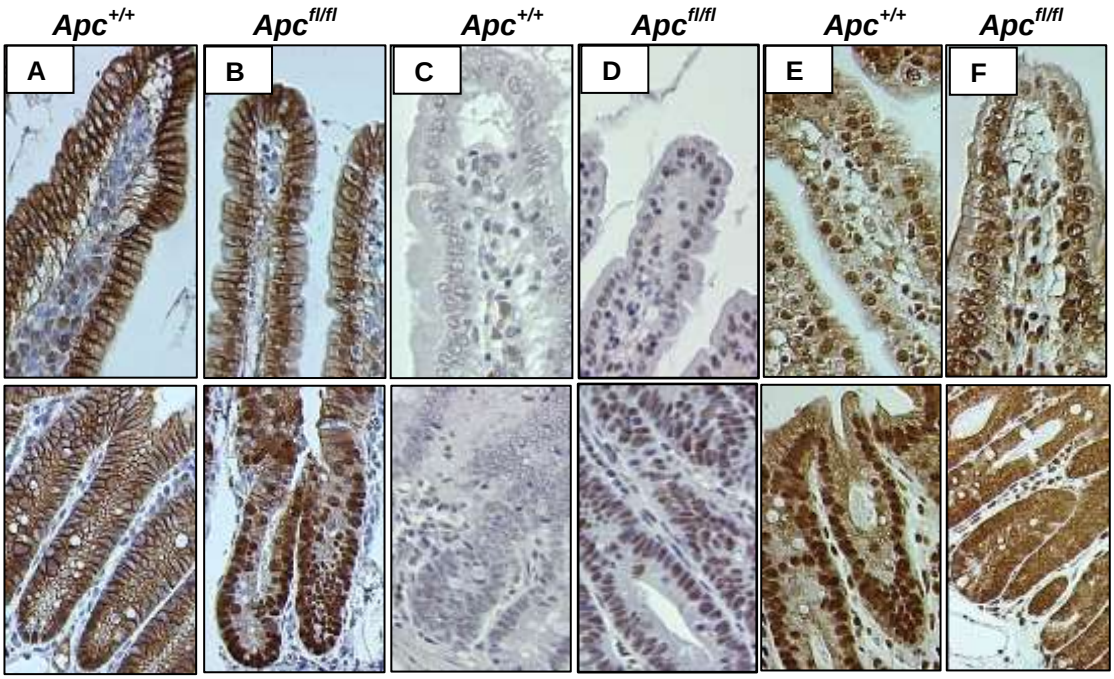


**Figure 5.1 Representiave images of paraffin embedded sections from murine small intestinal epithelium (top panel are villi and lower panel are crypts). A and B show *AhCre$^{+}$Apc$^{+/+}$* and *AhCre$^{+}$Apc$^{fl/fl}$* sections, respectively stained with anti-Beta catenin antibody; C and D are *AhCre$^{+}$Apc$^{+/+}$* and *AhCre$^{+}$Apc$^{fl/fl}$* sections, respectively stained with anti-SFRS2 antibody; E and F are *AhCre$^{+}$Apc$^{+/+}$* and *AhCre$^{+}$Apc$^{fl/fl}$* sections, respectively stained with anti-CDC5L antibody. All images are X40 objective original magnification.**

Beta catenin nuclear localisation indicated the presence of an active Wnt signalling pathway localised to the crypt areas of the small intestine in *AhCre*$^{+}$*Apc*$^{fl/fl}$ animals (figure 5.1B). SFRS2 did not show any observable expression in control intestinal epithelium (figure 5.1C). However, clear nuclear expression was observed in the *Apc*$^{fl/fl}$ tissue (figure 5.1D). The latter was mainly in the form of speckles. Interestingly, while CDC5L showed a predominantly nuclear staining pattern in control small intestinal tissue (figure 5.1E), it was detected in the cytoplasm either equally or more intensely in the *Apc* knockout tissues (figure 5.1F). The latter observation may be due to displacement of CDC5L from the nuclei into the cytoplasm following *Apc* deletion.

### 5.2.2 SFRS2 and CDC5L expression in *Apc*$^{Min/+}$ mice

The expression of SFRS2 and CDC5L was also assessed in neoplastic lesions in *Apc*$^{Min/+}$ mice. This model allows evaluation of a more extended period of Apc induced changes that lead to tumour formation. Below are representative images of IHC in this model (figure 5.2).

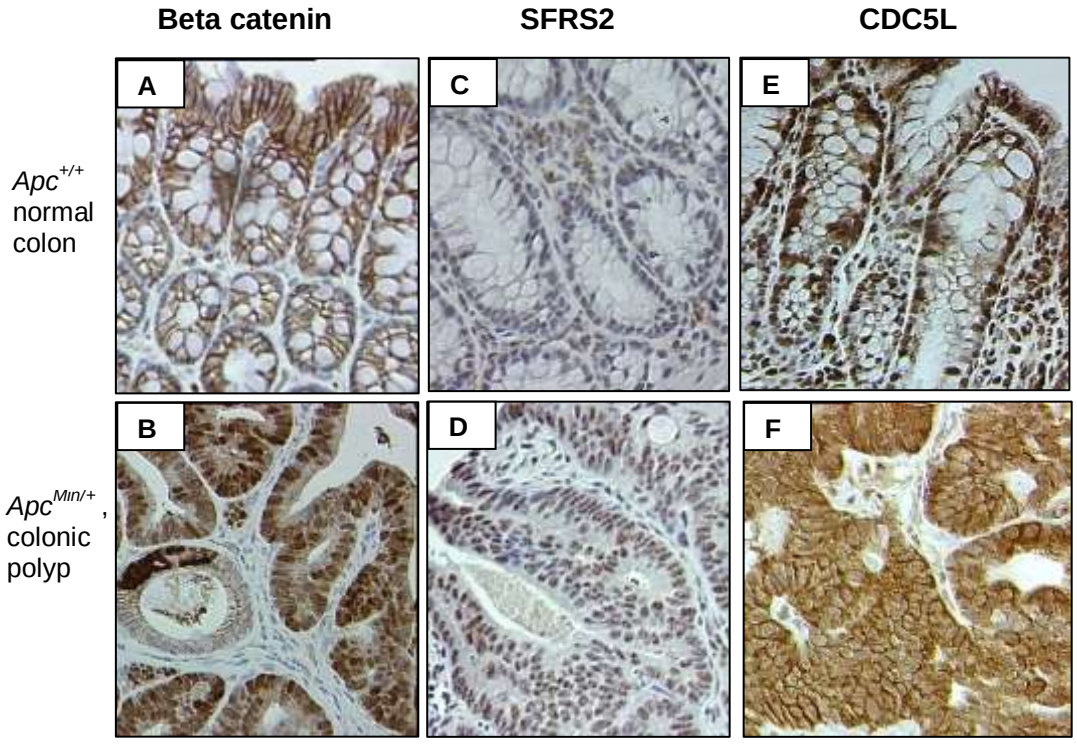


**Figure 5.2 Representative images of paraffin embedded sections from *Apc*$^{+/+}$ colonic mucosa (A, C and E) and colonic polyps in six month old *Apc*$^{Min/+}$ (B, D and F) mice. A and B show Beta catenin staining. C and D show SFRS2 staining. E and F show CDC5L staining. The experimental conditions were the same as those described in figure 5.1. All images are X40 magnification.**

Beta catenin staining showed evidence of active Wnt signalling in the polyps. Consistent with the findings from the *AhCre*$^{+}$*Apc*$^{fl/fl}$ mouse model, SFRS2 and CDC5L showed nuclear overexpression and increased cytoplasmic staining respectively in areas of adenoma. The interesting difference was that CDC5L expression was virtually absent from the nuclei in the adenomatous tissue (figure 5.2F), whereas nuclear staining was as strong as the cytoplasmic staining in the *AhCre*$^{+}$*Apc*$^{fl/fl}$ mice (figure 5.1F, crypt area). This may be due to the longer time these lesions take to develop in *Apc*$^{Min/+}$ mice compared to those in the *AhCre*$^{+}$*Apc*$^{fl/fl}$ mouse model.

### 5.2.3 Assessment of WNT pathway activation and SFRS2 and CDC5L expression in animal models of early and advanced intestinal tumourigensis using IHC

Due to the importance of WNT signalling pathway in colorectal tumourigensis, we investigated the state of this pathway in intestinal lesions from animal models known to have *Apc* deletion and a deranged Wnt pathway. *AhCre*$^{+}$*Apc*$^{fl/fl}$ and *Apc*$^{Min/+}$ mice represent the relatively early stages in which lesions are not transformed. The *AhCreER*$^{T+}$*Apc*$^{fl/+}$*Pten*$^{fl/fl}$ mouse represents a model of accelerated intestinal tumourigensis which leads to the formation of malignant lesions in the intestine [182]. This enhanced tumourigensis is due to the addition of *Pten* knockout to a background in which *Apc* is also deleted [182]. Figure 5.3 shows different time points during the colorectal tumourigensis process using these animals. Nuclear localisation of Beta catenin was used as a surrogate marker for Wnt pathway activity.

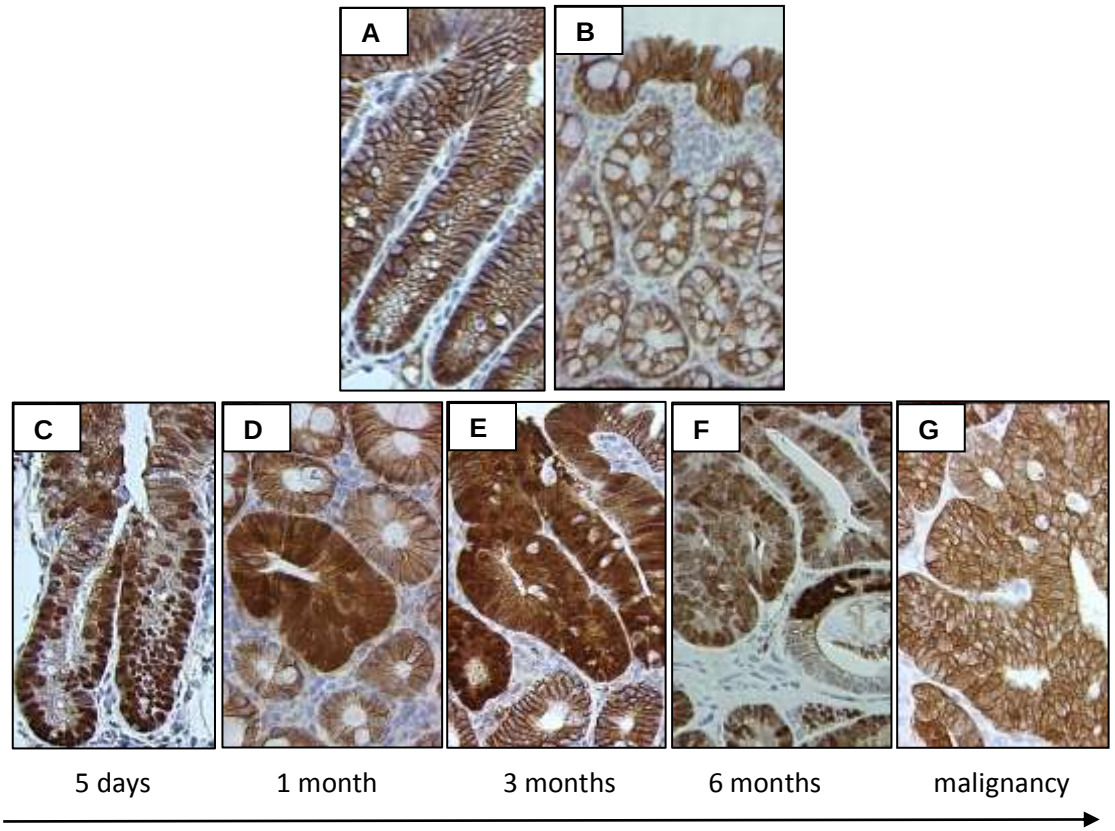


**Figure 5.3 Representative images of murine intestinal sections stained with anti-Beta catenin antibody showing Wnt pathway activity at different time points during intestinal tumourigenesis. The secondary antibody was from Dako. A) Small intestinal crypt from an *AhCre*$^{+}$*Apc*$^{+/+}$ mouse, (B) colonic section from *an Apc*$^{+/+}$ mouse. (C) Small intestinal crypt from an *AhCre*$^{+}$*Apc*$^{fl/fl}$ mouse, (D) neoplastic lesion from a one month old *Apc*$^{Min/+}$ mouse, (E) neoplastic lesion from a three month old *Apc*$^{Min/+}$ mouse, (F) neoplastic lesion from a six month old *Apc*$^{Min/+}$ mouse and (G) neoplastic lesion from an *AhCreER*$^{T+}$*Apc*$^{fl/+}$*Pten*$^{fl/fl}$ mouse. All images were taken with an X40 objective. Sections were from at least three mice in each group.**

As we showed previously (chapter 3), Beta catenin is mostly membranous under unstimulated conditions (figures 5.3 A and B). However, very early following *Apc* deletion, overexpression of Beta catenin occurs, which is manifested as nuclear translocation (figures 5.3 C, D, E and F). Interestingly, after transformation, Beta catenin overexpression persisted, but it was no longer localised to the nuclei (figure 5.3 G).

Due to the above observations, and because our candidate proteins are probably Wnt pathway dependent, we decided to study their expression in this tranformation model. We therefore stained intestinal lesions from *AhCreER*$^{T+}$*Apc*$^{fl/+}$*Pten*$^{fl/fl}$ mice

with anti-NAP1L1, RPL6 and SFRS2 (also FABP6, NCL and PHB) antibodies (sources of antibodies and experimental conditions were as described in chapter 3). Unfortunately, the antibodies used did not stain these sections. A possible reason for this is that a different fixation method (Methacarn, 60% absolute methanol, 30% chloroform and 10% glacial acetic acid) was used in the preparation of these sections. This fixative has been described as affecting the antigen binding efficiency of some antibodies [271]. Moreover, other factors might have been responsible such as the duration of the storage of the tissue slides; tissue slides that are more than 2 months old are often suboptimal for IHC.

However, when we stained sections from the same source with the anti-CDC5L antibody (under the same conditions described above) the results were interesting; below are representative images of CDC5L staining in *AhCreER$^{T+}$Apc$^{fl/+}$Pten$^{fl/fl}$* mice (figure 5.4).

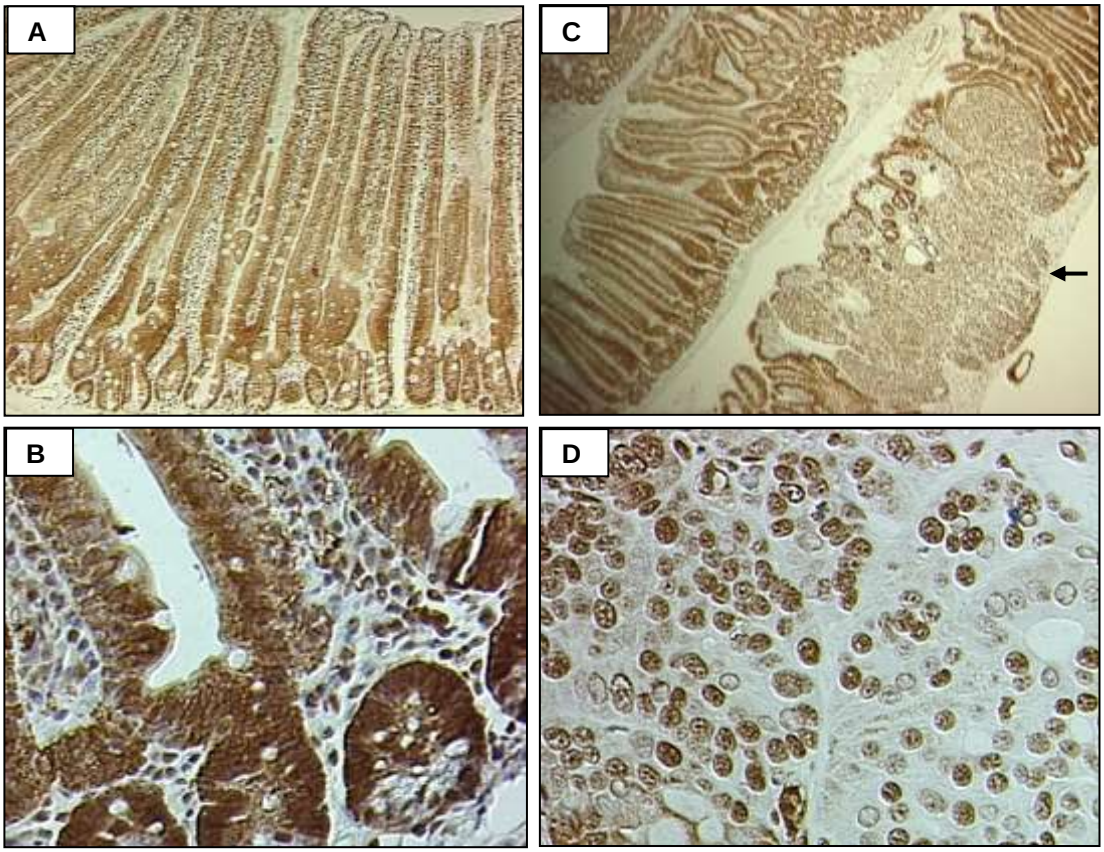


**Figure 5.4 Representative images of murine small intestinal sections stained with anti-CDC5L antibody (experimental conditions were the same as in figure 5.1). A and B) *AhCreER$^{T+}$Apc$^{fl/+}$Pten$^{+/+}$*. C and D) A malignant lesion from *AhCreER$^{T+}$Apc$^{fl/+}$Pten$^{fl/fl}$* mouse. The black arrow in (C) points to a lesion with submucosal invasion. A and C) are X5 original magnification whereas B and D are X40 original magnification. N= 3 mice.**

Before neoplastic transformation, CDC5L showed predominantly cytoplamic expression (figures 5.1F and 5.2F) whereas Beta catenin showed predominant nuclear expression (figures 5.1B and 5.2B). However, CDC5L showed almost exclusive nuclear staining (figure 5.4D) in malignant lesions in which Beta catenin was excluded from the nuclei (figure 5.3G). Although effects of fixation on CDC5L and Beta catenin staining cannot be excluded in *AhCreER$^{T+}$Apc$^{fl/+}$Pten$^{fl/fl}$* mice, this seems to be unlikely due to the presence of obvious staining patterns in the lesions and in the control tissue.

Unfortunately due to the limited number of sections available from the *AhCreER$^{T+}$Apc$^{fl/+}$Pten$^{fl/fl}$* mice, it was not possible to stain lesions from mice of different ages. However, the staining pattern observed was the same across lesions of different sizes. Moreover, despite the fact that SFRS2 staining was tried on different batches of tissue sections from *AhCreER$^{T+}$Apc$^{fl/+}$Pten$^{fl/fl}$* mice, no staining was observed. For the future, because of the potential importance of SFRS2 in *AhCreER$^{T+}$Apc$^{fl/+}$Pten$^{fl/fl}$* model, it would be ideal if tissues from this model could be generated and processed in a way that enable staining with commercially available anti-SFRS2 antibodies (namely formalin fixation).

### 5.3 Effect of SFRS2 knockdown on cellular proliferation and apoptosis in HCT116 and HT29 cells

Several reports have indicated a role for both SFRS2 and CDC5L in critical physiological processes such as proliferation, apoptosis and cell cycle distribution as well as pathological processes such as cancer development (as described earlier in this work). It was therefore important to investigate the role of SFRS2 and CDC5L in these processes as this may unveil novel diagnostic and/or therapeutic tools in the management of an important health problem such as CRC. Again, siRNA mediated knockdown of gene expression was used to down regulate SFRS2 in HCT116 and HT29 cells using the same transfection conditions established earlier (described in chapter four). Knockdown efficiency was assessed by western blot and qRT-PCR, while effects on cells were assessed using the previously described techniques of haemocytometer based cell counting as well as SRB and clonogenic assays. Results are shown below.

**SFRS2 knockdown in HCT116 cells**

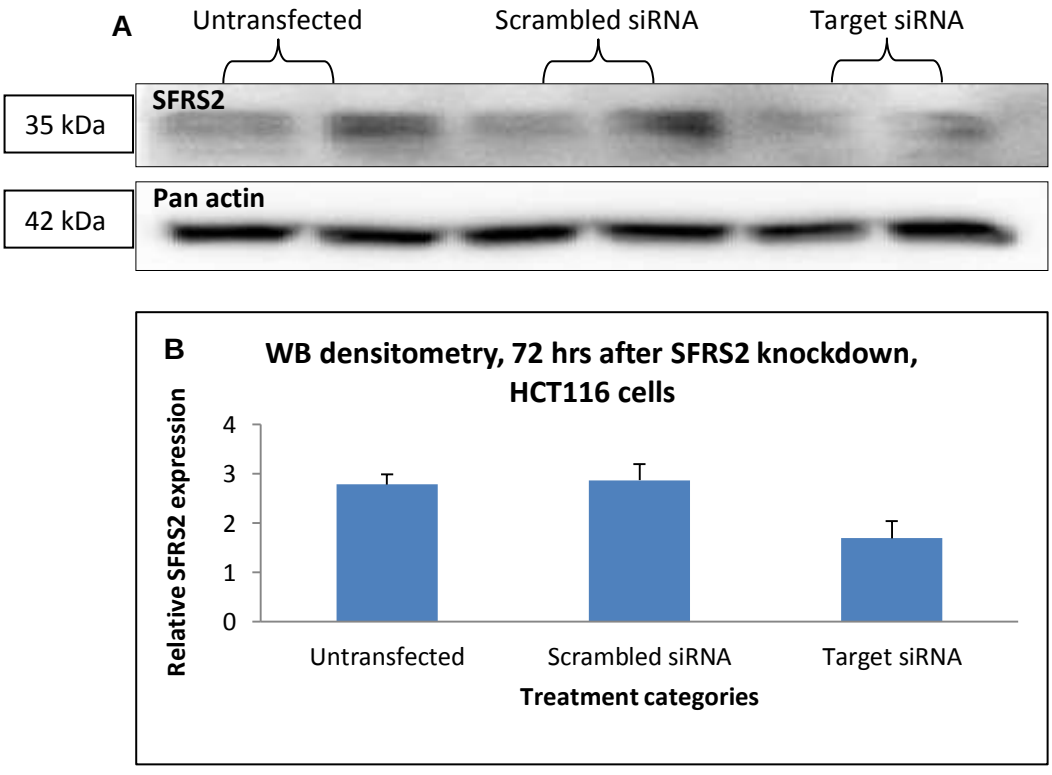


**Figure 5.5 A) Western blot (representative of 3 experiments) of HCT116 whole cell proteins probed with anti-SFRS2 antibody. Pan actin was used as loading control. B) Densitometry analysis of SFRS2 expression relative to untransfected cells (N3, n2). Error bars represent SD from means.**

It is obvious that the antibody used to probe the membranes did not produce optimal bands. Despite the above limitations, densitometry demonstrated some degree of knockdown relative to both control groups.

Different experimental conditions were tried to improve the western blot analysis of SFRS2 knockdown (as described in chapter three, p 132). Unfortunately no great improvement was achieved. Therefore, qRT-PCR was used to demonstrate knockdown as shown in figure 5.6.

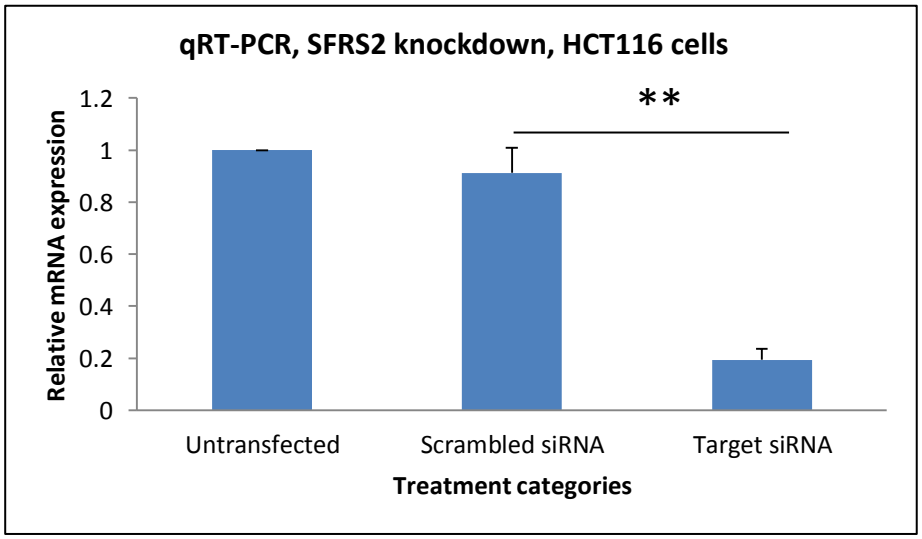


**Figure 5.6 qRT-PCR analysis of relative SFRS2 expression in HCT116 cells 72 hrs following its knockdown. Error bars represent standard deviation from means. N3, n3. ** p value < 0.01.**

There was an approximately 80% reduction in SFRS2 mRNA abundance (figure 5.6) in the target siRNA transfected group compared to that from the scrambled siRNA transfected group (p value 0.002).

Following the successful knockdown of SFRS2 in HCT116 cells, it was possible to assess cellular proliferation and apoptosis as shown below; preliminarily, numbers (counted using haemocytometer method) of attached cells (cultured) were used as indicators of proliferation and numbers of floating cells as indicators of apoptosis at the end of the predetermined time point.

Below (figure 5.3) are cell counting results following SFRS2 knockdown in HCT116 cells.

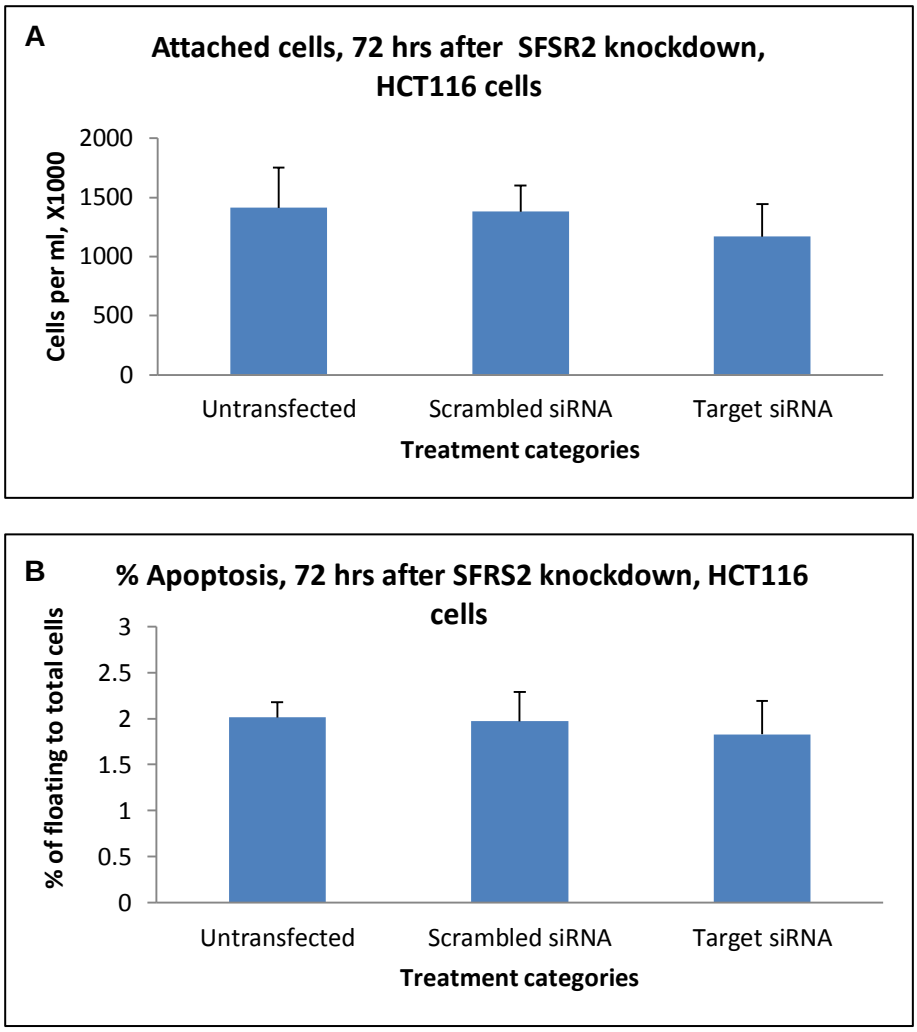


**Figure 5.7 Haemocytometer based cell counts. SFRS2 knockdown in HCT116 cells, 72 hrs time point. A) Change in attached cell number. B) Percentage of apoptotic cells to total cells per sample. Error bars represent standard deviation from the mean (N3, n2).**

Cell counting after transfection showed a small but non-significant effect of SFRS2 knockdown on cellular proliferation. More interestingly, floating cells showed a small but again non-significant reduction in numbers in the transfected group. This effect, although weak, may point to a role for SFRS2 in mediating apoptosis during colorectal tumourigensis (more details will be mentioned in the next sections).

As with HCT116 cells it was difficult to generate clear WB results with HT29 cells. Therefore, qRT-PCR was used to demonstrate the reduction in expression at the level of mRNA expression.

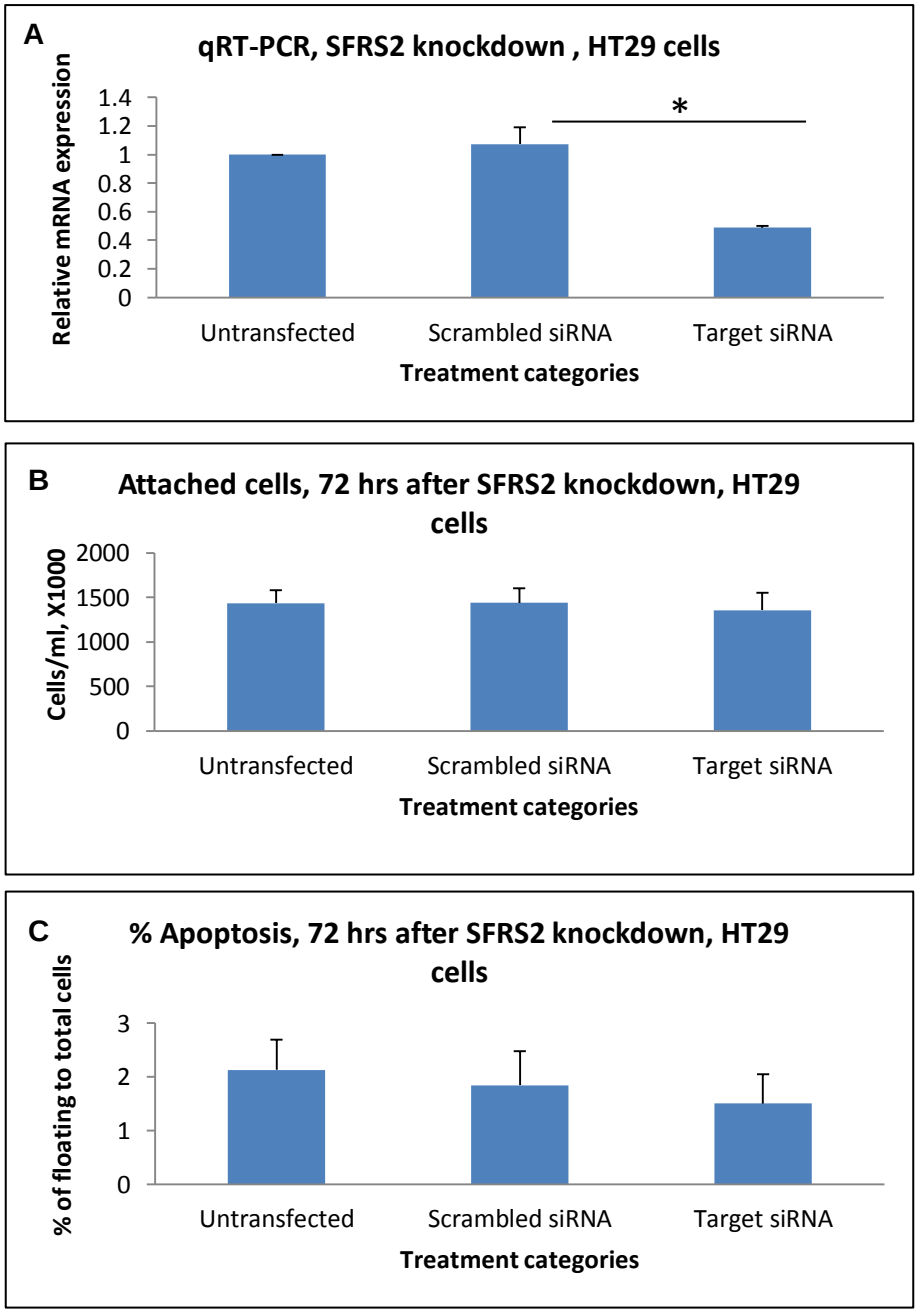


**Figure 5.8 SFRS2 knockdown in HT29 cells, 72 hrs time point. A) Relative SFRS2 mRNA expression (N3, n3). B) Change in attached cell number. C) Percentage of apoptotic cells to total cells per sample. Error bars represent standard deviation from the mean (N3, n2).**

The results from the cell counting method did not demonstrate any obvious effects of SFRS2 knockdown on proliferation and apoptosis in HT29 cells. The SRB assay was then used to assess the effect of SFRS2 knockdown on both HCT116 and HT29 cells as shown below.

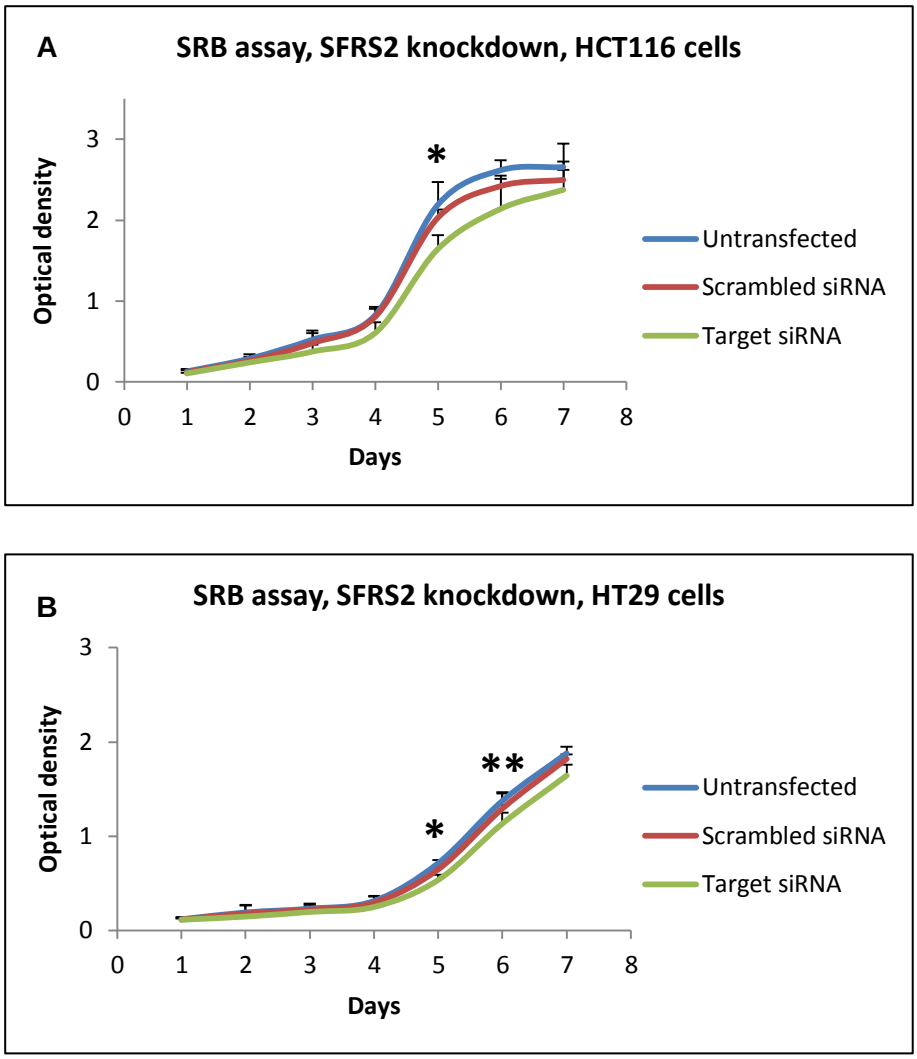


**Figure 5.9 SRB assay, HCT116 (A) and HT29 (B) cells showed a modest reduction in survival after knocking down SFRS2. Error bars represent standard deviation from the mean (N3, n6). * and **p values < 0.05 and < 0.01 respectively.**

The SRB assay demonstrated a small but statistically significant inhibitory effect of SFRS2 knockdown on proliferation in HCT116 (day 5) and HT29 (days 5 and 6) cells.

The survival of both cell lines following SFRS2 knockdown was also assessed using the clonogenic assay as shown below (figure 5.10).

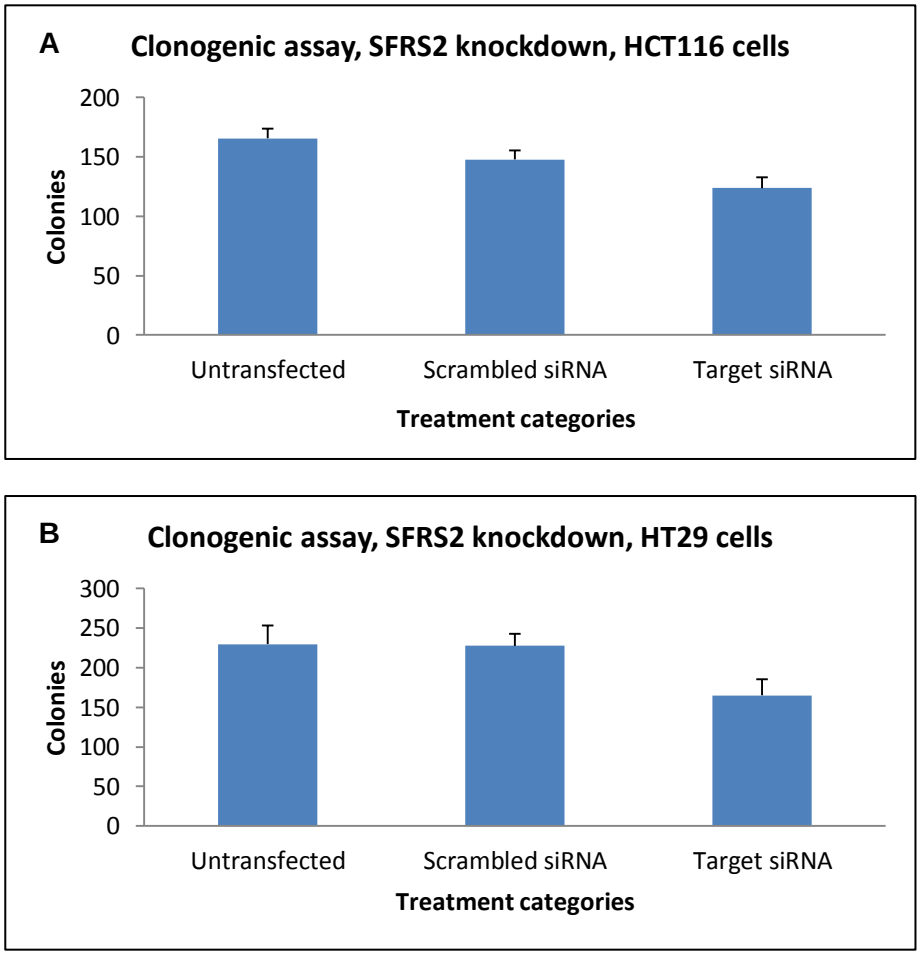


**Figure 5.10 Clonogenic survival assays. Both HCT116 cells (A) and HT29 cells (B) showed a mild reduction in survival and colony forming ability after SFRS2 knockdown. Error bars represent standard deviation from the mean (N3, n3).**

SFRS2 knockdown did not cause a significant effect on the ability of the cancer cells to survive. This is consistent with the results obtained from other techniques shown above.

## 5.4 Effect of CDC5L knockdown on cellular proliferation and apoptosis in HCT116 and HT29 cells

We included Cell division cycle 5 like (CDC5L) protein in our mechanistic studies because it has been mentioned in published literature that a possible interaction between this protein and our candidate protein, SFRS2 may exist. For instance, one report suggested a possible competition between these two proteins for the same binding molecule(s) [270].

CDC5L is an essential element for spliceosome assembly and catalysis [272]. Moreover, relatively recent studies have shown a direct role for this protein in the cellular response to DNA damage and cell cycle regulation [273]. It has also been suggested that CDC5L is required for G2M transition during the cell cycle [274]. Although CDC5L has not been well studied in CRC, it has been shown to be upregulated in human osteosarcoma and osteosarcoma cell lines [274].

To understand the role of CDC5L in CRC, we investigated its expression by IHC in various CRC models and we studied aspects of its role using siRNA knockdown techniques in HCT116 and HT29 cells. Below are the results for the knockdown experiments in HCT116 cells (figures 5.11 and 5.12).

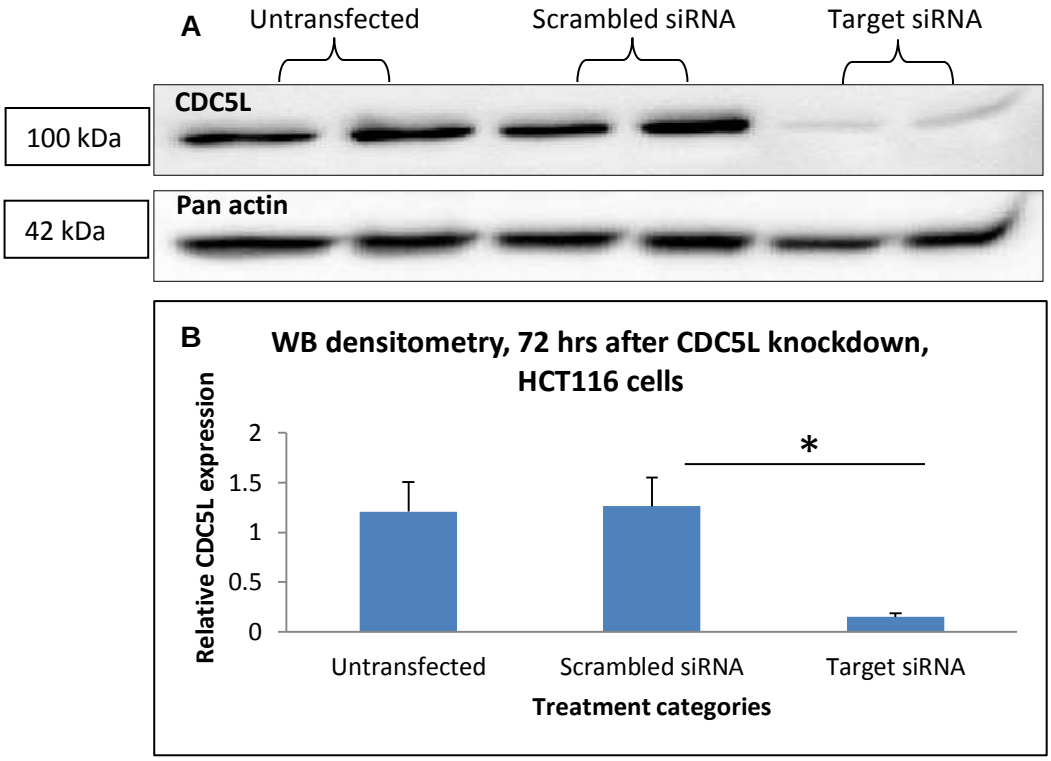


**Figure 5.11 A) Western blot of HCT116 whole cell proteins probed with anti-CDC5L antibody. Pan actin was used as loading control. B) Densitometry analysis of CDC5L expression relative to untransfected cells. Error bars represent standard deviation from the mean (N3, n2).**

Densitometry analysis demonstrated a 90% reduction (p value 0.03) in CDC5L expression in the target group using previously established experimental conditions (figure 5.11A). CDC5L knockdown had a significant inhibitory effect on cell proliferation and apoptosis in HCT116 cells as shown below (figure 5.12).

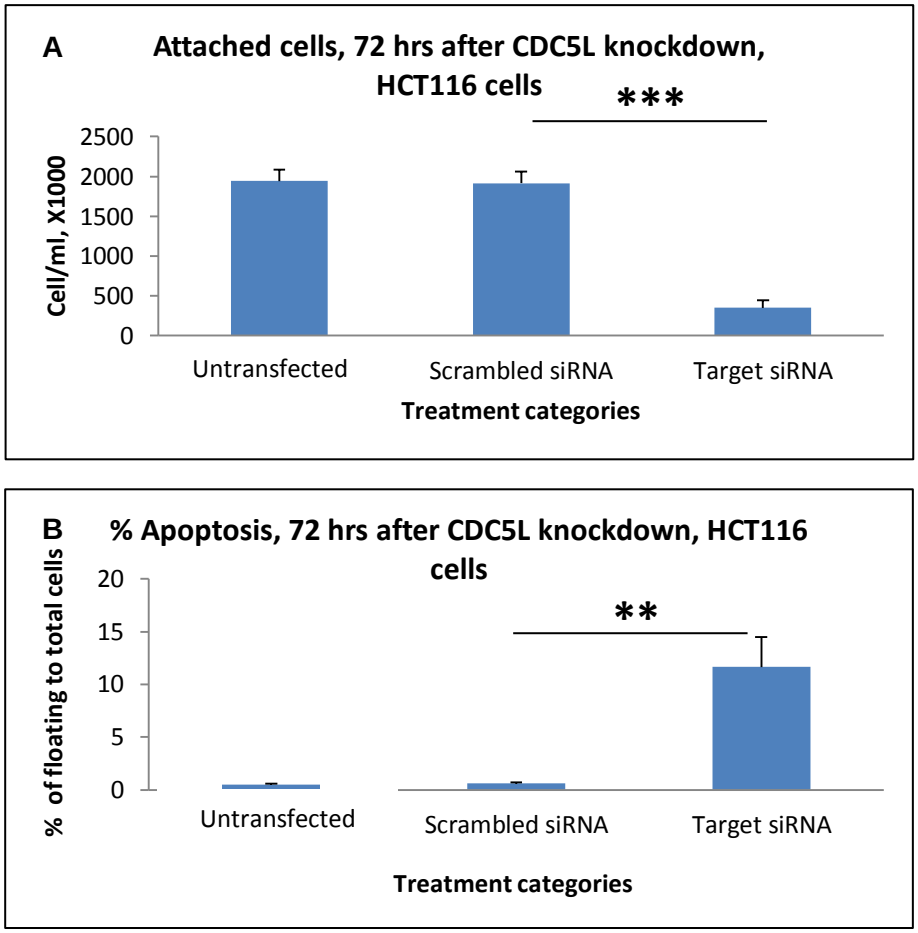


**Figure 5.12 Haemocytometer based cell counting. siRNA knockdown of CDC5L in HCT116 cells at the 72 hr time point. A) Change in attached cell number. B) Percentage of apoptotic cells relative to total cells per sample. Error bars represent standard deviation from the mean. (N3, n2). P value ** <0.01 and *** <0.001.**

In HCT116 cells the observed effect was dramatic and statistically significant for both parameters (figure 5.12 A and B). When the knockdown studies were repeated in HT29 cells (figures 5.13), the same impact on proliferation and apoptosis was observed, however the magnitude of the effect was slightly smaller (figure 5.14).

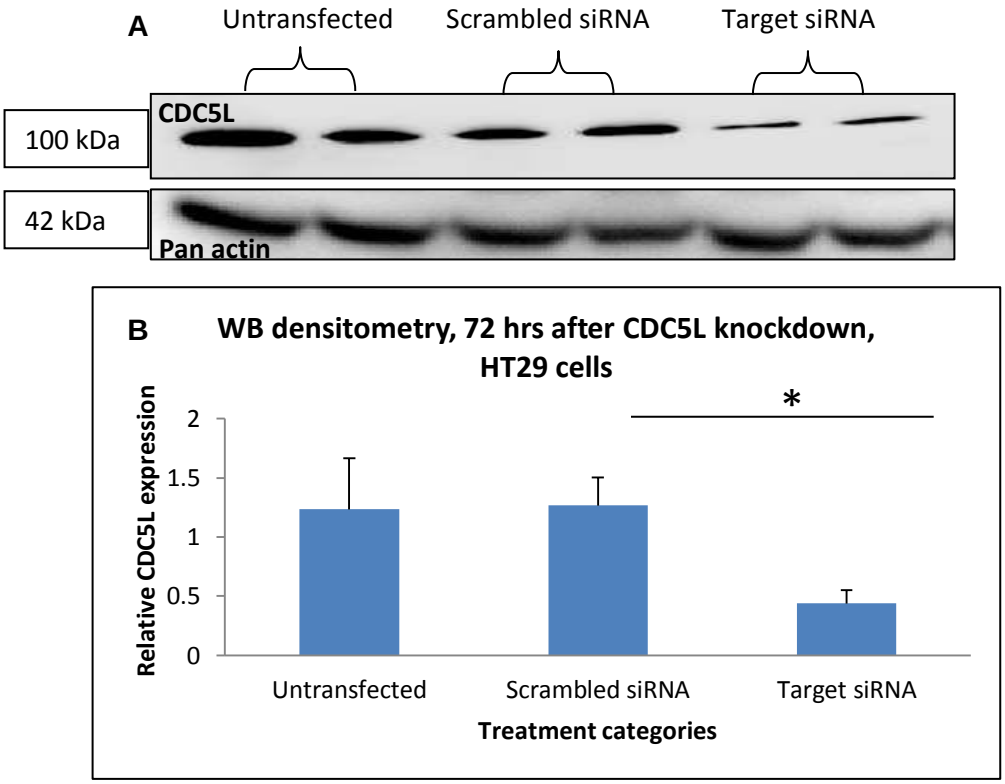


**Figure 5.13 A) Western blot of HT29 whole cell proteins probed with anti-CDC5L antibody. Pan actin was used as loading control. B) Densitometry analysis of CDC5L expression relative to untransfected cells. Error bars represent standard deviation from the mean (N3, n2).**

As with other proteins, HT29 cells demonstrated a lower knockdown efficiency for CDC5L (61%, p value 0.02). Consistent with the less efficient protein knockdown, proliferation and apoptosis changes were also less pronounced in HT29 cells as shown below (figure 5.14).

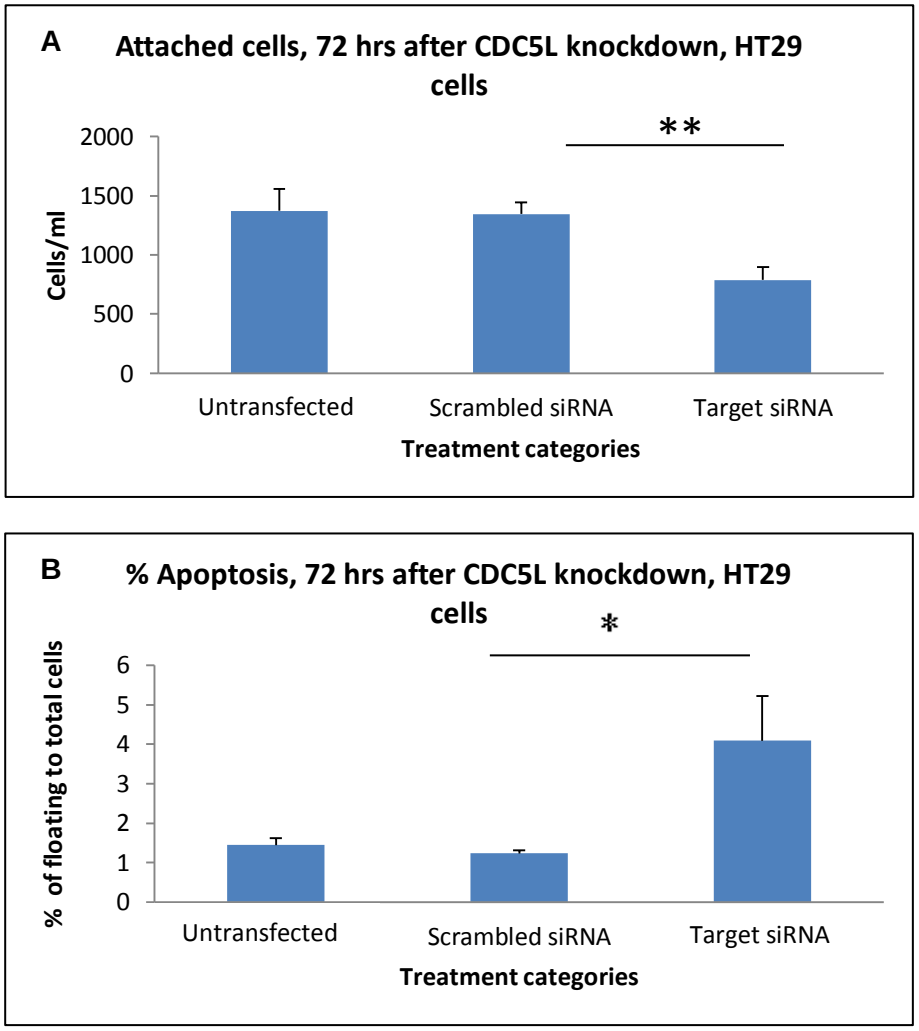


**Figure 5.14 Haemocytometer based cell counting. CDC5L knockdown in HT29 cells, 72 hrs time point. A) Change in attached cell number (** p value 0.0029). B) Percentage of apoptotic cells to total cells per sample (* p value 0.04). Error bars represent standard deviation from the mean. (N3, n2).**

Similar to HCT116 cells, HT29 cells demonstrated a statistically significant alteration in proliferation and apoptosis following CDC5L knockdown. However, the degree of the effect was reduced in HT29 cells in comparison to that in HCT116 cells, an observation that can possibly be explained by the reduced knockdown efficiency (60% vs. 90%) in the former.

As with the other proteins, the impact of knocking down CDC5L *in vitro* was further validated by SRB assay as shown below:

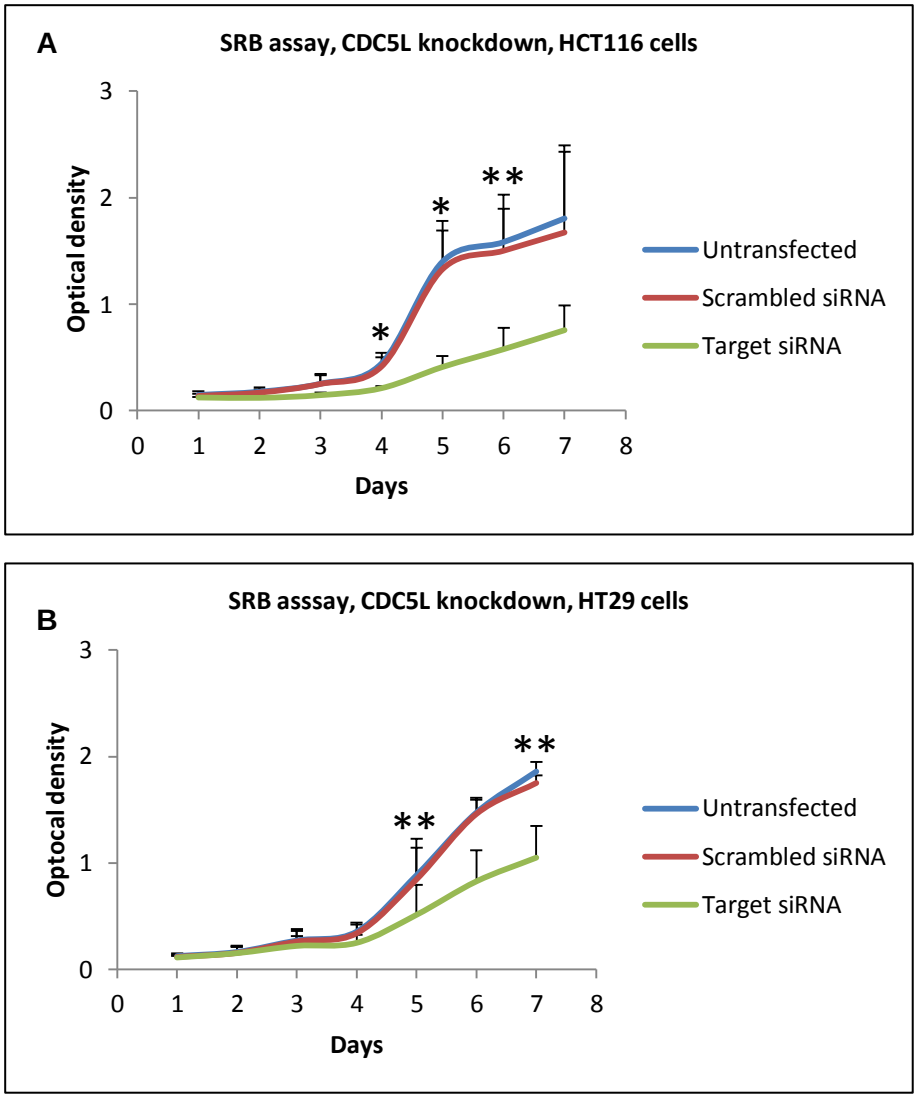


**Figure 5.15 SRB assay, HCT116 (a) and HT29 (B) cells showed a significant reduction in survival after knocking down CDC5L. Error bars represent standard deviation from the mean (N3, n6). * p value <0.05 and ** < 0.01.**

SRB assay results were in agreement with the cell counting results and showed a statistically significant inhibitory effect of CDC5L knockdown on cell proliferation in both HCT116 (days 4, 5 and 6) and HT29 (days 5 and 7) cells. Again the reduced transfection sensitivity of HT29 cells to CDC5L siRNA knockdown was also obvious in this assay.

The ability of cancer cells to survive by forming colonies, following CDC5L knockdown by siRNA was also assessed in HCT116 and HT29 cells as shown below (figure 5.16):

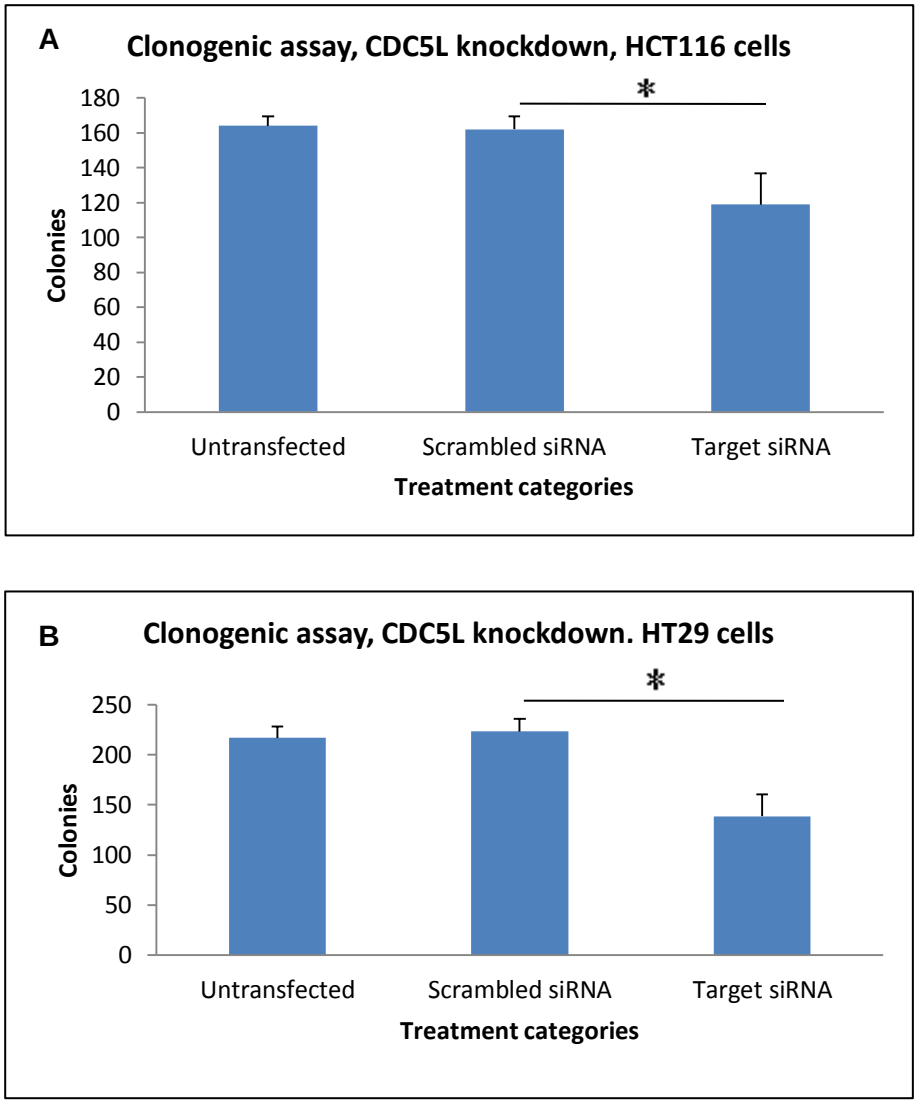


**Figure 5.16 Clonogenic survival assays. Both HCT116 cells (A) and HT29 cells (B) showed a significant reduction in survival and colony forming ability after CDC5L knockdown. Error bars represent standard deviation from the mean (N3, n3). * p value is < 0.05 (0.03 and 0.01 respectively).**

CDC5L knockdown significantly affected the ability of cancer cells to survive. This further supported the role of this protein in regulating cellular growth.

## 5.5 Assessment of cell cycle distribution following knockdown of SFRS2 and CDC5L

In the previous work shown in this chapter, we demonstrated that knocking down SFRS2 did not result in major effects on cellular proliferation and apoptosis. Therefore, it was important to try to study these parameters using alternative techniques. For this reason we used fluorescence activated cell sorting (FACS) to analyse the effect of SFRS2 knockdown on proliferation and apoptosis in HCT116 cells. The latter cells were chosen due to their greater sensitivity to siRNA mediated knockdown than HT29 cells. Moreover, it was similarly important to study the effect of CDC5L knockdown on these cellular parameters using FACS to further expand our comparison between these two molecules.

FACS is a widely used method for characterising and sorting different cell types in a heterogeneous cell population. This sorting is based on analysing cell size and volume as well as analysing the expression of cell surface and intracellular molecules. Moreover, it allows sorting the individual cells in the same cell group using multi-parameter analysis. The latter is achieved by measuring fluorescence activity produced by fluorescent labelled antibodies detecting proteins or ligands of specific cell associated molecules; for example detection of activated caspase 3 in apoptotic cells in a sample [44].

### 5.5.1 Effect of SFRS2 and CDC5L on cell cycle distribution

HCT116 cells (untransfected, scrambled siRNA and target siRNA groups) were prepared according to the conditions described in chapter four. After 72 hours, cells were harvested and fixed in methanol free formaldehyde and permeabilised in 90% methanol (technical details can be found in the relevant section of the methods chapter). At this point, cells were either used for immunostaining or stored at -20ºC for later use. The FACS experiments of cell cycle involved staining with propidium iodide (PI).

The preparation of FACS samples needed a lot of optimisation of conditions, such as working out the right settings for acquiring data from the samples. When the instrument was appropriately set up, 0.5-1x$10^6$ cells/sample were stained according to the steps mentioned in the methods section. Samples were run using a FACSCalibur machine and data were analysed using the free version of "FCSexpress

4 flow research edition" software. Below are representative images of the FACS analysis of HCT116 cell samples following the individual knockdown of SFRS2 and CDC5L.

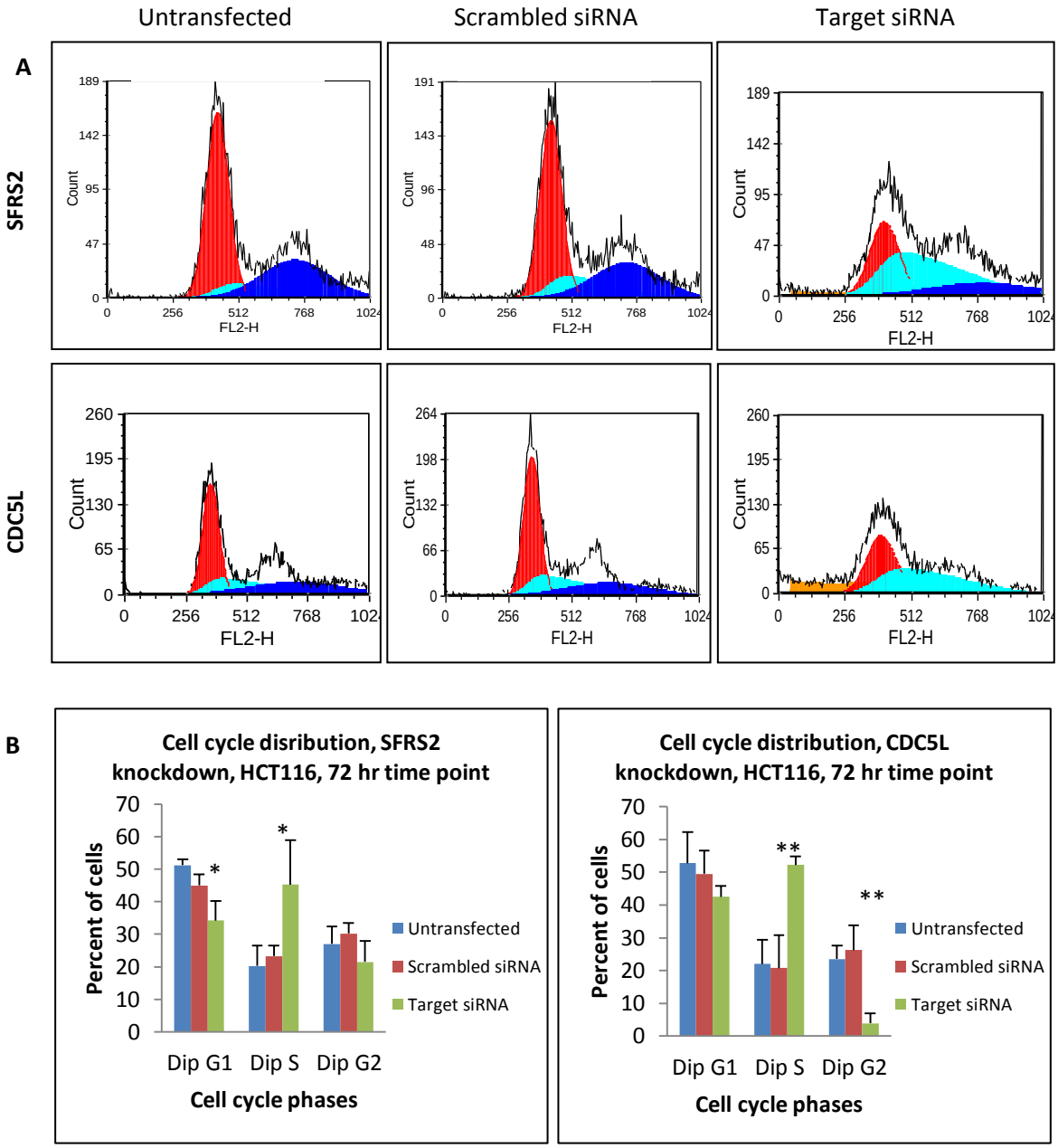


**Figure 5.17 Cell cycle analysis using FACS. A) shows HCT116 cells tranasfected with a SFRS2 target siRNA compared to the two control groups (upper panel) as well as the same cells transfected with a CDC5L target siRNA in comparison to the two control groups (lower panel). B) Shows the mean values of number of cells in each phase of the cell cycle. Error bars represent SD from the means. * and ** p values < 0.05 and <0.01 respectively. N4, n2.**

Consistent with the other techniques used to assess the effect of SFRS2 knockdown, FACS also showed less pronounced changes in the cell cycle as seen in figure 5.17A, upper panel. The two peaks are still seen with no obvious increase in the sub-G1 cell population in the target siRNA group. By contrast, CDC5L knockdown had more pronounced effects (figure 5.17A, lower panel); it resulted in almost complete obliteration of the G2 peak and a clear increase in the sub-G1 population. The latter observation is indicative of increased cell death. Again, FACS results supported the results from the other techniques used to assess the pathophysiological effects of CDC5L knockdown. Moreover, the reduction in the G2 population and the increase of cells in the S phase of the cell cycle make it difficult to suggest which checkpoint is affected. Knowing that these studies represent a snap shot through the cell cycle; the results may not be true representations of the end results of knocking down these proteins. However, the possible underlying disruption may involve arrest at both G1 and G2 check points.

### 5.6 Assessment of SFRS2 and CDC5L relationship in human CRC cell lines using immunocytochemistry

HCT116 and HT29 cells represent easily accessible models of CRC with active Wnt pathways. Therefore, we examined the expression of SFRS2 and CDC5L in these cells and correlated them with Wnt pathway activity.

As shown repeatedly in this work, HT29 cells were not easy to transfect. In addition, HT29 cells were only loosely attaching to the cover slips that were used during the staining process. Therefore, the results in this section are mainly focused on HCT116 cells, which were easier to transfect and attached to coverslips slightly better than HT29 cells.

HCT116 cells were again transfected in 6 well plates containing cover slips. The transfection process was as described before and the 72 hr time point was used. At the end of this time point, cells were fixed and premeabilised in 2% paraformaldehyde and 0.2% Triton X-100 in PBS respectively. Then the cells were processed with modified IHC protocols, in which xylene was not used and PBS was used to wash the cells instead of TBS. For all ICC, protocols did not include an antigen retrieval step as per IHC protocols performed on tissue sections. Below are representative images of the ICC experiments.

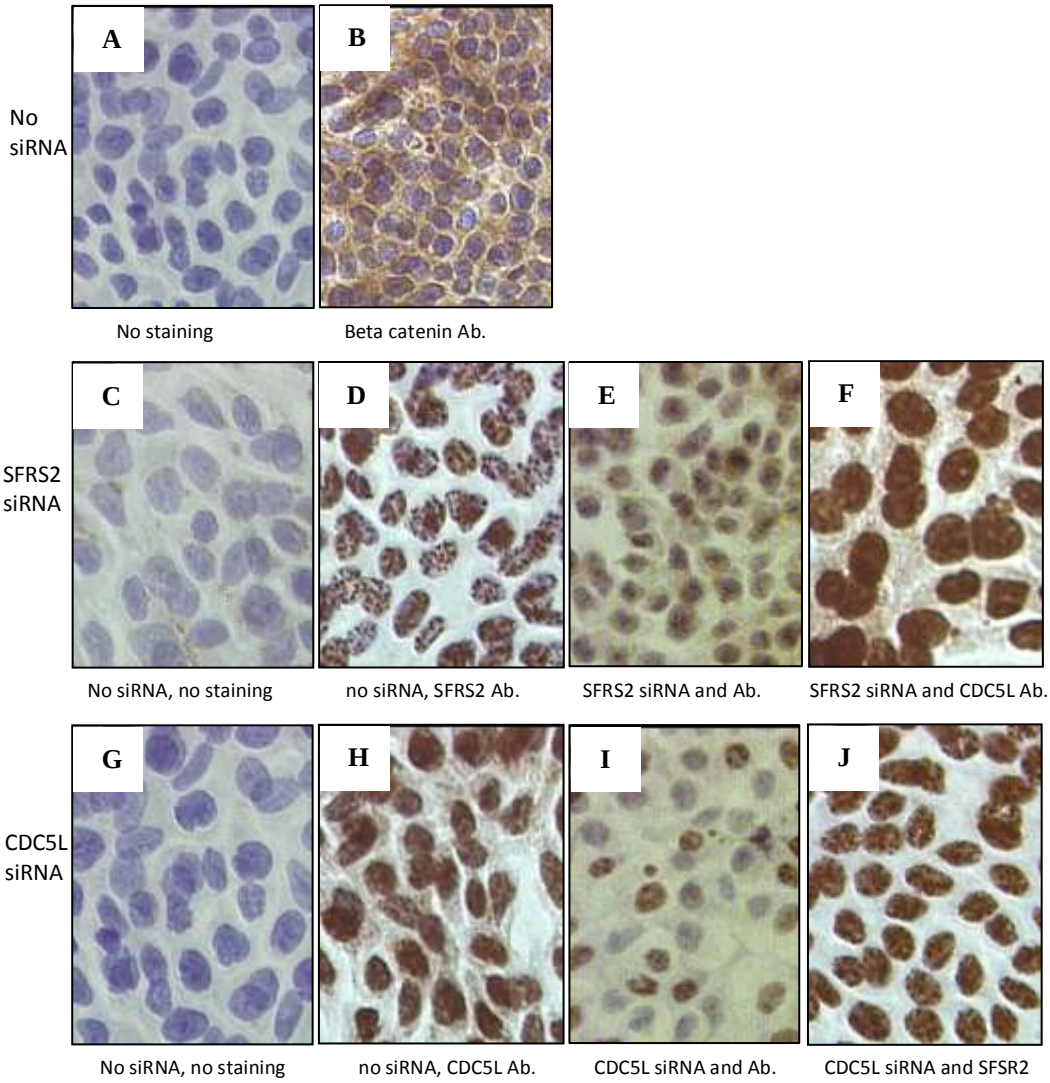


**Figure 5.18 shows ICC staining in HCT116 cells. A and B) show unstained untreated cells and untreated cells stained with anti-Beta catenin antibody respectively. D-F) show SFRS2 staining in untreated cells, SFRS2 staining in cells following SFRS2 target siRNA treatment and CDC5L staining in cells following SFRS2 target siRNA treatment respectively. H-J) show CDC5L staining in untreated cells, CDC5L staining in cells following CDC5L target siRNA treatment and SFRS2 staining in cells following CDC5L target siRNA treatment respectively. C and G) show unstained untreated control cells. Ab. = antibody. N2, n2.**

These images represent the best two experiments out of several that were performed. The main problem with the unsuccessful experiments was cell detachment during the staining process. Interestingly, in HCT116 cells, Beta catenin showed almost exclusively cytoplasmic staining. This is not surprising as we know that HCT116 cells were derived from an advanced and poorly differentiated CRC. There have been reports suggesting down regulation of Wnt pathway activity in the more advanced

stages of CRC [275, 276]. It is visually obvious that there was a successful knockdown of both SFRS2 and CDC5L. These observations support the results from western blots shown earlier in this chapter. Both proteins showed increased nuclear localisation following knocking down its proposed partner. However, this observation was more obvious for CDC5L following SFRS2 knockdown. We also tried to show this interdependent relationship between SFRS2 and CDC5L using western blot analysis of whole protein extracts from HCT116 cells (figure 5.19).

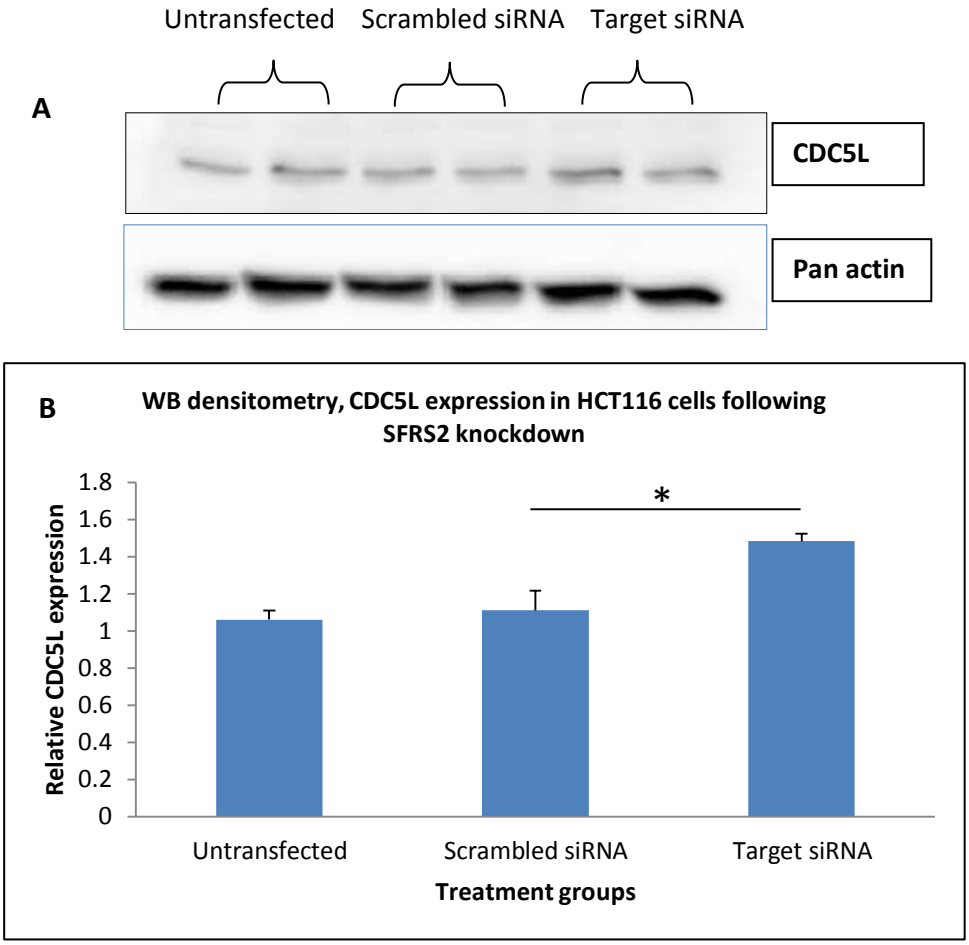


**Figure 5.19 Western blot analysis of CDC5L expression following SFRS2 knockdown in HCT116 cells. A) is a representative blot and B) is densitometry of relative expression of CDC5L following SFRS2 knockdown. N3, n2. * p value is less than 0.05.**

In this set of experiments, we tried to assess the expression of SFRS2 following the knockdown of CDC5L and vice versa. Unfortunately, SFRS2 antibodies as described before did not produce evenly measurable bands across the different experiments. CDC5L did however demonstrate small but significant (p value 0.02) upregulation following the knockdown of SFRS2 in HCT116 cells. Lack of time and resources

prevented the use of an alternative quantification technique such as qRT-PCR to assess SFRS2 expression following CDC5L knockdown. However, assessment of proteins and mRNAs are not interchangeable and also any interaction between two molecules does not necessarily involve changes in their absolute levels.

### 5.7 Assessment of rate and mechanism of apoptosis following SFRS2 and CDC5L knockdown

As mentioned before, although haemocytometer based cell counting allowed an approximate estimation of the rate of apoptosis following the knockdown of SFRS2 and CDC5L however, it was important to confirm these observations with a less observer dependent technique. Therefore, ICC and FACS analysis were used to achieve this. Figures 5.20 and 5.21 show the results from assessment of apoptosis in HCT116 cells after knocking down the above two proteins.

It has been reported that cisplatin treated cells exhibited increased expression of SFRS2 which in turn caused G2M cell cycle arrest and induced alternative splicing of caspase 8 [237]. Caspase 8 is known to be the initiator of the extrinsic pathway of apoptosis [277]. As we are proposing that CDC5L knockdown might be associated with over activity of SFRS2, it was a logical step to study the activity of caspase 8 following the knockdown of CDC5L. Therefore, caspase 8 activity was used as an indicator for the presence of apoptotic cells and was tested as a mechanism to explain the observed increase in apoptosis following the knockdown of CDC5L. However, a common step between the two pathways such as activated caspase 3 would be a better choice for studying the rate of overall apoptosis per se [44].

An increase in caspase 8 mediated apoptosis was noted in HCT116 cells following the knockdown of CDC5L as assessed by immunocytochemistry (figure 5.20). Again, knockdown of SFRS2, in agreement with previous results, did not cause any obvious increase in caspase 8 staining.

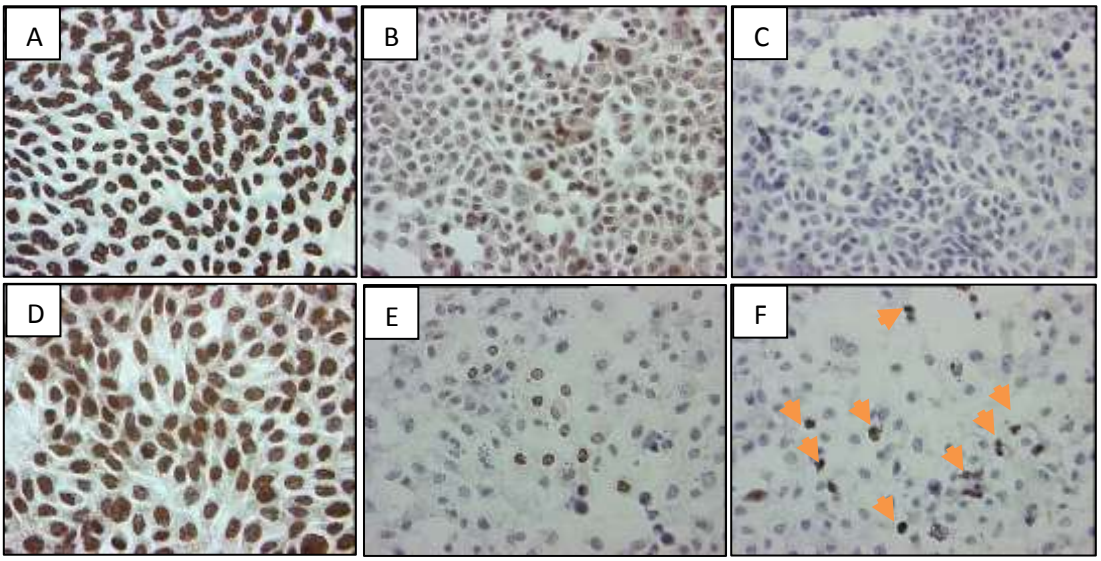


**Figure 5.20 Representative images of ICC in HCT116 cells. A) Shows untransfected cells/SFRS2 staining, B) shows cells transfected with SFRS2 specific siRNA/ SFRS2 staining and C) shows cells transfected with SFRS2 specific siRNA/ caspase 8 staining. D) Shows untransfected cells/CDC5L staining, E) shows cells transfected with CDC5L specific siRNA/ CDC5L staining and F) shows cells transfected with CDC5L specific siRNA/ caspase 8 staining. Arrows point to Caspase 8 positive cells. N2, n2. Images are X40 original magnification.**

Reduced cell numbers and increased caspase 8 staining in the cells in which CDC5L was knocked down (figure 5.20F) in comparison to cells transfected with an SFRS2 target siRNA, indicates increased rates of apoptosis and a role for caspase 8 in mediating this apoptosis in the former. These observations were validated with a set of FACS experiments using the same cells under the same knockdown conditions (figure 5.21).

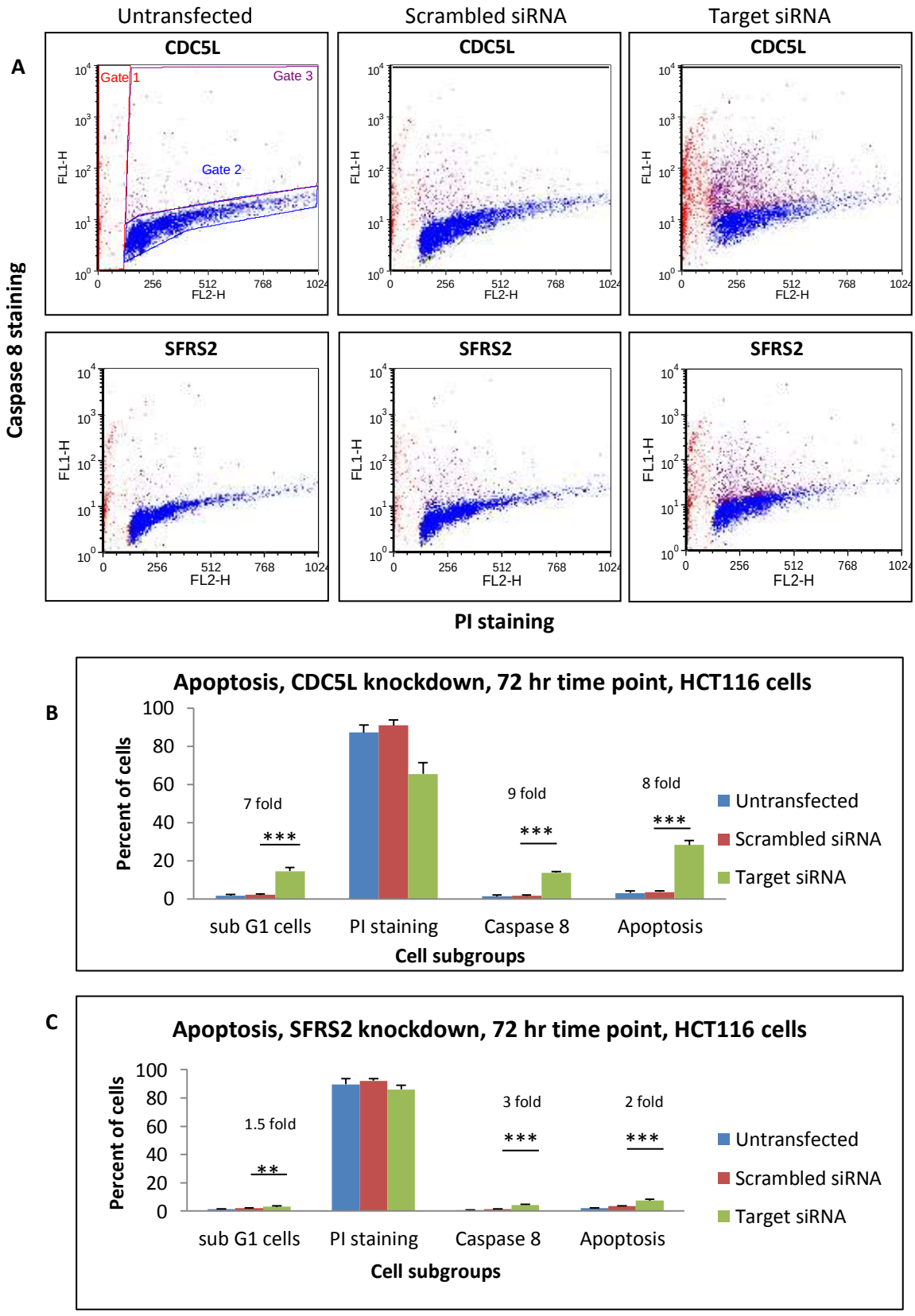


**Figure 5.21 Assessment of apoptosis in HCT116 cells following the knockdown of SFRS2 and CDC5L. A) Shows dot plots of cells stained with PI and anti-caspase8 antibody; the rate of apoptosis was estimated from the summation of caspase8 positive cells and the sub-G cells. B and C) show percentages of cell populations in section (A). Values are means ± SD. N4, n2.**

Again, consistent with the results shown above, CDC5L knockdown had a greater effect on the degree of apoptosis (figure 5.21). This was evident from a 9 fold increase (p value < 0.001) in the percentage of caspase 8 positive cells in the target siRNA group compared to the scrambled siRNA group. Moreover, the cell population consisting of caspase 8 positive and sub-G1 cells increased by 8 fold (p value <0.001) in the target siRNA group. These observations indicate the extent of cell cycle disruption and the parallel increase in apoptosis following CDC5L knockdown in HCT116 cells. On the other hand, SFRS2 knockdown had a lesser effect on cell death induction.

### 5.8 Role of p53 in mediating apoptosis following SFRS2 and CDC5L knockdown in HCT116 cells

The balance between cellular proliferation and apoptosis is a critical process throughout life; the changes to this balance during aging and carcinogenesis may contribute to the increase in the incidence of uncontrolled cellular growth encountered [278]. Evidence supporting this concept comes from studies of GIT aging in rats, which showed an increase in proliferation and a reduction in apoptosis with increased age [279]. Similarly, cancer cells have increased metabolism with increased proliferative activity and maintenance of de-differentiation. They can produce embryonic proteins and stay immortal by evading apoptosis [280]. Moreover, proteins regulating apoptosis often show distinctive expression profiles in cancer and senescent cells. Examples for the latter suggestion include down regulation of p53 [281] and upregulation of the antiapoptotic protooncogene Bcl2 [282]. Furthermore, p53 is thought to play an important role in various cellular processes such as cell cycle regulation, DNA replication and apoptosis [283]. SFRS2 and CDC5L have both been clearly linked to alternative splicing and cell cycle regulation and it is now strongly believed that coordinated proapoptotic splicing is linked to cell cycle checkpoints through mechanisms that are not fully understood. Therefore, it was important to study these two proteins in relation to p53 in the setting of CRC.

In the siRNA experiments that involved knockdown of SFRS2 and CDC5L, there were changes in the amount of apoptosis induced in HCT116 cells (which have wild type p53) as demonstrated by haemocytometer based counting and FACS analysis. Therefore, to evaluate the role of p53 in this apoptosis, HCT116 cells with knockout

p53 [185] were also subjected to the same siRNA knockdown experiments. Below are figures showing a comparison between the rates of apoptosis in HCT116 cells with WT p53 versus those with knockout p53.

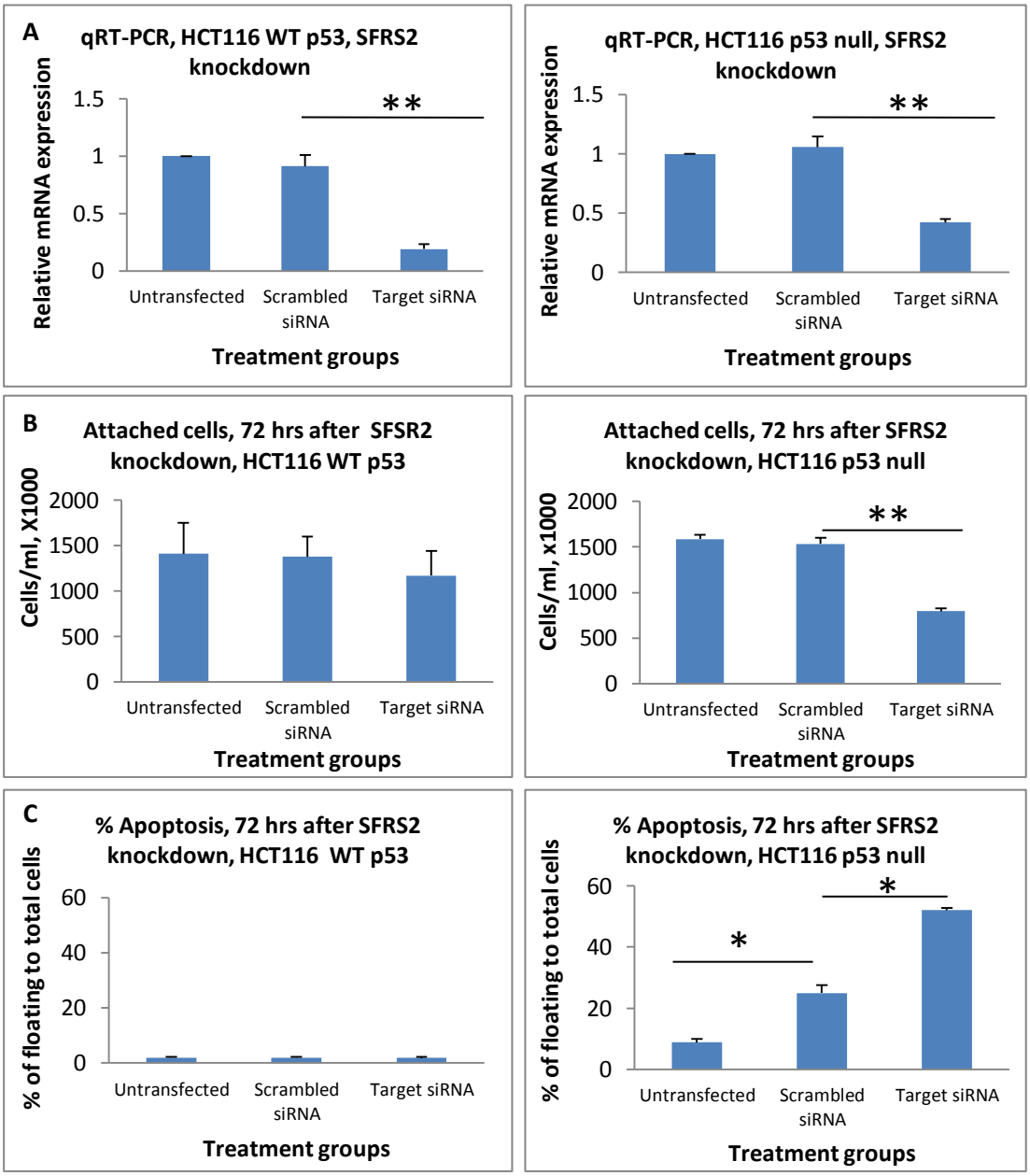


**Figure 5.22 Assessment of proliferation and apoptosis in attached HCT116 cells 72 hrs following the knockdown of SFRS2. A) Shows relative expression of SFRS2 mRNA in HCT116 WT p53 vs. knockout p53. B) Shows haemocytometer based counting of attached cells in the above cell groups. C) Shows percentage of apoptosis to total sample cells in the same cell groups. Values are means ±SD. * and ** p values are <0.05 and 0.01 respectively. N3, n2.**

Following successful knockdown of SFRS2 in both cell lines, attached and floating cells were counted. There was more obvious inhibition of cellular proliferation in cells with knockout p53 in comparison to cells with wild type p53. Although p53 null

HCT116 cells showed more significant increase in apoptotic cells after treatment with SFRS2 target siRNA, however this effect was also observed in the scrambled siRNA treated cells. This is suggesting an increased sensitivity of these cells to toxic conditions.

The same above experiments were repeated with CDC5L targeted siRNA in HCT116 cells with WT and knockout p53. Figure 5.23 demonstrates the efficiency of knockdown using western blotting.

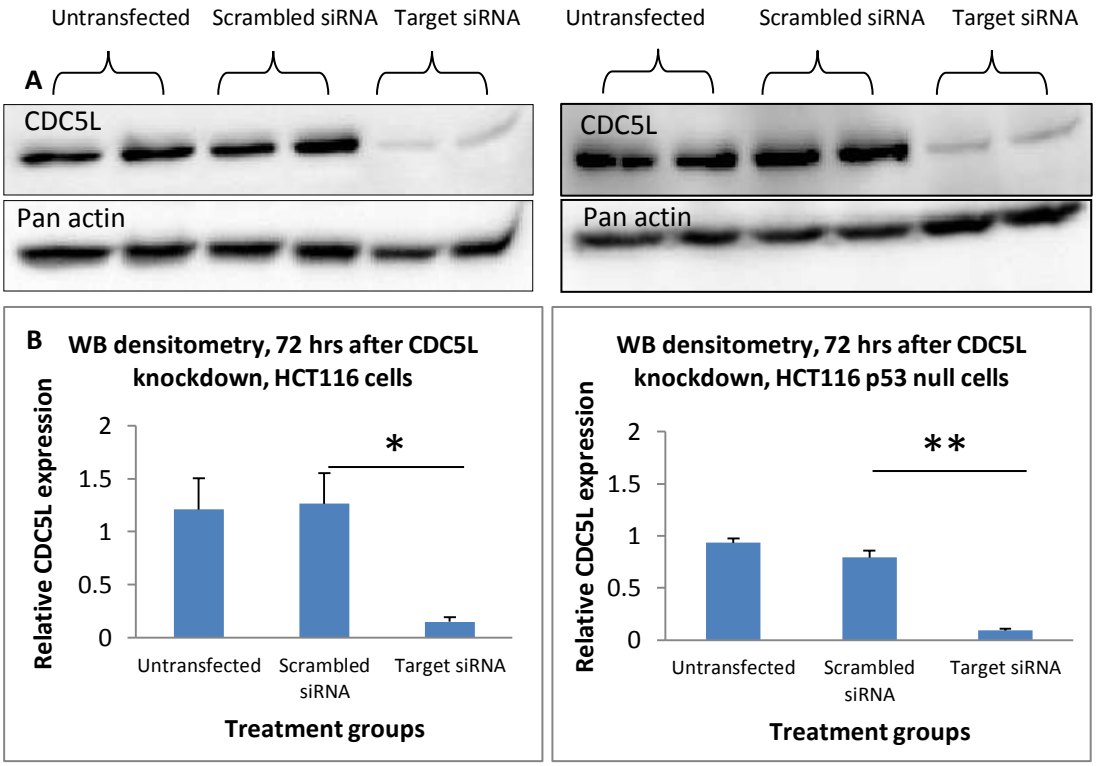


**Figure 5.23 siRNA mediated knockdown of CDC5L in HCT116 WT p53 cells (left panel) and HCT116 knockout p53 cells (right panel). A) Shows western blots of whole proteins extracts from both cells. B) Shows densitometry analysis of relative CDC5L expression in both cell lines. Values are means ±SD. * and ** p values are < 0.05 and 0.01 respectively. N3, n2.**

It is evident from both cell lines that there is efficient and significant knockdown of CDC5L expression in both cell lines.

Again both attached and floating cells were counted as demonstrated below in figure 5.24.

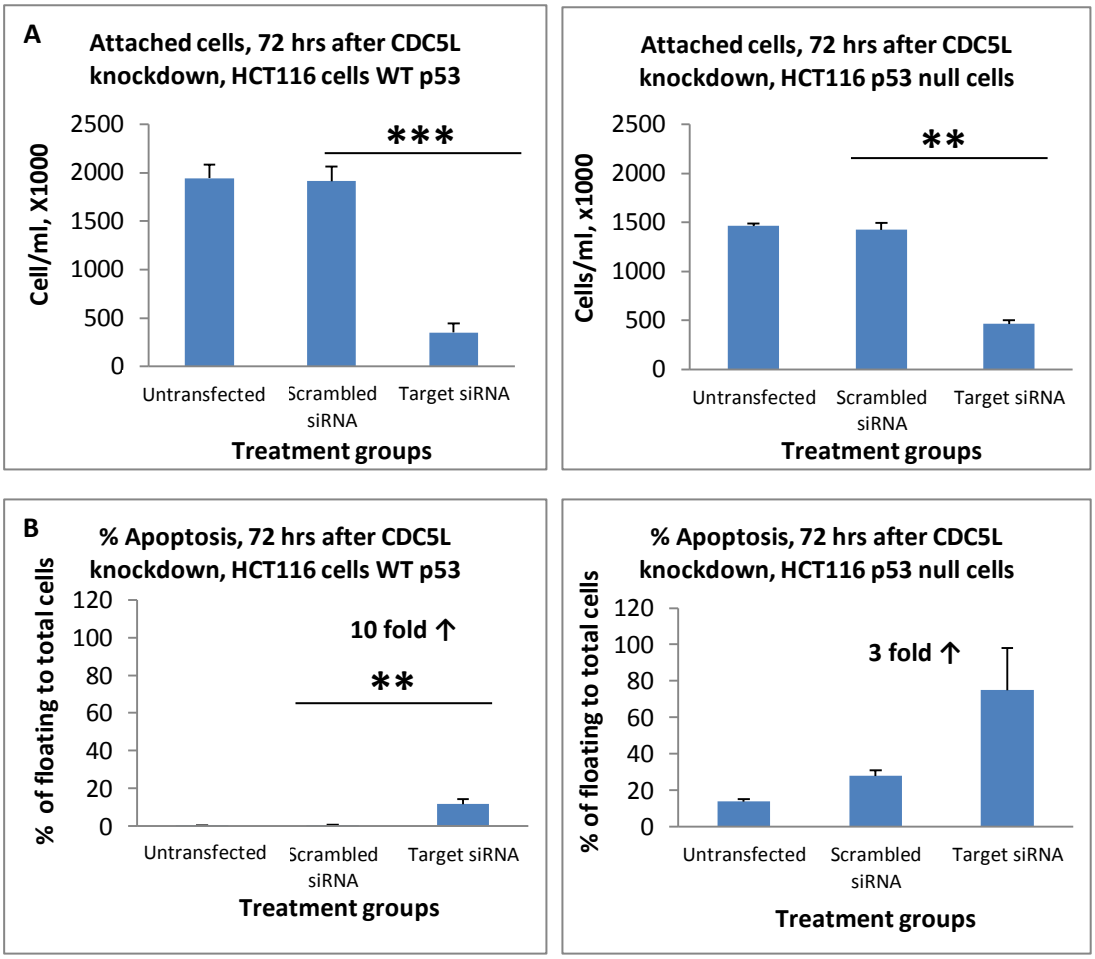


**Figure 5.24 Haemocytometer based cell counting following the knockdown of CDC5L in HCT116 cells WT p53 vs. knockout p53. A) Shows cellular proliferation represented by attached cells. B) Shows degree of apoptosis represented by the percentage of floating cells to total cells in each sample. Values are means ±SD. ** and *** p values are < 0.01 and 0.001 respectively. N3, n2.**

In contrast to SFRS2 knockdown, CDC5L knockdown caused a stronger inhibition of cellular proliferation in the presence of p53. This was also associated with a greater degree of apoptosis in the same cell group.

## 5.9 Discussion

The aim of this chapter was to study the role of the protein SFRS2 in critical cellular functions that could have a fundamental impact on the course of colorectal tumourigeneis.

SFRS2 belongs to the serine rich (SR) family of proteins that are well known for their role in constitutive and alternative splicing (AS) of precursor messenger RNA (pre-mRNA) [234]. In recent years, defects in alternative splicing have been frequently identified in various cancer related processes. The vast majority of human genes undergo alternative splicing, with the production of functionally different protein isoforms from the same gene. Therefore, this high throughput machinery can have dramatic effects upon tumourigenesis [170].

Cell division cycle 5 like (CDC5L) protein is an essential component of the spliceosome assembly and catalysis [272]. In addition to pre-mRNA splicing, CDC5L has also been shown to have direct links to cellular response to DNA damage and cell cycle regulation [273]. Similar to SFRS2, there are a few reports about its role in cancer; for instance it has been shown that CDC5L plays an important role in human osteosarcoma development [274].

A number of research groups have suggested that SFRS2 and CDC5L may interact. One research group stated that both these molecules compete for the same binding molecule and that overexpression of nuclear CDC5L displaced SFRS2 into the cytoplasm in cell lines [270]. Also, spliceosome analysis studies have shown that SFRS2 and CDC5L co-purify [284]. Both proteins function within the nucleus, a fact further supporting a possible interaction. Additionally, another group has suggested that hnRNPs (CDC5L is usually linked to these molecules during alternative splicing) and SR proteins bind to the same areas of pre-mRNAs, the G rich areas [272]. An example of this interaction is the observation that over expression of hnRNP A1 promotes degradation of caspase 2 via modulating its splicing, resulting in the inclusion of exon 9 and production of an anti-apoptotic molecule which mediates tumour survival while SFRS2 over expression promotes the opposite [285]. Another possible point of interaction could be a molecule needed by CDC5L to remain in the nucleus and hence functional, namely pleiotropic regulator 1 (PLRG1)

[286, 287]. Deficiency of PLRG1 has been shown to cause a similar impact on cell cycle and apoptosis as that caused by CDC5L knockdown [286].

Due to the above observations that support the existence of a functional interaction between SFRS2 and CDC5L and as both proteins have not been well studied in CRC, IHC was initially used to examine the amount and sub-cellular localisation of SFRS2 and CDC5L during early and late phases of colorectal tumourigenesis. For this purpose, $AhCre^{+}Apc^{fl/fl}$ and $Apc^{Min/+}$ mice were used as models of early neoplasia and $AhCreER^{T+}Apc^{fl/+}Pten^{fl/fl}$ mice as a model of invasive disease. Early after *Apc* deletion in the $AhCre^{+}Apc^{fl/fl}$ mouse, there was nuclear translocation of Beta catenin, nuclear over expression of SFRS2 and cytoplasmic displacement of CDC5L (figure 5.1). In $Apc^{Min/+}$ mice (figure 5.2), with advancement of tumourigenesis in the form of polyps, the same changes were also observed; apart from the fact that the cells in the polyp area showed almost complete cytoplasmic localisation of CDC5L. This observation may be explained by the longer time that these lesions take to develop, whereas $AhCre^{+}Apc^{fl/fl}$ mice were sacrificed within 5 days of *Apc* deletion.

When the above three proteins were examined in malignant lesions from $AhCreER^{T+}Apc^{fl/+}Pten^{fl/fl}$ mice, Beta catenin showed cytoplasmic overexpression and CDC5L was re-localised into the nucleus (figures 5.3 and 5.4). Unfortunately, despite the use of three batches of tissue from $AhCreER^{T+}Apc^{fl/+}Pten^{fl/fl}$ mice, SFRS2 staining was not successful in most sections that had invasive lesions. However, initial studies on human malignant tissues have suggested cytoplasmic displacement of SFRS2, as will be discussed in more detail in chapter 6.

To further investigate the role of SFRS2 and CDC5L during colorectal tumourigensis, we knocked down their expression in two CRC cell lines. Interestingly, SFRS2 down regulation only had a modest effect on cellular proliferation. This was more pronounced in HCT116 cells as with other proteins studied in this thesis. However, this change in proliferation was not associated with a parallel increase in apoptosis. On the contrary, the trend observed was a reduction in the number of apoptotic cells. This was indicated by a reduced number of floating cells in the cells transfected with the SFRS2 siRNA (figures 5.7B and 5.8C). However, these findings were statistically not significant. Interestingly, there have been published reports of a role for SFRS2 in cell cycle control and induction of

apoptosis. Specifically, in a recent study of cell lines treated with cisplatin, SFRS2 (overexpression) was shown to induce cell cycle G2M arrest and to induce modulation of caspase 8 pre-mRNA splicing to increase apoptosis [237]. Also in similar work, it has been observed that E2F1 in response to DNA damage, increases the expression of SFRS2 to activate the apoptotic genes *c-flip, caspases 8* and *9* and *Bcl-x* [234].

Similar to all our other candidate biomarkers, the biological role of SFRS2 is likely to be multifaceted and context dependent. Therefore, one explanation for the reduction in the number of proliferating cells (assessed by various techniques) observed after SFRS2 knockdown is based on a report that suggests that p53 is activated after SFRS2 down regulation. This in turn causes G2M arrest via p21 [288].

We also knocked down CDC5L expression in HCT116 and HT29 cell lines and compared the effects of this to those of SFRS2 knockdown in an attempt to further understand their combined role during colorectal carcinogenesis. Unlike SFRS2 knockdown, CDC5L knockdown had a dramatic and significant inhibitory effect on cellular proliferation and survival in both HCT116 and HT29 cell lines (by cell counting, SRB and clonogenic assays), but again the effect was more pronounced in the HCT116 cell line. Also, CDC5L knockdown was associated with an obvious increase in apoptosis. The role of CDC5L in regulation of cell cycle progression and cellular proliferation described by other research groups may explain the inhibitory effect of CDC5L knockdown on cellular proliferation observed in our *in vitro* studies [284]. For instance, it has been suggested that CDC5L is required for G2M transition; by shortening this phase, CDC5L facilitates cell entry into mitosis [274]. On the other hand, inhibition of CDC5L prolongs the G2 phase and delays entry into mitosis [284]. Moreover, it has been reported that CDC5L is completely cytoplasmic in inactive cells in the absence of serum, whereas the addition of serum (inducing proliferation) to the cells caused nuclear translocation of CDC5L [289]. All the above observations suggest that CDC5L is involved with positive regulation of the cell cycle and cellular proliferation.

The cell cycle was the other aspect studied in this chapter to investigate the role of SFRS2 during colorectal tumourigenesis. The knockdown of SFRS2 and CDC5L had

variable effects on cell cycle distribution (figure 5.17). However, CDC5L knockdown caused a greater effect on both the cell cycle and rate of apoptosis. This supports our hypothesis that SFRS2 is more critical during the earlier stages of colorectal tumourigenesis and that CDC5L has pro-proliferative properties that are involved in cancer development.

Cell cycle distribution analysis following CDC5L knockdown showed a reduction in the G2 cell population and a relative increase in the S phase cell population (figure 5.17). This observation agrees with other publications in which it was shown that CDC5L knockdown prolonged G2M transition and delayed entry into mitosis [284]. Also, it agrees with our proposal that this could be due to SFRS2 over activity, as it has been reported that overexpression of the latter causes G2M arrest and induces apoptosis via switching on the apoptotic profile of certain regulators of apoptosis as described above (G2 cell death) [237].

SFRS2 knockdown mainly caused an increase in the S phase cell population (figure 5.17). This disagrees with other observations which have suggested that G2M arrest or G1/S arrest (reduced S phase cells has been suggested to be due primarily to G2M arrest) [288] occur following SFRS2 knockdown [235, 288]. However, it is consistent with our proposal that SFRS2 knockdown causes CDC5L over activity, since the latter shortens G2M transition and promotes mitosis. Having said that, PI based analysis of the cell cycle relies on analysis of a single time point and does not fully show the percentage of cells in the different phases due to overlap between the various phases [290]. Therefore, the use of markers for specific cell cycle phases such as pulsed 5'-bromo-2'-deoxyuridine (BrdU) and phosphorylated histone H3 for S phase and M phase respectively may provide better estimations of the proportions of cells in each phase [291, 292].

It has been shown that Cdc2 and Chk kinases are required for G2M transition, such that DNA damage induces Chk kinases, which in turn inhibit Cdc2 [293, 294]. Western blotting was used to assess the expression of these two proteins following the knockdown of both CDC5L and SFRS2 in HCT116 cells in an attempt to understand how these proteins mediate their effects on the cell cycle. Unfortunately however no conclusive results were obtained within the time frame available, despite several modifications to the experimental protocols.

In addition to the functional comparison we made between SFRS2 and CDC5L, immunocytochemistry (ICC) (figure 5.18) was also used to assess the possible interaction between these two molecules as a more direct tool. Although mild, SFRS2 demonstrated increased nuclear expression following CDC5L knockdown in HCT116 cells. CDC5L also demonstrated a more robust increase in nuclear localisation following SFRS2 knockdown in these cells. The latter increase was confirmed by western blot analysis (figure 5.19) of CDC5L expression following treatment with SFRS2 siRNAs. Unfortunately, western blot validation of the change in SFRS2 expression following CDC5L knockdown was not possible, due to technical issues related to the primary antibodies used. Interestingly, Beta catenin demonstrated almost no nuclear expression in HCT116 cells. Generally, the above results may support our hypothesis that SFRS2 and CDC5L interact during the course of colorectal tumourigenesis.

The purpose of this study was also to assess the apoptotic pathway that is possibly associated with SFRS2 and CDC5L by using the siRNA knockdown technique. Although the haemocytometer method for counting floating cells in the culture media from each sample was a good initial indicator of the rate of apoptosis, it was essential to validate these data with more robust techniques such as ICC and FACS. In FACS analysis, in addition to cellular size, caspase 8 was used, because it both assessed apoptosis and was proposed as a potential mechanism involved in the apoptosis related to SFRS2 and CDC5L. Alternative splicing of Caspase 8 by SFRS2 has been reported to induce apoptosis during G2/M cell cycle arrest mediated by overexpression of the latter [237].

This proposal was initially supported by the ICC results (figure 5.20) which showed increased caspase 8 staining following the knockdown of CDC5L in HCT116 cells. In the FACS analysis, CDC5L knockdown in HCT116 cells (figure 5.21) was associated with a 7 fold increase in sub-G1 cells ($p$ value $<0.001$), a 9 fold increase in caspase 8 positive cells ($p$ value $< 0.001$) and an 8 fold increase in overall apoptosis (summation of sub-G1 cells and caspase 8 positive cells) in the target siRNA group compared to the negative control group. These data agree with the proposal that CDC5L knockdown may be associated with SFRS2 over activity or nuclear presence that in turn mediates apoptosis via activating caspase 8. Western blot assessment of activation of caspase 8 was also attempted following the

knockdown of CDC5L in HCT116 cells. However, unfortunately the antibody used did not yield conclusive results.

SFRS2 knockdown was associated with a much weaker apoptotic response. There was a 1.5 fold increase in sub-G1 cells, a 3 fold increase in caspase 8 positive cells and a 2 fold increase in total apoptosis.

Since p53 is mutated in 30-60% of CRC cases [47], it was also important to examine the role of this tumour suppressor in the apoptosis that was associated with the knockdown of our two proteins. The transcription factor p53 is activated by various cellular responses that result in an insult to the DNA. This in turn causes the activation of a wide range of genes that exert tumour suppressive effects such as inhibition of the cell cycle and induction of apoptosis [295].

SFRS2 knockdown resulted in increased amount of apoptosis in p53 knockout HCT116 cells (figure 5.22). This observation suggests activation of non-canonical apoptotic pathways or direct activation of downstream mechanisms bypassing p53. This can be attributed to cell cycle arrest that has been shown to induce apoptosis via modifying the alternative splicing of regulators of apoptosis independent of canonical apoptosis pathways. For example, stimuli that activate the G2/M checkpoint have been shown to trigger pro-apoptotic Bcl-x splicing [236]. In conclusion, SFRS2 abnormalities seem to involve DNA damage that mediates G2M arrest via p53 dependent and independent mechanisms. This suggestion is supported by two studies; one study in cell lines which showed G2M cell cycle arrest via p21 as a result of activation of p53 following SFRS2 knockdown and another study in mice in which knocking out p53 in an SFRS2 knockout model did not prevent the lethality of SFRS2 depletion [288].

Apoptosis associated with CDC5L knockdown was greater (10 fold vs. 3 fold increase) in the presence of WT p53 (figure 5.24). This observation suggests that CDC5L knockdown may also involve an insult to the DNA with resultant activation of p53. Moreover, increased caspase 8 activity following the knockdown of CDC5L may be linked to p53, as it has been reported that caspase 8 is an essential mediator of p53 dependent apoptosis induced by etoposide in HNSCC cells [296]. Again WB analysis was used to detect direct activation of p53 and caspase 8 following the knockdown of CDC5L in HCT116 cells, but no bands were detected under standard

experimental conditions. Although some modifications were tried such as changing antibody dilutions and the incubation duration and temperature, neither time nor resources allowed further optimisation of these conditions.

### 5.10 Conclusions

The observations made in this chapter may suggest that during the early (benign) stages of colorectal neoplasia, the Wnt pathway regulates the rates of proliferation and apoptosis via different mechanisms including SFRS2 over expression and cytoplasmic displacement of CDC5L. In contrast, upon tumour invasion, as Wnt pathway activity reduces (as demonstrated by loss of nuclear Beta catenin), proliferative stimuli (CDC5L nuclear re-localisation) overcome the apoptotic ones (loss of SFRS2 expression in the malignant lesions can further support this assumption) and possibly result in tumour progression. This scenario is not new to the field of oncology, since many reports have pointed to the balance between proliferative and apoptotic mechanisms during the benign stages of tumourigeneis and that this balance is lost in favour of proliferative mechanisms upon transformation [278, 279].

Taking the above observations into account, together with reports suggesting that Beta-catenin promotes apoptosis in several cell systems independent of G1/S regulators [297] and overexpression of a stable form of Beta catenin or inhibition of endogenous Beta-catenin degradation in epidermal keratinocyte cells induces a G2 cell cycle arrest and leads to apoptosis, these results propose a role for Beta-catenin (Wnt pathway) in the control of cell cycle and apoptosis at the G2/M cell cycle check point in normal and transformed epidermal keratinocytes [298]. This suggests that tight control of Beta-catenin levels is required to ensure correct progression of cells through the cell cycle. Therefore, SFRS2 may be an autoregulatory mechanism mediated by the WNT pathway to fine tune its functions.

The coordination between cell cycle, alternative splicing and apoptosis is critical in maintaining the balance between proliferative and apoptotic mechanisms. It has been shown that loss of balance favouring proliferation occurs during aging and carcinogenesis. Alternative splicing is high throughput machinery that can radically change cell fate. A critical example is the fine tuning existing between pro and anti-apoptotic factors that is orchestrated by alternative splicing. Alternative splicing is

greatly altered in tumours, however its causes and consequences are still unknown. A disturbance in this balance has been shown to mediate apoptosis resistance in a mechanism independent of the canonical apoptosis pathways. Therefore, studying alternative splicing mediated factors contributing to tumour expansion can unveil therapeutic targets that may have fewer side effects.

Our direct and indirect observations suggest that SFRS2 and CDC5L function on opposite sides of the equation, in such a way that SFRS2 is mediating the apoptotic arm while CDC5L promotes proliferation. However, due to the complexity of the process of alternative splicing which seems to mediate opposite functions using the same molecules, more direct tests should be implemented to more clearly define this relationship. For example;

- Finding a common molecule between the two proteins using immunopreciptation for instance and then studying its splicing profile in various conditions in which SFRS2 and CDC5L have been up or down regulated. Up regulation studies may be more conclusive, but may need more time and resources than knockdown studies.
- Using qRT-PCR to investigate the relative expression of SFRS2 following CDC5L knockdown and vice versa. However, it is not necessary that the interaction between SFRS2 and CDC5L involves changes in their levels, therefore quantifying one after knocking down the other may not provide the final answer.

Also more robust techniques will need to be used to study the role of SFRS2 in apoptosis for example:

- *In vitro* activation or over-activation of the Wnt pathway and analysis of the resultant changes in SFRS2 level and apoptosis.
- *In vitro* induction of apoptosis using cytotoxic agents and analysis of SFRS2 level as well as studying the effects of SFRS2 knockdown on induced apoptosis.

# Chapter six

# The expression of candidate protein biomarkers in human colorectal cancer

## 6. The expression of candidate biomarker proteins in human colorectal cancer

### 6.1 Introduction

At the beginning of this work as described in chapter three, we demonstrated that six out of nine proteins studied showed obvious differential staining in two mouse models of intestinal tumourigenesis using IHC. Moreover, it was also possible to study the expression of proteins such as CDC5L and Cyclin E that have been shown to be functionally related to some of these candidate biomarkers.

These proteins have not previously been extensively studied in human cancers and in CRC in particular. Although IHC is unlikely to provide mechanistic insights into the roles of these proteins during colorectal carcinogenesis, we hope that it would be a good starting point from which more specific and in depth studies could be set out.

In this chapter, IHC was used to study the expression of several candidate biomarkers and their related proteins in samples of human CRC. The same optimised experimental conditions shown in chapter three were used in this work.

The samples (biopsies or surgical resection specimens) were provided by Mr Paul Sutton with documentation of diagnosis and staging. The fixation process and storage conditions of these samples were however not known at the time these experiments were carried out. Five patients per tumour stage were included and the samples were grouped as: normal colon, benign adenomas, polyp cancers and Dukes' A to D CRC. Normal colonic tissues were obtained from patients who had undergone colonoscopy for non-malignant conditions (with samples being taken from normal looking colon). Human samples and ethics committee approval were obtained by Mr Paul Sutton, Countess of Chester Hospital.

Sections from each sample were stained with haematoxylin and eosin to show the histology of each tumour. Then IHC was used to study the expression of each protein during the different stages of CRC.

Aims

1. To assess the immunohistochemical expression patterns of candidate biomarkers in relation to the different stages of CRC

2. To examine the relationship between CDC5L and Cyclin E expression and that of their potential partner proteins during human CRC development

### 6.2 Haematoxylin and eosin (H and E) staining based histology of the samples

H and E is the standard method used to assess the histopathology of cancers based on their morphology. H and E images are shown in figure 6.1 as a histological reference for the different stages of CRC.

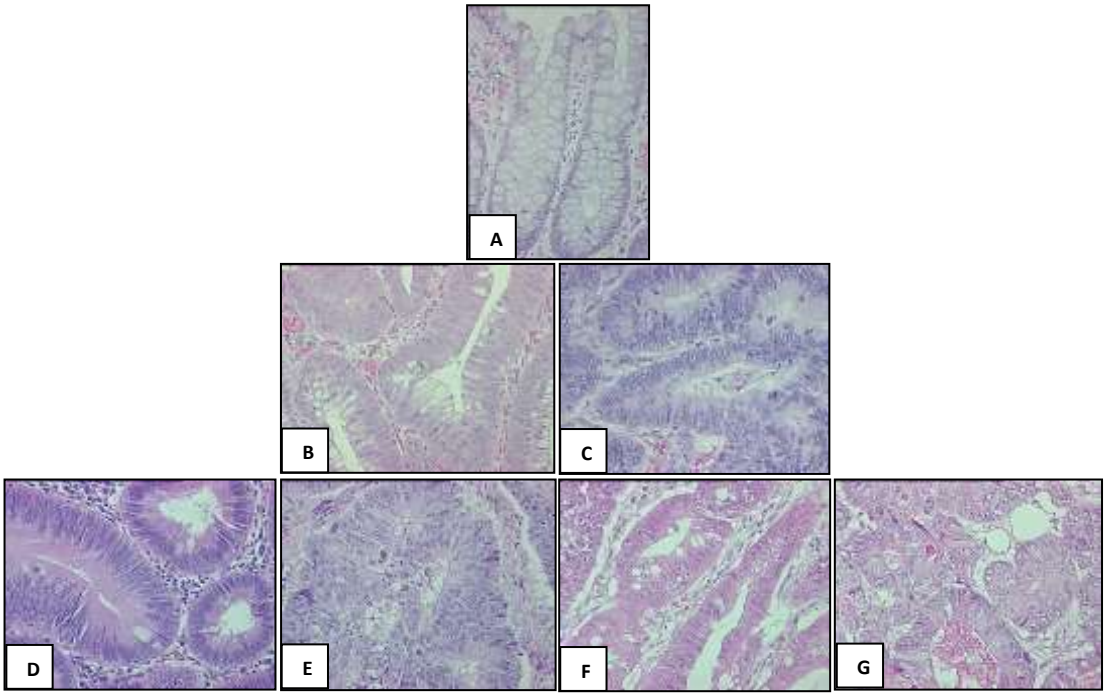


**Figure 6.1 Haematoxylin and Eosin stained human colonic sections. A) Shows normal colon, B) shows benign adenoma, C) shows polyp cancer and D-E) show Dukes' A to D CRC respectively. All images are X40 original magnification.**

Although the histological appearance of each stage may vary according to the behaviour of the individual tumour, these images can be used as a general guide for how CRC changes during the different stages. Moreover, staging is not only based on the morphological changes but also on the invasion to the different surrounding structures as well as on distant metastasis. Refer to table 1.1 (p18) for more details.

### 6.3 Immunohistochemistry evaluation of the expression of candidate biomarker proteins

IHC is a good method for studying the association between changes in the expression of a particular protein and the histopathological and clinical behaviour of a tumour.

IHC is also widely used to understand the distribution and localisation of biomarkers and differentially expressed proteins in different parts of a biological tissue.

All images are representative, since whole tumour sections were examined from five patients per histological stage.

### 6.3.1 Assessment of WNT pathway activity in normal and neoplastic human colon

The canonical WNT signalling pathway plays a critical role in development, tissue homeostasis and cancer [68]. Cell fate, cell growth and cellular proliferation have all been reported to be regulated by this pathway. The complex relationship between the WNT pathway and cellular functions extends to mechanisms that control progression through the cell cycle. Consequently, aberrations of the WNT pathway during development or later in life can have catastrophic outcomes including cancer development [68]. Not surprisingly, the majority of human CRCs are initiated by abnormal activation of the WNT pathway [299]. However, the downstream mechanisms mediating this tumourigeneis are not yet fully understood [205].

It was evident in chapter three that *Apc* deletion caused immediate derangement of the WNT pathway as demonstrated by nuclear re-localisation of Beta catenin in the areas of the $AhCre^{+}Apc^{fl/fl}$ mouse where DNA recombination occurred. Moreover, colonic neoplastic lesions in $Apc^{Min/+}$ mice also demonstrated evidence of altered WNT activity. The proteins examined in this thesis also demonstrated the most obvious changes in expression patterns in the same tissue compartments where the Wnt pathway was active. It is therefore important to investigate the role of the WNT signalling pathway in human subjects and then correlate that with the expression of our candidate biomarker proteins. This will inform about the significance of WNT signalling pathway activation during human colorectal tumourigenesis.

The same antibody to Beta catenin was used as in chapter three and the same experimental conditions were used in the IHC work that involved human colonic tissue samples. Figure 6.2 shows representative images of Beta catenin expression in samples from the various stages of human CRC.

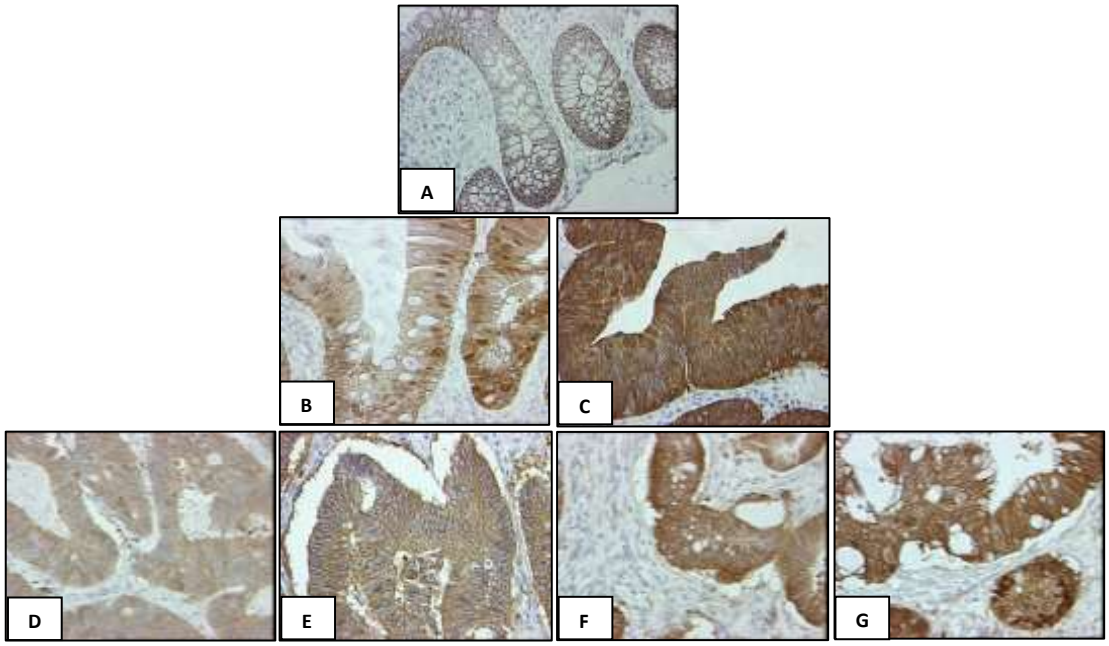


**Figure 6.2 Representative IHC images of Beta catenin expression in human CRC. Images A to G represent normal colonic epithelium, small adenomatous polyp, polyp cancer, Dukes' A, Dukes B', Dukes' C and Dukes' D CRC respectively. All images are X40 original magnification. N=5 patients per tumour stage.**

Under un-stimulated conditions Beta catenin is cytoplasmic and membrane bound [59]. Normal colonic epithelium also demonstrated membranous localisation of Beta catenin (figure 6.2A). Consistent with the findings in the mouse models (chapter three), the earliest stages of colorectal cancer development, particularly adenomas, demonstrated increased nuclear localisation of Beta catenin (figure 6.2B). Interestingly, overexpression of Beta catenin continued with the progression of the lesions, however nuclear localisation was not the predominant distribution pattern anymore.

Due to the inter-tumour heterogeneity described with many cancers [300] and to have a more objective assessment of the expression of Beta catenin and other candidate biomarkers in these samples, the intensity of nuclear and cytoplasmic staining of the various proteins was scored from 0-3. Zero represented no staining while 3 represented the most intense staining (figure 6.3). Scoring was performed by scanning the slides under a light microscope according to the following criteria:

- Included tissues were more than 70% intact
- More than 70% of the specimen had acceptable staining

- The predominant staining pattern (more than 50-70% of the included tissue) was considered. It was not possible to determine the percentage of each minor variation in intensity because we were scoring two parameters (nuclear and cytoplasmic).
- Artefacts were ignored

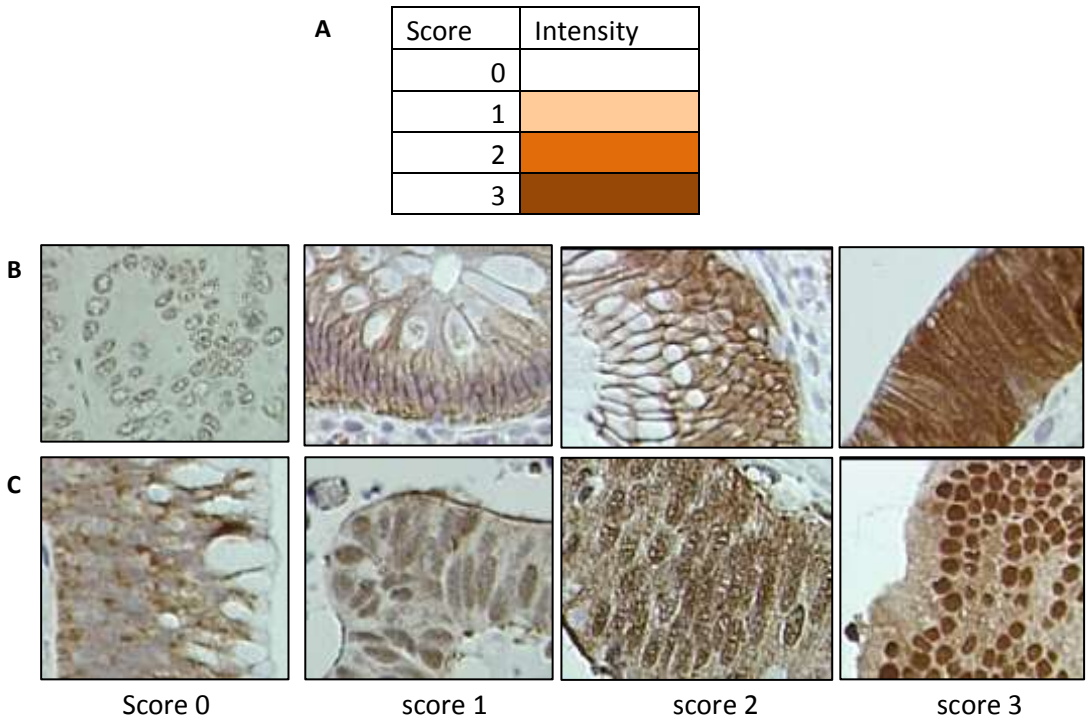


**Figure 6.3 Colour guide in the quick scoring used for all candidate proteins. A) Cartoon representation of colour intensities with corresponding scores. B) Representative IHC images for the different cytoplasmic (B) and nuclear (C) staining intensities with the respective scores.**

Intra-scorer variation was checked by re-scoring some slides on a different occasion with the scorer being blinded from knowing the slide label and tumour stage. Results were then compared as shown below in figure 6.4.

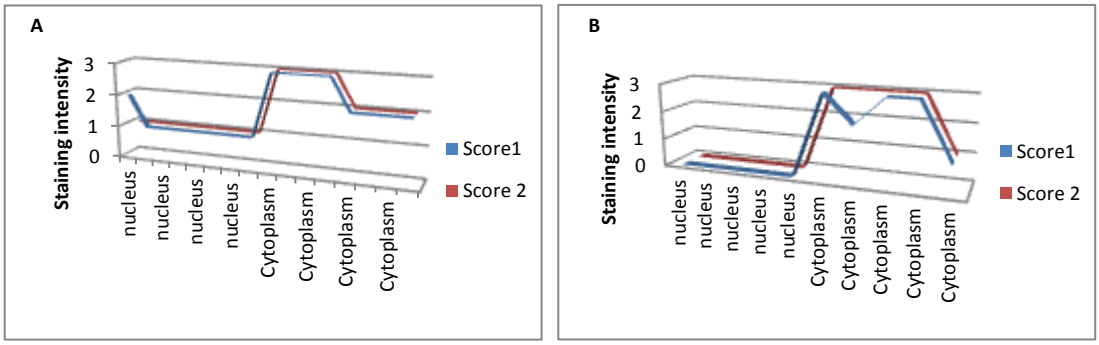


**Figure 6.4 Re-scoring of staining intensity for some proteins on a different date. A) Shows rescoring of Beta catenin expression in 8 patients with benign colonic polyps. In graph (A) each tick mark on the X axis represents a data point from one patient. B) shows rescoring of PHB expression in 5 patients with polyp cancers.**

Rescoring was performed on several of the proteins and the results were acceptably close between the two rounds of scoring as demonstrated in two examples shown in figure 6.4.

Figure 6.5 below shows the scoring of nuclear and cytoplasmic Beta catenin staining in specimens representing the different stages of human CRC development.

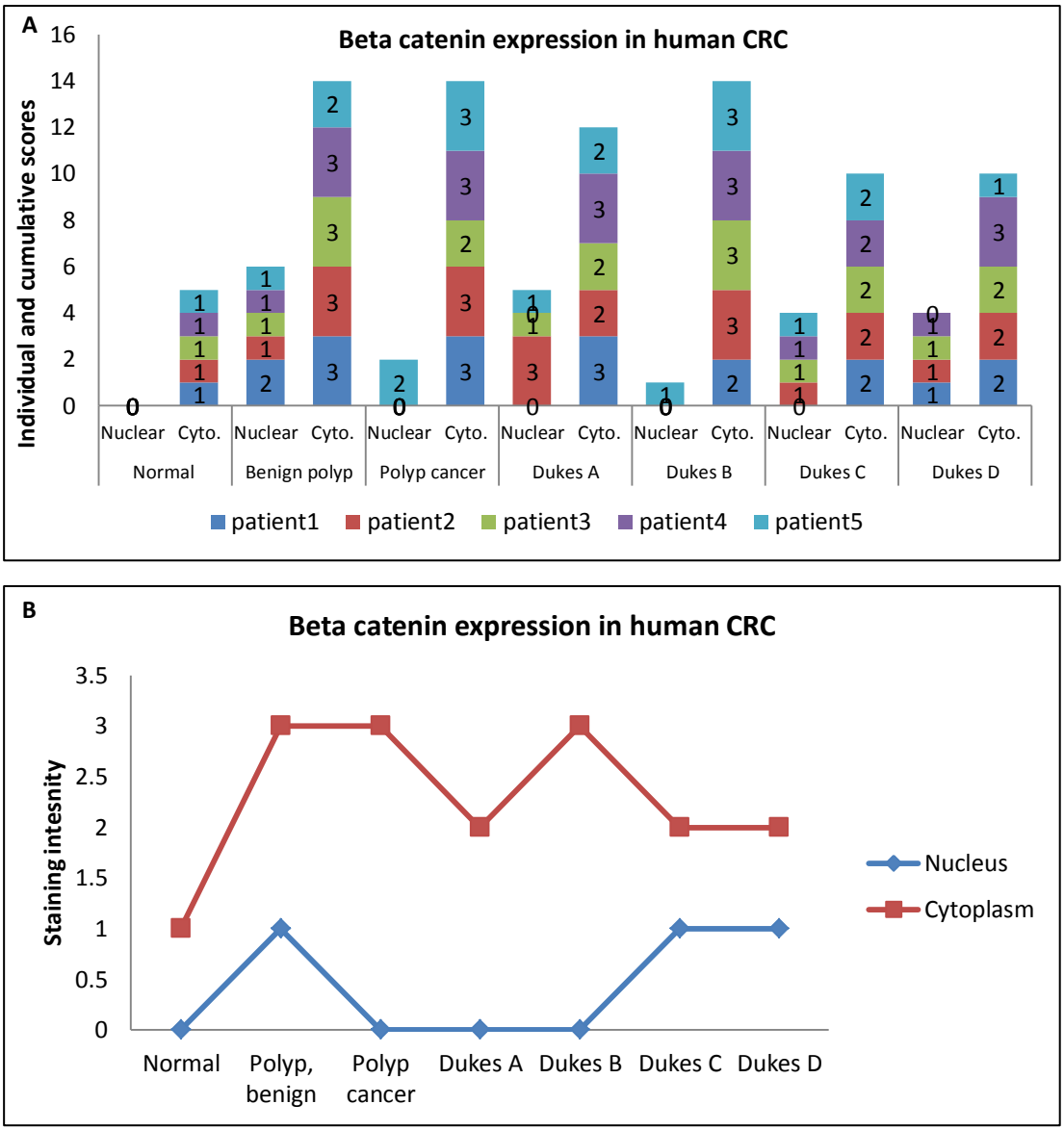


**Figure 6.5 Nuclear and cytoplasmic Beta catenin staining scores in all stages of human CRC. For each histological stage, five patient's samples were scored. A) Each segment represents a raw data point and each bar represents the cumulative staining intensity. B) Each data point represents the mode within each group. Cyto.= cytoplasmic.**

Mouse models showed more consistent staining in the benign stages as seen in colonic polyps from six month old *Apc*$^{Min/+}$ mice and the intestinal crypts of *AhCre*$^{+}$*Apc*$^{fl/fl}$ mice. However, it is not surprising that the same consistency was not recapitulated in human CRC. This may be due to the following reasons:

- Lesions studied in mice were all about the same age while polyps from humans were harvested at different time points during tumourigenesis.

- Experimental mice share the same genetic and environmental conditions while humans differ in these conditions.
- It is documented that the type of *Apc* mutation determines the level of Beta catenin [63]. This observation supports the role of genetic background in determining tumour behaviour.

Despite the above heterogeneity, Beta catenin expression appeared to be higher during the earliest stages of CRC development. Moreover, if we add up nuclear and cytoplasmic Beta catenin levels, we can see the total level is lowest in the normal colon and then it is upregulated, but almost the same during the other stages. This suggests a role for the nuclear Beta catenin/WNT pathway particularly during the early stages of colorectal tumourigenesis.

### 6.3.2 NAP1L1 expression in human CRC

NAP1L1 is a novel protein in the area of carcinogenesis that has not been studied extensively. Its upregulation has been reported in few studies; for example it has been shown to be upregulated in hepatoblastomas [301]. Moreover, in a study involving relative mRNA level comparison between human CRC samples and normal adjacent tissues involving 15 patients, a 2 - 9 fold increase in the level of *NAP1L1* was seen in cancerous tissue in 7 patients [150]. Therefore studying NAP1L1 expression in human CRC samples using IHC may further clarify the role of NAP1L1 in this disease.

NAP1L1 protein expression was studied in the various stages of human colorectal tumourigenesis using samples from 5 patients for each stage. Figure 6.6 shows representative images for NAP1L1 expression in early and advanced cases of human CRC.

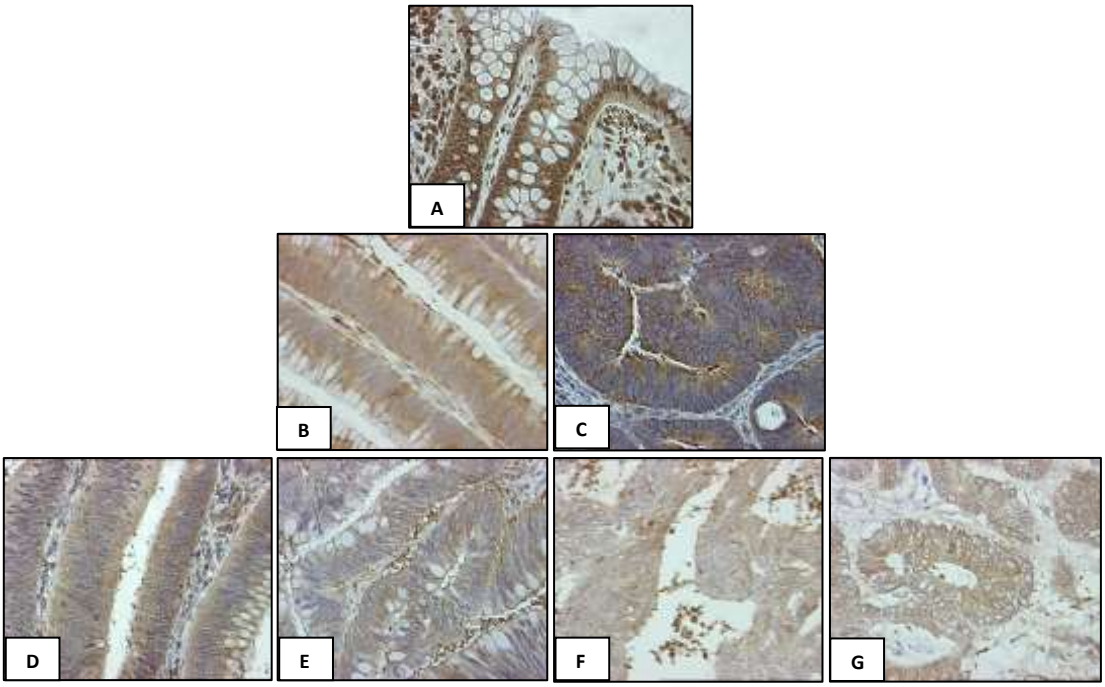


**Figure 6.6 Immunohistochemical NAP1L1 expression in human CRC. Images A-G represent normal colonic epithelium, benign colonic adenoma, colonic polyp cancer, Dukes' A, Dukes' B, Dukes' C and Dukes' D stages CRC respectively. N=5 patients per stage.**

In agreement with a previous report that described NAP1L1 as a nuclear protein [148], NAP1L1 showed nuclear localisation in the normal colon. Again, consistent with the findings from IHC studies in animal models, NAP1L1 demonstrated cytoplasmic displacement and nuclear sparing immediately after the start of neoplasia development. Interestingly, the change does not seem to involve an obvious increase in the total level of NAP1L1 expression.

Scoring of NAP1L1 expression in normal and neoplastic colonic tissues was performed (figure 6.7) following the same criteria as those used for Beta catenin.

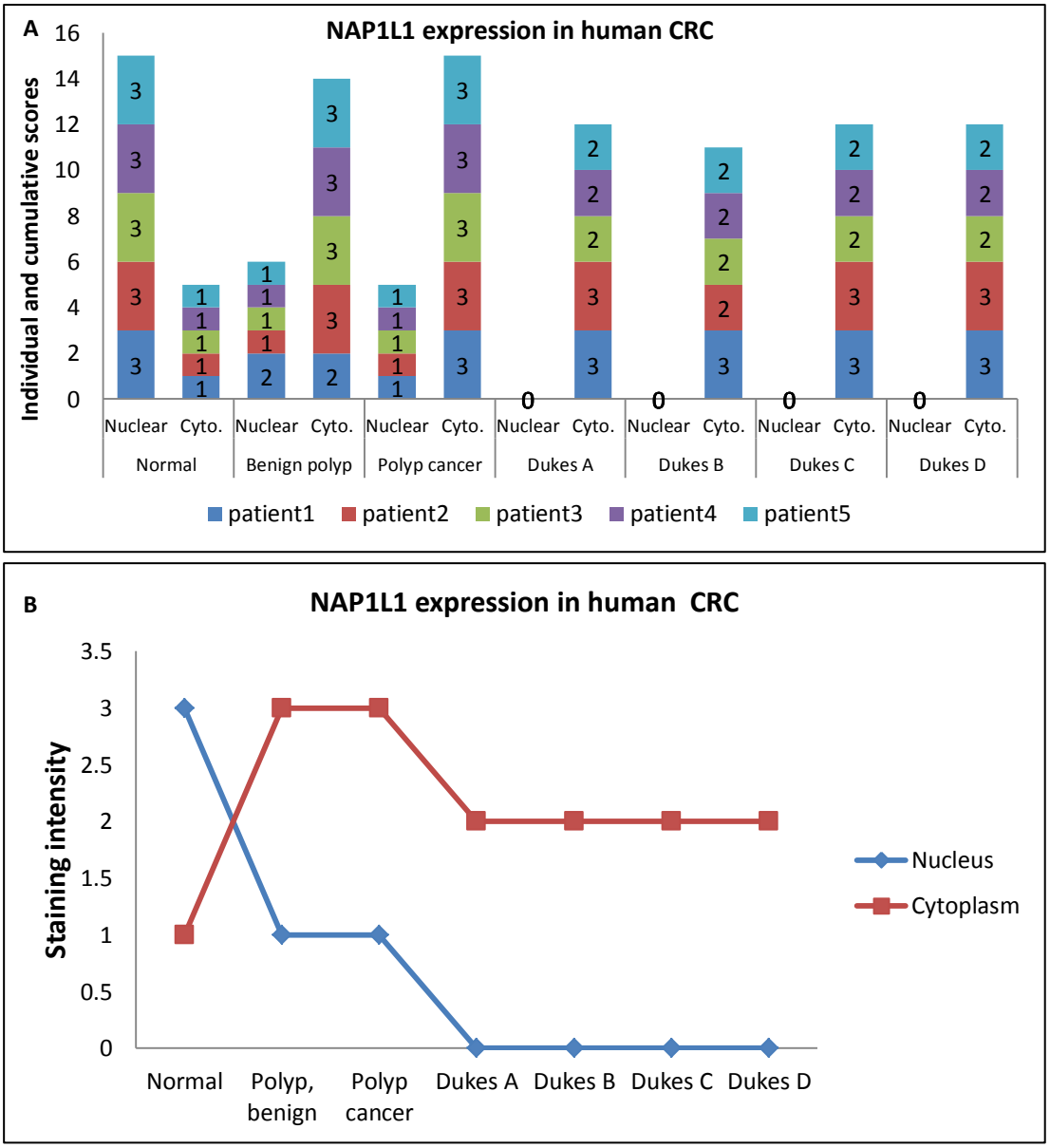


**Figure 6.7 Scoring results for NAP1L1 expression as detected by IHC in samples from normal and neoplastic human colon. N=5 patients per stage. A) Represents raw data and B) represents the mode values within each group. Cyto.= cytoplasmic.**

Strong nuclear expression of NAP1L1 was obvious in the normal colon. The early stages of colorectal neoplasia were associated with a reduction in the nuclear expression of NAP1L1 while after invasion there was complete loss of nuclear NAP1L1 expression. A more quantitative technique such as western blotting or qPCR may be superior for assessing changes in total NAP1L1 level.

### 6.3.3 RPL6 expression in human CRC

Similar to NAP1L1, RPL6 has not been well studied in CRC. This protein however also showed upregulation in the mouse models previously studied. Moreover, *in vitro*, RPL6 knockdown caused significant inhibition of cellular proliferation with a simultaneous increase of apoptosis. The same antibody and experimental conditions used in chapter three were also used in the IHC experiments involving human colonic tissue samples.

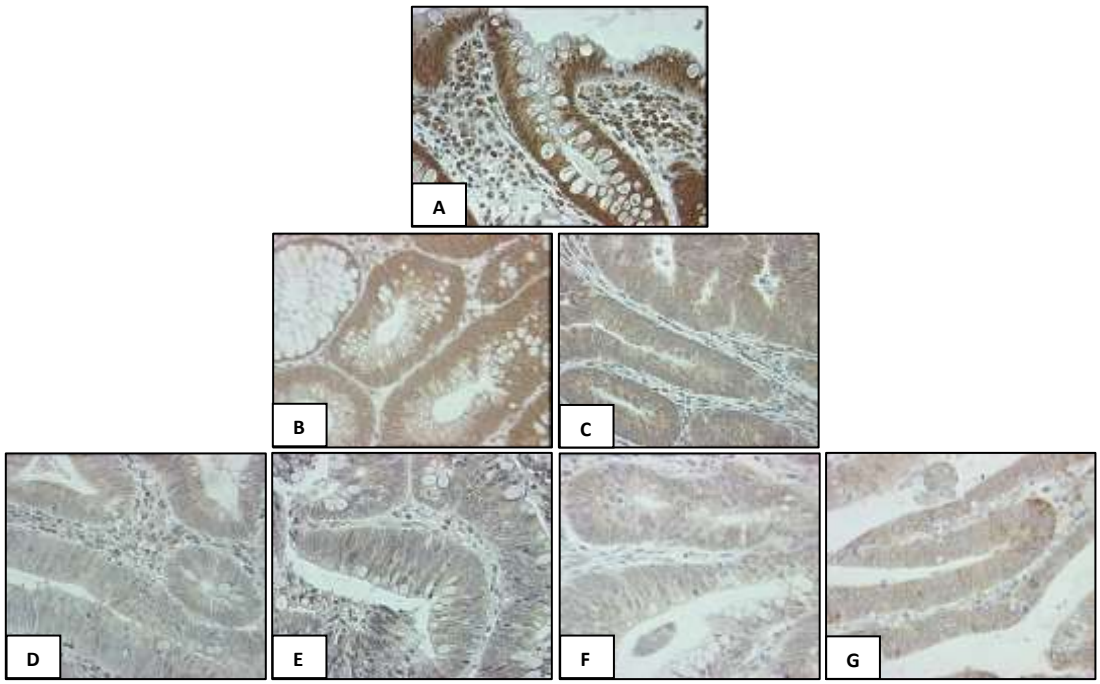


**Figure 6.8 RPL6 expression in human CRC. Images A-G represent normal colonic epithelium, benign colonic adenoma, colonic polyp cancer, Dukes' A, Dukes' B, Dukes' C and Dukes D' stages CRC respectively. N=5 patients per stage.**

Consistent with the results from the animal studies, RPL6 showed nuclear localisation early during colorectal tumourigenesis as seen in the benign adenoma sample. Nuclear expression was absent in the more advanced tumour stages.

Scoring of the staining intensity of nuclear and cytoplasmic RPL6 expression was performed on five patients for each stage of CRC as shown in figure 6.9.

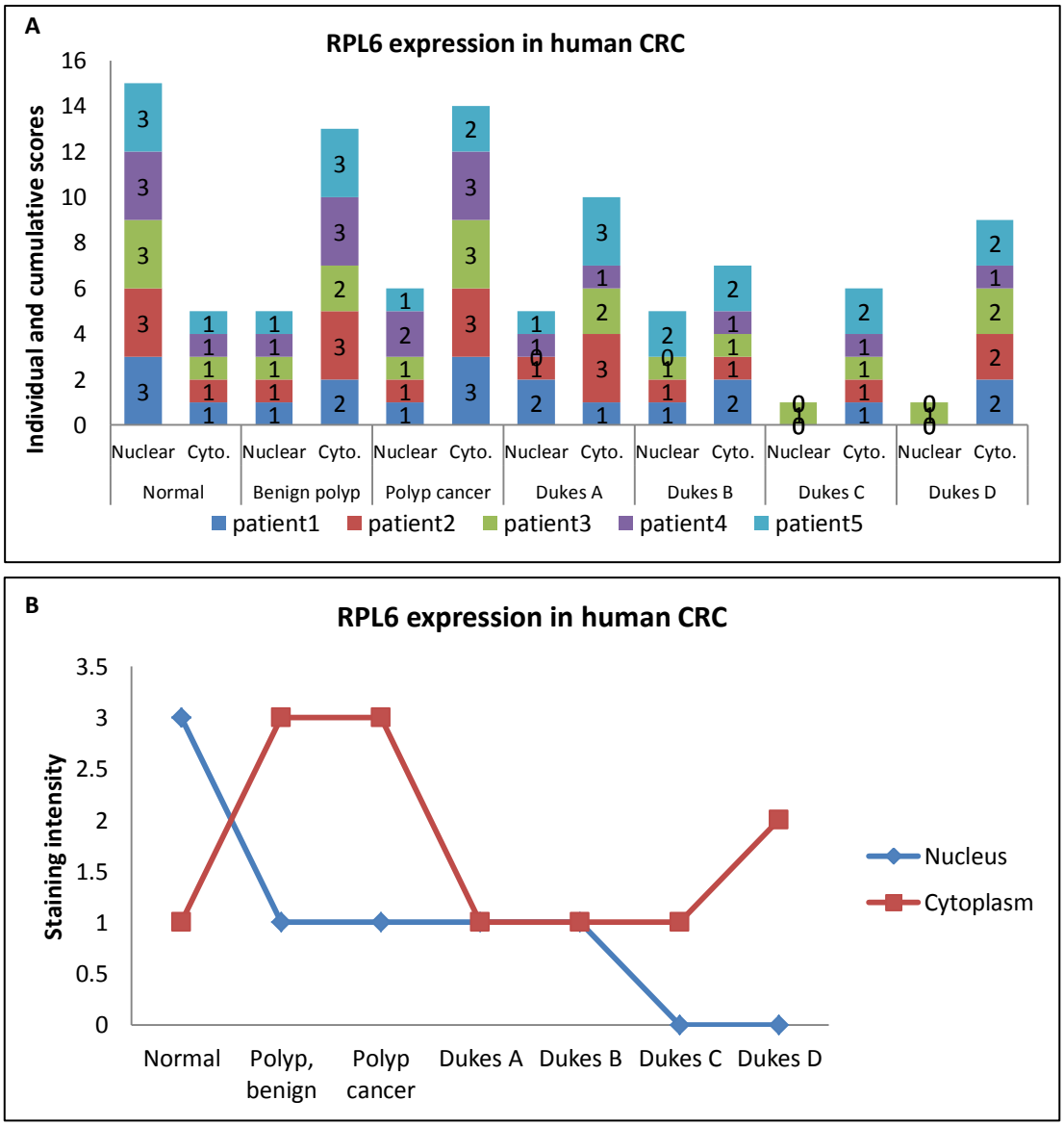


**Figure 6.9 Scoring results for RPL6 expression as detected by IHC in samples from normal and neoplastic human colon. N=5 patients per stage. A) Represents raw data and B) represents the mode values within each group. Cyto.= cytoplasmic.**

Unlike the animal models, nuclear expression of RPL6 was strong in normal colonic epithelium. Then with the start of the neoplastic process, RPL6 started to shift into the cytoplasm. Almost no nuclear expression was seen in the more advanced tumours. This suggests a WNT dependent role of RPL6 in early but not late colorectal tumourigenesis. Also these results showed that RPL6 was a nuclear protein under normal conditions. Moreover, these observations are in agreement with studies which have reported cytoplasmic localisation of RPL6 in human gastric cancer tissues [163].

We have previously studied whether RPL6 interacts with Cyclin E during colonic tumour development *in vitro* and in mouse models. Therefore, we decided to also study this relationship in human CRC. The same experimental conditions employed in chapter three were used to study Cyclin E expression in human colonic tissues. Figure 6.10 shows representative IHC images of Cyclin E expression and figure 6.11 shows the scoring results from IHC experiments of five subjects per histological stage.

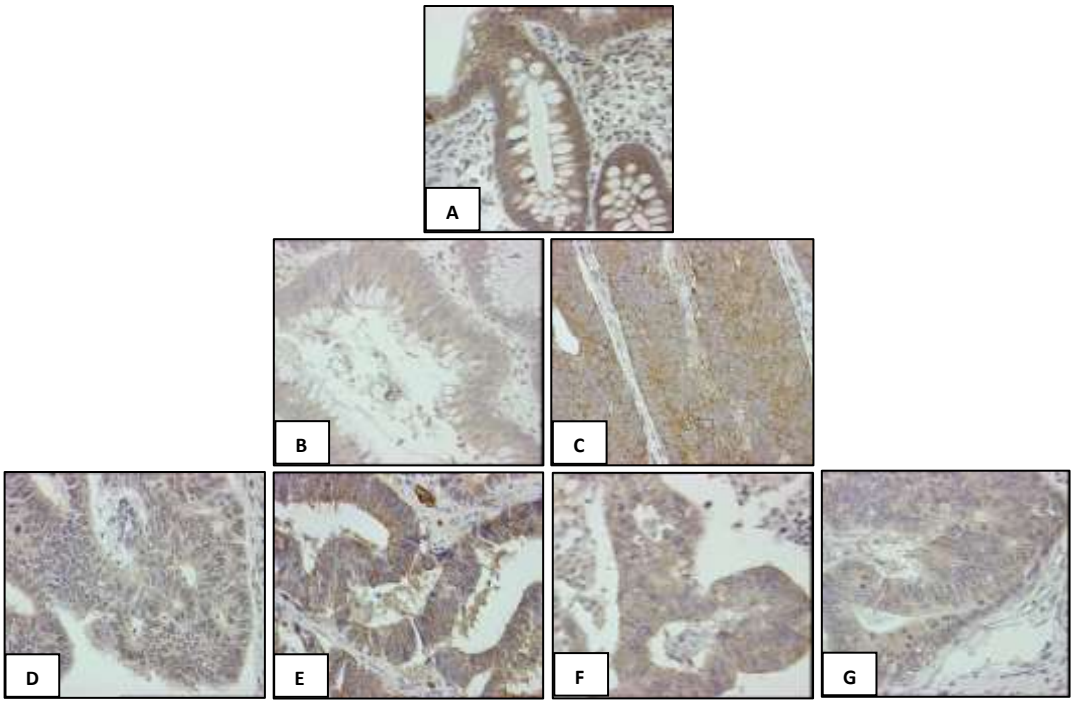


**Figure 6.10 IHC results of Cyclin E expression in human CRC. Images A-G represent normal colonic epithelium, benign colonic adenoma, colonic polyp cancer, Dukes' A, Dukes' B, Dukes' C and Dukes' D stages CRC respectively. N=5 patients per stage.**

Although animal studies did not show co-expression of RPL6 and Cyclin E as shown in chapter three, both proteins showed cytoplasmic localisation in human CRC. Despite this co-expression, no clear change in Cyclin E expression was seen in the above images. Because the above images are only representative of a larger scale experiment, figure 6.11 is shown to depict the results from five patients per stage.

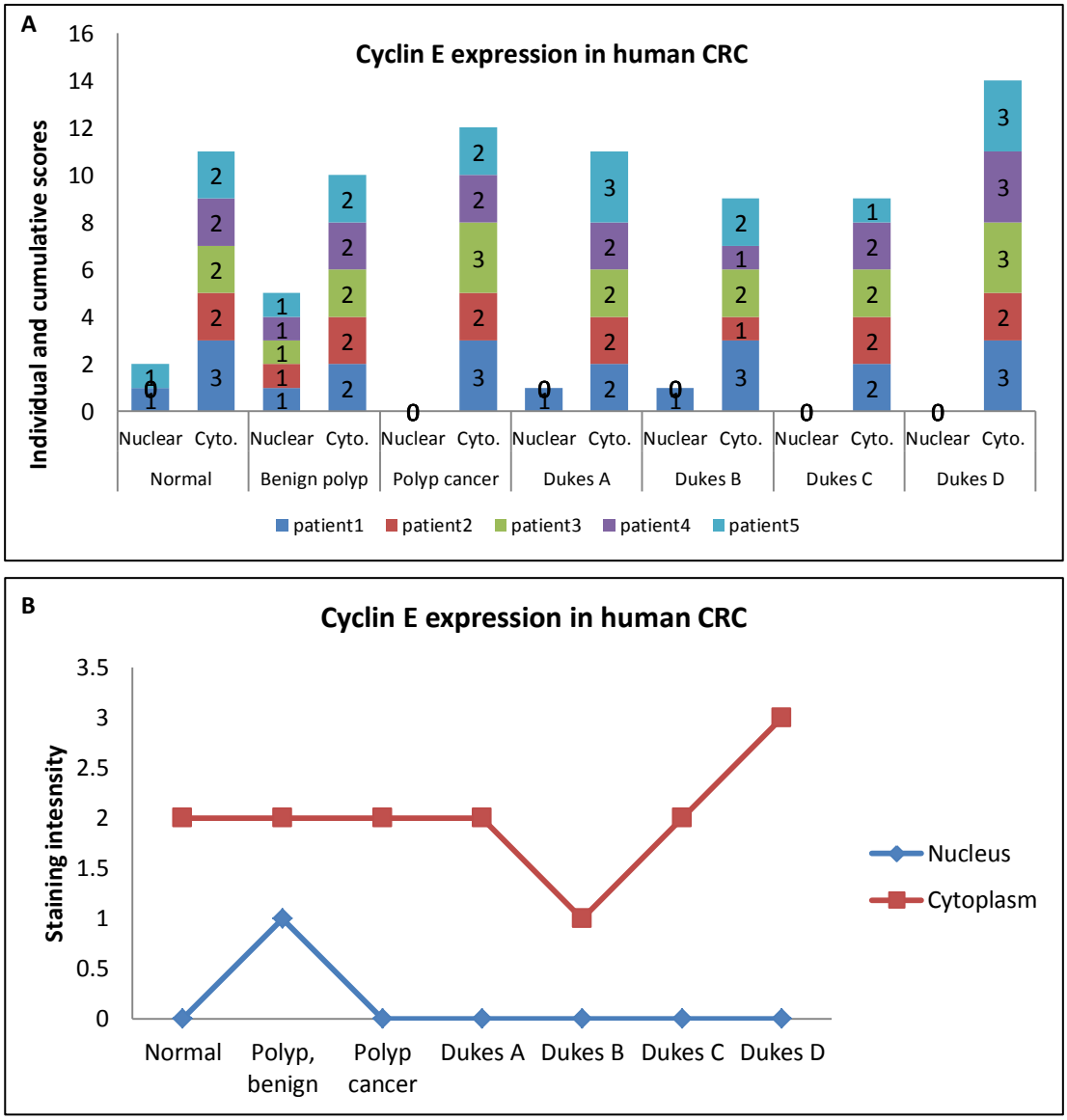


**Figure 6.11 Scoring results for Cyclin E expression as detected by IHC in samples from normal and neoplastic human colon. A) Represents raw data and B) represents the mode values within each group. Cyto.= cytoplasmic.**

Cyclin E expression was cytoplasmic and did not alter in the various stages of CRC studied. The highest expression can be seen in Dukes' D cancers. Interestingly, both RPL6 and Cyclin E showed the highest cytoplasmic to nuclear ratio in the most advanced stage of CRC. This finding may support the suggestion made by one research group that Cyclin E mediate effects of RPL6 in tumourigenesis [163].

### 6.2.4 PHB expression in human CRC

PHB showed mild changes in its level of expression in the animal studies, suggesting a small role if any for this protein during early colorectal tumourigenesis. Unfortunately, the anti-PHB antibody was among the antibodies that did not work in the animal model of advanced colorectal tumourigenesis. Similar to the other proteins studied in this thesis, PHB has also not been well studied in human CRC. Optimised IHC experimental conditions (as outlined in chapter three) were therefore used to study PHB expression in human CRC samples. Figure 6.12 shows representative images of an experiment that involved 5 patients per histological stage.

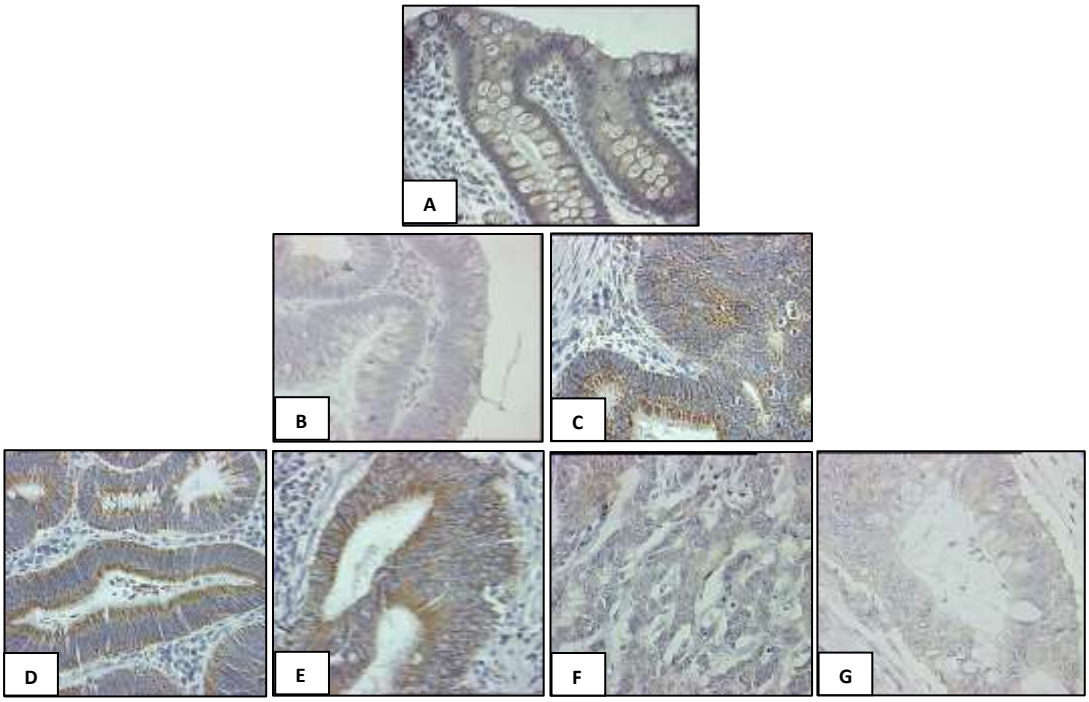


**Figure 6.12 assessment of PHB expression in the various stages of human CRC. A-G represent normal colonic epithelium, benign colonic adenoma, colonic polyp cancer, Dukes' A, Dukes' B, Dukes' C and Dukes D' stages CRC respectively. N=5 patients per stage.**

Although no major change of expression was seen in some adenomas (as shown in figure 6.12B), there was an obvious increase in the brown staining in the cytoplasm of colonic epithelial cells from the early stages of colorectal cancer (C-E). To further validate these results, tissue sections from all five patients in each stage were scored as demonstrated in figure 6.13.

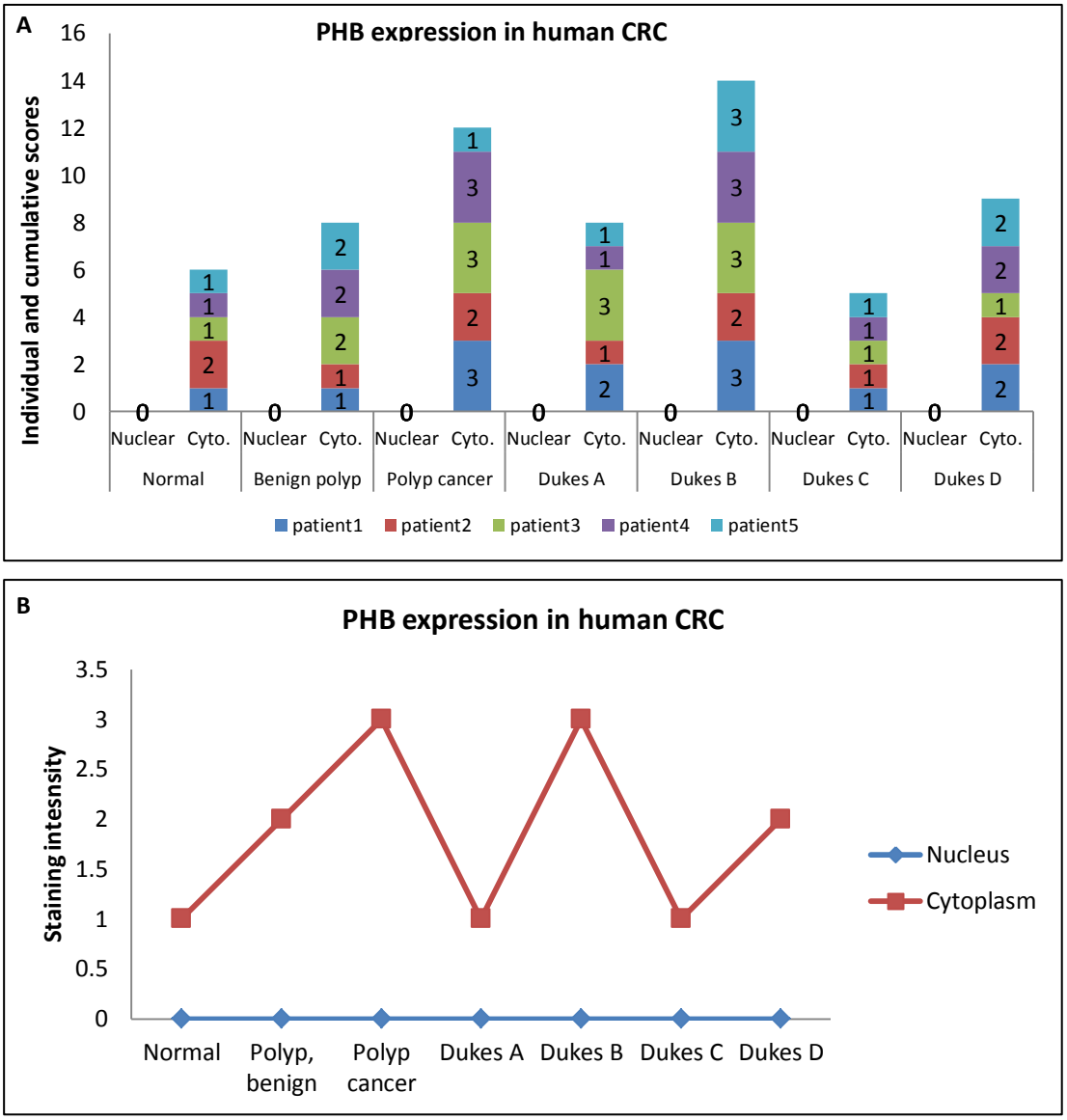


**Figure 6.13 Cytoplasmic and nuclear PHB staining intensity in the various stages of human CRC. N=5 patients per stage. A) Represents raw data and B) represents the mode values within each group. Cyto. = cytoplasmic**

The scoring results (figure 6.13) demonstrate that there was an increase in PHB level in benign polyps, polyp cancers, as well as Dukes' A and Dukes' B cancers. This further confirms the changes that were seen visually in figure 6.12. Moreover, these results are in agreement with quantitative RT-PCR data produced by a previous colleague (Dr. Fei Song, unpublished work) in human CRC tissues vs. normal adjacent tissues. She showed that PHB was mainly overexpressed in Dukes' A and B stages colorectal tumours.

### 6.3.5 NCL expression in human CRC

NCL was another protein that demonstrated overexpression in the animal models of early CRC. Therefore, it was selected to be tested in human colonic tissue samples. Below (figure 6.14) are representative images of NCL IHC that included five patients for each histopathological stage and used the same optimised experimental conditions as were described in chapters two and three.

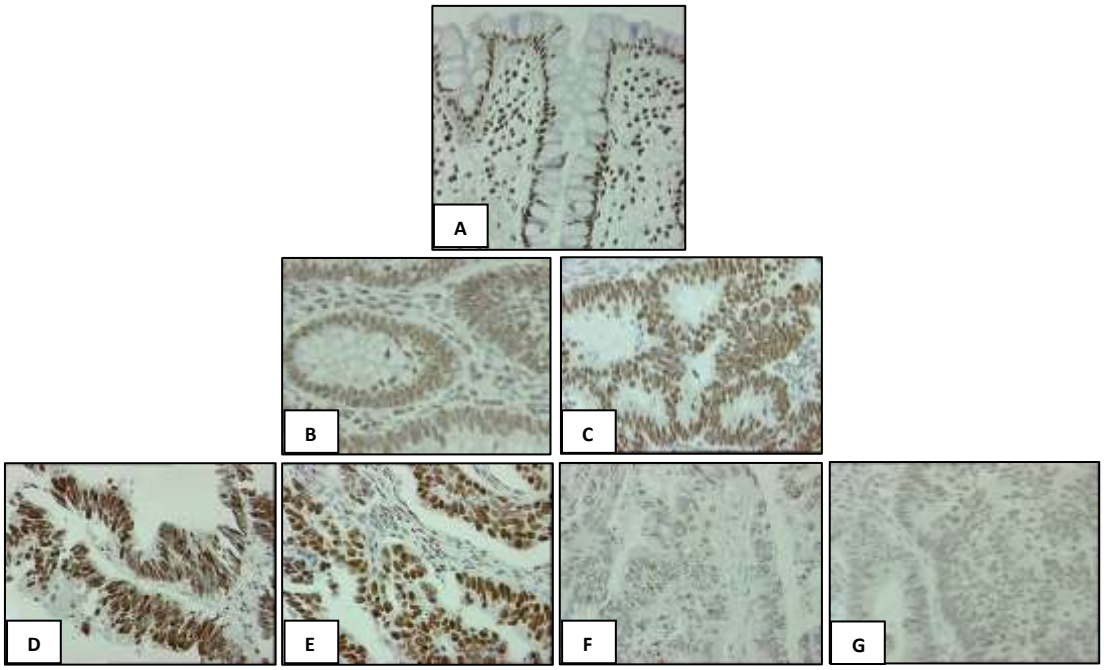


**Figure 6.14 representative images of IHC staining of NCL in human CRC tissues. Images A-G represent normal colonic epithelium, benign colonic adenoma, colonic polyp cancer, Dukes' A, Dukes' B, Dukes' C and Dukes' D stages CRC respectively. N=5 patients per stage.**

In the animal studies, NCL demonstrated overexpression early during colonic tumourigenesis. Interestingly, in human samples, it was visually obvious that NCL was down regulated in Dukes' C and D stages. This protein could therefore be useful as a prognostic or predictive marker if this observation is confirmed in larger scale studies.

All tissue sections in the above experiment were scored (figure 6.15) to produce a more objective assessment of NCL expression during the course of CRC progression.

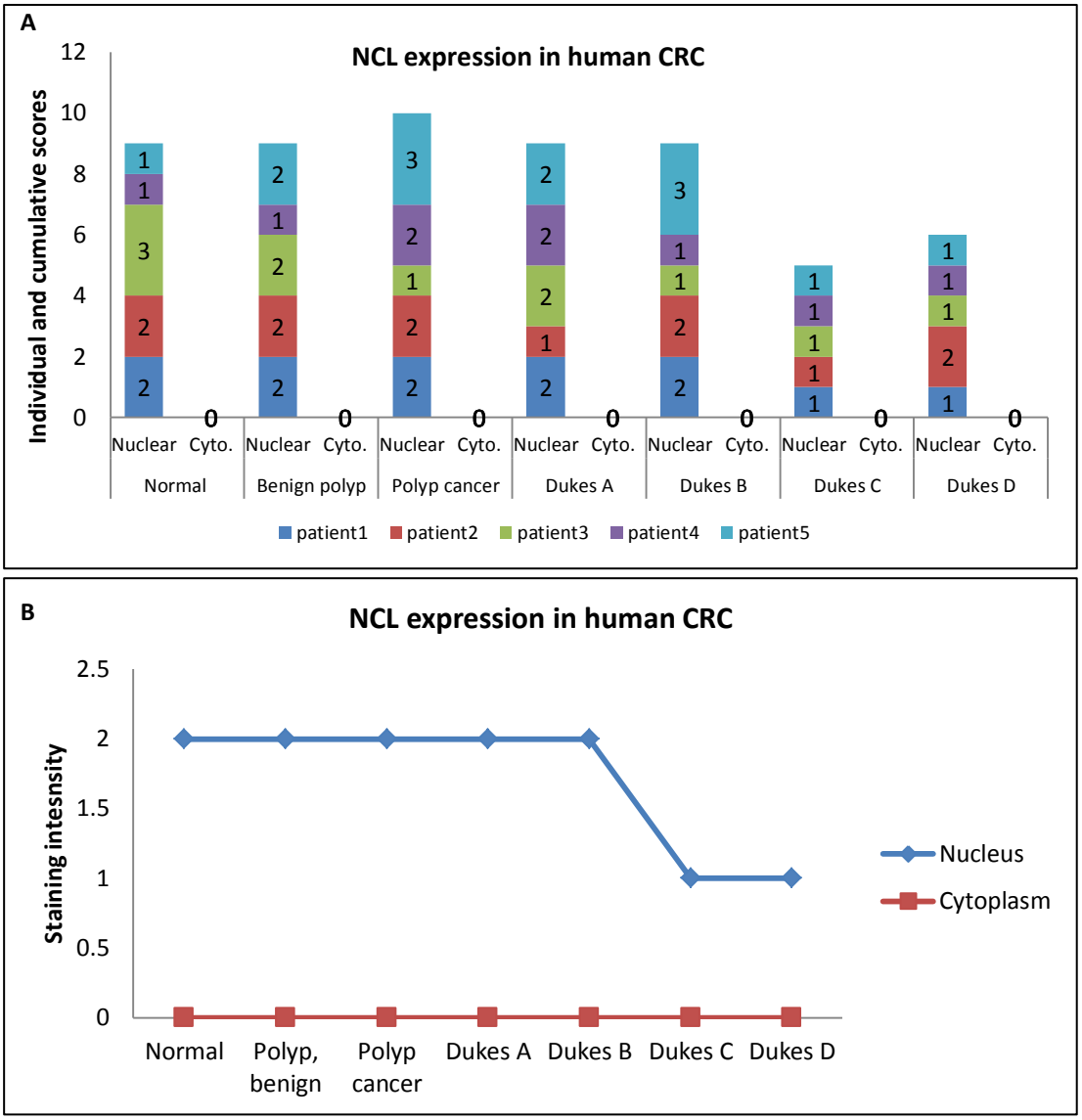


**Figure 6.15 Scoring results for NCL staining intensity in the various stages of human CRC. N=5 patients per stage. A) Represents raw data and B) represents the mode values within each group. Cyto. = cytoplasmic.**

In agreement with the images in figure 6.14, scoring demonstrated that NCL did not show obvious changes in expression except in Dukes' C and D stages, where it showed an obvious reduction in staining intensity in comparison to normal colonic tissue.

### 6.3.6 Assessment of SFRS2 and CDC5L expression in correlation with WNT pathway activity

As described in chapter five, SFRS2 and CDC5L may interact during colorectal carcinogenesis. In the IHC experiments performed on animal models of early colorectal tumourigenensis that we showed in chapter three, SFRS2 demonstrated nuclear over expression while CDC5L showed cytoplasmic displacement in areas where the WNT signalling pathway was shown to be active. CDC5L also showed nuclear re-localisation in the animal model of more advanced intestinal tumourigenesis (*AhCreER*$^{T+}$*Apc*$^{fl/+}$*Pten*$^{fl/fl}$ mouse). Unfortunately two anti-SFRS2 antibodies did not work on the tissue sections from this mouse model. We have now investigated the expression of these proteins during human colorectal tumour development.

Below (figure 6.16) are representative images from each CRC stage. For each stage, samples from five patients were used.

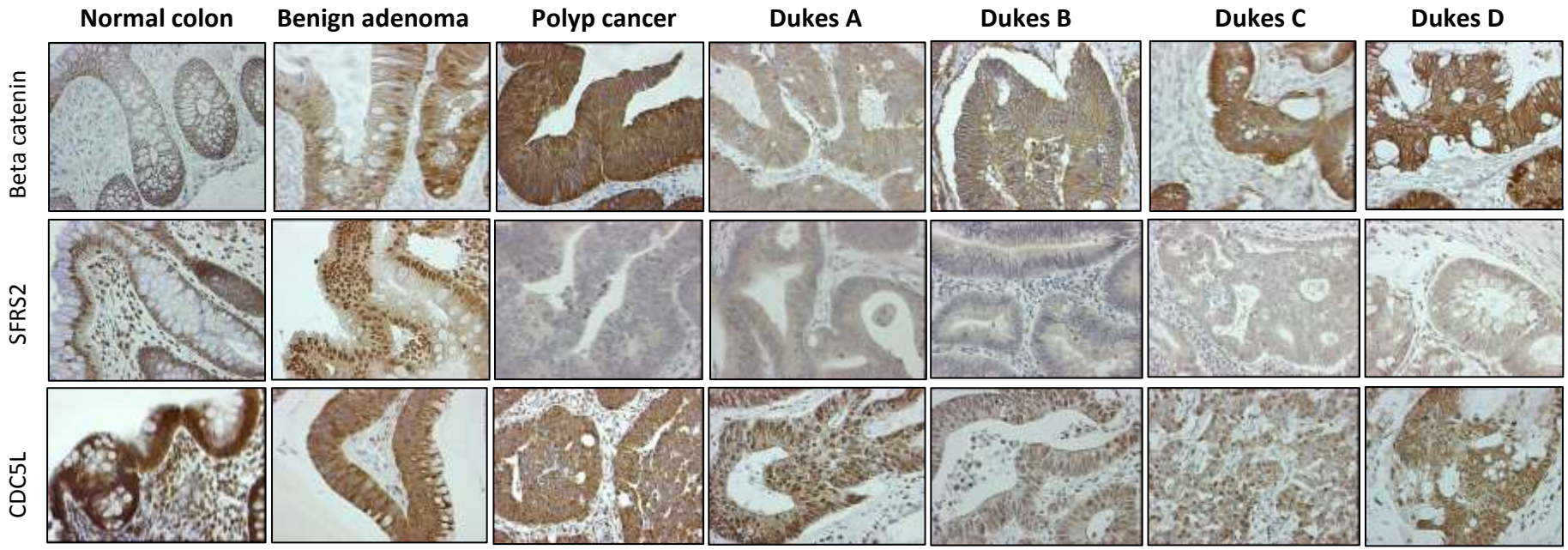


**Figure 6.16 shows assessment of SFRS2 and CDC5L expression in correlation with WNT pathway activity.**

These representative images from a subset of patients show loss of nuclear Beta catenin after the benign adenoma stage. At this stage, similar to the animal models described in chapter three, there was a simultaneous nuclear over expression of SFRS2 and cytoplasmic displacement of CDC5L. In the polyp cancer samples, SFRS2 started to show loss of nuclear activity while CDC5L expression remained cytoplasmic. From the stage of Dukes' A cancers onwards, CDC5L started to regain nuclear localisation. N= 5 or more samples per tumour stage.

As with Beta catenin, scoring was carried out on the sections stained with anti-SFSR2 and anti-CDC5L antibodies.

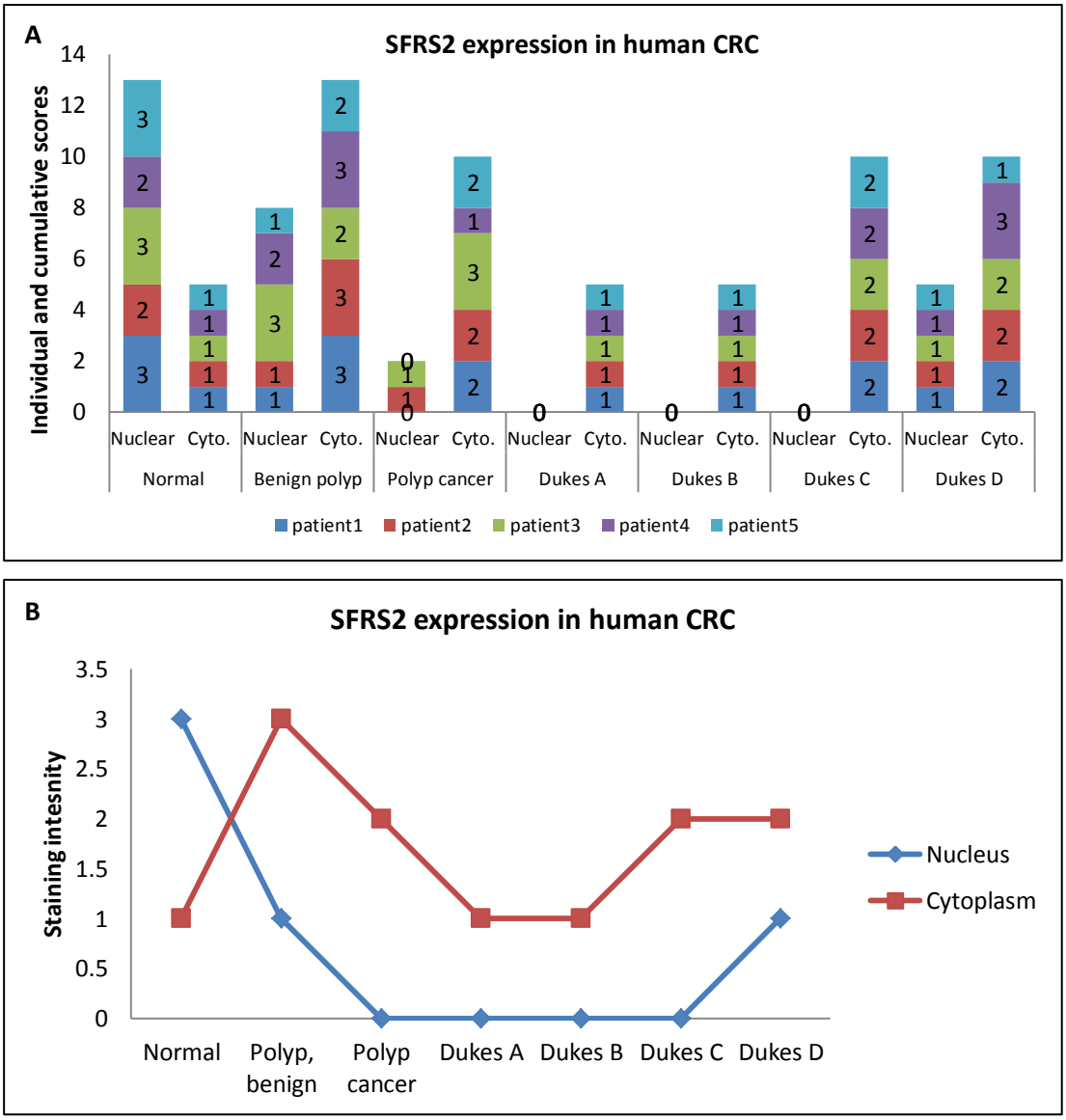


**Figure 6.17 Scoring results for SFRS2 expression in five patients per histopathological stage of human CRC. A) Represents raw data and B) represents the mode values within each group. Cyto. = cytoplasmic.**

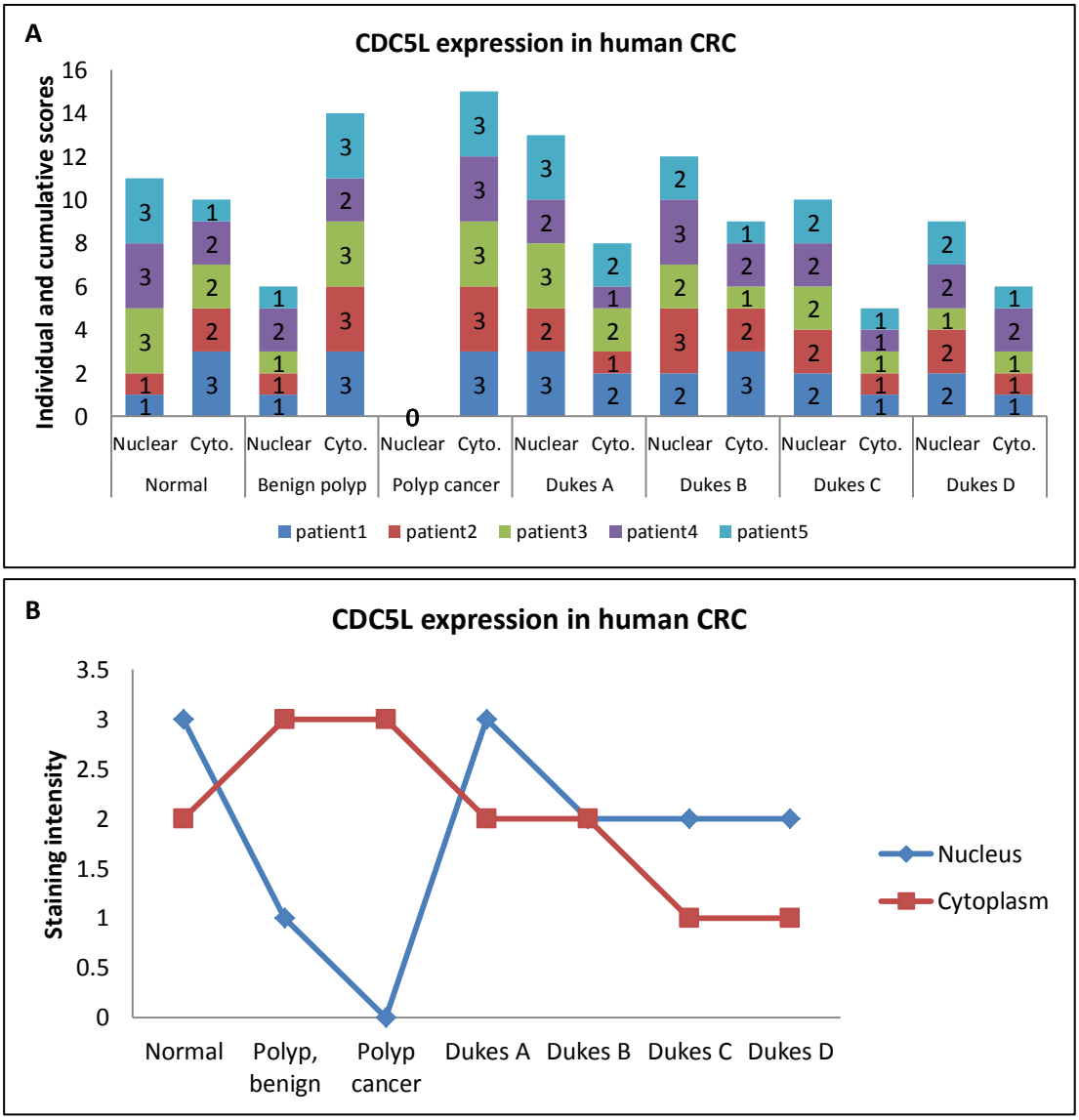


**Figure 6.18 Scoring results for CDC5L expression in five patients per histopathological stage of human CRC. A) Represents raw data and B) represents the mode values within each group. Cyto. = cytoplasmic.**

Consistent with the images shown in figure 6.16, SFRS2 started to be observed in the cytoplasm as early as the benign adenoma stage and became almost completely cytoplasmic after that. On the contrary, CDC5L demonstrated more cytoplasmic staining initially, whereas it was predominantly re-localised to the nucleus after the polyp cancer stage. This observation indirectly shows opposite locations for the two proteins at least for most stages of CRC and for the more advanced ones in particular. These observations further support the preliminary findings that we showed in the mouse model of invasive disease. Moreover, they fill in the gap left in the data from this animal model, due to technical issues related to the anti-SFRS2 antibodies.

To further elucidate the relationship between SFRS2 and CDC5L in correlation with WNT pathway activity, a more detailed scoring was carried out using a modified H score [302, 303]. This scoring was based on assessing 10 random X40 images for each individual tumour. One tumour was scored from each patient and five patients were included per histological stage; normal, benign adenoma, polyp cancer and Dukes' stages A to D CRCs. Images were taken using a Leica laser capture micro-dissection microscope.

The three proteins included in this assessment need to be nuclear to be functional. Therefore, only nuclear expression was scored as an indicator of the activity of each protein during the different stages of CRC. The intensity of staining was scored as 0, 1, 2 and 3 representing negative, weak, intermediate and strong staining respectively (figure 6.19). The total number of cells in each field and the number of cells stained at each intensity were counted. Then the percentage of cells in each intensity group was calculated. Then H score was calculated using the formula; H Score = (% of cells stained at intensity category 1 x 1) + (% of cells stained at intensity category 2 x 2) + (% of cells stained at intensity category 3 x 3). An H-Score between 0 and 300 was obtained where 300 was equal to 100% of tumour cells stained strongly (3+) (figure 6.19).

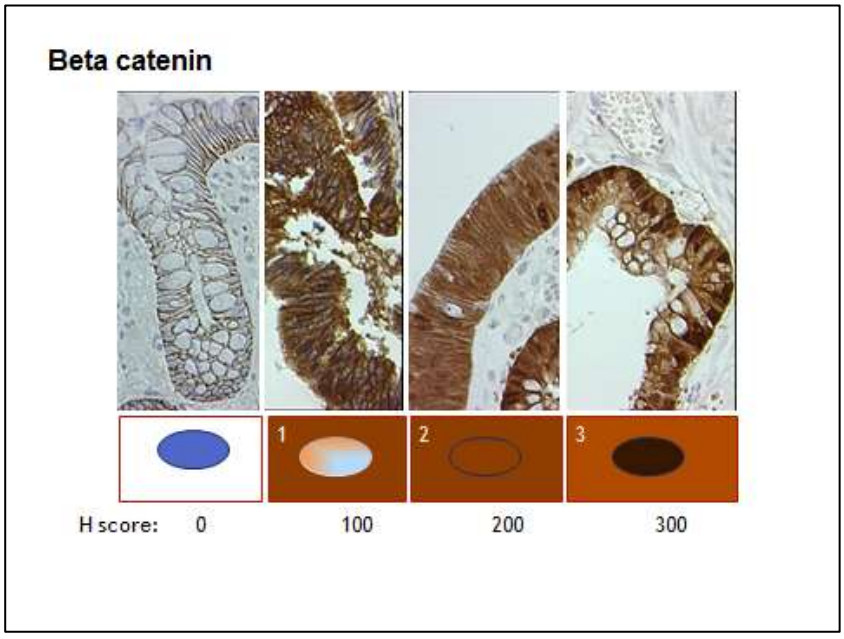


**Figure 6.19 an example illustrating the different nuclear staining intensities and their corresponding scorings.**

Cells were counted manually using imageJ 1.47v software (plugins; analyse/cell counter). Intra-scorer variation was checked by rescoring the fields taken from one patient for each protein at a different date. Figure 6.20 shows rescoring results for both SFRS2 and CDC5L.

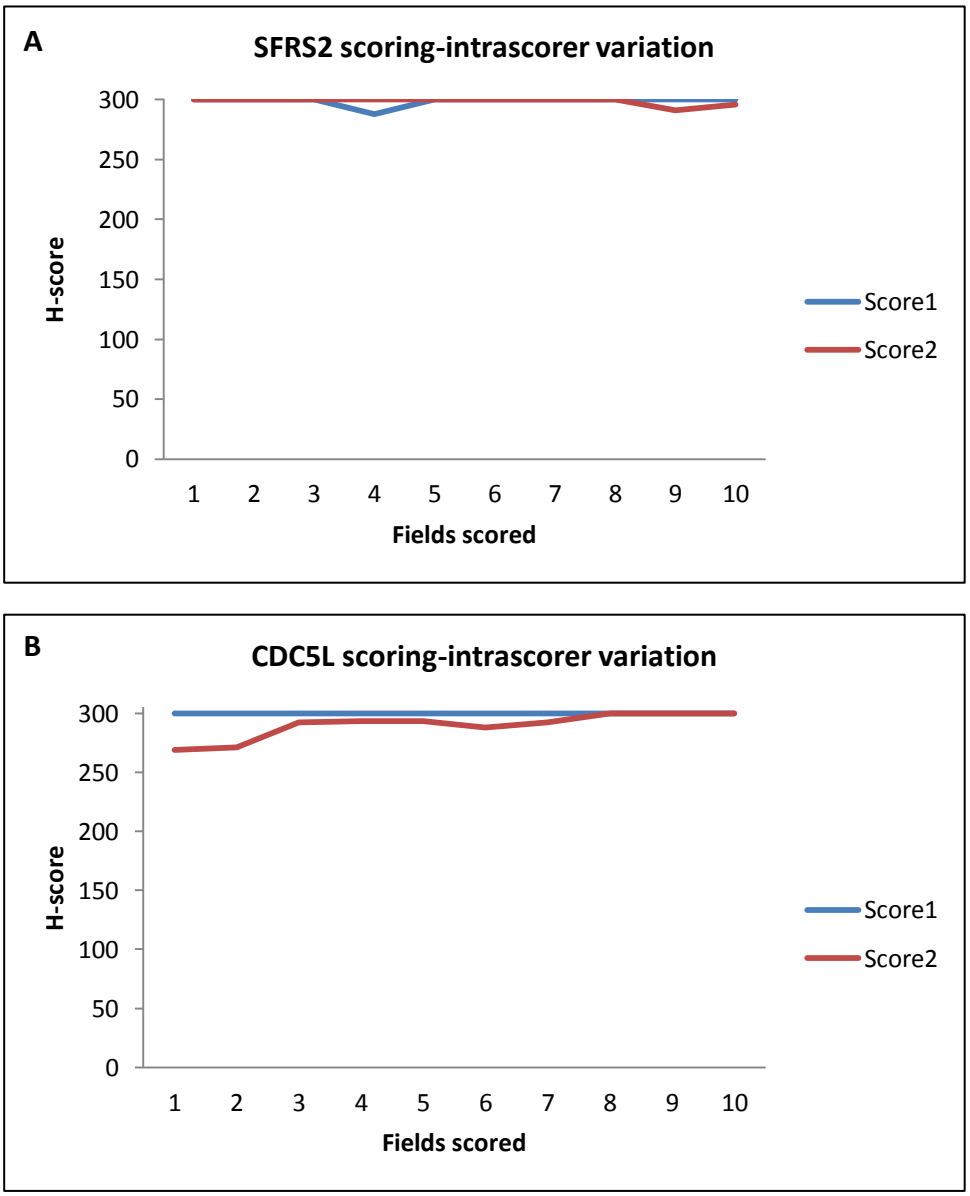


**Figure 6.20 Analysis of intra-scorer variation. A) Shows two scorings for SFRS2 staining in the benign adenoma stage of CRC. B) Shows two scorings for CDC5L staining in Dukes' A stage of CRC. The scorings were performed more than two weeks apart. N=10 images.**

After scoring several hundreds of fields for three different proteins, rescoring of randomly chosen patients and tumour stages at a different date with the scorer being blinded to the first round of scoring results is an effective way of assessing intra-scorer variation. Results were compared with those from the same patient (images were already labelled).

Figure 6.21 below, shows the distribution of data points from five patients per stage for each protein.

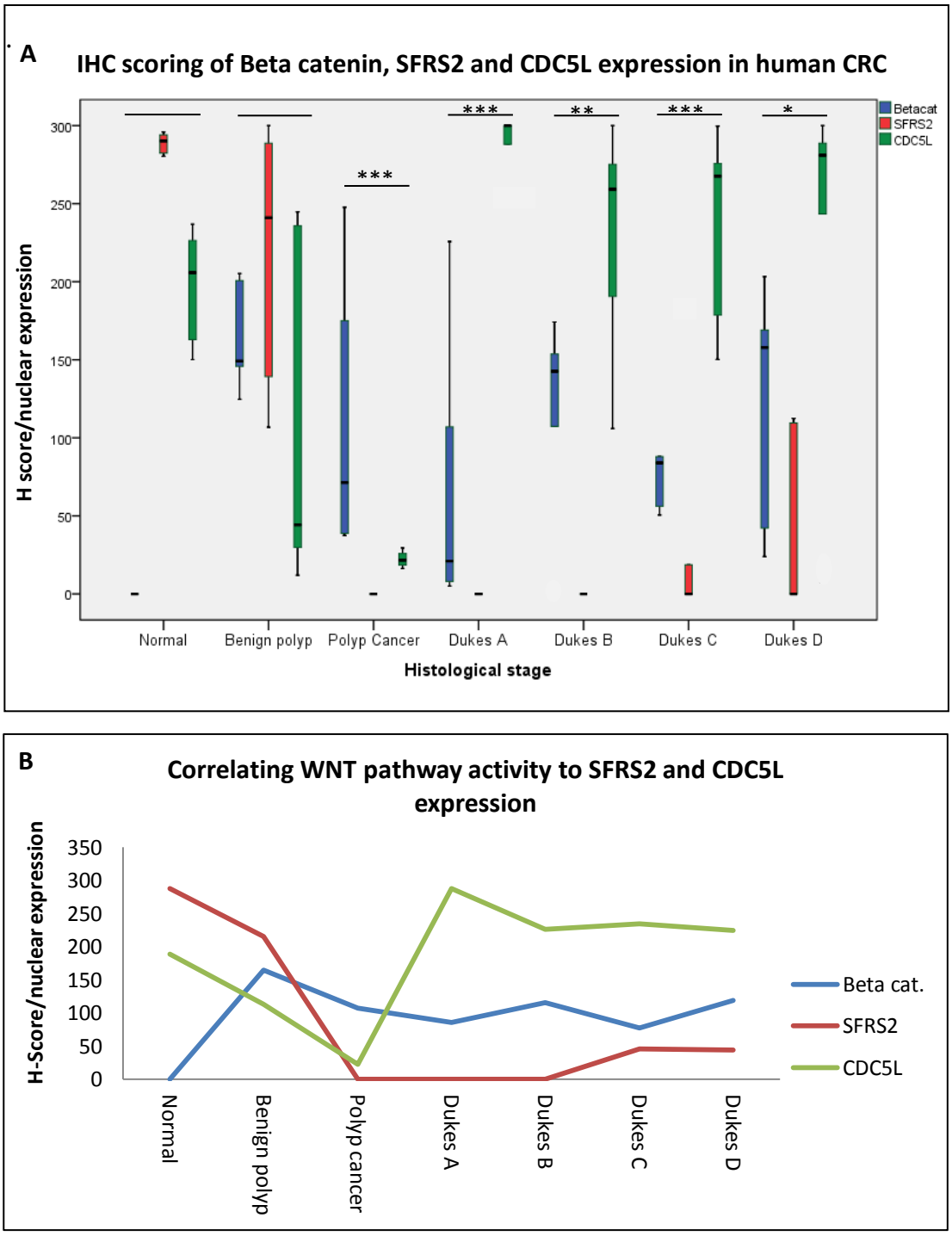


**Figure 6.21 H-score data from IHC analysis of nuclear expression of Beta catenin, SFRS2 and CDC5L in human CRC. A) Each box represents mean H-scores from five patients. Each mean represents ten H-scores from each individual tumour. B) Shows levels of SFRS2 and CDC5L correlated with WNT pathway activity. N=5 patients per stage. Within each histological stage, non-parametric (Kruskal-Wallis) one way ANOVA was used to assess the statistical significance of the difference. P values *, ** and *** are less than 0.05, 0.01 and 0.001 respectively. Beta cat = Beta catenin.**

H-Score data (figures 6.20 and 6.21) supported what has already been shown in figures 6.16-6.19. The inverse relationship between SFRS2 and CDC5L expression is obvious in all Dukes' stages. Moreover, in agreement with the notion that Wnt pathway activity is down regulated during the more advanced stages of CRC, WNT pathway activity remained weak throughout the tumourigenesis process after the benign polyp stage.

Detailed statistical analysis of the H-score data was also performed. The mean or median values for the expression of each protein in five patients from each histopathological stage were compared to those from the normal patients. SPSS version 20 was used to assess the statistical significance of any existing difference. Dunnett's test was used to compare each group to the control group (normal colon).

Beta catenin was significantly different in benign adenoma, Dukes'B and Dukes'D stages of CRC when compared to its expression in normal colon. SFRS2 expression was significantly different in all stages but the benign adenoma stage from that in normal colon. CDC5L expression was only significantly different in the polyp cancer stage when compared to its expression in normal colon.

## 6.4 Discussion

Following the validation of changes in the expression of selected proteins in the setting of *Apc* deletion in animals, it was important to also investigate the expression of these proteins in human subjects. Therefore, in this chapter, immunohistochemistry was used to evaluate the expression of these proteins in colonic tissues from patients who had different stages of CRC as well as normal colon. Five patients were used from each histopathological stage.

The activity of the Wnt signalling pathway was evaluated using Beta catenin staining (figure 6.3 and 6.4). It was obvious from the representative images that there is over expression of Beta catenin throughout the tumourigensis process. In early adenomas, there were scattered areas of increased nuclear expression of Beta catenin. In the more advanced stages, there was a predominant cytoplasmic over expression of this protein. This was verified by scoring both the intensity of cytoplasmic and nuclear staining. Scoring results agreed with what is shown in figure 6.3, as the most prominent nuclear expression of Beta catenin was noted at the early adenoma stage. Also, there was a marked increase in cytoplasmic expression of Beta catenin initially, and then some reduction was noted in the amount of both cytoplasmic and overall staining in the more advanced stages (Dukes' C and D).

A more homogenous expression of Beta catenin was observed in the animal models. Variation in the fixation conditions used for the human tissues may have had an important effect on the heterogeneity of IHC results. Moreover, the variability in genetic and environmental conditions may also have affected the results seen in humans. Unlike humans, laboratory animals share the same genetic backgrounds and live in controlled environments, making it possible for different mice to have similar lesions with similar expression profiles. Moreover, lesions in animals develop within a known time frame, whereas in humans lesions are detected at different ages.

Furthermore, there is an increasing body of evidence which suggests that *Apc* deletion is not the only factor responsible for the nuclear translocation of Beta catenin. Because APC mutations are found in most if not all cases of CRC, the heterogeneity in the distribution pattern of nuclear Beta catenin in most CRCs supports this approach. Therefore, other genetic or epigenetic factors might be involved in this process [304, 305]. One interesting paper analysed the patterns of

nuclear Beta catenin expression in 88 colonic adenomas ranging from early to more advanced cases with the beginning of invasive growth. The authors reported a heterogeneous pattern of nuclear Beta catenin expression with the most significant correlation of nuclear Beta catenin expression being with the size but not the grade of dysplasia observed in an adenoma [306]. Also, the same paper reported a perfect correlation between nuclear Beta catenin and c-Myc expression, but no correlation between adenoma size and proliferative activity and no significant correlation between nuclear Beta catenin expression and proliferative activity [306]. This same group found that highly proliferating areas in large adenomas and rapidly proliferating small adenomas did not exhibit high nuclear Beta catenin expression. They suggested a possible mechanism for this; undetectable low levels of nuclear Beta catenin contribute to proliferation while high levels of nuclear Beta catenin contribute to resistance against progression of larger lesions towards more invasive phenotypes by depressing certain pro-proliferative genes [306]. Alternatively both nuclear Beta catenin and c-Myc may not be directly involved in regulating cell proliferation during the early stages of tumourigenesis. The authors suggested that induction of proliferation at these stages is an APC effect, independent of Beta catenin [306].

A study by Samowitz *et al.* demonstrated that mutations in Beta catenin with normal APC status are found more commonly in smaller adenomas rather than in late adenomas and cancers [307]. Interestingly they reported 5 mm as a threshold size above which Beta catenin mutations rapidly decrease. This polyp size has also been defined as a threshold for detecting observable levels of nuclear Beta catenin expression. This could mean that both Beta catenin and APC individually can induce some degree of hyperproliferation, but further tumour progression with a concomitant increase in nuclear Beta catenin expression needs APC mutations as a basic defect [306]. This implies that APC mutations can do more than reducing the degradation of Beta catenin [306].

Consistent with the pattern of Beta catenin expression in our samples (figure 6.4), a study by Takayama *et al.*, involving a number of human cancers such as oesophageal, gastric and colorectal, found that down regulation of Beta catenin was associated with malignant transformation [275]. Down regulation of Beta catenin was observed in 11 out of 22 CRC samples and this was associated with poorer

differentiation. Moreover, it has also been suggested that the WNT pathway dominates in the early stages of sporadic CRC development [276].

In the same context, but with different results, a study using human cell lines and a zebra fish model of CRC, showed that APC loss was not sufficient to induce nuclear translocation of Beta catenin. It was only possible for nuclear Beta catenin to accumulate and for an adenoma to progress after secondary K-Ras mutations occurred in a RAF1/RAC1 dependent manner [308]. Similarly, it has been found that human colonic adenomas and cancers are associated with significantly higher cytoplasmic but not nuclear Beta catenin expression than normal colon [309]. Moreover, nuclear Beta catenin expression was observed only in advanced carcinoma tissue and not in any adenomas associated with familial adenomatous polyposis coli (FAP) or sporadic adenomas. In a similar study by Anderson *et al.*, nuclear Beta catenin expression was not found in 90% of polyps taken from FAP patients, but was present in 50% of cancers examined [310].

Due to the observation mentioned above, it is appropriate to conclude with the following quotation "It is now widely accepted that the inappropriate localization of β-catenin to the nucleus is a key oncogenic process. The basic understanding of Wnt signalling whereby β-catenin translocates to the nucleus simply as a result of cytosolic accumulation may be an over simplification in many contexts. In reality the systems regulating nuclear β-catenin entry are likely to be multi-factorial and highly context-dependent. However, this should not perturb efforts to uncover these mechanisms since they are likely to be of significant therapeutic interest in malignancy" [311].

NAP1L1 staining in human samples showed results (figures 6.6 and 6.7) that were consistent with our results the animal studies. Early after the start of colorectal neoplasia, NAP1L1 was displaced into the cytoplasm. It became almost completely cytoplasmic in all four invasive cancer stages. However, results (figure 6.7) did not suggest any obvious increase in the overall amount of cellular NAP1L1 protein.

Our results demonstrated that NAP1L1 was a nuclear protein in the normal human colon. A role in proliferation has been reported for NAP1L1 by some research groups. Also in our work (chapter four) siRNA knockdown of NAP1L1 in human CRC cell lines resulted in a modest inhibitory effect on cellular proliferation.

Therefore, one can speculate that this displacement may be part of a protective mechanism within cells against further uncontrolled proliferation.

We were not able to find any published report of NAP1L1 expression in human CRC. Therefore, we hope that this piece of work may be a starting point for more in depth studies involving this protein. Also, because reports are contradictory about NAP1L1 sub-cellular localisation, it is difficult to judge the consequences of the cytoplasmic displacement of NAP1L1.

RPL6 has been shown by a previous colleague in our department (Dr. Fei Song) to follow a pattern of expression similar to that of NAP1L1 in unpublished work that involved ELISA evaluation of serum samples from patients at the different stages of CRC. Therefore, it was not surprising to also find similarity between these two proteins in this piece of work. Although RPL6 retained some nuclear staining throughout the colorectal tumourigenesis process (figure 6.9), its expression was characterised by predominantly cytoplasmic expression as soon as neoplasia started.

We (chapter four, siRNA studies) and others have shown a role for RPL6 in regulating the proliferation of cancer cells. Therefore, similar to NAP1L1, RPL6 nuclear exclusion during the tumourigeneis process may be a protective mechanism to control growth and prevent the further progression of colorectal neoplasia.

Cyclin E has been extensively studied for its role in tumourigenesis and increased expression has been correlated with adverse outcomes in breast cancer and a number of other tumours. However, its role needs further investigation, especially in CRC. Cyclin E has been suggested to have similar effects on cell cycle as RPL6 (G1/S transition) and one study has shown the co-expression of these two proteins in human gastric cancer samples [163]. Moreover, this paper suggested that Cyclin E mediated the effects of RPL6 on the cell cycle. Therefore, we included Cyclin E in our experiments on human CRC. In agreement with these observations and our prior observations in animal studies (chapter four), Cyclin E and RPL6 showed co-expression in the cytoplasm of malignant colonic epithelial cells.

Consistent with the reports shown in the introduction chapter (section 1.6.9) which suggested that PHB was associated with the more advanced stages of CRC, PHB demonstrated cytoplasmic over expression after the early polyp stage of colorectal

tumour development. The highest expression was noted in Dukes' B stage samples. This was also consistent with the data from the unpublished work of Dr Fei Song described above. She demonstrated increased PHB concentrations mainly in the sera of patients with Dukes' A and B CRC.

NCL was also one of the proteins that showed differential staining in the animal studies reported in chapter three. It showed early nuclear over expression in the *AhCre*$^{+}$*Apc*$^{fl/fl}$ mice and in colonic polyps from *Apc*$^{Min/+}$ mice. In human subjects, there was no obvious over expression of NCL during the early stages of colorectal tumour development (figures 6.14 and 6.15). In contrast, there was an obvious down regulation of NCL staining intensity in the more advanced stages (Dukes' C and D) (figures 6.14 and 6.15). This finding could be quite interesting, since NCL has been reported to negatively regulate c-Myc promoter driven transcription via binding to c-Myc G-quadreplex structures [169]. Therefore, down regulation of NCL may be associated with c-Myc driven proliferation. However, the role of NCL during tumourigenesis can vary according to its sub-cellular location. For example, cell surface NCL has been shown to promote tumour growth, angiogenesis and proliferation [312].

To follow up our analysis of the proposed relationship between SFRS2 and CDC5L during colorectal carcinogenesis, these two proteins were also included in our experiments involving human CRC samples. Although, SFRS2 showed obvious over expression in the Wnt active areas in the animal models described in chapter three of this thesis, this was not the case in human CRC. Unlike the animal models, there was no clear over expression of SFRS2 in early adenomatous polyps, but interestingly cytoplasmic displacement of SFRS2 was noted thereafter (figure 6.16). This was coincident with a reduction in WNT pathway activity in these lesions. Again in agreement with our results in animal models, CDC5L showed cytoplasmic displacement in early and advanced colonic adenomas (figures 6.16-6.19). It then demonstrated nuclear re-localisation in invasive cancers (Dukes' A-D stages) with some remaining cytoplasmic staining (same above figures). These findings were further supported by the results of detailed H-scoring that was performed to correlate the activity of SFRS2 and CDC5L with each other and with WNT pathway activity during colorectal carcinogenesis (figure 6.21). Although, the reduction in the level of Beta catenin was not large, it still could have dramatic effects on tumour behaviour.

This is supported by the findings of other research groups who suggested pro-proliferative effects for low levels of Beta catenin and anti-proliferative effects for high levels of this protein [275]. Therefore, it is tempting to speculate that this reduction in the level of Beta catenin was responsible for the cytoplasmic displacement of SFRS2 and nuclear re-localisation of CDC5L in the later stages of CRC.

### 6.5 Conclusion

In human CRC, WNT pathway activity is heterogeneous, with a modest down regulation occurring in the more advanced stages. The proteins investigated in this chapter showed results consistent with those described in the animal studies described in chapter three. NAP1L1 and RPL6 demonstrated cytoplasmic expression early after the start of the neoplastic process. Cyclin E showed co-expression with RPL6 with no obvious changes in expression level being observed. PHB showed over expression after transformation and it was most obvious in advanced adenomas, Dukes' A and Dukes' B cancers. There was a down regulation in the level of NCL in the more advanced stages of CRC (Dukes' C and D). Therefore, these candidate proteins may be potential biomarkers both individually and as a panel for the different stages of CRC.

Our findings about SFRS2 and CDC5L expression in human CRC further augmented our proposal that these two proteins have opposite functions during colorectal tumourigensis and that they are regulated at least in part by WNT pathway activity.

# Chapter seven

# Discussion

# 7. Discussion

Although the early and critical role of *Apc* mutation in most if not all CRCs has been well documented, the molecular mechanistic consequences of loss of Apc function are not well understood [44, 313]. Moreover, issues with delays in diagnosis and targeted therapy are major contributors to the relatively high mortality and morbidity associated with CRC. Therefore, studying the events that follow *Apc* deletion may reveal new aspects about early colorectal tumourigenesis and help to modify disease outcome. By studying the concomitant changes in the intestinal proteome of a mouse model of acute intestinal *Apc* deletion (*AhCre*$^{+}$*Apc*$^{fl/fl}$ mouse), our group has identified several upregulated proteins. Based on the above findings and other data generated in our group, we hypothesised that these proteins are upregulated at early time points following *Apc* deletion and that they are therefore potential key proteins that may serve as novel biomarkers or therapeutic targets in the management of CRC. We have tested this hypothesis using animal and cell line models of CRC and clinical samples obtained from patients with this disease.

In the animal studies involving samples from *AhCre*$^{+}$*Apc*$^{fl/fl}$ and *Apc*$^{Min/+}$ mice as models of early colorectal tumourigenesis, we were able to confirm the over expression of six out of nine proteins studied. These proteins were NAP1L1, RPL6, SFRS2, PHB, FABP6 and NCL. These proteins have not previously been shown to be Wnt target genes, but they have been implicated in regulating a wide range of important cellular functions such as cellular proliferation, progression through the cell cycle, apoptosis, alternative splicing and protein translation. Derangement of one or more of these processes has well been linked to various tumourigenesis processes [226].

Also in these animal studies, we tried to explore mechanistic aspects about our proteins. Therefore, using mainly IHC and based on other published data, we studied Cyclin E and CDC5L as partners for RPL6 and SFRS2 respectively during colorectal tumourigenesis. In this part of the study we also included a mouse model of invasive CRC, the *AhCreER*$^{T+}$*Apc*$^{fl/+}$*Pten*$^{fl/fl}$ mouse.

*In vitro* studies (using HCT116 and HT29 cells) were also undertaken to identify whether selected proteins had causative or correlative roles during colorectal tumourigenesis. Based on other independent data generated in our group, NAP1L1,

RPL6 and SFRS2 were selected for this part of the study. Moreover, we used this system to further explore the hypothesised interaction between SFRS2 and CDC5L.

Although animals are good pre-clinical disease models however, significant variation can exist in disease behaviour between animals and humans. Therefore, before investigating these proteins in large clinical trials it was wise to validate at least our principal findings from the animal models in clinical samples obtained from patients with CRC. For this purpose we used IHC to study the expression of those proteins which showed overexpression in our earlier animal studies. Due to the inter- and intra-tumour heterogeneity of IHC results, modified scoring systems were used to further augment our findings in these clinical studies.

### 7.1 Analysis of NAP1L1 expression in clinical samples and animal/cell line models of CRC

Similar to several other selected candidate biomarker proteins that we studied in this thesis, NAP1L1 has not previously been extensively studied in colorectal tumourigenesis. In our work, NAP1L1 localisation under normal conditions varied between animal and human samples. In the animal models NAP1L1 mainly showed cytoplasmic expression, whereas in the non-cancerous parts of the human CRC samples it showed predominantly nuclear expression. This variability is also found in papers describing NAP1L1 subcellular position in normal tissues [148, 149]. In the pathologic areas, NAP1L1 showed predominant and sometimes exclusively cytoplasmic expression immediately after *Apc* deletion in the $AhCre^{+}Apc^{fl/fl}$ mice, in the benign adenomas in $Apc^{Min/+}$ mice and in human subjects. In the animal model of invasive disease, the NAP1L1 antibody did not produce valid results, but in human CRC NAP1L1 expression remained cytoplasmic throughout the neoplastic process (including the invasive stages). Since NAP1L1 has been shown to play a role in regulating cell proliferation and as NAP1L1 is believed to shuttle essential molecules into the nucleus from the cytoplasm [149, 211], a cytoplasmic localisation of NAP1L1 suggests that it may act as a driver in the tumourigenesis process. This was further supported by the inhibition of proliferation that we observed upon knocking down NAP1L1 expression in human colon adenocarcinoma cell lines. Our findings support a previous report which has suggested that NAP1L1 may be a therapeutic target for CRC [211].

## 7.2 Analysis of RPL6 expression in clinical samples and animal/cell line models of CRC

RPL6 has also not previously been well studied in colorectal tumourigenesis. Although it has been described as a constituent of ribosomes, RPL6 is not necessarily only a cytoplasmic protein. It is now accepted that ribosomal proteins also have other extra-ribosomal functions [162, 163]. This may therefore explain why we observed RPL6 expression in both the nucleus and cytoplasm of wild type control mice and in normal human colon samples. Early after *Apc* deletion in both mouse models, there was an obvious increase in the nuclear proportion of this protein. In contrast, in human CRC samples, cytoplasmic RPL6 expression was predominantly observed in benign adenomas as well as the more advanced tumour stages. This observation was similar to that reported by another research group in human gastric cancer samples [163]. RPL6 expression knockdown in cell line models of human CRC resulted in a dramatic inhibition of cellular proliferation, reduced colony formation and increased apoptosis. These findings agree with data from studies on gastric cancer cell lines which have suggested that RPL6 has oncogenic properties and that it regulates cellular proliferation, survival and resistance to drug induced apoptosis [164]. Moreover, RPL6 knockdown in gastric cancer cell lines appeared to cause similar effects to those that we observed in colon cancer cell lines [163].

The concordance in expression between RPL6 and NAP1L1 in human CRC tissue samples shown by IHC was also found by mRNA analysis of these two proteins by a previous colleague (Dr Fei Song) in unpublished work comparing tissues from the various stages of CRC and normal adjacent colon.

It has been suggested that Cyclin E mediates the effects of RPL6 on G1/S transition and cellular proliferation, thus contributing to the oncogenic properties of this protein. It has also been shown that RPL6 and Cyclin E are co-expressed in human gastric cancer [163, 231]. In $AhCre^{+}Apc^{fl/fl}$ mice, Cyclin E demonstrated increased staining in the granules of Paneth cells, whereas in colonic adenomas from $Apc^{Min/+}$ mice, it showed cytoplasmic displacement in comparison to the colon of wild type mice. This disagreed with the above suggestion, as RPL6 mainly showed nuclear overexpression in these two animal models. However, in the clinical samples both proteins were mainly localised in the cytoplasm during the various stages of CRC. This difference between human subjects and experimental animals may be due to the

longer time human tumours take to develop allowing for more stable phenotypes. It has also been shown that siRNA mediated RPL6 knockdown in gastric cancer cell lines resulted in down regulation of Cyclin E [163]. Unfortunately, the Western blot experiments that we carried out to assess Cyclin E abundance following RPL6 knockdown were unsuccessful due to technical issues related to the anti-Cyclin E antibody that we used.

### 7.3 Analysis of SFRS2 and CDC5L expression and their interaction in clinical samples and animal/cell line models of CRC

SFRS2 and CDC5L are nuclear proteins that have been shown to be involved in a similar range of cellular functions such as regulating alternative splicing and cell cycle progression [170, 270]. Neither protein has previously been extensively studied in colorectal cancer. Moreover, there have been suggestions of a possible interaction between these two molecules. One direct observation was made by a group in 2002, who reported that nuclear overexpression of CDC5L caused cytoplasmic displacement of SFRS2 [270]. Therefore, we hypothesised that SFRS2 and CDC5L may interact during colorectal tumourigenesis. In our animal studies, SFRS2 showed nuclear overexpression both in $AhCre^{+}Apc^{fl/fl}$ mice and in the neoplastic lesions that arose in $Apc^{Min/+}$ mice, whereas CDC5L was displaced into the cytoplasm. When we examined these two proteins in an animal model of invasive colorectal tumours, the $AhCreER^{T+}Apc^{fl/+}Pten^{fl/fl}$ mouse, CDC5L showed relocalisation into the nucleus. Although SFRS2 IHC was not successful in this mouse model, SFRS2 did show cytoplasmic displacement in all the invasive stages of human CRC that were assessed in this study. Also, in agreement with these findings, CDC5L showed predominantly nuclear localisation in the more advanced stages of human CRC. Further in agreement with our hypothesis, we observed nuclear overexpression of CDC5L following SFRS2 knockdown in HCT116 cells and vice versa.

When we studied the effects of these two proteins *in vitro* by knocking down their expressions in human colonic adenocarcinoma cell lines, CDC5L down regulation caused a dramatic inhibition of cellular proliferation and survival in addition to an obvious increase in the amount of apoptosis observed. This agrees with observations made by other research groups which have described CDC5L as a pro-proliferative protein [274, 284, 289]. In contrast, SFRS2 knockdown caused weak non-significant effects on cellular proliferation and only resulted in a small reduction in the amount

of apoptosis observed. Based on the latter observation it was tempting to hypothesise that SFRS2 plays a role in mediating apoptosis. This could lead to the speculation that SFRS2 may be partly responsible for the increased apoptosis that has been observed in *AhCre*$^{+}$*Apc*$^{fl/fl}$ mice [44] as these animals also demonstrated overexpression of nuclear SFRS2. SFRS2 has previously been directly linked to apoptosis in a number of published studies. For example, it has been shown that SFRS2 overexpression mediated cisplatin treatment and DNA damage-induced apoptosis via modulating the alternative splicing of caspase 8, caspase 9, c-flip and Bcl-x [234, 237]. Taking these observations together, as well as the observed increase in nuclear SFRS2 abundance following CDC5L knockdown in HCT116 cells, we further speculated that SFRS2 may contribute to the increase in apoptosis that we observed following the knockdown of CDC5L. Moreover, SFRS2 overactivity following CDC5L knockdown may explain the loss of G2 peak of the cell cycle (figure 5.17), as it has been reported that SFRS2 causes G2M arrest and activation of regulators of apoptosis [237].

Despite the overall increased sensitivity of *p53* knockout cells to the mild toxicity of the transfection process itself, as indicated by increased cell death in cells transfected with scrambled siRNA, CDC5L knockdown caused more apoptosis in HCT116 cells with WT p53 in comparison to HCT116 cells with knockout p53. This may also explain the observed increase in caspase 8 activity in these cells, as it has been shown that caspase 8 is an essential mediator of p53 dependent apoptosis [296]. In contrast, SFRS2 knockdown caused a more pronounced increase in the amount of apoptosis in p53 null HCT116 cells. This may be attributed to the effect of SFRS2 knockdown on the G2M checkpoint, resulting in the activation of downstream regulators of apoptosis such as Bcl-x independent of canonical apoptosis pathways [236]. These observations suggest that SFRS2 over expression (following CDC5L knockdown) can mediate p53 dependent apoptosis, whereas SFRS2 knockdown may induce non-canonical apoptosis pathways or molecules downstream of p53.

## 7.4 Analysis of PHB and NCL expression in human samples and animal/cell line models of CRC

PHB and NCL were also studied in this thesis as potential biomarkers of CRC. PHB showed mild cytoplasmic overexpression in the animal models of early colorectal tumourigenesis, *AhCre*$^{+}$*Apc*$^{fl/fl}$ and *Apc*$^{Min/+}$ mice. In human CRC samples, PHB showed more obvious cytoplasmic overexpression in the more advanced stages of the disease, namely polyp cancers, Dukes'A and Dukes' B cancers. Interestingly, these observations of an association between PHB and advanced CRC agree with other published reports. For example, Chen *et al*. reported that PHB was over expressed in human CRC with the most obvious increase in expression being in poorly differentiated cancers [213]. In addition, PHB's promoter has been shown to be susceptible to the actions of c-Myc [239], which has in turn been shown to be important in the later stages of CRC [60].

NCL demonstrated an obvious increase in nucleolar staining early after *Apc* deletion in *AhCre*$^{+}$*Apc*$^{fl/fl}$ *and Apc*$^{Min/+}$ mice. In human samples representing the early stages of CRC however, no obvious increase in the staining intensity of NCL was noted in comparison to normal colon. However, the total amount of this protein might be increased due to the larger nuclei and more densely packed cells within tumours. Interestingly, there was a reduction in the intensity of NCL staining in the two most advanced tumour stages, Dukes' C and D cancers. Since NCL has been shown to regulate critical cellular functions such as ribosomal biogenesis, DNA and RNA metabolism and cellular response to stress [167], it is not surprising that NCL upregulation was observed in the crypts of *AhCre*$^{+}$*Apc*$^{fl/fl}$ mice and in the colonic adenomas of *Apc*$^{Min/+}$ mice. This could be due to the hyper-proliferative state that follows *Apc* deletion in these areas. The down regulation of NCL expression that we observed in advanced human colorectal cancers may be related to c-Myc activity, as this has been shown to be negatively regulated by NCL [169].

### 7.5 Limitations of the studies carried out and possible steps for improvement

Developing and validating new protein biomarkers of a malignancy is not easy. Despite the fact that countless studies have been carried out for this purpose, a limited number of biomarker proteins have made their way into routine clinical practice. This is attributed to the complex nature of malignant processes and this complexity is due to multi-level regulation of biological functions which often widens the search area beyond feasibility. For the same reason, efforts are now focusing on finding genetic fingerprints and mechanisms to define more specific features of a malignancy that can be used to modify one or more aspects of its management [314].

The *AhCre*$^{+}$*Apc*$^{fl/fl}$ mouse is a novel *in vivo* model of an induced Wnt signalling pathway in the intestine. It allows study of the immediate events and underlying molecular changes that follow acute intestinal *Apc* deletion. However, in human CRC there is a long period of heterozygosity before the stage of loss of heterozygosis. This may involve many biological changes in the microenvironment of the tumour, which might contribute to any difference observed between *AhCre*$^{+}$*Apc*$^{fl/fl}$ mice and *Apc*$^{Min/+}$ mice or humans.

*Apc*$^{Min/+}$ mice are not exempt either, since their death before malignant transformation causes an interruption in the process of mapping changes in the expression of candidate biomarker proteins based on the histological progression of lesions. Therefore, it would be good to analyse the expression of our proteins in lesions at different time points from a mouse model that shows tumour progression to invasive disease, thereby studying benign and malignant lesions from the same mouse model. A good candidate for this would be the *AhCreER*$^{T+}$*Apc*$^{fl/+}$*Pten*$^{fl/fl}$ mouse. Although we did perform a few preliminary experiments, lack of samples precluded more detailed investigation of this model and further work is needed.

HCT116 and HT29 cell lines harbour mutations in elements of the Wnt pathway rendering it active, however HT29 cells also still have other mechanisms for regulating Beta catenin activity such as PTEN protein. In contrast HCT116 cells have defective Beta catenin which is resistant to degradation. This difference might have been a contributor to the variation in transfection results observed between the two cell lines. Therefore, for validation purposes, it might have been better to use cell

lines with more similar genetic profiles such that they all have the same primary genetic defect, *Apc* mutation in our case. This agrees with a recent call for emphasis on the importance of cell line genotype authentication and characterisation before selecting *in vitro* models for descriptive and functional research [315].

HCT116 and HT29 cells were originally derived from poorly differentiated and moderately differentiated human colonic adenocarcinomas respectively. This means that using these cells to investigate a protein such as SFRS2 which we think it is important early in the tumourigenesis process, may be misleading. Therefore, it might be better in future to study this protein in a cell line which was derived from an earlier neoplastic lesion such as an adenoma cell line. Such cell lines are however more difficult to grow and manipulate.

Transient RNA interference using siRNA mediated knockdown of gene expression has also some limitations such as off target effects which the manufacturer has tried to keep minimal via multiple modifications of the siRNAs including the use of a pool of siRNAs to increase efficacy at lower doses. Also, the type of cells, rate of cell proliferation and importance of the target protein in regulating cell proliferation will all affect the outcome of gene knockdown. This may include rate of transfection and sustainability of knockdown. Therefore, stable transfection, albeit more expensive and time consuming may ultimately provide a better reflection of the role of a target gene.

When it comes to studying the proposed interaction between SFRS2 and CDC5L, upregulating one protein at a time may also provide more direct clues about their effects on the alternative splicing process.

In the studies which we performed using clinical samples, differences in genetics, environment and age of lesions may all have contributed to the variation that we observed in staining patterns between human and animal samples. Moreover, non-standardised fixation conditions during the collection of human samples may also have affected the results that we obtained. Ensuring similar fixation conditions might dramatically improve the reproducibility of future results using this experimental approach.

## 7.6 Future work plans and medical implications of the studies that have been carried out

The importance of the studies described in this thesis lies in the fact that we have investigated novel proteins that have been postulated to be involved in colorectal tumourigensis. Our studies were designed to prepare for more specific and larger studies that will be needed to take these proteins into clinical practice.

There are many research opportunities that could be developed from this project. The potential biomarker proteins could be examined in a large prospective clinical trial and then results could be correlated with clinical data from these patients. With the aid of appropriate analysis and statistical tools, this may also unveil markers that may predict response to therapy and/or overall prognosis. The patients in the national CRC screening programme represent an excellent opportunity for these types of assessments, because of the good documentation of their clinical course. Moreover, studying the blood/serum level of one or more of the candidate biomarker proteins which showed early upregulation following *Apc* deletion in participants of the national CRC screening programme could validate whether one or more of these proteins is a potential screening tool for this disease.

As far as therapy is concerned, studying the effects of knocking down NAP1L1 and RPL6 in adenoma cell lines may indicate whether targeting either of these proteins has any merit as a chemopreventive measure for CRC. The effect of blocking CDC5L on tumour progression should also be tested in animal models of colon cancer, particularly of invasive disease.

The mechanistic studies that we conducted have generated promising initial data that have supported the hypothesis that the balance between SFRS2 and CDC5L expression is important in regulating apoptosis, possibly via a caspase 8 dependent mechanism and potentially involving alternative splicing. This should be further explored using new antibodies and optimised experimental conditions to quantify the expression of SFRS2 following CDC5L knockdown and *vice versa* using western blotting. Alternatively, qRT-PCR could be used to investigate this. Immunoprecipitation could also be used to find a common target molecule shared by both SFRS2 and CDC5L. The splicing profile of this target molecule could be

studied by up or down regulating one protein at a time to more robustly assess the antagonism that we propose exists between these two proteins.

Using IHC in *in vivo* models, we have demonstrated that SFRS2 is up-regulated in the setting of an induced Wnt pathway. Inducing Wnt pathway activity in cell lines and then assessing the level of SFRS2 (by WB or qRT-PCR) would further validate this observation. Also, more specific tests could be implemented to study the role of SFRS2 in apoptosis; for example assessing the number of apoptotic cells following the induction of apoptosis in colon cancer cell lines in the presence and absence of SFRS2. Also, the level of SFRS2 could be assessed before and after inducing apoptosis using western blotting or qRT-PCR.

In *p53* knockout HCT116 cells, SFRS2 knockdown caused obvious effects on cell proliferation and apoptosis. Therefore, FACS analysis could be used to study the cell cycle distribution, apoptosis rate and caspase 8 activity in these cells following the knockdown of SFRS2. This might reveal more details about the role of SFRS2 in regulating apoptosis and the pathway involved. Also FACS or western blotting could be used to study the activity of p53 and/or its target proteins in this context.

### 7.7 Conclusions

In the studies carried out in this thesis, we were able to confirm the overexpression of six novel candidate biomarker proteins in animal models of early colorectal tumourigensis. We were also able to validate these changes in human clinical samples of early CRC. Moreover, the clinical studies have also shown that some of these proteins are also involved in the invasive stages of the disease.

Our data suggest that these proteins individually or as panels are promising candidate biomarkers that may be useful for screening as well as predicting response to therapy and prognosis of CRC. Based on their pro-proliferative properties, NAP1L1, RPL6 and CDC5L should also be further tested as potential therapeutic targets for CRC.

Our observations support the notion that nuclear Beta catenin expression is reduced during the more advanced stages of colorectal carcinogenesis and that this is associated with adverse outcomes. Several direct and indirect observations made in this work have also supported the hypothesis that SFRS2 and CDC5L interact during the course of colorectal tumourigenesis. Based on data from this thesis and other

published papers, SFRS2 over activity may at least partly mediate the apoptosis that is observed in animal models following *Apc* deletion and that followed CDC5L knockdown *in vitro*. This could be p53 dependent and may involve modulating the alternative splicing of proapoptotic molecules such as caspase 8. As SFRS2 knockdown induced apoptosis that was observed in HCT116 cells with deleted p53, this may bypass p53 by activating downstream apoptotic molecules or involve non-canonical apoptotic pathways.

Whether cyclin E mediates the oncogenic effects of RPL6 during colorectal tumourigensis and whether it has any role in regulating the composition of the stem cell niche in the small intestine remain unclear. More specific studies are required to address this question.

The studies described in this thesis have therefore presented several proteins as promising biomarkers or therapeutic targets for colorectal cancer. Also, they have revealed possible new aspects about the molecular events that follow *Apc* deletion in the colon. The data justify the need for more research in this area.

# References

## 8. References


1. Nichita C, Ciarloni L, Monnier-Benoit S, Hosseinian S, Dorta G, Ruegg C: **A novel gene expression signature in peripheral blood mononuclear cells for early detection of colorectal cancer**. *Aliment Pharmacol Ther* 2014.
2. **Cancer Research UK** [http://www.cancerresearchuk.org/cancer-info/cancerstats/types/bowel/]-19Nov2013.
3. Bresalier RS: **Early detection of and screening for colorectal neoplasia**. *Gut and liver* 2009, **3**(2):69-80.
4. Zhang J, Lv L, Ye Y, Jiang K, Shen Z, Wang S: **Comparison of metastatic lymph node ratio staging system with the 7th AJCC system for colorectal cancer**. *Journal of cancer research and clinical oncology* 2013, **139**(11):1947-1953.
5. Greene FL: **Staging of colon and rectal cancer: from endoscopy to molecular markers**. *Surgical endoscopy* 2006, **20 Suppl 2**:S475-478.
6. Dukes CE, Bussey HJ: **The spread of rectal cancer and its effect on prognosis**. *British journal of cancer* 1958, **12**(3):309-320.
7. Astler VB, Coller FA: **The prognostic significance of direct extension of carcinoma of the colon and rectum**. *Annals of surgery* 1954, **139**(6):846-852.
8. Jimenez CR, Knol JC, Meijer GA, Fijneman RJ: **Proteomics of colorectal cancer: overview of discovery studies and identification of commonly identified cancer-associated proteins and candidate CRC serum markers**. *Journal of proteomics* 2010, **73**(10):1873-1895.
9. Fairley TL, Cardinez CJ, Martin J, Alley L, Friedman C, Edwards B, Jamison P: **Colorectal cancer in U.S. adults younger than 50 years of age, 1998-2001**. *Cancer* 2006, **107**(5 Suppl):1153-1161.
10. Haggar FA, Boushey RP: **Colorectal cancer epidemiology: incidence, mortality, survival, and risk factors**. *Clinics in colon and rectal surgery* 2009, **22**(4):191-197.
11. Carethers JM: **Proteomics, genomics, and molecular biology in the personalized treatment of colorectal cancer**. *Journal of gastrointestinal surgery : official journal of the Society for Surgery of the Alimentary Tract* 2012, **16**(9):1648-1650.

12. de Jong AE, Morreau H, Nagengast FM, Mathus-Vliegen EM, Kleibeuker JH, Griffioen G, Cats A, Vasen HF: **Prevalence of adenomas among young individuals at average risk for colorectal cancer**. *The American journal of gastroenterology* 2005, **100**(1):139-143.
13. Lynch HT, Lynch JF: **Genetics of colonic cancer**. *Digestion* 1998, **59**(5):481-492.
14. Cruz-Bustillo Clarens D: **Molecular genetics of colorectal cancer**. *Revista espanola de enfermedades digestivas : organo oficial de la Sociedad Espanola de Patologia Digestiva* 2004, **96**(1):48-59.
15. Powell SM, Petersen GM, Krush AJ, Booker S, Jen J, Giardiello FM, Hamilton SR, Vogelstein B, Kinzler KW: **Molecular diagnosis of familial adenomatous polyposis**. *The New England journal of medicine* 1993, **329**(27):1982-1987.
16. Guillem JG, Smith AJ, Calle JP, Ruo L: **Gastrointestinal polyposis syndromes**. *Current problems in surgery* 1999, **36**(4):217-323.
17. Sieber OM, Lipton L, Crabtree M, Heinimann K, Fidalgo P, Phillips RK, Bisgaard ML, Orntoft TF, Aaltonen LA, Hodgson SV *et al*: **Multiple colorectal adenomas, classic adenomatous polyposis, and germ-line mutations in MYH**. *The New England journal of medicine* 2003, **348**(9):791-799.
18. Burt RW: **Colon cancer screening**. *Gastroenterology* 2000, **119**(3):837-853.
19. Colussi D, Brandi G, Bazzoli F, Ricciardiello L: **Molecular pathways involved in colorectal cancer: implications for disease behavior and prevention**. *International journal of molecular sciences* 2013, **14**(8):16365-16385.
20. Grande M, Milito G, Attina GM, Cadeddu F, Muzi MG, Nigro C, Rulli F, Farinon AM: **Evaluation of clinical, laboratory and morphologic prognostic factors in colon cancer**. *World journal of surgical oncology* 2008, **6**:98.
21. Fearon ER, Vogelstein B: **A genetic model for colorectal tumorigenesis**. *Cell* 1990, **61**(5):759-767.
22. Worthley DL: **Colorectal carcinogenesis: Road maps to cancer.** *World journal of Gastroenterology* 2007:3784-3791.

23. Potter JD: **Colorectal cancer: molecules and populations**. *Journal of the National Cancer Institute* 1999, **91**(11):916-932.
24. Leary RJ, Lin JC, Cummins J, Boca S, Wood LD, Parsons DW, Jones S, Sjoblom T, Park BH, Parsons R *et al*: **Integrated analysis of homozygous deletions, focal amplifications, and sequence alterations in breast and colorectal cancers**. *Proceedings of the National Academy of Sciences of the United States of America* 2008, **105**(42):16224-16229.
25. Jass JR, Whitehall VL, Young J, Leggett BA: **Emerging concepts in colorectal neoplasia**. *Gastroenterology* 2002, **123**(3):862-876.
26. Jass JR: **Serrated adenoma of the colorectum and the DNA-methylator phenotype**. *Nature clinical practice Oncology* 2005, **2**(8):398-405.
27. Grady WM: **Genomic instability and colon cancer**. *Cancer metastasis reviews* 2004, **23**(1-2):11-27.
28. Takayama T, Ohi M, Hayashi T, Miyanishi K, Nobuoka A, Nakajima T, Satoh T, Takimoto R, Kato J, Sakamaki S *et al*: **Analysis of K-ras, APC, and beta-catenin in aberrant crypt foci in sporadic adenoma, cancer, and familial adenomatous polyposis**. *Gastroenterology* 2001, **121**(3):599-611.
29. Vogelstein B, Fearon ER, Kern SE, Hamilton SR, Preisinger AC, Nakamura Y, White R: **Allelotype of colorectal carcinomas**. *Science* 1989, **244**(4901):207-211.
30. Ogino S, Goel A: **Molecular classification and correlates in colorectal cancer**. *The Journal of molecular diagnostics : JMD* 2008, **10**(1):13-27.
31. Smith G, Carey FA, Beattie J, Wilkie MJ, Lightfoot TJ, Coxhead J, Garner RC, Steele RJ, Wolf CR: **Mutations in APC, Kirsten-ras, and p53--alternative genetic pathways to colorectal cancer**. *Proceedings of the National Academy of Sciences of the United States of America* 2002, **99**(14):9433-9438.
32. Carethers JM: **The cellular and molecular pathogenesis of colorectal cancer**. *Gastroenterology clinics of North America* 1996, **25**(4):737-754.
33. Hahn M, Saeger HD, Schackert HK: **Hereditary colorectal cancer: clinical consequences of predictive molecular testing**. *International journal of colorectal disease* 1999, **14**(4-5):184-193.
34. Kinzler KW, Vogelstein B: **Cancer-susceptibility genes. Gatekeepers and caretakers**. *Nature* 1997, **386**(6627):761, 763.

35. Groden J, Thliveris A, Samowitz W, Carlson M, Gelbert L, Albertsen H, Joslyn G, Stevens J, Spirio L, Robertson M *et al*: **Identification and characterization of the familial adenomatous polyposis coli gene**. *Cell* 1991, **66**(3):589-600.
36. Horii A, Nakatsuru S, Ichii S, Nagase H, Nakamura Y: **Multiple forms of the APC gene transcripts and their tissue-specific expression**. *Human molecular genetics* 1993, **2**(3):283-287.
37. Beroud C, Soussi T: **APC gene: database of germline and somatic mutations in human tumors and cell lines**. *Nucleic acids research* 1996, **24**(1):121-124.
38. Fodde R, Smits R, Clevers H: **APC, signal transduction and genetic instability in colorectal cancer**. *Nature reviews Cancer* 2001, **1**(1):55-67.
39. Fearnhead NS, Britton MP, Bodmer WF: **The ABC of APC**. *Human molecular genetics* 2001, **10**(7):721-733.
40. Huelsken J, Birchmeier W: **New aspects of Wnt signaling pathways in higher vertebrates**. *Current opinion in genetics & development* 2001, **11**(5):547-553.
41. Fodde R: **The multiple functions of tumour suppressors: it's all in APC**. *Nature cell biology* 2003, **5**(3):190-192.
42. Draviam VM, Shapiro I, Aldridge B, Sorger PK: **Misorientation and reduced stretching of aligned sister kinetochores promote chromosome missegregation in EB1- or APC-depleted cells**. *The EMBO journal* 2006, **25**(12):2814-2827.
43. Shih IM, Zhou W, Goodman SN, Lengauer C, Kinzler KW, Vogelstein B: **Evidence that genetic instability occurs at an early stage of colorectal tumorigenesis**. *Cancer research* 2001, **61**(3):818-822.
44. Sansom OJ, Reed KR, Hayes AJ, Ireland H, Brinkmann H, Newton IP, Batlle E, Simon-Assmann P, Clevers H, Nathke IS *et al*: **Loss of Apc in vivo immediately perturbs Wnt signaling, differentiation, and migration**. *Genes & development* 2004, **18**(12):1385-1390.
45. Jiang Y, Kimchi ET, Staveley-O'Carroll KF, Cheng H, Ajani JA: **Assessment of K-ras mutation: a step toward personalized medicine for patients with colorectal cancer**. *Cancer* 2009, **115**(16):3609-3617.

46. Vogelstein B, Fearon ER, Hamilton SR, Kern SE, Preisinger AC, Leppert M, Nakamura Y, White R, Smits AM, Bos JL: **Genetic alterations during colorectal-tumor development**. *The New England journal of medicine* 1988, **319**(9):525-532.
47. Mills AA: **p53: link to the past, bridge to the future**. *Genes & development* 2005, **19**(18):2091-2099.
48. Iacopetta B: **TP53 mutation in colorectal cancer**. *Human mutation* 2003, **21**(3):271-276.
49. Kaur G, Masoud A, Raihan N, Radzi M, Khamizar W, Kam LS: **Mismatch repair genes expression defects & association with clinicopathological characteristics in colorectal carcinoma**. *The Indian journal of medical research* 2011, **134**:186-192.
50. Hoeijmakers JH: **Genome maintenance mechanisms for preventing cancer**. *Nature* 2001, **411**(6835):366-374.
51. Dietmaier W, Wallinger S, Bocker T, Kullmann F, Fishel R, Ruschoff J: **Diagnostic microsatellite instability: definition and correlation with mismatch repair protein expression**. *Cancer research* 1997, **57**(21):4749-4756.
52. Taketo M: **Reviews in basic and clinical gastroenterology; mouse models of colon cance**. *Gastroenterolgy* 2009:780-798.
53. Levitt NC, Hickson ID: **Caretaker tumour suppressor genes that defend genome integrity**. *Trends in molecular medicine* 2002, **8**(4):179-186.
54. Bariol C, Suter C, Cheong K, Ku SL, Meagher A, Hawkins N, Ward R: **The relationship between hypomethylation and CpG island methylation in colorectal neoplasia**. *The American journal of pathology* 2003, **162**(4):1361-1371.
55. Jones PA, Baylin SB: **The fundamental role of epigenetic events in cancer**. *Nature reviews Genetics* 2002, **3**(6):415-428.
56. Clevers H: **Wnt/beta-catenin signaling in development and disease**. *Cell* 2006, **127**(3):469-480.
57. Clevers H, Nusse R: **Wnt/beta-catenin signaling and disease**. *Cell* 2012, **149**(6):1192-1205.

58. Barth AI, Nathke IS, Nelson WJ: **Cadherins, catenins and APC protein: interplay between cytoskeletal complexes and signaling pathways**. *Current opinion in cell biology* 1997, **9**(5):683-690.
59. Polakis P: **The oncogenic activation of beta-catenin**. *Current opinion in genetics & development* 1999, **9**(1):15-21.
60. Myant K, Sansom OJ: **Wnt/Myc interactions in intestinal cancer: partners in crime**. *Experimental cell research* 2011, **317**(19):2725-2731.
61. Katoh M, Katoh M: **WNT signaling pathway and stem cell signaling network**. *Clinical cancer research : an official journal of the American Association for Cancer Research* 2007, **13**(14):4042-4045.
62. Burgess AW, Faux MC, Layton MJ, Ramsay RG: **Wnt signaling and colon tumorigenesis--a view from the periphery**. *Experimental cell research* 2011, **317**(19):2748-2758.
63. Albuquerque C, Breukel C, van der Luijt R, Fidalgo P, Lage P, Slors FJ, Leitao CN, Fodde R, Smits R: **The 'just-right' signaling model: APC somatic mutations are selected based on a specific level of activation of the beta-catenin signaling cascade**. *Human molecular genetics* 2002, **11**(13):1549-1560.
64. Mahmoud NN, Boolbol SK, Bilinski RT, Martucci C, Chadburn A, Bertagnolli MM: **Apc gene mutation is associated with a dominant-negative effect upon intestinal cell migration**. *Cancer research* 1997, **57**(22):5045-5050.
65. Sierra J, Yoshida T, Joazeiro CA, Jones KA: **The APC tumor suppressor counteracts beta-catenin activation and H3K4 methylation at Wnt target genes**. *Genes & development* 2006, **20**(5):586-600.
66. Reya T, Clevers H: **Wnt signalling in stem cells and cancer**. *Nature* 2005, **434**(7035):843-850.
67. Kim KA, Kakitani M, Zhao J, Oshima T, Tang T, Binnerts M, Liu Y, Boyle B, Park E, Emtage P *et al*: **Mitogenic influence of human R-spondin1 on the intestinal epithelium**. *Science* 2005, **309**(5738):1256-1259.
68. Niehrs C, Acebron SP: **Mitotic and mitogenic Wnt signalling**. *The EMBO journal* 2012, **31**(12):2705-2713.
69. van Amerongen R, Nusse R: **Towards an integrated view of Wnt signaling in development**. *Development* 2009, **136**(19):3205-3214.

70. Korinek V, Barker N, Moerer P, van Donselaar E, Huls G, Peters PJ, Clevers H: **Depletion of epithelial stem-cell compartments in the small intestine of mice lacking Tcf-4**. *Nature genetics* 1998, **19**(4):379-383.
71. Barker N, van Es JH, Kuipers J, Kujala P, van den Born M, Cozijnsen M, Haegebarth A, Korving J, Begthel H, Peters PJ *et al*: **Identification of stem cells in small intestine and colon by marker gene Lgr5**. *Nature* 2007, **449**(7165):1003-1007.
72. Barker N, Ridgway RA, van Es JH, van de Wetering M, Begthel H, van den Born M, Danenberg E, Clarke AR, Sansom OJ, Clevers H: **Crypt stem cells as the cells-of-origin of intestinal cancer**. *Nature* 2009, **457**(7229):608-611.
73. Okamoto R, Watanabe M: **Molecular and clinical basis for the regeneration of human gastrointestinal epithelia**. *Journal of gastroenterology* 2004, **39**(1):1-6.
74. Marshman E, Booth C, Potten CS: **The intestinal epithelial stem cell**. *BioEssays : news and reviews in molecular, cellular and developmental biology* 2002, **24**(1):91-98.
75. Brittan M, Wright NA: **Stem cell in gastrointestinal structure and neoplastic development**. *Gut* 2004, **53**(6):899-910.
76. Batlle E, Henderson JT, Beghtel H, van den Born MM, Sancho E, Huls G, Meeldijk J, Robertson J, van de Wetering M, Pawson T *et al*: **Beta-catenin and TCF mediate cell positioning in the intestinal epithelium by controlling the expression of EphB/ephrinB**. *Cell* 2002, **111**(2):251-263.
77. Sato T, van Es JH, Snippert HJ, Stange DE, Vries RG, van den Born M, Barker N, Shroyer NF, van de Wetering M, Clevers H: **Paneth cells constitute the niche for Lgr5 stem cells in intestinal crypts**. *Nature* 2011, **469**(7330):415-418.
78. Janssen KP, Alberici P, Fsihi H, Gaspar C, Breukel C, Franken P, Rosty C, Abal M, El Marjou F, Smits R *et al*: **APC and oncogenic KRAS are synergistic in enhancing Wnt signaling in intestinal tumor formation and progression**. *Gastroenterology* 2006, **131**(4):1096-1109.
79. Korinek V, Barker N, Morin PJ, van Wichen D, de Weger R, Kinzler KW, Vogelstein B, Clevers H: **Constitutive transcriptional activation by a beta-catenin-Tcf complex in APC-/- colon carcinoma**. *Science* 1997, **275**(5307):1784-1787.

80. Morin PJ, Sparks AB, Korinek V, Barker N, Clevers H, Vogelstein B, Kinzler KW: **Activation of beta-catenin-Tcf signaling in colon cancer by mutations in beta-catenin or APC**. *Science* 1997, **275**(5307):1787-1790.
81. van de Wetering M, Sancho E, Verweij C, de Lau W, Oving I, Hurlstone A, van der Horn K, Batlle E, Coudreuse D, Haramis AP *et al*: **The beta-catenin/TCF-4 complex imposes a crypt progenitor phenotype on colorectal cancer cells**. *Cell* 2002, **111**(2):241-250.
82. Lamlum H, Ilyas M, Rowan A, Clark S, Johnson V, Bell J, Frayling I, Efstathiou J, Pack K, Payne S *et al*: **The type of somatic mutation at APC in familial adenomatous polyposis is determined by the site of the germline mutation: a new facet to Knudson's 'two-hit' hypothesis**. *Nature medicine* 1999, **5**(9):1071-1075.
83. Bjorklund P, Akerstrom G, Westin G: **Accumulation of nonphosphorylated beta-catenin and c-myc in primary and uremic secondary hyperparathyroid tumors**. *The Journal of clinical endocrinology and metabolism* 2007, **92**(1):338-344.
84. Zhang Y, Liu C, Duan X, Ren F, Li S, Jin Z, Wang Y, Feng Y, Liu Z, Chang Z: **CREPT/RPRD1B, a recently identified novel protein highly expressed in tumors, enhances the beta-catenin.TCF4 transcriptional activity in response to Wnt signaling**. *The Journal of biological chemistry* 2014, **289**(33):22589-22599.
85. Taketo MM, Edelmann W: **Mouse models of colon cancer**. *Gastroenterology* 2009, **136**(3):780-798.
86. Clarke CM, Plata C, Cole B, Tsuchiya K, La Spada AR, Kapur RP: **Visceral neuropathy and intestinal pseudo-obstruction in a murine model of a nuclear inclusion disease**. *Gastroenterology* 2007, **133**(6):1971-1978.
87. Maddison K, Clarke AR: **New approaches for modelling cancer mechanisms in the mouse**. *The Journal of pathology* 2005, **205**(2):181-193.
88. Bilger A, Shoemaker AR, Gould KA, Dove WF: **Manipulation of the mouse germline in the study of Min-induced neoplasia**. *Seminars in cancer biology* 1996, **7**(5):249-260.
89. Moser AR, Pitot HC, Dove WF: **A dominant mutation that predisposes to multiple intestinal neoplasia in the mouse**. *Science* 1990, **247**(4940):322-324.

90. Su LK, Kinzler KW, Vogelstein B, Preisinger AC, Moser AR, Luongo C, Gould KA, Dove WF: **Multiple intestinal neoplasia caused by a mutation in the murine homolog of the APC gene**. *Science* 1992, **256**(5057):668-670.
91. Aoki K, Tamai Y, Horiike S, Oshima M, Taketo MM: **Colonic polyposis caused by mTOR-mediated chromosomal instability in Apc+/Delta716 Cdx2+/- compound mutant mice**. *Nature genetics* 2003, **35**(4):323-330.
92. Romagnolo B, Berrebi D, Saadi-Keddoucci S, Porteu A, Pichard AL, Peuchmaur M, Vandewalle A, Kahn A, Perret C: **Intestinal dysplasia and adenoma in transgenic mice after overexpression of an activated beta-catenin**. *Cancer research* 1999, **59**(16):3875-3879.
93. Harada N, Tamai Y, Ishikawa T, Sauer B, Takaku K, Oshima M, Taketo MM: **Intestinal polyposis in mice with a dominant stable mutation of the beta-catenin gene**. *The EMBO journal* 1999, **18**(21):5931-5942.
94. Colnot S, Romagnolo B, Lambert M, Cluzeaud F, Porteu A, Vandewalle A, Thomasset M, Kahn A, Perret C: **Intestinal expression of the calbindin-D9K gene in transgenic mice. Requirement for a Cdx2-binding site in a distal activator region**. *The Journal of biological chemistry* 1998, **273**(48):31939-31946.
95. Takaku K, Oshima M, Miyoshi H, Matsui M, Seldin MF, Taketo MM: **Intestinal tumorigenesis in compound mutant mice of both Dpc4 (Smad4) and Apc genes**. *Cell* 1998, **92**(5):645-656.
96. Munoz NM, Upton M, Rojas A, Washington MK, Lin L, Chytil A, Sozmen EG, Madison BB, Pozzi A, Moon RT *et al*: **Transforming growth factor beta receptor type II inactivation induces the malignant transformation of intestinal neoplasms initiated by Apc mutation**. *Cancer research* 2006, **66**(20):9837-9844.
97. Tanaka T: **Colorectal carcinogenesis: Review of human and experimental animal studies**. *Journal of carcinogenesis* 2009, **8**:5.
98. Chu FF, Esworthy RS, Chu PG, Longmate JA, Huycke MM, Wilczynski S, Doroshow JH: **Bacteria-induced intestinal cancer in mice with disrupted Gpx1 and Gpx2 genes**. *Cancer research* 2004, **64**(3):962-968.
99. Van der Sluis M, De Koning BA, De Bruijn AC, Velcich A, Meijerink JP, Van Goudoever JB, Buller HA, Dekker J, Van Seuningen I, Renes IB *et al*:

**Muc2-deficient mice spontaneously develop colitis, indicating that MUC2 is critical for colonic protection**. *Gastroenterology* 2006, **131**(1):117-129.

100. Jobin C: **Colorectal cancer: looking for answers in the microbiota**. *Cancer discovery* 2013, **3**(4):384-387.

101. Yang Y, Jobin C: **Microbial imbalance and intestinal pathologies: connections and contributions**. *Disease models & mechanisms* 2014, **7**(10):1131-1142.

102. Arthur JC, Perez-Chanona E, Muhlbauer M, Tomkovich S, Uronis JM, Fan TJ, Campbell BJ, Abujamel T, Dogan B, Rogers AB *et al*: **Intestinal inflammation targets cancer-inducing activity of the microbiota**. *Science* 2012, **338**(6103):120-123.

103. Bonnet M, Buc E, Sauvanet P, Darcha C, Dubois D, Pereira B, Dechelotte P, Bonnet R, Pezet D, Darfeuille-Michaud A: **Colonization of the human gut by E. coli and colorectal cancer risk**. *Clinical cancer research : an official journal of the American Association for Cancer Research* 2014, **20**(4):859-867.

104. Dove WF, Clipson L, Gould KA, Luongo C, Marshall DJ, Moser AR, Newton MA, Jacoby RF: **Intestinal neoplasia in the ApcMin mouse: independence from the microbial and natural killer (beige locus) status**. *Cancer research* 1997, **57**(5):812-814.

105. Sauer B: **Inducible gene targeting in mice using the Cre/lox system**. *Methods* 1998, **14**(4):381-392.

106. **Introduction to cre-lox system** [http://cre.jax.org/introduction.html]-11Dec2013.

107. Clarke AR: **Cancer genetics: mouse models of intestinal cancer**. *Biochemical Society transactions* 2007, **35**(Pt 5):1338-1341.

108. Shibata H, Toyama K, Shioya H, Ito M, Hirota M, Hasegawa S, Matsumoto H, Takano H, Akiyama T, Toyoshima K *et al*: **Rapid colorectal adenoma formation initiated by conditional targeting of the Apc gene**. *Science* 1997, **278**(5335):120-123.

109. He TC, Sparks AB, Rago C, Hermeking H, Zawel L, da Costa LT, Morin PJ, Vogelstein B, Kinzler KW: **Identification of c-MYC as a target of the APC pathway**. *Science* 1998, **281**(5382):1509-1512.

110. Sansom OJ, Meniel VS, Muncan V, Phesse TJ, Wilkins JA, Reed KR, Vass JK, Athineos D, Clevers H, Clarke AR: **Myc deletion rescues Apc deficiency in the small intestine**. *Nature* 2007, **446**(7136):676-679.

111. Tanaka T, Tanaka M, Tanaka T, Ishigamori R: **Biomarkers for colorectal cancer**. *International journal of molecular sciences* 2010, **11**(9):3209-3225.

112. Levin B, Lieberman DA, McFarland B, Andrews KS, Brooks D, Bond J, Dash C, Giardiello FM, Glick S, Johnson D *et al*: **Screening and surveillance for the early detection of colorectal cancer and adenomatous polyps, 2008: a joint guideline from the American Cancer Society, the US Multi-Society Task Force on Colorectal Cancer, and the American College of Radiology**. *Gastroenterology* 2008, **134**(5):1570-1595.

113. Baxter NN, Goldwasser MA, Paszat LF, Saskin R, Urbach DR, Rabeneck L: **Association of colonoscopy and death from colorectal cancer**. *Annals of internal medicine* 2009, **150**(1):1-8.

114. Brenner H, Chang-Claude J, Seiler CM, Rickert A, Hoffmeister M: **Protection from colorectal cancer after colonoscopy: a population-based, case-control study**. *Annals of internal medicine* 2011, **154**(1):22-30.

115. Greenberger NJ: **Current diagnosis and treatment: Gastroenterology, Hepatology and Endoscopy**. USA: McGraw-Hill companies Inc.; 2009.

116. Holme O, Bretthauer M, Fretheim A, Odgaard-Jensen J, Hoff G: **Flexible sigmoidoscopy versus faecal occult blood testing for colorectal cancer screening in asymptomatic individuals**. *The Cochrane database of systematic reviews* 2013, **9**:CD009259.

117. Atkin WS, Edwards R, Kralj-Hans I, Wooldrage K, Hart AR, Northover JM, Parkin DM, Wardle J, Duffy SW, Cuzick J *et al*: **Once-only flexible sigmoidoscopy screening in prevention of colorectal cancer: a multicentre randomised controlled trial**. *Lancet* 2010, **375**(9726):1624-1633.

118. Carethers JM: **DNA Testing and Molecular Screening for Colon Cancer**. *Clinical gastroenterology and hepatology : the official clinical practice journal of the American Gastroenterological Association* 2013.

119. Boynton KA, Summerhayes IC, Ahlquist DA, Shuber AP: **DNA integrity as a potential marker for stool-based detection of colorectal cancer**. *Clinical chemistry* 2003, **49**(7):1058-1065.

120. Lidgard GP, Domanico MJ, Bruinsma JJ, Light J, Gagrat ZD, Oldham-Haltom RL, Fourrier KD, Allawi H, Yab TC, Taylor WR *et al*: **Clinical performance of an automated stool DNA assay for detection of colorectal neoplasia**. *Clinical gastroenterology and hepatology : the official clinical practice journal of the American Gastroenterological Association* 2013, **11**(10):1313-1318.

121. Lin JS, Webber EM, Beil TL, Goddard KA, Whitlock EP. In: *Fecal DNA Testing in Screening for Colorectal Cancer in Average-Risk Adults.* Rockville (MD); 2012.

122. Imperiale TF: **Noninvasive screening tests for colorectal cancer**. *Digestive diseases* 2012, **30 Suppl 2**:16-26.

123. Hardcastle JD, Chamberlain JO, Robinson MH, Moss SM, Amar SS, Balfour TW, James PD, Mangham CM: **Randomised controlled trial of faecal-occult-blood screening for colorectal cancer**. *Lancet* 1996, **348**(9040):1472-1477.

124. Lindholm E, Brevinge H, Haglind E: **Survival benefit in a randomized clinical trial of faecal occult blood screening for colorectal cancer**. *The British journal of surgery* 2008, **95**(8):1029-1036.

125. Lowenfels AB: **Fecal occult blood testing as a screening procedure for colorectal cancer**. *Annals of oncology : official journal of the European Society for Medical Oncology / ESMO* 2002, **13**(1):40-43.

126. Parente F, Boemo C, Ardizzoia A, Costa M, Carzaniga P, Ilardo A, Moretti R, Cremaschini M, Parente EM, Pirola ME: **Outcomes and cost evaluation of the first two rounds of a colorectal cancer screening program based on immunochemical fecal occult blood test in northern Italy**. *Endoscopy* 2013, **45**(1):27-34.

127. Jean-Jacques M, Kaleba EO, Gatta JL, Gracia G, Ryan ER, Choucair BN: **Program to improve colorectal cancer screening in a low-income, racially diverse population: a randomized controlled trial**. *Annals of family medicine* 2012, **10**(5):412-417.

128. Logan RF, Patnick J, Nickerson C, Coleman L, Rutter MD, von Wagner C, English Bowel Cancer Screening Evaluation C: **Outcomes of the Bowel Cancer Screening Programme (BCSP) in England after the first 1 million tests**. *Gut* 2012, **61**(10):1439-1446.

129. Jain KK: **Handbook of biomarkers**. USA: SprigerScience+Businessmedia; 2010.

130. Church TR, Wandell M, Lofton-Day C, Mongin SJ, Burger M, Payne SR, Castanos-Velez E, Blumenstein BA, Rosch T, Osborn N *et al*: **Prospective evaluation of methylated SEPT9 in plasma for detection of asymptomatic colorectal cancer**. *Gut* 2014, **63**(2):317-325.

131. Lorusso G, Ruegg C: **The tumor microenvironment and its contribution to tumor evolution toward metastasis**. *Histochemistry and cell biology* 2008, **130**(6):1091-1103.

132. Alaoui-Jamali MA, Xu YJ: **Proteomic technology for biomarker profiling in cancer: an update**. *Journal of Zhejiang University Science B* 2006, **7**(6):411-420.

133. de Wit M, Fijneman RJ, Verheul HM, Meijer GA, Jimenez CR: **Proteomics in colorectal cancer translational research: biomarker discovery for clinical applications**. *Clinical biochemistry* 2013, **46**(6):466-479.

134. Duffy MJ: **Carcinoembryonic antigen as a marker for colorectal cancer: is it clinically useful?** *Clinical chemistry* 2001, **47**(4):624-630.

135. Perkins GL, Slater ED, Sanders GK, Prichard JG: **Serum tumor markers**. *American family physician* 2003, **68**(6):1075-1082.

136. Shimwell NJ, Wei W, Wilson S, Wakelam MJ, Ismail T, Iqbal T, Johnson PJ, Martin A, Ward DG: **Assessment of novel combinations of biomarkers for the detection of colorectal cancer**. *Cancer biomarkers : section A of Disease markers* 2010, **7**(3):123-132.

137. Hundt S, Haug U, Brenner H: **Blood markers for early detection of colorectal cancer: a systematic review**. *Cancer epidemiology, biomarkers & prevention : a publication of the American Association for Cancer Research, cosponsored by the American Society of Preventive Oncology* 2007, **16**(10):1935-1953.

138. Roessler M, Rollinger W, Palme S, Hagmann ML, Berndt P, Engel AM, Schneidinger B, Pfeffer M, Andres H, Karl J *et al*: **Identification of nicotinamide N-methyltransferase as a novel serum tumor marker for colorectal cancer**. *Clinical cancer research : an official journal of the American Association for Cancer Research* 2005, **11**(18):6550-6557.

139. Wu CC, Chen HC, Chen SJ, Liu HP, Hsieh YY, Yu CJ, Tang R, Hsieh LL, Yu JS, Chang YS: **Identification of collapsin response mediator protein-2 as a potential marker of colorectal carcinoma by comparative analysis of cancer cell secretomes**. *Proteomics* 2008, **8**(2):316-332.

140. Saydam O, Shen Y, Wurdinger T, Senol O, Boke E, James MF, Tannous BA, Stemmer-Rachamimov AO, Yi M, Stephens RM *et al*: **Downregulated microRNA-200a in meningiomas promotes tumor growth by reducing E-cadherin and activating the Wnt/beta-catenin signaling pathway**. *Molecular and cellular biology* 2009, **29**(21):5923-5940.

141. Yang L, Belaguli N, Berger DH: **MicroRNA and colorectal cancer**. *World journal of surgery* 2009, **33**(4):638-646.

142. Boland CR, Sinicrope FA, Brenner DE, Carethers JM: **Colorectal cancer prevention and treatment**. *Gastroenterology* 2000, **118**(2 Suppl 1):S115-128.

143. Clark-Langone KM, Sangli C, Krishnakumar J, Watson D: **Translating tumor biology into personalized treatment planning: analytical performance characteristics of the Oncotype DX Colon Cancer Assay**. *BMC cancer* 2010, **10**:691.

144. Hochwald SN, Lind DS, Malaty J, Copeland EM, 3rd, Moldawer LL, MacKay SL: **Antineoplastic therapy in colorectal cancer through proteasome inhibition**. *The American surgeon* 2003, **69**(1):15-23.

145. Ribic CM, Sargent DJ, Moore MJ, Thibodeau SN, French AJ, Goldberg RM, Hamilton SR, Laurent-Puig P, Gryfe R, Shepherd LE *et al*: **Tumor microsatellite-instability status as a predictor of benefit from fluorouracil-based adjuvant chemotherapy for colon cancer**. *The New England journal of medicine* 2003, **349**(3):247-257.

146. Palles C, Cazier JB, Howarth KM, Domingo E, Jones AM, Broderick P, Kemp Z, Spain SL, Guarino E, Salguero I *et al*: **Germline mutations affecting the proofreading domains of POLE and POLD1 predispose to colorectal adenomas and carcinomas**. *Nature genetics* 2013, **45**(2):136-144.

147. Hammoudi A, Song F, Reed KR, Jenkins RE, Meniel VS, Watson AJ, Pritchard DM, Clarke AR, Jenkins JR: **Proteomic profiling of a mouse model of acute intestinal Apc deletion leads to identification of potential**

**novel biomarkers of human colorectal cancer (CRC)**. *Biochemical and biophysical research communications* 2013, **440**(3):364-370.

148. Kidd M, Modlin IM, Mane SM, Camp RL, Eick G, Latich I: **The role of genetic markers--NAP1L1, MAGE-D2, and MTA1--in defining small-intestinal carcinoid neoplasia**. *Annals of surgical oncology* 2006, **13**(2):253-262.

149. Okuwaki M, Kato K, Nagata K: **Functional characterization of human nucleosome assembly protein 1-like proteins as histone chaperones**. *Genes to cells : devoted to molecular & cellular mechanisms* 2010, **15**(1):13-27.

150. Line A, Slucka Z, Stengrevics A, Silina K, Li G, Rees RC: **Characterisation of tumour-associated antigens in colon cancer**. *Cancer immunology, immunotherapy : CII* 2002, **51**(10):574-582.

151. Nagata T, Takahashi Y, Ishii Y, Asai S, Sugahara M, Nishida Y, Murata A, Chin M, Schichino H, Koshinaga T *et al*: **Profiling of genes differentially expressed between fetal liver and postnatal liver using high-density oligonucleotide DNA array**. *International journal of molecular medicine* 2003, **11**(6):713-721.

152. Nicol SM, Fuller-Pace FV: **Analysis of the RNA helicase p68 (Ddx5) as a transcriptional regulator**. *Methods in molecular biology* 2010, **587**:265-279.

153. Wilson BJ, Bates GJ, Nicol SM, Gregory DJ, Perkins ND, Fuller-Pace FV: **The p68 and p72 DEAD box RNA helicases interact with HDAC1 and repress transcription in a promoter-specific manner**. *BMC molecular biology* 2004, **5**:11.

154. Fuller-Pace FV, Moore HC: **RNA helicases p68 and p72: multifunctional proteins with important implications for cancer development**. *Future oncology* 2011, **7**(2):239-251.

155. Causevic M, Hislop RG, Kernohan NM, Carey FA, Kay RA, Steele RJ, Fuller-Pace FV: **Overexpression and poly-ubiquitylation of the DEAD-box RNA helicase p68 in colorectal tumours**. *Oncogene* 2001, **20**(53):7734-7743.

156. Karhemo PR, Rivinoja A, Lundin J, Hyvonen M, Chernenko A, Lammi J, Sihto H, Lundin M, Heikkila P, Joensuu H *et al*: **An extensive tumor array**

**analysis supports tumor suppressive role for nucleophosmin in breast cancer**. *The American journal of pathology* 2011, **179**(2):1004-1014.

157. Borer RA, Lehner CF, Eppenberger HM, Nigg EA: **Major nucleolar proteins shuttle between nucleus and cytoplasm**. *Cell* 1989, **56**(3):379-390.

158. Wang D, Umekawa H, Olson MO: **Expression and subcellular locations of two forms of nucleolar protein B23 in rat tissues and cells**. *Cellular & molecular biology research* 1993, **39**(1):33-42.

159. Grisendi S, Mecucci C, Falini B, Pandolfi PP: **Nucleophosmin and cancer**. *Nature reviews Cancer* 2006, **6**(7):493-505.

160. Feuerstein N, Spiegel S, Mond JJ: **The nuclear matrix protein, numatrin (B23), is associated with growth factor-induced mitogenesis in Swiss 3T3 fibroblasts and with T lymphocyte proliferation stimulated by lectins and anti-T cell antigen receptor antibody**. *The Journal of cell biology* 1988, **107**(5):1629-1642.

161. Feuerstein N, Chan PK, Mond JJ: **Identification of numatrin, the nuclear matrix protein associated with induction of mitogenesis, as the nucleolar protein B23. Implication for the role of the nucleolus in early transduction of mitogenic signals**. *The Journal of biological chemistry* 1988, **263**(22):10608-10612.

162. Lai MD, Xu J: **Ribosomal proteins and colorectal cancer**. *Current genomics* 2007, **8**(1):43-49.

163. Gou Y, Shi Y, Zhang Y, Nie Y, Wang J, Song J, Jin H, He L, Gao L, Qiao L *et al*: **Ribosomal protein L6 promotes growth and cell cycle progression through upregulating cyclin E in gastric cancer cells**. *Biochemical and biophysical research communications* 2010, **393**(4):788-793.

164. Du J, Shi Y, Pan Y, Jin X, Liu C, Liu N, Han Q, Lu Y, Qiao T, Fan D: **Regulation of multidrug resistance by ribosomal protein l6 in gastric cancer cells**. *Cancer biology & therapy* 2005, **4**(2):242-247.

165. Wu CH, Sahoo D, Arvanitis C, Bradon N, Dill DL, Felsher DW: **Combined analysis of murine and human microarrays and ChIP analysis reveals genes associated with the ability of MYC to maintain tumorigenesis**. *PLoS genetics* 2008, **4**(6):e1000090.

166. Ohmachi T, Inoue H, Mimori K, Tanaka F, Sasaki A, Kanda T, Fujii H, Yanaga K, Mori M: **Fatty acid binding protein 6 is overexpressed in**

**colorectal cancer**. *Clinical cancer research : an official journal of the American Association for Cancer Research* 2006, **12**(17):5090-5095.

167. Watanabe T, Hirano K, Takahashi A, Yamaguchi K, Beppu M, Fujiki H, Suganuma M: **Nucleolin on the cell surface as a new molecular target for gastric cancer treatment**. *Biological & pharmaceutical bulletin* 2010, **33**(5):796-803.

168. Hovanessian AG, Soundaramourty C, El Khoury D, Nondier I, Svab J, Krust B: **Surface expressed nucleolin is constantly induced in tumor cells to mediate calcium-dependent ligand internalization**. *PloS one* 2010, **5**(12):e15787.

169. Gonzalez V, Guo K, Hurley L, Sun D: **Identification and characterization of nucleolin as a c-myc G-quadruplex-binding protein**. *The Journal of biological chemistry* 2009, **284**(35):23622-23635.

170. David CJ, Manley JL: **Alternative pre-mRNA splicing regulation in cancer: pathways and programs unhinged**. *Genes & development* 2010, **24**(21):2343-2364.

171. Thakur A, Bollig A, Wu J, Liao DJ: **Gene expression profiles in primary pancreatic tumors and metastatic lesions of Ela-c-myc transgenic mice**. *Molecular cancer* 2008, **7**:11.

172. Tang D, Kang R, Zeh HJ, 3rd, Lotze MT: **High-mobility group box 1 and cancer**. *Biochimica et biophysica acta* 2010, **1799**(1-2):131-140.

173. Sims GP, Rowe DC, Rietdijk ST, Herbst R, Coyle AJ: **HMGB1 and RAGE in inflammation and cancer**. *Annual review of immunology* 2010, **28**:367-388.

174. Volp K, Brezniceanu ML, Bosser S, Brabletz T, Kirchner T, Gottel D, Joos S, Zornig M: **Increased expression of high mobility group box 1 (HMGB1) is associated with an elevated level of the antiapoptotic c-IAP2 protein in human colon carcinomas**. *Gut* 2006, **55**(2):234-242.

175. Kuniyasu H, Chihara Y, Takahashi T: **Co-expression of receptor for advanced glycation end products and the ligand amphoterin associates closely with metastasis of colorectal cancer**. *Oncology reports* 2003, **10**(2):445-448.

176. Mishra S, Ande SR, Nyomba BL: **The role of prohibitin in cell signaling**. *The FEBS journal* 2010, **277**(19):3937-3946.

177. Zhou P, Qian L, D'Aurelio M, Cho S, Wang G, Manfredi G, Pickel V, Iadecola C: **Prohibitin reduces mitochondrial free radical production and protects brain cells from different injury modalities**. *The Journal of neuroscience : the official journal of the Society for Neuroscience* 2012, **32**(2):583-592.

178. Gamble SC, Odontiadis M, Waxman J, Westbrook JA, Dunn MJ, Wait R, Lam EW, Bevan CL: **Androgens target prohibitin to regulate proliferation of prostate cancer cells**. *Oncogene* 2004, **23**(17):2996-3004.

179. Kang X, Zhang L, Sun J, Ni Z, Ma Y, Chen X, Sheng X, Chen T: **Prohibitin: a potential biomarker for tissue-based detection of gastric cancer**. *Journal of gastroenterology* 2008, **43**(8):618-625.

180. Zhu B, Zhai J, Zhu H, Kyprianou N: **Prohibitin regulates TGF-beta induced apoptosis as a downstream effector of Smad-dependent and -independent signaling**. *The Prostate* 2010, **70**(1):17-26.

181. Yang HB, Song W, Chen LY, Li QF, Shi SL, Kong HY, Chen P: **Differential expression and regulation of prohibitin during curcumin-induced apoptosis of immortalized human epidermal HaCaT cells**. *International journal of molecular medicine* 2014, **33**(3):507-514.

182. Marsh V, Winton DJ, Williams GT, Dubois N, Trumpp A, Sansom OJ, Clarke AR: **Epithelial Pten is dispensable for intestinal homeostasis but suppresses adenoma development and progression after Apc mutation**. *Nature genetics* 2008, **40**(12):1436-1444.

183. Kemp R, Ireland H, Clayton E, Houghton C, Howard L, Winton DJ: **Elimination of background recombination: somatic induction of Cre by combined transcriptional regulation and hormone binding affinity**. *Nucleic acids research* 2004, **32**(11):e92.

184. Bunz F, Hwang PM, Torrance C, Waldman T, Zhang Y, Dillehay L, Williams J, Lengauer C, Kinzler KW, Vogelstein B: **Disruption of p53 in human cancer cells alters the responses to therapeutic agents**. *The Journal of clinical investigation* 1999, **104**(3):263-269.

185. McNamara AV, Barclay M, Watson AJ, Jenkins JR: **Hsp90 inhibitors sensitise human colon cancer cells to topoisomerase I poisons by depletion of key anti-apoptotic and cell cycle checkpoint proteins**. *Biochemical pharmacology* 2012, **83**(3):355-367.

186. Nishisho I, Nakamura Y, Miyoshi Y, Miki Y, Ando H, Horii A, Koyama K, Utsunomiya J, Baba S, Hedge P: **Mutations of chromosome 5q21 genes in FAP and colorectal cancer patients**. *Science* 1991, **253**(5020):665-669.

187. Wang Z, Vogelstein B, Kinzler KW: **Phosphorylation of beta-catenin at S33, S37, or T41 can occur in the absence of phosphorylation at T45 in colon cancer cells**. *Cancer research* 2003, **63**(17):5234-5235.

188. Bradford MM: **A rapid and sensitive method for the quantitation of microgram quantities of protein utilizing the principle of protein-dye binding**. *Analytical biochemistry* 1976, **72**:248-254.

189. Smith PK, Krohn RI, Hermanson GT, Mallia AK, Gartner FH, Provenzano MD, Fujimoto EK, Goeke NM, Olson BJ, Klenk DC: **Measurement of protein using bicinchoninic acid**. *Analytical biochemistry* 1985, **150**(1):76-85.

190. Gao Y, Liu XL, Li XR: **Research progress on siRNA delivery with nonviral carriers**. *International journal of nanomedicine* 2011, **6**:1017-1025.

191. Elbashir SM, Harborth J, Lendeckel W, Yalcin A, Weber K, Tuschl T: **Duplexes of 21-nucleotide RNAs mediate RNA interference in cultured mammalian cells**. *Nature* 2001, **411**(6836):494-498.

192. Bumcrot D, Manoharan M, Koteliansky V, Sah DW: **RNAi therapeutics: a potential new class of pharmaceutical drugs**. *Nature chemical biology* 2006, **2**(12):711-719.

193. Zamore PD, Tuschl T, Sharp PA, Bartel DP: **RNAi: double-stranded RNA directs the ATP-dependent cleavage of mRNA at 21 to 23 nucleotide intervals**. *Cell* 2000, **101**(1):25-33.

194. Li J, Chen YC, Tseng YC, Mozumdar S, Huang L: **Biodegradable calcium phosphate nanoparticle with lipid coating for systemic siRNA delivery**. *Journal of controlled release : official journal of the Controlled Release Society* 2010, **142**(3):416-421.

195. Barichello JM, Ishida T, Kiwada H: **Complexation of siRNA and pDNA with cationic liposomes: the important aspects in lipoplex preparation**. *Methods in molecular biology* 2010, **605**:461-472.

196. Spagnou S, Miller AD, Keller M: **Lipidic carriers of siRNA: differences in the formulation, cellular uptake, and delivery with plasmid DNA**. *Biochemistry* 2004, **43**(42):13348-13356.

197. Ramachandran PV, Ignacimuthu S: **RNA interference--a silent but an efficient therapeutic tool**. *Applied biochemistry and biotechnology* 2013, **169**(6):1774-1789.

198. Hamilton AJ, Baulcombe DC: **A species of small antisense RNA in posttranscriptional gene silencing in plants**. *Science* 1999, **286**(5441):950-952.

199. Tebes SJ, Kruk PA: **The genesis of RNA interference, its potential clinical applications, and implications in gynecologic cancer**. *Gynecologic oncology* 2005, **99**(3):736-741.

200. Hanedi AF: **Physiological importance of various NFKB family members in regulating intestinal responses to injury**. *PhD thesis.* Liverpool, UK: University of Liverpool; 2013.

201. Vichai V, Kirtikara K: **Sulforhodamine B colorimetric assay for cytotoxicity screening**. *Nature protocols* 2006, **1**(3):1112-1116.

202. Franken NA, Rodermond HM, Stap J, Haveman J, van Bree C: **Clonogenic assay of cells in vitro**. *Nature protocols* 2006, **1**(5):2315-2319.

203. **Introduction to Flow Cytometry** [http://www.abcam.com/index.html?pageconfig=resource&rid=11446]-8Feb2014.

204. Kinzler KW, Vogelstein B: **Lessons from hereditary colorectal cancer**. *Cell* 1996, **87**(2):159-170.

205. Jarde T, Evans RJ, McQuillan KL, Parry L, Feng GJ, Alvares B, Clarke AR, Dale TC: **In vivo and in vitro models for the therapeutic targeting of Wnt signaling using a Tet-ODeltaN89beta-catenin system**. *Oncogene* 2013, **32**(7):883-893.

206. Valenta T, Hausmann G, Basler K: **The many faces and functions of beta-catenin**. *The EMBO journal* 2012, **31**(12):2714-2736.

207. Schwarz-Romond T: **Three decades of Wnt signalling**. *The EMBO journal* 2012, **31**(12):2664.

208. Shoemaker AR, Gould KA, Luongo C, Moser AR, Dove WF: **Studies of neoplasia in the Min mouse**. *Biochimica et biophysica acta* 1997, **1332**(2):F25-48.

209. Ponder BA, Schmidt GH, Wilkinson MM, Wood MJ, Monk M, Reid A: **Derivation of mouse intestinal crypts from single progenitor cells**. *Nature* 1985, **313**(6004):689-691.

210. Schmidt GH, Winton DJ, Ponder BA: **Development of the pattern of cell renewal in the crypt-villus unit of chimaeric mouse small intestine**. *Development* 1988, **103**(4):785-790.

211. Simon HU, Mills GB, Kozlowski M, Hogg D, Branch D, Ishimi Y, Siminovitch KA: **Molecular characterization of hNRP, a cDNA encoding a human nucleosome-assembly-protein-I-related gene product involved in the induction of cell proliferation**. *The Biochemical journal* 1994, **297 ( Pt 2)**:389-397.

212. Tripathi K, Parnaik VK: **Differential dynamics of splicing factor SC35 during the cell cycle**. *Journal of biosciences* 2008, **33**(3):345-354.

213. Chen D, Chen F, Lu X, Yang X, Xu Z, Pan J, Huang Y, Lin H, Chi P: **Identification of prohibitin as a potential biomarker for colorectal carcinoma based on proteomics technology**. *International journal of oncology* 2010, **37**(2):355-365.

214. Yang A, Shi G, Zhou C, Lu R, Li H, Sun L, Jin Y: **Nucleolin maintains embryonic stem cell self-renewal by suppression of p53 protein-dependent pathway**. *J Biol Chem* 2011, **286**(50):43370-43382.

215. Goodwin GH, Sanders C, Johns EW: **A new group of chromatin-associated proteins with a high content of acidic and basic amino acids**. *European journal of biochemistry / FEBS* 1973, **38**(1):14-19.

216. Lee H, Park M, Shin N, Kim G, Kim YG, Shin JS, Kim H: **High mobility group box-1 is phosphorylated by protein kinase C zeta and secreted in colon cancer cells**. *Biochemical and biophysical research communications* 2012, **424**(2):321-326.

217. Kang HJ, Lee H, Choi HJ, Youn JH, Shin JS, Ahn YH, Yoo JS, Paik YK, Kim H: **Non-histone nuclear factor HMGB1 is phosphorylated and secreted in colon cancers**. *Laboratory investigation; a journal of technical methods and pathology* 2009, **89**(8):948-959.

218. Ellerman JE, Brown CK, de Vera M, Zeh HJ, Billiar T, Rubartelli A, Lotze MT: **Masquerader: high mobility group box-1 and cancer**. *Clinical cancer*

*research : an official journal of the American Association for Cancer Research* 2007, **13**(10):2836-2848.

219. Liu Y, Zhang F, Zhang XF, Qi LS, Yang L, Guo H, Zhang N: **Expression of Nucleophosmin/NPM1 correlates with migration and invasiveness of colon cancer cells**. *Journal of biomedical science* 2012, **19**(1):53.

220. Okuda M: **The role of nucleophosmin in centrosome duplication**. *Oncogene* 2002, **21**(40):6170-6174.

221. Li QF, Tang J, Liu QR, Shi SL, Chen XF: **Localization and altered expression of nucleophosmin in the nuclear matrix during the differentiation of human hepatocarcinoma SMMC-7721 cells induced by HMBA**. *Cancer investigation* 2010, **28**(10):1004-1012.

222. Li Z, Boone D, Hann SR: **Nucleophosmin interacts directly with c-Myc and controls c-Myc-induced hyperproliferation and transformation**. *Proc Natl Acad Sci U S A* 2008, **105**(48):18794-18799.

223. Moyes LH, McEwan H, Radulescu S, Pawlikowski J, Lamm CG, Nixon C, Sansom OJ, Going JJ, Fullarton GM, Adams PD: **Activation of Wnt signalling promotes development of dysplasia in Barrett's oesophagus**. *The Journal of pathology* 2012, **228**(1):99-112.

224. Levy DB, Smith KJ, Beazer-Barclay Y, Hamilton SR, Vogelstein B, Kinzler KW: **Inactivation of both APC alleles in human and mouse tumors**. *Cancer research* 1994, **54**(22):5953-5958.

225. Paoni NF, Feldman MW, Gutierrez LS, Ploplis VA, Castellino FJ: **Transcriptional profiling of the transition from normal intestinal epithelia to adenomas and carcinomas in the APCMin/+ mouse**. *Physiological genomics* 2003, **15**(3):228-235.

226. Hanahan D, Weinberg RA: **The hallmarks of cancer**. *Cell* 2000, **100**(1):57-70.

227. Attia M, Forster A, Rachez C, Freemont P, Avner P, Rogner UC: **Interaction between nucleosome assembly protein 1-like family members**. *Journal of molecular biology* 2011, **407**(5):647-660.

228. Zlatanova J, Seebart C, Tomschik M: **Nap1: taking a closer look at a juggler protein of extraordinary skills**. *FASEB journal : official publication of the Federation of American Societies for Experimental Biology* 2007, **21**(7):1294-1310.

229. Wu Q, Gou Y, Wang Q, Jin H, Cui L, Zhang Y, He L, Wang J, Nie Y, Shi Y *et al*: **Downregulation of RPL6 by siRNA inhibits proliferation and cell cycle progression of human gastric cancer cell lines**. *PLoS One* 2011, **6**(10):e26401.

230. Ruggero D, Pandolfi PP: **Does the ribosome translate cancer?** *Nature reviews Cancer* 2003, **3**(3):179-192.

231. Amsterdam A, Sadler KC, Lai K, Farrington S, Bronson RT, Lees JA, Hopkins N: **Many ribosomal protein genes are cancer genes in zebrafish**. *PLoS Biol* 2004, **2**(5):E139.

232. Henry JL, Coggin DL, King CR: **High-level expression of the ribosomal protein L19 in human breast tumors that overexpress erbB-2**. *Cancer research* 1993, **53**(6):1403-1408.

233. Wang Q, Yang C, Zhou J, Wang X, Wu M, Liu Z: **Cloning and characterization of full-length human ribosomal protein L15 cDNA which was overexpressed in esophageal cancer**. *Gene* 2001, **263**(1-2):205-209.

234. Merdzhanova G, Edmond V, De Seranno S, Van den Broeck A, Corcos L, Brambilla C, Brambilla E, Gazzeri S, Eymin B: **E2F1 controls alternative splicing pattern of genes involved in apoptosis through upregulation of the splicing factor SC35**. *Cell Death Differ* 2008, **15**(12):1815-1823.

235. Ma K, He Y, Zhang H, Fei Q, Niu D, Wang D, Ding X, Xu H, Chen X, Zhu J: **DNA methylation-regulated miR-193a-3p dictates resistance of hepatocellular carcinoma to 5-fluorouracil via repression of SRSF2 expression**. *The Journal of biological chemistry* 2012, **287**(8):5639-5649.

236. Moore MJ, Wang Q, Kennedy CJ, Silver PA: **An alternative splicing network links cell-cycle control to apoptosis**. *Cell* 2010, **142**(4):625-636.

237. Edmond V, Moysan E, Khochbin S, Matthias P, Brambilla C, Brambilla E, Gazzeri S, Eymin B: **Acetylation and phosphorylation of SRSF2 control cell fate decision in response to cisplatin**. *The EMBO journal* 2011, **30**(3):510-523.

238. Tsai HW, Chow NH, Lin CP, Chan SH, Chou CY, Ho CL: **The significance of prohibitin and c-Met/hepatocyte growth factor receptor in the progression of cervical adenocarcinoma**. *Human pathology* 2006, **37**(2):198-204.

239. Nijtmans LG, Artal SM, Grivell LA, Coates PJ: **The mitochondrial PHB complex: roles in mitochondrial respiratory complex assembly, ageing and degenerative disease**. *Cellular and molecular life sciences : CMLS* 2002, **59**(1):143-155.

240. Asamoto M, Cohen SM: **Prohibitin gene is overexpressed but not mutated in rat bladder carcinomas and cell lines**. *Cancer letters* 1994, **83**(1-2):201-207.

241. Williams K, Chubb C, Huberman E, Giometti CS: **Analysis of differential protein expression in normal and neoplastic human breast epithelial cell lines**. *Electrophoresis* 1998, **19**(2):333-343.

242. Fellenberg J, Dechant MJ, Ewerbeck V, Mau H: **Identification of drug-regulated genes in osteosarcoma cells**. *International journal of cancer Journal international du cancer* 2003, **105**(5):636-643.

243. Bugler B, Caizergues-Ferrer M, Bouche G, Bourbon H, Amalric F: **Detection and localization of a class of proteins immunologically related to a 100-kDa nucleolar protein**. *European journal of biochemistry / FEBS* 1982, **128**(2-3):475-480.

244. Woo RA, Poon RY: **Cyclin-dependent kinases and S phase control in mammalian cells**. *Cell cycle* 2003, **2**(4):316-324.

245. Resnitzky D, Gossen M, Bujard H, Reed SI: **Acceleration of the G1/S phase transition by expression of cyclins D1 and E with an inducible system**. *Molecular and cellular biology* 1994, **14**(3):1669-1679.

246. Duong MT, Akli S, Macalou S, Biernacka A, Debeb BG, Yi M, Hunt KK, Keyomarsi K: **Hbo1 is a cyclin E/CDK2 substrate that enriches breast cancer stem-like cells**. *Cancer research* 2013, **73**(17):5556-5568.

247. Koff A, Giordano A, Desai D, Yamashita K, Harper JW, Elledge S, Nishimoto T, Morgan DO, Franza BR, Roberts JM: **Formation and activation of a cyclin E-cdk2 complex during the G1 phase of the human cell cycle**. *Science* 1992, **257**(5077):1689-1694.

248. Trimarchi JM, Lees JA: **Sibling rivalry in the E2F family**. *Nature reviews Molecular cell biology* 2002, **3**(1):11-20.

249. Geng Y, Lee YM, Welcker M, Swanger J, Zagozdzon A, Winer JD, Roberts JM, Kaldis P, Clurman BE, Sicinski P: **Kinase-independent function of cyclin E**. *Molecular cell* 2007, **25**(1):127-139.

250. Geng Y, Yu Q, Sicinska E, Das M, Schneider JE, Bhattacharya S, Rideout WM, Bronson RT, Gardner H, Sicinski P: **Cyclin E ablation in the mouse**. *Cell* 2003, **114**(4):431-443.

251. Lee HO, Davidson JM, Duronio RJ: **Endoreplication: polyploidy with purpose**. *Genes & development* 2009, **23**(21):2461-2477.

252. Scaltriti M, Eichhorn PJ, Cortes J, Prudkin L, Aura C, Jimenez J, Chandarlapaty S, Serra V, Prat A, Ibrahim YH *et al*: **Cyclin E amplification/overexpression is a mechanism of trastuzumab resistance in HER2+ breast cancer patients**. *Proceedings of the National Academy of Sciences of the United States of America* 2011, **108**(9):3761-3766.

253. Song F: **Early colon cancer model: analysis of cited1 in vivo and in vitro**. Liverpool, UK: University of Liverpool; 2009.

254. Barker CR, Hamlett J, Pennington SR, Burrows F, Lundgren K, Lough R, Watson AJ, Jenkins JR: **The topoisomerase II-Hsp90 complex: a new chemotherapeutic target?** *International journal of cancer Journal international du cancer* 2006, **118**(11):2685-2693.

255. Ruggero D, Grisendi S, Piazza F, Rego E, Mari F, Rao PH, Cordon-Cardo C, Pandolfi PP: **Dyskeratosis congenita and cancer in mice deficient in ribosomal RNA modification**. *Science* 2003, **299**(5604):259-262.

256. Nikitenko NA, Prassolov VS: **Non-Viral Delivery and Therapeutic Application of Small Interfering RNAs**. *Acta naturae* 2013, **5**(3):35-53.

257. Persad S, Troussard AA, McPhee TR, Mulholland DJ, Dedhar S: **Tumor suppressor PTEN inhibits nuclear accumulation of beta-catenin and T cell/lymphoid enhancer factor 1-mediated transcriptional activation**. *The Journal of cell biology* 2001, **153**(6):1161-1174.

258. Shen CH, Clark DJ: **DNA sequence plays a major role in determining nucleosome positions in yeast CUP1 chromatin**. *The Journal of biological chemistry* 2001, **276**(37):35209-35216.

259. Drozdov I, Kidd M, Nadler B, Camp RL, Mane SM, Hauso O, Gustafsson BI, Modlin IM: **Predicting neuroendocrine tumor (carcinoid) neoplasia using gene expression profiling and supervised machine learning**. *Cancer* 2009, **115**(8):1638-1650.

260. Li L, Gong H, Yu H, Liu X, Liu Q, Yan G, Zhang Y, Lu H, Zou Y, Yang P: **Knockdown of nucleosome assembly protein 1-like 1 promotes dimethyl**

**sulfoxide-induced differentiation of P19CL6 cells into cardiomyocytes**. *J Cell Biochem* 2012, **113**(12):3788-3796.

261. Narla A, Ebert BL: **Ribosomopathies: human disorders of ribosome dysfunction**. *Blood* 2010, **115**(16):3196-3205.
262. Bai D, Zhang J, Xiao W, Zheng X: **Regulation of the HDM2-p53 pathway by ribosomal protein L6 in response to ribosomal stress**. *Nucleic acids research* 2014, **42**(3):1799-1811.
263. Myant K, Sansom O: **Efficient Wnt mediated intestinal hyperproliferation requires the cyclin D2-CDK4/6 complex**. *Cell division* 2011, **6**(1):3.
264. Corin I, Larsson L, Bergstrom J, Gustavsson B, Derwinger K: **A study of the expression of Cyclin E and its isoforms in tumor and adjacent mucosa, correlated to patient outcome in early colon cancer**. *Acta oncologica* 2010, **49**(1):63-69.
265. Hwang HC, Clurman BE: **Cyclin E in normal and neoplastic cell cycles**. *Oncogene* 2005, **24**(17):2776-2786.
266. Garabedian EM, Roberts LJ, McNevin MS, Gordon JI: **Examining the role of Paneth cells in the small intestine by lineage ablation in transgenic mice**. *The Journal of biological chemistry* 1997, **272**(38):23729-23740.
267. Mosca E, Alfieri R, Merelli I, Viti F, Calabria A, Milanesi L: **A multilevel data integration resource for breast cancer study**. *BMC systems biology* 2010, **4**:76.
268. Orford K, Orford CC, Byers SW: **Exogenous expression of beta-catenin regulates contact inhibition, anchorage-independent growth, anoikis, and radiation-induced cell cycle arrest**. *The Journal of cell biology* 1999, **146**(4):855-868.
269. Smith CW, Valcarcel J: **Alternative pre-mRNA splicing: the logic of combinatorial control**. *Trends in biochemical sciences* 2000, **25**(8):381-388.
270. Engemann H, Heinzel V, Page G, Preuss U, Scheidtmann KH: **DAP-like kinase interacts with the rat homolog of Schizosaccharomyces pombe CDC5 protein, a factor involved in pre-mRNA splicing and required for G2/M phase transition**. *Nucleic acids research* 2002, **30**(6):1408-1417.
271. Hayat MA: **Microscopy, immunohistochemistry and antigen retrieval methods**. USA: Kluwer academic publlishers; 2002.

272. Lleres D, Denegri M, Biggiogera M, Ajuh P, Lamond AI: **Direct interaction between hnRNP-M and CDC5L/PLRG1 proteins affects alternative splice site choice**. *EMBO reports* 2010, **11**(6):445-451.

273. Zhang N, Kaur R, Akhter S, Legerski RJ: **Cdc5L interacts with ATR and is required for the S-phase cell-cycle checkpoint**. *EMBO reports* 2009, **10**(9):1029-1035.

274. Lu XY, Lu Y, Zhao YJ, Jaeweon K, Kang J, Xiao-Nan L, Ge G, Meyer R, Perlaky L, Hicks J *et al*: **Cell cycle regulator gene CDC5L, a potential target for 6p12-p21 amplicon in osteosarcoma**. *Molecular cancer research : MCR* 2008, **6**(6):937-946.

275. Takayama T, Shiozaki H, Shibamoto S, Oka H, Kimura Y, Tamura S, Inoue M, Monden T, Ito F, Monden M: **Beta-catenin expression in human cancers**. *The American journal of pathology* 1996, **148**(1):39-46.

276. Serafino A, Moroni N, Zonfrillo M, Andreola F, Mercuri L, Nicotera G, Nunziata J, Ricci R, Antinori A, Rasi G *et al*: **WNT-pathway components as predictive markers useful for diagnosis, prevention and therapy in inflammatory bowel disease and sporadic colorectal cancer**. *Oncotarget* 2014, **5**(4):978-992.

277. Boatright KM, Renatus M, Scott FL, Sperandio S, Shin H, Pedersen IM, Ricci JE, Edris WA, Sutherlin DP, Green DR *et al*: **A unified model for apical caspase activation**. *Molecular cell* 2003, **11**(2):529-541.

278. Leiszter K, Galamb O, Sipos F, Krenacs T, Veres G, Wichmann B, Kalmar A, Patai AV, Toth K, Valcz G *et al*: **Sporadic colorectal cancer development shows rejuvenescence regarding epithelial proliferation and apoptosis**. *PloS one* 2013, **8**(10):e74140.

279. Xiao ZQ, Moragoda L, Jaszewski R, Hatfield JA, Fligiel SE, Majumdar AP: **Aging is associated with increased proliferation and decreased apoptosis in the colonic mucosa**. *Mechanisms of ageing and development* 2001, **122**(15):1849-1864.

280. Ukraintseva SV, Yashina AI: **Cancer as "rejuvenescence"**. *Annals of the New York Academy of Sciences* 2004, **1019**:200-205.

281. Soussi T, Dehouche K, Beroud C: **p53 website and analysis of p53 gene mutations in human cancer: forging a link between epidemiology and carcinogenesis**. *Human mutation* 2000, **15**(1):105-113.

282. Aggarwal S, Gupta S: **Increased apoptosis of T cell subsets in aging humans: altered expression of Fas (CD95), Fas ligand, Bcl-2, and Bax**. *Journal of immunology* 1998, **160**(4):1627-1637.

283. Taira N, Yamaguchi T, Kimura J, Lu ZG, Fukuda S, Higashiyama S, Ono M, Yoshida K: **Induction of amphiregulin by p53 promotes apoptosis via control of microRNA biogenesis in response to DNA damage**. *Proceedings of the National Academy of Sciences of the United States of America* 2014, **111**(2):717-722.

284. Ajuh P, Kuster B, Panov K, Zomerdijk JC, Mann M, Lamond AI: **Functional analysis of the human CDC5L complex and identification of its components by mass spectrometry**. *The EMBO journal* 2000, **19**(23):6569-6581.

285. Jiang ZH, Zhang WJ, Rao Y, Wu JY: **Regulation of Ich-1 pre-mRNA alternative splicing and apoptosis by mammalian splicing factors**. *Proceedings of the National Academy of Sciences of the United States of America* 1998, **95**(16):9155-9160.

286. Kleinridders A, Pogoda HM, Irlenbusch S, Smyth N, Koncz C, Hammerschmidt M, Bruning JC: **PLRG1 is an essential regulator of cell proliferation and apoptosis during vertebrate development and tissue homeostasis**. *Molecular and cellular biology* 2009, **29**(11):3173-3185.

287. Bernstein HS, Coughlin SR: **Pombe Cdc5-related protein. A putative human transcription factor implicated in mitogen-activated signaling**. *The Journal of biological chemistry* 1997, **272**(9):5833-5837.

288. Xiao R, Sun Y, Ding JH, Lin S, Rose DW, Rosenfeld MG, Fu XD, Li X: **Splicing regulator SC35 is essential for genomic stability and cell proliferation during mammalian organogenesis**. *Mol Cell Biol* 2007, **27**(15):5393-5402.

289. Bernstein HS, Coughlin SR: **A mammalian homolog of fission yeast Cdc5 regulates G2 progression and mitotic entry**. *The Journal of biological chemistry* 1998, **273**(8):4666-4671.

290. Crissman HA, Hirons GT: **Staining of DNA in live and fixed cells**. *Methods in cell biology* 1994, **41**:195-209.

291. Juan G, Traganos F, Darzynkiewicz Z: **Methods to identify mitotic cells by flow cytometry**. *Methods in cell biology* 2001, **63**:343-354.

292. Poot M, Silber JR, Rabinovitch PS: **A novel flow cytometric technique for drug cytotoxicity gives results comparable to colony-forming assays**. *Cytometry* 2002, **48**(1):1-5.

293. Norbury C, Nurse P: **Animal cell cycles and their control**. *Annual review of biochemistry* 1992, **61**:441-470.

294. Zhao H, Piwnica-Worms H: **ATR-mediated checkpoint pathways regulate phosphorylation and activation of human Chk1**. *Molecular and cellular biology* 2001, **21**(13):4129-4139.

295. Vogelstein B, Lane D, Levine AJ: **Surfing the p53 network**. *Nature* 2000, **408**(6810):307-310.

296. Liu J, Uematsu H, Tsuchida N, Ikeda MA: **Essential role of caspase-8 in p53/p73-dependent apoptosis induced by etoposide in head and neck carcinoma cells**. *Molecular cancer* 2011, **10**:95.

297. Kim K, Pang KM, Evans M, Hay ED: **Overexpression of beta-catenin induces apoptosis independent of its transactivation function with LEF-1 or the involvement of major G1 cell cycle regulators**. *Molecular biology of the cell* 2000, **11**(10):3509-3523.

298. Olmeda D, Castel S, Vilaro S, Cano A: **Beta-catenin regulation during the cell cycle: implications in G2/M and apoptosis**. *Molecular biology of the cell* 2003, **14**(7):2844-2860.

299. Giles RH, van Es JH, Clevers H: **Caught up in a Wnt storm: Wnt signaling in cancer**. *Biochimica et biophysica acta* 2003, **1653**(1):1-24.

300. Potts SJ, Krueger JS, Landis ND, Eberhard DA, Young GD, Schmechel SC, Lange H: **Evaluating tumor heterogeneity in immunohistochemistry-stained breast cancer tissue**. *Laboratory investigation; a journal of technical methods and pathology* 2012, **92**(9):1342-1357.

301. Nagata T, Takahashi Y, Ishii Y, Asai S, Nishida Y, Murata A, Koshinaga T, Fukuzawa M, Hamazaki M, Asami K *et al*: **Transcriptional profiling in hepatoblastomas using high-density oligonucleotide DNA array**. *Cancer genetics and cytogenetics* 2003, **145**(2):152-160.

302. Budwit-Novotny DA, McCarty KS, Cox EB, Soper JT, Mutch DG, Creasman WT, Flowers JL, McCarty KS, Jr.: **Immunohistochemical analyses of estrogen receptor in endometrial adenocarcinoma using a monoclonal antibody**. *Cancer research* 1986, **46**(10):5419-5425.

303. Costa WH, Rocha RM, Cunha IW, Guimaraes GC, Zequi Sde C: **Immunohistochemical expression of CD44s in renal cell carcinoma lacks independent prognostic significance**. *International braz j urol : official journal of the Brazilian Society of Urology* 2012, **38**(4):456-465.

304. Brabletz T, Jung A, Hermann K, Gunther K, Hohenberger W, Kirchner T: **Nuclear overexpression of the oncoprotein beta-catenin in colorectal cancer is localized predominantly at the invasion front**. *Pathology, research and practice* 1998, **194**(10):701-704.

305. Hugh TJ, Dillon SA, Taylor BA, Pignatelli M, Poston GJ, Kinsella AR: **Cadherin-catenin expression in primary colorectal cancer: a survival analysis**. *British journal of cancer* 1999, **80**(7):1046-1051.

306. Brabletz T, Herrmann K, Jung A, Faller G, Kirchner T: **Expression of nuclear beta-catenin and c-myc is correlated with tumor size but not with proliferative activity of colorectal adenomas**. *The American journal of pathology* 2000, **156**(3):865-870.

307. Samowitz WS, Powers MD, Spirio LN, Nollet F, van Roy F, Slattery ML: **Beta-catenin mutations are more frequent in small colorectal adenomas than in larger adenomas and invasive carcinomas**. *Cancer research* 1999, **59**(7):1442-1444.

308. Phelps RA, Chidester S, Dehghanizadeh S, Phelps J, Sandoval IT, Rai K, Broadbent T, Sarkar S, Burt RW, Jones DA: **A two-step model for colon adenoma initiation and progression caused by APC loss**. *Cell* 2009, **137**(4):623-634.

309. Kobayashi M, Honma T, Matsuda Y, Suzuki Y, Narisawa R, Ajioka Y, Asakura H: **Nuclear translocation of beta-catenin in colorectal cancer**. *British journal of cancer* 2000, **82**(10):1689-1693.

310. Anderson CB, Neufeld KL, White RL: **Subcellular distribution of Wnt pathway proteins in normal and neoplastic colon**. *Proceedings of the National Academy of Sciences of the United States of America* 2002, **99**(13):8683-8688.

311. Morgan RG, Ridsdale J, Tonks A, Darley RL: **Factors Affecting the Nuclear Localization of beta-Catenin in Normal and Malignant Tissue**. *Journal of cellular biochemistry* 2014.

312. Destouches D, El Khoury D, Hamma-Kourbali Y, Krust B, Albanese P, Katsoris P, Guichard G, Briand JP, Courty J, Hovanessian AG: **Suppression of tumor growth and angiogenesis by a specific antagonist of the cell-surface expressed nucleolin**. *PloS one* 2008, **3**(6):e2518.

313. Song JH, Huels DJ, Ridgway RA, Sansom OJ, Kholodenko BN, Kolch W, Cho KH: **The APC network regulates the removal of mutated cells from colonic crypts**. *Cell reports* 2014, **7**(1):94-103.

314. Belmont PJ, Budinska E, Jiang P, Sinnamon MJ, Coffee E, Roper J, Xie T, Rejto PA, Derkits S, Sansom OJ *et al*: **Cross-species analysis of genetically engineered mouse models of MAPK-driven colorectal cancer identifies hallmarks of the human disease**. *Disease models & mechanisms* 2014, **7**(6):613-623.

315. Ahmed D, Eide PW, Eilertsen IA, Danielsen SA, Eknaes M, Hektoen M, Lind GE, Lothe RA: **Epigenetic and genetic features of 24 colon cancer cell lines**. *Oncogenesis* 2013, **2**:e71.

# Appendix

# 9 Appendix

## 9.1 List of published abstracts

- S A Ibrahim; K R Reed; F Song; A Hammoudi; D M Pritchard; J R Jenkins. Validation of two APC-dependent potential biomarkers of colorectal carcinogenesis. Gut 2012 Vol: 61(Suppl 2):A8-A8. DOI: 10.1136/gutjnl-2012-302514a.18
- Shahram A. Ibrahim, Karen R. Reed, Alan R. Clarke, D. M. Pritchard, John R. Jenkins. SFRS2 and CDC5L Interaction: An insight Into Downstream Events Following APC Deletion During Colorectal Carcinogenesis. Gastroenterology, Volume 144, Issue 5, Supplement 1, Pages S-353–S-354, May 2013
- Shahram Ibrahim, Karen Reed, Abeer Hammoudi, Alan Clarke, Mark Pritchard, John Jenkins. Human tissue validation of potential biomarkers for colorectal cancer. Poster presentation at the 2013 NCRI conference.
- Shahram Ibrahim, Karen Reed, Abeer Hammoudi, Alan Clarke, Mark Pritchard, John Jenkins. SFRS2 and CDC5L interaction: An insight into downstream events following APC deletion during colorectal carcinogenesis. Poster presentation at the 2013 NCRI conference.